Open-File Report of Geological Survey of Japan, no. 557

The 1st Workshop of Asia-Pacific Region Global Earthquake and Volcanic Eruption Risk Management

G-EVER1

Abstracts

Volume

Feb. 22-25, 2012

Tsukuba, Japan

Kirishima-Shinmoedake Volcanic Eruption, Jan. 27, 2011

The 2011 off the Pacific coast of Tohoku Earthquake, March 11, 2011

http://www.gsj.jp/Event/AsiaPacific/indexE.html

The 1st Workshop of Asia-Pacific Region Global Earthquake and Volcanic Eruption Risk Management (G-EVER1)

Abstracts Volume

February 22-25, 2012
Auditorium, AIST Tsukuba Central, Tsukuba, Japan

Hosted by
Geological Survey of Japan (GSJ), National Institute of Advanced Industrial Science and Technology (AIST)

Supported by
Ministry of Economy, Trade and Industry (METI)
Ministry of Education, Culture, Sports, Science and Technology (MEXT)
Ministry of Foreign Affairs of Japan (MOFA)
Japan Meteorological Agency (JMA)
Geographical Information Authority of Japan (GSI)
National Research Institute for Earth Science and Disaster Prevention (NIED)
Building Research Institute (BRI)
Earthquake Research Institute, University of Tokyo (ERI)
Disaster Prevention Research Institute, Kyoto University (DPRI)
United States Geological Survey (USGS)
EuroGeoSurveys (EGS)
The Institute of Geological and Nuclear Sciences Ltd. of New Zealand (GNS Science)
Asian Disaster Reduction Center (ADRC)
Coordinating Committee for Geoscience Programmes in East and Southeast Asia (CCOP)
Circum Pacific Council (CPC)
Global Earthquake Model (GEM)
The International Union of Geodesy and Geophysics (IUGG)
International Association of Seismology and Physics of the Earth's Interior (IASPEI)
International Association of Volcanology and Chemistry of the Earth's Interior (IAVCEI)
Geological Society of Japan (GSJ)
Seismological Society of Japan (SSJ)
Volcanological Society of Japan (VSJ)
Japan Association for Quaternary Research (JAQUR)

The 1st Workshop of Asia-Pacific Region Global Earthquake and Volcanic Eruption Risk Management (G-EVER1)

Abstracts Volume
Editors
Eikichi Tsukuda, Yutaka Takahashi, Shinji Takarada, Akira Takada, Yasuto Kuwahara, Takashi Azuma, Naoji Koizumi and Yuzo Ishikawa

Open-File Report of Geological Survey of Japan, no. 557

Published by the Geological Survey of Japan (GSJ), National Institute of Advanced Industrial Science and Technology (AIST), 1-1-1 Higashi, Tsukuba, 305-8567, Japan.
Pages: 140, Feb. 22, 2012

Preface

As shown by the 2011 off the Pacific coast of Tohoku Earthquake, Asia-Pacific Region is an area with high risk of catastrophic natural disasters such as earthquakes and volcanic eruptions. Once a disaster occurs, in today's highly globalized economy, it can create unpredictable turmoil all over the world, not just in the affected area. These global-scale disasters are crucial for the sustainable development of the global economy to ensure human security. Japan is a country of plate convergence. Since the 1995 Hyogoken-Nanbu (Kobe) earthquake, extensive studies have been done in Japan, such as nation wide active fault surveys, development of high density seismograph networks and GPS crustal deformation monitoring system. Our knowledge on earthquakes is improved dramatically and observation and study results are systematically transferred to the society. However, it is fare to say that our understanding on earthquakes is still limited and farther studies should be done for the mitigation of seismic disasters. One of impediments to the development of geologic hazard studies is the infrequency of occurrence in a limited area. This makes it difficult to promote hypothesis and test processes. This may be solved by the international correlational study because geologic hazards are not less frequent phenomena any more. Now is the time to establish an effective international framework where we collaborate and develop a system to gather information on disaster mitigation in Asia-Pacific Region, including Japan.

Here are the purposes of the workshop. 1) To enhance collaboration among geological institutes within the Asian Circum-Pacific Region and rearrange existing information about the future risk for global earthquakes and volcanic disasters, 2) to build international and national networks, set up a website, and establish a consortium so that we can share and provide the information, 3) to create the environment to promote cooperative research, including personnel training, in the area with little information, especially in developing countries, and 4) to evaluate the risk of business activities in the Asia-Pacific region and seek to develop new business opportunities to provide information on the risk of catastrophic natural disasters. Through this full research of natural disasters, we can contribute to the society. Grasping disaster risk in advance enables us to reduce the damage from large-scale disasters, which are expected to cause worldwide impact on the economy. By improving the database for hazard risk information, we can assist international economic activities in formulating their BCP, and various private businesses concerning risk reduction, non life insurance.

Eikichi TSUKUDA

Program manager for the 1st Workshop of Asia-Pacific Region Global Earthquake and Volcanic Eruption Risk Management (G-EVER 1)

Director-General of the Geological Survey of Japan, AIST

G-EVER1 Program (22-25 Feb. 2011)

22 February (Wed)

9:00 - 10:00: Registration

Opening Session (10:00 - 10:15, Main Room, 2F)

Chairman: Yasuto Kuwahara (GSJ, AIST)
10:00 - 10:05: Welcome Address
Hirokazu Kato (AIST Fellow)
10:05 - 10:15: Opening Remarks
Eikichi Tsukuda (Director General of the Geological Survey of Japan, AIST)

Recent Earthquakes and Volcanic Eruptions (10:15 - 11:45, 13:00 – 15:00, Main Room, 2F)

Chairman: Akira Takada (GSJ, AIST)
10:15 - 10:45: The 1991 Eruption of Pinatubo Volcano, Philippines, and its Muddy Aftermath 1
Chris Newhall (Earth Observatory of Singapore)
10:45 - 11:15: The 2010-2011 Eruptions in Iceland: UK Impacts and Response 5
Sue Loughlin (BGS), Stephen Mobbs (Univ. of Leeds) and Steve Sparks (Univ. of Bristol)
11:15 - 11:45: The 2011 Eruption of Shinmoedake, Kirishima Volcano, Japan 7
Hiroshi Shinohara (GSJ, AIST)

Group Photo (11:45 - 12:00)

Lunch (12:00 - 13:00)

Chairman: Masataka Ando (Academia Sinica)
13:00 - 13:30: Earthquake and Tsunami Disaster Mitigation after the 2004 Indian Ocean and 2011 Tohoku Tsunamis 11
Kenji Satake (ERI, Tokyo Univ.)
13:30 - 14:00: Paleotsunami Study along the Pacific Coast of Tohoku, Japan 15
Yukinobu Okamura, Yuichi Namegaya, Yuki Sawai, Masanobu Shishikura (GSJ, AIST), Kenji Satake (ERI, Tokyo Univ.)
14:00 - 14:30: Strong Motion Observation System and Project Plan in China 17
Li Xiaojun (China Earthquake Administration)
14:30 - 15:00: Disaster Process after the 3.11 East Japan Earthquake and Tsunami Disaster 21
Norio Maki (DPRI, Kyoto Univ.)

15:00 - 15:20: Coffee Break

Report of Asia-Pacific Region, part 1 (15:20 - 17:20, Main Room, 2F)

Chairman: Takashi Azuma (GSJ, AIST)
15:20 - 15:40: The Earthquakes, Volcanic and Tsunami Risk Management on Kamchatka 25
Evgeny Gordeev (Inst. of Volcanology and Seismology, FEBRAS)
15:40 - 16:00: Earthquake, Tsunami and Volcano Information Issued by Japan Meteorological Agency and its Endeavor for Further Applicable Tsunami Information 27
Takeshi Koizumi (Japan Meteorological Agency)
16:00 - 16:20: Roles of Geodetic Methods on Volcanic Eruption Prediction 28
Makoto Murakami (Hokkaido Univ.)
16:20 - 16:40: 1952 Near Pyongyang, North Korean Earthquake and it's Tectonic Implication around the Region 29
Myung-Soon Jun (KIGAM) and Tae-Seob Kang (Pukyong National Univ.)
16:40 - 17:00: Seismic Hazard Assessment in Taiwan: Insights from Historical Seismicity and Radar Interferometry Analyses 31
Sin-Mei Ng (Chinese Culture Univ.)
17:00 - 17:20: Establishment of Taiwan Volcano Observatory at Tatun 32
Cheng-Horng Lin (Academia Sinica)

Welcome Dinner (18:00 - 20:00, Foyer, 1F)

23 February (Thu)

Report of Asia-Pacific Region, part 2 (8:30 - 11:40, Main Room, 2F)

Chairman: Motoo Ukawa (NIED)
8:30 - 8:50: Interviewing Insights Regarding the High Fatalities Inflicted by the Tohoku Earthquake 33
Masataka Ando (Academia Sinica), Mizuho Ishida (JAMSTEC), Yoshinari Hayashi (Kansai Univ.) and Chiharu Mizuki (Hokkaido Univ.)
8:50 - 9:10: Current Earthquake and Volcanic Risk Management Activities in the Philippines 35
Renato Solidum (PHIVOLCS)
9:10 - 9:30: Eathquake and Tsunami Hazard Assessment in Coastal Areas of Vietnam and Measures for a Seismic Risk Mitigation 37
Bui Cong Que and Nguyen Hong Phuong (VAST)
9:30 - 9:50: Application of a GIS for Earthquake Hazard Assessment and Risk Mitigation in Vietnam . 38
Nguyen Hong Phuong (VAST)

9:50 - 10:10: Coffee Break

Chairman: Yasuto Kuwahara (GSJ, AIST)
10:10 - 10:30: Earthquake Risk Management in Thailand; Current Status and Future Implication 39
Niran Chaimanee (CCOP)
10:30 - 10:50: Strategy on Volcano and Earthquake Hazards Mitigation in Indonesia 41

Surono (Center of Volcanology and Geological Hazard Mitigation)
10:50 - 11:05: Creating of Earthquake Hazard Map: an Effort to Mitigate Earthquake Disaster (Case study: Sulawesi Island Earthquake Hazard Map) 42
Sri Hidayati, Athanasius Cipta and Rahayu Robiana (Center of Volcanology and Geological Hazard Mitigation)
11:05 -11:20: Vulnerability, Capacity and Community Empowerment in Hazard Zone Areas, a Challenge in Hazard Mitigation in Indonesia 46
Supriyati Andreastuti (Center of Volcanology and Geological Hazard Mitigation)
11:20 - 11:40: Geoscience as a Component of an All-of-Government Approach to Recovery from the Canterbury Earthquake Sequence of 2010-2011 47
Kelvin Berryman (GNS Science)

Lunch (11:40 - 13:00)

Database and risk management (13:00 - 17:20, Main Room, 2F)

Chairman: Shinji Takarada (GSJ, AIST)

13:00 - 13:20: VHub – a Virtual Community and Cyberinfrastructure for Collaboration in Volcano Research and Risk Mitigation 48
Greg Valentine (State Univ. of New York)
13:20 - 13:40: Growth of International Collaboration in Monitoring Volcanic Ash Eruptions in the North Pacific 50
John Eichelberger and Christina Neal (USGS)
13:40 - 14:00: EOS Activities toward Volcanic Risk Mitigation 54
Chris Newhall (Earth Observatory of Singapore)
14:00 - 14:20: Recent Volcanic Crises in the USA and Europe: Some Case Studies 56
Bruce F. Houghton (Hawaii Univ.), R.J. Carey (Univ. of Tasmania), C.A. Gardnerc, C.A. Neald (USGS), and T. Thordarson (Univ. of Edinburgh)
14:20 - 14:40: VOGRIPA and the 'Global Volcano Model' 60
Steve Sparks, Sian Crosweler (Univ. of Bristol), Sue Loughlin (BGS), Lee Siebert, Paul Kimberly (Smithonian Institution), Natalie Ortiz, Laura Hobbs (Univ. of South Florida), Koji Kiyosugi and Shinji Takarada (GSJ, AIST)
14:40 - 15:00: The Role of Multidisciplinary Research and Collaboration for Improving the Resilience of Communities to Volcanic Rrisk 62
David Johnston, Graham Leonard, Emma Doyle, Julia Becker (GNS Science), Douglas Paton (Univ. of Tasmania), Kevin Ronan (Central Queensland Univ.), Bruce Houghton (Univ. of Hawai), Chris Gregg (East Tennessee State Univ.), Shane Cronin (Massey Univ.), Tom Wilson (Univ. of Canterbury), Carol Stewart (GNS Science), Jan Lindsay (Univ. of Auckland), Gill Jolly, Sally Grant (GNS Science), and Victoria Sword-Daniels (Univ. College London)

15:00 - 16:00: Coffee Break **[Poster session core time]**

Chairman: Naoji Koizumi (GSJ, AIST)
16:00 - 16:20: Public Release of Estimated Impact-based Alerts for Global Earthquakes using the U.S. Geological Survey's PAGER System 66
David J. Wald, Kishor S. Jaiswal, K. D. Marano (USGS), and D. Bausch (Federal Emergency Management Agency)
16:20 - 16:40: Extreme Seismic Hazards and Societal Implication 70
Alik Ismail-Zadeh (Russian Academy of Science)
16:40 - 17:00: The Global Earthquake Model: Building an Open Source Seismic Risk Model for the World 72
Ross Stein (USGS)
17:00 - 17:20: The IISEE Earthquake Catalog, "Catalog of Damaging Earthquakes in the World", "IISEE-NET", and BRI Strong Motion Observation 74
Tatsuhiko Hara (Building Research Institute)
17:20 - 17:40: GEO Grid Disaster Response Applications and its Activity for the 2011 Tohoku, Japan Earthquake and Tsunami 78
Masashi Matsuoka (GSJ, AIST), Naotaka Yamamoto, Hirokazu Yamamoto, Ryosuke Nakamura, Kazuki Nakamura, Shinsuke Kodama, Yuko Takeyama, Koki Iwao, Akihide Kamei, Sarawut Ninsawat, Satoshi Tsuchida (ITRI, AIST), Minoru Urai (GSJ, AIST), Isao Kojima, Yoshio Tanaka, and Satoshi Sekiguchi (ITRI, AIST)
17:40 - 18:00: National Seismic Hazard Maps for Japan and Seismic Hazard Assessment after the 2011 Tohoku-oki Earthquake 82
Hiroyuki Fujiwara (NIED)

24 February (Fri)

Group Discussion (9:00 - 10:30, 2F Main room, Middle Room, 1F)

- Database section (Chairmen: Chris Newhall and Yuzo Ishikawa)
- Risk assessment-management section (Chairmen: Ross Stein and John Eichelberger)

10:30 - 11:00: Coffee Break

General Discussion (11:00 - 12:00, Main Room, 2F)

Chairman: Toshitsugu Fujii (Crisis & Env. Management Policy Inst.), Yuzo Ishikawa (GSJ, AIST)
Comment: Shigeo Aramaki (Yamanashi Inst. of Environmental Sci.)

Summary and Ending Remarks: Eikichi Tsukuda (GSJ, AIST)

Poster Session: 10:00, 22 February to 12:00, 24 February
Core Time: 15:00-16:00, 23 March at Foyer, First Floor

P 1 Web Computing Service (WCS) for Detecting Land Cover Change Caused by Volcanic Eruptions Using Web Map Service (WMS), Frequency Based Change Detection Algorithm and PALSAR 84
Joel Bandibas, Daisake Kawabata, Minoru Urai, Asep Saepuloh, Koji Wakita (GSJ, AIST)

P 2 National Seismic Hazard Maps for Japan and Seismic Hazard Assessment after the 2011 Tohoku-oki Earthquake 88
Toshikazu Yoshioka, Fujika Miyamoto (GSJ, AIST)

P 3 Active Fault Database of Japan: Gathering and Spreading Active Fault Data for Earthquake Risk Management 90
Minoru Urai (GSJ, AIST)

P 4 ASTER Image Database for Volcanoes 92
Kuniaki Nishiki, Shun Nakano, Tatsuyuki Ueno, Jun'ichi Itoh, Isoji Miyagi (GSJ, AIST)

P 5 The Geological Database of Quaternary Volcanoes in Japan 93
Hiroaki Takahashi, Mitsuhiro Nakagawa, Yuichiro Tanioka (Hokkaido Univ.), Evgeny Gordeev (Inst. of Volcanology and Seismology, FEBRAS), Alexander Khanchuk (Far Eastern Geological Inst., FEBRAS), Victor Bykov (Inst. of Tectonics and Geophysics, FEBRAS), Boris Levin (Inst. of Marine Geology and Geophysics, FEBRAS), Mikhail Gerasimenko (Inst. of Applied Mathematics, FEBRAS), Nikolay Schestakov (Far Eastern National Univ.), Alexey Malovichko (Geophysical Survey Headquarter), Victor Chebrov (Inst. of Applied Mathematics), Yury Levin (Far Eastern National Univ.), Larisa Gunbin (Geophysical Survey headquarter)

P 6 Japan-Russia Scientific Research Activities for Earthquake, Tsunami and volcanic Disaster Mitigation in Northwestern Pacific Region 95
Shinji Takarada (GSJ, AIST), Shinsuke Kodama (ITRI, AIST), Takahiro Yamamoto, Minoru Urai (GSJ, AIST)

P 7 GEO Grid Volcanic Gravity Flow Simulation System for the Next-generation Real-time Hazard Mapping: an Application to the Recent 2011 Eruption at Shinmoedake, Kirishima Volcano, Japan 99
Tomokazu Kobayashi, Mikio Tobita, Takuya Nishimura, Shinzaburo Ozawa, Hisashi Suito, Tetsuro Imakiire (GSI)

P 8 GPS- and InSAR-derived Crustal Deformation and Estimated Fault Models of the 2011 Tohoku Earthquake and the Induced Inland Earthquakes 103
Tomokazu Kobayashi, Mikio Tobita (Geospatial Information Authority)

P 9 Seismic Gap and a Series of Large Earthquakes along the Sunda Trench and the Sumatran Fault 105
Asep Saepuloh, Minoru Urai (GSJ, AIST)

P 10 Characterizing Pyroclastic Flow Deposits of a Large Eruption of Mt. Merapi in 2010 using ALOS/PALSAR and ASTER data 109
Observation Network of Groundwater and Crustal Deformation for Forecasting the Tokai, Tonankai and Nankai Earthquakes

Norio Matsumoto, Naoji Koizumi (GSJ, AIST)

P 11 Long-term Variation of Pre-Caldera Volcanic Activity in Bali and in Tengger Caldera Region, East Java 110
Kiyoshi Toshida, Shingo Takeuchi (Central Research Institute of Electric Power Industry), Ryuta Furukawa, Akira Takada (GSJ, AIST), Supriyati Andreastuti, Nugraha Kartadinata, Anjar Heriwaseso, Oktory Prambada, A. Rosgandika Mulyana, Asep Nursurim (Center for Volcanology and Geological Hazard Mitigation)

P 12 Explosive Eruptions Associated with Batur and Bratan Calderas, Bali, Indonesia 114
Ryuta Furukawa, Akira Takada (GSJ, AIST), Kiyoshi Toshida (CRIEPI), Supriyati Andreastuti, Eka Kadarsetia, Nugraha Kartadinata, Anjar Heriwaseso, Oktory Prambada, Yudi Wahyudi, Nizar Firmansyah (CVGHM)

P 13 Development of Risk Assessment Simulation Tool for Optimal Control of a Low Probability - High Consequence Disaster 116
Hiroki Yotsumoto, Kikuo Yoshida, Hiroshi Genchi, Kiyotaka Tahara, Kiyotaka Tsunemi, Hideo Kajihara, Yuji Wada, Ryoji Makino, Kazuya Inoue (RISS, AIST), Yukinobu Okumura, Yasuto Kuwahara, Haruo Horikawa, Masayuki Yoshimi, Yuichi Namegaya (GSJ, AIST)

P 14 Geological Evaluation of Frequency and Process of Caldera-forming Eruption: A Compiled Study of Indonesian Caldera Volcanoes 119
Akira Takada, Ryuta Furukawa (GSJ, AIST), Kiyoshi Toshida (CRIEPI), Supriyati Andreastuti, Nugraha Kartadinata (CVGHM)

P 15 On the Prediction of Scaling Relationships Governing the Runouts of Short-lived Fluidized Granular Flows 122
Laurence Girolami (Université Blaise Pascal, GSJ, AIST), T.H. Druitt, O. Roche (Université Blaise Pascal)

P 16 The Observation with Remote GNSS Monitoring System 124
Eiichirou Harima (GSI)

P 17 To Monitor the Baegdusan Volcano before the Next Magmatic Eruption 125
Aurélien Dupont, Sung-Hyo Yun (Pusan National University)

P 18 The Impacts on Structures by Volcanic Eruption– a Case Study of the 1990-1995 Eruption on Unzen Volcano, Japan 128
Daisuke Nagai (Mt. Unzen Disaster Memorial Hall)

P 19 Re-evaluation of Mw of the 1707 Hoei Earthquake 129
Yuzo Ishikawa (GSJ, AIST)

P 20 Long-term and Short-term Volcanic Risk Assessment Based on New Geologic Maps of Tokachidake and Tarumae Volcanoes, Northern Japan 130
Yoshihiro Ishizuka, Ryuta Furukawa (GSJ, AIST)

P 21 How Many Explosive Eruptions are Missing from the Geologic Record? Analysis of the Quaternary Record of Large Magnitude Explosive Eruptions in Japan 132
Koji Kiyosugi, C.B. Connor (Univ. of South Florida), R. S. J. Sparks, H. S. Crosweller (Univ. of Bristol), L. Siebert (Smithonian Institute), S. Takarada (GSJ, AIST)

P 22 Electric Power Failures in the 2011 off the Pacific Coast of Tohoku Earthquake 136

Gaku Shoji, Dai Takahashi (Tsukuba Univ.)

P 23 Design for Hybrid Database System for Volcanological Research and Outreach Program on Eruptive History 140

Mitsuru Okuno, Naoyuki Tsuruta (Fukuoka Univ.), Yukihisa Nishizono (Fukuoka Univ., West Japan Engineering Consultations Inc.), Masayuki Torii (Kumamoto Gakuen Univ.), Hirohito Inakura (West Japan Engineering Consultations Inc.), Tetsuo Kobayashi (Fukuoka Univ., Kagoshima Univ.), Members of the International Research Center for Eruptive History and Informatics

Field Excursion

<24 Feb. (Fri)>

13:15 Departure from AIST

move to the accommodation in Gotemba City (“Toki-no-sumika”)

<25 Feb. (Sat)>

1) Mt. Fuji and its productions

*the Hoei crater of Mt. Fuji

*the Gotemba volcanic debris avalanche

*the Mishima lava

2) Defense against Tsunami

*artificial barrier along the Suruga Bay

3) Active tectonics in the northern Izu Peninsula

*Tanna fault

* View from the Jukkoku Pass (cable car)

ca. 19:00 Arrival at AIST

Oral Session

Main Room (Second Floor)

The 1991 eruption of Pinatubo Volcano, Philippines, and its muddy aftermath

C.G. Newhall

Earth Observatory of Singapore, Nanyang Technological Univ., 50 Nanyang Ave, N2-01a-10, Singapore 639798

For the first time, modern monitoring captured the pre-, syn-, and post-eruption signatures of a sulfur-rich, plinian, caldera-forming eruption. Deposits of past eruptions told that a giant eruption was possible; however, no one knew exactly what precursors to expect.

The eruption began with a tiny steam-blast explosion on April 2, 1991, growth of a lava dome from June 7-12, 1991, and a series of sixteen moderate size explosive events from June 12-June 15. The climactic eruption occurred on June 15, 1991, lasted 3.5 hours, and produced about 5 km^3 of magma. The products, frothy pumice and ash with a bulk volume of about 10 km^3, were spread on the slopes of the volcano and across the South China Sea. A new 2.5-km-diameter caldera was formed at the summit of the volcano, which later filled with a lake.

A number of new concepts arose, and some others, previously suspected, were resoundingly confirmed by study of this eruption. In order of occurrence, these include:

- The M 7.8 Luzon earthquake of July 16, 1990, 100 km NE of Pinatubo, apparently started a chain of events that led to Pinatubo's large eruption in June 1991. A plausible but admittedly unproven mechanism is that movement of crust during the earthquake increased compression in the Pinatubo area by ~1 bar and squeezed basalt magma up from depth (see Bautista et al, 1996). Contrary to a widespread belief among the indigenous Aeta people, geothermal drilling in 1988-1990 did not cause the eruption; rather, the eruption was more likely a delayed response to the 1990 earthquake.

- A modest volume of basalt intruded a ~100 km^3 body of residual, viscous, crystal-rich dacite magma 8-12 km beneath the volcano. Mixing of the two began at least 30-45 days before magma was erupted, perhaps around the time of opening steam blasts in early April 1991. Mixing continued for weeks, some <1 week before eruption. Mixing of magmas was widely known before Pinatubo. From Pinatubo, its timeframe is unusually well constrained, by experimental work on mineral disequilibria of the Pinatubo rocks and by records of deep long-period (magmatic) earthquakes ~35 km deep in early June, late May, and perhaps earlier. (see papers by White 1996 on deep earthquakes; Mori et al 1996 on the large preeruption dacite reservoir; and Pallister et al 1996; Rutherford and Devine 1996; and M. Coombs, pers. commun.)

- Many of the early precursory earthquakes were 5 km northwest of Pinatubo, rather than directly beneath the volcano. Similar patterns have now been recognized at many volcanoes, and probably reflect complex interaction between magma intrusions, regional tectonics, and hydrothermal systems. R. White refers to these as distal VT earthquakes and they should be seen as the effects of intrusions but not the loci of those intrusions.

- Precursors began as early as mid-March but until early June, Pinatubo's geologic past was the main reason to suspect that a large eruption was pending. Strong magma-related long-period earthquakes didn't begin in the shallow crust until after the mixture of basalt and dacite had already formed a lava dome and moderately large explosive eruptions began on June 12, 1991 (see Harlow et al 1996; Power et al 1996)

- There may have been a significant expulsion of acidic groundwater from Pinatubo, because water samples collected on April 8-10, 1.5 km downstream from a known thermal area, had pH 2.45 vs. a baseline pH of 7.6-8.0. All fish had been killed in two river systems draining the north side of Pinatubo (Sabit et al 1996). Similar expulsions of groundwater have

occurred at Matsushiro, Japan and at Huila, Colombia, and the most likely explanation is volumetric compression of the shallow crust.

- Pinatubo's eruption was unusually powerful because the volcano had been dormant for ~500 years and had apparently trapped incoming carbon dioxide, water, sulfur dioxide, and other magmatic gases so effectively that these volatiles saturated the melt and then formed a discrete phase of volatile bubbles. Evidence for this accumulation came from discovery of 17 Mt of SO_2 by the Total Ozone Mapping Spectrometer (TOMS) on the Nimbus satellite, many times more than could have been dissolved in the magma that was erupted. It now appears that many magmas are saturated with carbon dioxide and water and contain excess volatiles as bubbles, even deep beneath volcanoes. High volatile contents make them more prone to disturbance by fresh influx of magma from below, and more prone to explosive eruption. (see papers by Wallace and Gerlach 1994; Gerlach et al 1996; Wallace 2001).

- The eruption column of the climactic eruption seems to have simultaneously fed high-energy pyroclastic surges and a tephra fall layer from its upper reaches and more voluminous but shorter pyroclastic flows from a lower source that might have spilled over the rim of the developing crater. The latter built large pyroclastic fans, and slumps from the growing fans formed deposit-derived ("secondary") pyroclastic flows that reached to approximately the same distances (~15 km) as the high-energy pyroclastic surges

.

- The climactic eruption was recorded seismically around the world as very long period Rayleigh waves with frequencies of 3.68 and 4.44 mHz. These reflected coupling of atmospheric resonance from the huge eruption cloud back into the solid earth (Kanamori and Mori 1992; Zürn and Widmer 1996; Tahira et al 1996)

- The large release of SO_2 during the eruption spread throughout the stratosphere, was a welcome tracer for many atmospheric studies, and lowered average global surface temperature by 0.5^{o}C for about 2 years.

Areas at risk from pyroclastic flows were successfully forecast, but just barely. A hazard map was drawn hastily from air photos and from spot checking by geologists on the ground. Stacked by the side of roads, sacks of pumice for stone-washed jeans were a quick tip-off to nearby excavations in pyroclastic flow deposits. Radiocarbon ages were approximated even before gamma counting was complete. The hazard map was drawn to represent a worst-case scenario but, in retrospect, we learned that the worst case was much worse. Fortunately, the 1991 eruption turned out to be relatively small for Pinatubo. Appearance of the small lava dome on June 7 rather than a plinian eruption made us worry briefly that no explosive phase would follow, but still-escalating seismicity and SO_2 argued that the dome was simply the degassed tip of otherwise gas-rich magma and that explosions would follow.

The date of eruption was also successfully forecast, also just barely. A simple alert scheme was adopted in mid-May. COSPEC measurements started at that time indicated that magma was involved (alert level 2). The seismic network was completed by the end of May. Alert level 3 (eruption possible within 2 weeks) was raised on June 5, alert level 4 (eruption possible within 24 hours) was raised on June 7, and alert level 5 (explosive eruption in progress) was raised on June 9. In fact, that on June 9 was based on mistaken identification of a billowing ash cloud that looked very much like a pyroclastic flow but was actually cold, but this very understandable mistake turned out to be a blessing in disguise because many people were waiting for the highest alert level before they would evacuate. A lava dome began to extrude on June 7, Clark Air Base was evacuated on June 10, the first large explosive eruptions began on June 12, and the climactic eruption occurred on June 15. We were lucky that magma ascent progressed to eruption without major interruption.

Pyroclastic flows from the eruption completely devastated an area of about 400 km^2 around the volcano. Fortunately, all but about 100 of the indigenous Aeta residents of this area had evacuated before the climactic phase of the eruption. Ashfall from the eruption caused many roofs to collapse, especially because rain from Typhoon Yunya made the ash much heavier that it would otherwise have been. About 100 persons died from pyroclastic flows inside the evacuated areas; about 300 persons

died under outside the evacuated areas from collapsed roofs. Sadly, about 500 Aeta children died from measles in evacuation camps. About 85,000 people were evacuated from the most dangerous areas before the climactic eruption, and at least 10,000 of these people were saved from certain death by such evacuations.

Ash from the June 15 eruption, including a large component of fine-grained co-ignimbrite ash, was encountered by 13 flights, and many other flights were grounded by the ash (Casadevall et al 1996). Most of these encounters occurred far downwind from Pinatubo and none caused a near-crash. However, coming as they did just before the long-scheduled 1st International Symposium on Volcanic Ash and Aviation Safety in Seattle (July 1991), they helped catalyze development of the worldwide network of Volcanic Ash Advisory Centers (VAAC's).

Renewed seismicity in July 1992 led to concern about more explosive eruptions. However, the fresh intrusion of basalt into the now-degassed dacite reservoir was unable to do more than mix and extrude gently, albeit with much seismicity. This and subsequent seismic quiet and diminishing CO_2 gas (see below) leads to some assurance – though not 100% -- that Pinatubo will sleep again for an extended period.

Lahars began during the eruption and continued for roughly a decade thereafter.

- More than half of the debris on Pinatubo's slopes was washed by rain-induced lahars and sediment-laden streamflow into the surrounding lowlands, adding to Pinatubo's broad alluvial fans. Villages and towns were buried by up to 10 m of sediment. Thresholds for lahar formation dropped dramatically as a result of fine ash on the surface that prevented infiltration of rainfall. Early on, as little as 10 mm of rain in 30 min was sufficient to trigger lahars. Sediment yields in the first few years broke previous world records by 1-2 orders of magnitude and as of 2000 were still close to the levels of previous records (see Janda et al 1996; Hayes et al 2001). Many scales of sabo works were attempted. In the end, progressively larger and larger works were built as lahar volumes decreased and the two matched each other by about 1996. In terms of economic losses and human displacements, post-eruption hydrologic hazards exceeded those of the eruption itself. As was true also for the eruption, citizens, engineers, and officials had difficulty imagining the large scale of the hazard that they faced.

- In a fascinating and worrisome paradox, surface water of the caldera lake in mid-2000 was 30^oC while that at 60-m depth it was $\geq 70^oC$! Salinity and suspended sediment differences were wholly inadequate to explain how such a temperature inversion could persist. The lake overturned soon thereafter. Apparently, CO_2 bubbles in the water column had stabilized hot water at depth through the early history of the lake until late 2000 or earliest 2001, by which time CO_2 flux had diminished enough to allow lake overturn and mixing. (By November 2010, CO_2 flux had decreased further and the lake remained thoroughly mixed, per study by F. Schwandner, B. Christenson, MC Arpa, and the author).

- By August 2000, the new caldera lake had a volume of nearly 200×10^6 m^3, was rising more than 12 m/y, and had approximately 14 m of freeboard remaining. By September 2001 the caldera lake was nearly ready to spill through a notch in the crater rim. Although there was initially debate about whether the uppermost part of the notch was stable, all eventually concluded that it could be eroded. Approximately 20 m thickness of loose material in the notch would have been eroded rapidly, releasing a large flood. A plan was made to trench down to water level and intentionally induce scouring removal of all of the loose material in the dam. The downstream town of Botolan would be evacuated on the morning on which the last plug would be removed, the flood would pass with risk only to property, and, assuming that Botolan was not destroyed, residents could return home in the evening. A 5-meter deep trench was dug, all by hand and with a small water pump, the town was evacuated, and plug was removed. Unfortunately, conservative engineers had changed the plan to a non-scouring gradient so no scouring occurred. However, in the next typhoon (July 2002) water level rose quickly, scoured out 23 m of the dam, and generated a large lahar that

narrowly missed destroying Botolan (Bornas et al., 2003). The trenching certainly helped save Botolan.

- A lingering legacy of the lahars and sediment is that many river channels surrounding Pinatubo remain clogged. As a result, flooding continues, as in Botolan in 2009 and in San Fernando almost every year.

Official and public response to the eruption and subsequent lahars at Pinatubo was generally very constructive. There was a close partnership between scientists, engineers, civil and military authorities, the news media, and the public. Some responses were controversial and some skepticism was voiced, to be sure, but in the broad picture, what needed to be done was done. In such crises, scientists must have the courage to outline even worst-case scenarios and, at the same time, the wisdom to put those in proper context with smaller events. To keep people safe, scientists must also accept the risk of giving false alarms. For their part, public officials must be willing to act quickly on the scientists' concerns. And both the public officials and the general public must understand and be willing to accept uncertainties and the risk of false alarms. All must act as a team. Much credit for that team is owed to the late Dr. Ray Punongbayan of PHIVOLCS. Teamwork saved >10,000 lives and averted > USD 0.5 billion of property damage and other economic disruption. Costs incurred to mitigate deaths from the eruption were a few million USD; costs to mitigate the lahar hazard was roughly USD 1 billion.

At least 400 earth scientists seized scientific opportunities presented by Pinatubo. Among these were at least 30-40 graduate students who are now (or will soon be) new leaders in volcanology and related fields. The same holds true in atmospheric sciences. Pinatubo was a signal event for our sciences and we were privileged to participate.

References

All cited 1996 papers are in:

Newhall, C.G. and Punongbayan, R.S., eds., 1996, Fire and Mud, Eruptions and Lahars of Pinatubo Volcano, Philippines. PHIVOLCS and Univ. of Washington Press. 1126 pp. Full-text online at http://pubs.usgs.gov/pinatubo.

Other references:

Bornas M.A. and PHIVOLCS Quick Response Team, 2003 Evaluation, proposed solution & current status of the crater lake breakout problem, Mount Pinatubo, Philippines. Poster at IUGG, Sapporo.

Hayes S.K., Montgomery D.R., Newhall C.G., 2002, Fluvial sediment transport and deposition following the 1991 eruption of Mount Pinatubo, Philippines: Geomorphology, v. 45, p. 211-224.

Kanamori, H., Mori, J., Harmonic excitation of mantle Rayleigh waves by the 1991 eruption of Mount Pinatubo, Philippines, Geophys. Res. Lett., 19, 721-724, 1992.

Newhall, C.G., Power, J.A., and Punongbayan, R.S., 2002, Pinatubo: "to make grow:" Science, v. 295, 1241-1242.

Wallace, P.J., 2001, Volcanic SO2 emission and the abundance and distribution of exsolved gas in magma bodies. J. Volcanol. Geotherm. Res. 108, 85-106.

Wallace, P., Gerlach, T.M., 1994, Magmatic vapor source for sulfur dioxide released during volcanic eruptions: Evidence from Mount Pinatubo, Science, 265, 497-499

The 2010-11 eruptions in Iceland: UK impacts and response

Sue Loughlin[a], Stephen Mobbs[b]; Steve Sparks[c]

[a]*British Geological Survey, West Mains Road, Edinburgh, EH9 3LA, UK*
[b]*National Centre for Atmospheric Science School of Earth and Environment, University of Leeds, Leeds LS2 9JT, UK*
[c]*Dept. of Earth Sciences, University of Bristol, Wills Memorial Building, Queen's Road, Bristol, BS8 1RJ, UK*

The regulatory response to the subglacial eruption at Eyjafjalljökull volcano on the Eastern Volcanic Zone in southern Iceland in April 2010 resulted in major economic impacts and significant disruption to air passengers. The total global economic losses caused by the crisis amount to $5 billion in lost GDP [1]. The regulations were quickly modified by the UK Civil Aviation Authority in discussion with regulators, airlines and jet engine manufacturers to allow flying at predicted low ash concentrations. The International Civil Aviation Authority (ICAO) are now working at long term recommendations and procedures for dealing with volcanic ash [e.g. 2]. Predicted ash concentrations from eruptions in Iceland are based on dispersion models run by the London Volcanic Ash Advisory Centre (UK Meteorological Office). Real-time data and observations of key parameters (plume height, eruption rate, particle size distribution) and characteristics of the dispersing ash/gas cloud are needed for the model. If data is not available, assumptions are made about source parameters in particular, based on empirical evidence and past events [e.g. 3]. Improved acquisition and assimilation of satellite, airborne and ground-based observations and data would enhance the forecasting procedure [e.g 4].

The UK government was not prepared in 2010 for the impacts of volcanic eruptions on the UK. A Scientific Advisory Group in Emergencies was tasked by government to discuss a range of critical issues. Volcanoes are now in the UK National Risk Register, valuable interdisciplinary networks have been built-up, relevant research is being carried out and the UK government Civil Contingencies Secretariat is taking a proactive role in preparing for future eruptions in Iceland and elsewhere. Strong links between the UK and Iceland in both research and operations have been enhanced in the last two years, supported by an MoU.

A NERC-funded multi-disciplinary project is underway to develop numerical models that more-accurately represent the dynamics of weak plumes, it aims to better characterise volcanic ash for remote sensing retrievals and is developing improved ground-based and airborne monitoring

techniques for future eruptions. Many other projects are also underway.

A great deal of research and development is required, in particular bringing together volcanologists, atmospheric scientists, meteorologists and engineers in order to deal with the scientific and operational challenges. One of the key challenges to the scientific community is to find novel ways to support decision-making in the face of considerable uncertainty.

References

[1] Oxford Economics, The Economic Impacts of Air Travel restrictions Due to Volcanic Ash, A report prepared for Airbus. 2010.
http://www.oef.com/free/pdfs/volcanicupdate.pdf

[2] EUR DOC 019 - Volcanic Ash Contingency Plan EUR and NAT Regions (2nd Edition)
http://www.paris.icao.int/documents_open/show_file.php?id=334

[3] Witham, C. S., Hort, M. C., Potts, R., Sevranckx, R., Husson, P., and Bonnardot, F. 2007. Comparison of VAAC atmospheric dispersion models using the 1 November 2004 Grimsvotn eruption. Meteorological Applications, 14, 27-38.

[4] Bonadonna, C., Folch, A., Loughlin, S. And Puempel, H. 2011. Bulletin of Volcanology, 74, 1-10.

The 2011 eruption of Shinmoedake, Kirishima volcano, Japan

Hiroshi Shinohara

[a]*Institute of Geology and Geoinformation, Geological Survey of Japan, AIST, 1-1-1 Higashi, Tsukuba, Ibaraki 305-8567, Japan*

Kirishima volcano is a composite volcano with more than 20 small volcanoes within 20x30 km area, in southern Kyushu, SW Japan. Historic eruption of the volcanoe occurred at Ohachi, Iwoyama and Shimoedake volcanoes, which locate within a few km distance (Imura and Kobayashi, 2001), and the current eruption occurred at the Shinmoedake volcano where significant magmatic eruptions was not observed for about 300 years. The 2011 eruptive activity started with a small phreato-magmatic eruption on 19th Jan. and followed by the sub-Plinian eruptions occurred on 26th - 27th Jan. The sub-Plinian eruption column reached about 7 km above the volcano and ejected about 3x10^{7} tons of pyroclasts (Furukawa et al., 2011). Immediately after the explosive eruptions, lava extrusion started and filled the summit crater within a few days with lava volume of 2x10^{7} m^{3} (Miyagi, 2011). Then intermittent Vulcanian eruptions occurred in the summit crater filled with lavas. Intensity and frequency of Vulcanican

Fig. 1 Sub-Plinian eruption of Shinmoedake, Kirishima volcano

Fig. 2 Summit crater of Shinmoedake filled with lava (Feb. 3, 2001, photo by Y. Kawanabe).

eruptions were large in February and March but decreased with time. Most recent eruption occurred at the end of August but significant volcanic gas emission still continues (JMA, Monthly Report).

The 2011 eruptive activity was preceded by several small scale phreatic- phreatomagmatic eruption occurred in 2008 and 2011. GPS monitoring by Geospatial information authority in Japan (GIS) and other institutes showed that continuous inflation of the volcano was stared in January 2010 at inflation source depth of 6 km and is considered as a long-term precursory phenomenon of the January 2011 eruption. In contrast, significant increase of seismic activity nor ground deformation was not observed just before the January 19 and 26 eruptions. One of the significant precursory phenomenon of the sub-Plinian eruption was ejection of pumiceous ash by the January 19th eruption in spite of the small scale (Fig. 3). Such pumiceous ash was not observed in the ejecta by the small scale eruptions in 2008. Therefore, the January 19th eruption is not phreatic eruption activated by magma but

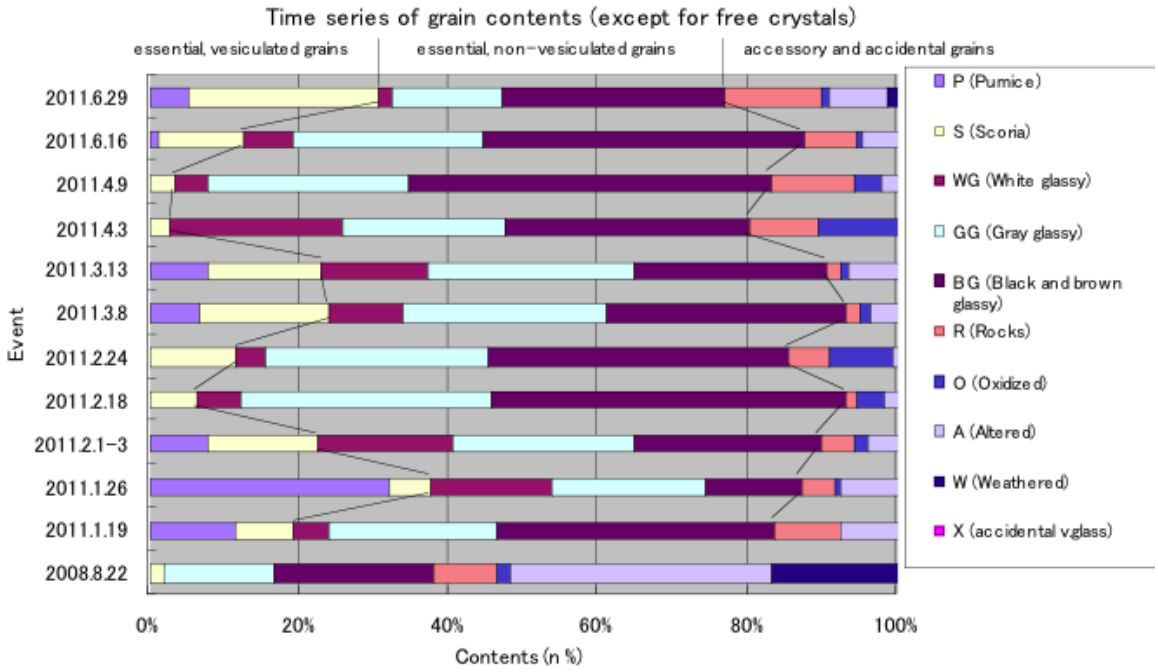

Fig. 3 Variation of ash composition of Shinmoedake ash samples in terms of grain types (Ooishi et al., 2011).

the eruption directly caused by magma ascent.

Geological Survey of Japan is measuring volcanic ash constituents to monitor variation of the eruptive activity (Fig. 3; Ooishi et al., 2011). The ashes consist of various grains including vesicular pumice and scoria grains, dense-blocky glass fragments, lithic fragments, crystals and altered fragments. Proportion of each grain type varies with change of eruptive style and intensity. It is quite

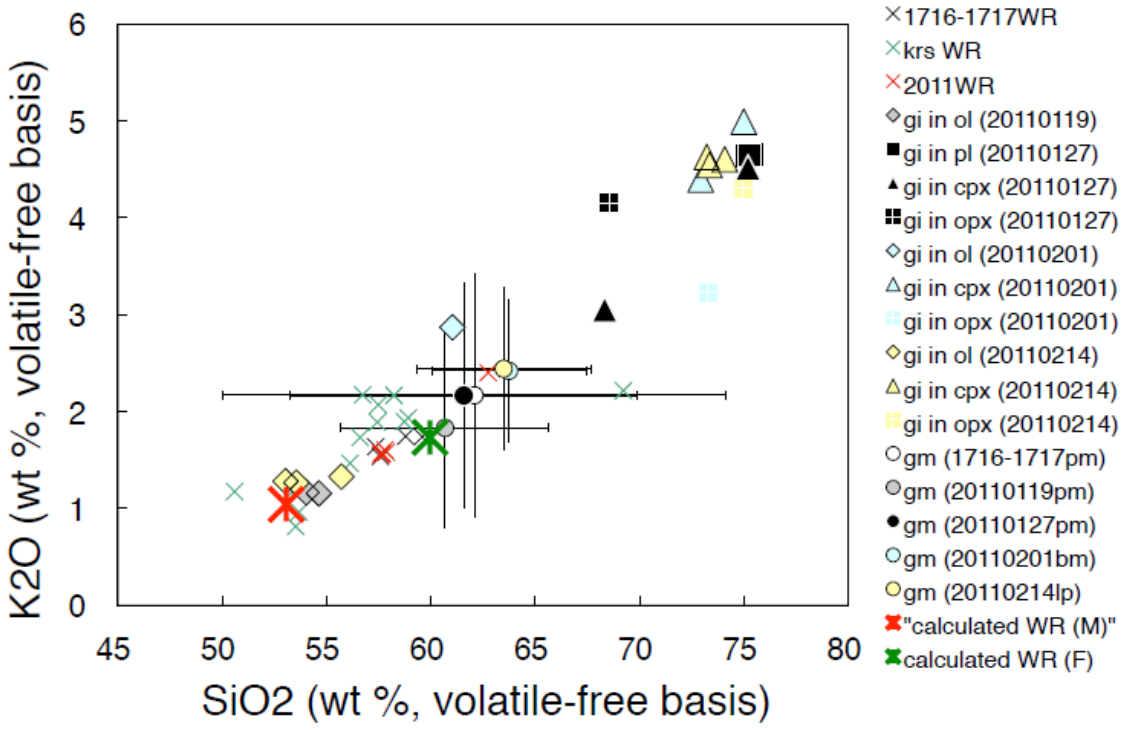

Fig. 4 Composition of whole rock, melt inclusion glass and groundmass. (Saito et al., 2011)

natural to observe a large percentage of pumice grains in the January 26th eruption, but similar pumice grains were observed also in ashes ejected by Vulcanian eruptions. This observation suggests that the Vulcanian eruptions are caused by the magma accumulated in the summit crater, but are caused by newly ascended magma. This idea is consistent with observation of continuous volcanic gas emission with SO_2 flux more than 100 t/d (JMA Monthly Report).

The 2011 magma is mainly andesite with SiO_2=57 wt.% with minor amount of dacite with SiO_2=62 wt.% (Fig. 4). These magma compositions are similar with those of magmas erupted by the latest magmatic eruption at Shinmoedake in 1746-1717. Composition and chemical zoning of phenocrysts and melt inclusions indicate that the erupted magma was formed by magma mixing (Saito et al., 2011). Phase equilibrium and mass balance calculated with MELTS program revealed that the erupted magma was created by intrusion of basaltic magma to highly crystallized andesitic magma chamber (Miyagi et al., 2011). The large ranges of melt inclusion composition from basaltic to rhyolitic melt agrees with the mixing model. The mixing model indicates that the erupted magma is a mixture the basalt and andesite mush with 1:2 proportion.

The time-scale after the magma-mixing to eruption was estimated based on Mg concentration zoning of magnetite phenocrysts (Tomiya et al., 2011). At least two different time-scale mixing were estimated; 1) mixing more than 30 days before, and 2) mixing within several days. The first type is likely created by continuous injection of basaltic magmas to the andesite mush and the second type mixing may corresponds the mixing event triggered the eruption. The Mg-zoning became smaller in the ejecta of February eruptions, indicating that the Vulcanian eruptions were caused by the magma mixed in January.

References

Imura, R., and Kobayashi, T. 2001. Geological map of Kirishima volcano. Geological Map of Volcanoes 11, Geol. Surv. Japan, (in Japanese with English abstract).

Earthquake and Tsunami Disaster Mitigation after the 2004 Indian Ocean and 2011 Tohoku Tsunamis

Kenji Satake

Earthquake Research Institute, the University of Tokyo, 1-1-1 Yayoi, Bunkyo-ku, Tokyo 113-0032 Japan

Introduction

The 2004 Sumatra-Andaman earthquake (M 9.1) generated the Indian Ocean tsunami, which is the worst tsunami disaster in human history with the total casualties of more than 230,000. The 2011 Tohoku earthquake (M 9.0) also generated one of the devastating tsunamis in Japan, with casualties near 20,000. While the countries around the Indian Ocean were not prepared for such giant earthquakes and tsunamis before 2004, Japan was equipped with long-term forecast of great earthquakes and the most developed tsunami warning and mitigation systems. Because gigantic (M~9) earthquakes occur infrequently, and not historically recorded in Indian Ocean and around Japan, both the 2004 and 2011 earthquake surprised not only general public but also many seismologists. Paleoseismological studies in recent years, however, indicated that similar earthquakes occurred in the past in both regions. I will review recent developments in coastal paleoseismology and tsunami warning/mitigation system.

Long-term Forecast of Great Earthquakes and the March 11 Tohoku Earthquake

After the 1995 Kobe earthquake (M 7.3 with more than 6,000 fatalities), the Japanese government set up the Headquarters of Earthquake Research Promotion (HERP). One of the goals of HERP was to make national seismic hazard map, which indicates distribution of 30 year probability of ground shaking beyond a certain level (e.g., seismic intensity 6-lower on the Japanese scale). Such probabilistic ground shaking was computed from long-term forecast of earthquakes, i.e. probabilities of earthquake occurrence on more than 100 inland active faults and about 20 segments in subduction zones.

The long-term forecast of great (M>7) earthquakes along subduction zones around Japan - the Kuril and Japan trenches and Nankai trough- was estimated by Earthquake Research Committee (ERC), one of the HERP committees, based on the past recurrence history of earthquakes. For example, in the Miyagi-oki region, M ~7.5 earthquakes have repeated since 1793 with an average interval of 37 years, from which the probability of another earthquake with similar size was calculated as 99 % in the next 30 years. Because the oldest event in 1793 seemed to have ruptured the neighboring Southern Sanriku region, the forecast estimated the earthquake size could be as large as M 8.0, if both segments rupture simultaneously. Most tsunami hazard maps calculated tsunami inundation zones from such a high probability scenario of simultaneous rupture (M~8.0), although a tsunami earthquake (Tsunami magnitude Mt 8.2, recently revised to be 8.6-9.0) with occurrence probability of 20 % in 30 years was also forecasted in any part of a zone along the Japan trench.

The 2011 Tohoku earthquake was a giant (M = 9.0) earthquake. The rupture started from the southern Sanriku region and expanded to Miyagi-oki, but the source region extended over central Sanriku, Fukushima-oki and a part of Ibaraki-oki region, as well as near Japan trench (*e.g.*, Ide *et al.*, 2011; Ozawa *et al.*, 2011). The maximum slip, more than 30 m, was much larger than that for the

anticipated Miyagi-oki earthquake. This earthquake generated devastating tsunami. Along the Sanriku coast, the maximum tsunami heights were nearly 40 m, similar to that of 1896 Sanriku "tsunami earthquake." In Sendai plain, the tsunami inundated more than 5 km from the coast, much more extensive than the predicted inundation area in the tsunami hazard maps, but similar to the distribution of the AD 869 tsunami deposits.

Paleoseismological Studies and Varability of Earthquake Size

A Japanese national history book depicts strong shaking, collapse of houses, and a large area of tsunami flooding around Sendai in AD 869 caused about 1000 fatalities. Tsunami deposits from this earthquake have been mapped for more than 4 km from the present coast line of Sendai plain (*e.g.*, Minoura *et al.*, 2001; Sawai *et al.*, 2008). Along the Kuril subduction zone, unusually large earthquakes occurred with approximately 500 year intervals (Nanayama *et al.*, 2003; Sawai *et al.*, 2009), with the last earthquake in the 17th century.

Paleoseismological studies conducted since the 2004 Indian Ocean tsunami revealed that a giant earthquake similar to the Sumatra-Andaman earthquake (M 9.1) occurred several hundred years ago. Studies of tsunami deposits made in Sumatra Island (Monecke *et al.*, 2008), Thai coast (Jankaew *et al.*, 2008), Andaman Island (Malik *et al.*, 2011) and Indian Coast (Rajendran *et al.*, 2011) show evidence of past tsunamis. Coseismic coastal uplifts were inferred from marine terraces in Myanmar (Aung *et al.*, 2008) or microatolls in Andaman Island (Kayanne et al., 2010) and Sumatra Island (Sieh *et al.*, 2008). Evidence of past coseismic subsidence was found in southern Andaman Island (Malik *et al.*, 2011).

These paleoseismological studies also indicate variability of past earthquakes. The date of penultimate Sumatra-Andaman earthquake was estimated at around AD 1300 - 1450 in Thailand, AD 1290 - 1400 in Sumatra, but much later, post AD 1600 in Andaman Island. These variable dates may indicate that the last earthquake was not exactly the same type as the 2004 Sumatra-Andaman earthquake.

Such a variability in size of past earthquakes or supercycle of earthquake recurrence (Sieh *et al*., 2008) was also found in subduction zones around the Pacific Ocean (Satake and Atwater, 2008). Historical tsunami heights or coastal changes from the large recurrent earthquakes along Nankai trough also show a variability. In southern Chile, the 1960 earthquake was much larger than the previously recorded earthquakes in historical literature in 1837 and 1737, and similar to the 1575 earthquake (Cisernas *et al.*, 2005). In Cascadia subduction zone of North America, giant earthquakes similar to the 1700 earthquake seems to have occurred at approximately 500 years interval, but the detailed studies show that recurrence interval and size of past earthquakes also seem to be variable (Atwater *et al.*, 2005).

Variable recurrence patterns, revealed from paleoseismological data for much longer time range than historical records, indicate a difficulty in long-term forecast for future earthquakes. Date and size of past earhtquakes estimated from hisotircal data or paleoseismological surveys are used to calculate the probability for future occurrence. While most long-term forecasts assume recurrence of characteristic earthquakes, they may need to consider the variability. This is more important and urgent in several subduction zones, such as the Kuril subduction zone off Hokkaido or the Sunda subduction zone off Sumatra, which might have entered in an active period of great earthquakes.

Tsunami Warning and Mitigation Systems

Lack of a tsunami warning system in the Indian Ocean contributed to the severity of the 2004 Indian Ocean tsunami. At the 2005 IOC general assembly, it was proposed and adopted to organize ICGs (Intergovernmental Coordination Groups) in oceans and basins other than the Pacific. They are ICG/IOTWS (ICG for the Indian Ocean Tsunami Warning and Mitigation System), ICG/NEAMTWC (ICG for the Tsunami Early Warning and Mitigation System in the northeastern Atlantic, the Mediterranean and connected seas), and ICG/CARIBE-EWS (ICG for Tsunami and Coastal Hazards Warning System for the Caribbean and Adjacent Regions). The ICG/ITSU for the Pacific, which was active since 1968, has been renamed as ICG/PTWS (ICG for the Pacific Tsunami Warning and Mitigation System).

With coordination with ICG/IOTWS, three regional Tsunami Warning Centers were established in the Indian Ocean countries. They are at German-Indonesian Tsunami Early Warning System (GITEWS) in BMKG (Badan Meteorologi Klimatologi dan Geofisika), Joint Australian Tsunami Warning Centre (Bureau of Meteorology and Geoscience Australia), and Indian National Tsunami Early Warning System in INCOIS (Indian Centre for Ocean Information Services). These centers are staffed 24 hours a day and 7 days a week to monitor seismic activity and tsunami occurrence. These systems rely on seismic and sea-level monitoring and pre-made numerical simulation. In recent tsunamigenic earthquakes, they issue tsunami warning messages in about 5 minutes.

At the time of the 2011 March 11 earthquake, Japan Meteorological Agency (JMA) issued tsunami warning within 3 minutes of the earthquake. They also announced expected tsunami heights (6 m in Miyagi and 3 m in Iwate and Fukushima prefectures) based on the preliminary earthquake size (M 7.9). After detection of actual tsunami on offshore tsunami gauges, they updated the information on expected tsunami heights, but this updated information did not reach all the coastal communities because the power failure occurred and residents already started evacuation. JMA is revising the tsunami warning system and messages to be issued. The technical revision of the system includes use of various and redundant methods to estimate the earthquake size in a few minutes, systematic use of offshore tsunami observation data. They also plan to assume a largest possible size of earthquake, if the initial estimate of the earthquake is beyond a certain level (M~8). While the current warning system predicts tsunami heights in 8 different levels (0.5, 1, 2, 3, 4, 6, 8 and more than 10 m) based on tsunami simulation, the revised messages are issued in 5 levels considering the uncertainties and corresponding evacuation actions to be taken. The message statements are also revised so that public can easily understand the anticipated tsunami hazard.

Tsunami warning for “tsunami earthquake,” an earthquake that generated much larger tsunamis than expected from seismic magnitude, needs improvements. Recent Mentawai, Indonesia, earthquake (M 7.2) in October 2010 caused 4-7 m tsunami and about 500 casualties in Pagai Islands. Our survey and interview indicated that coastal residents did not escape to high ground, because the earthquake shaking was weaker than the other recent earthquakes that did not cause tsunami. Identification of “tsunami earthquakes” is possible by using broad-band seismic records, but quick estimation within a few minutes and dissemination of such message to coastal residents who felt weak shaking are still left as challenges.

References

Aung,T.T., Satake, K., Okamura, Y., Shishikura, M., Win Swe, Hla Saw, Ting Lwin Swe, Soe Thura Tun, and Thura Aung, 2008, Geological evidence for three great earthquakes in past 3400 years

off Myanmar, *J. Earthq. Tsunami*, 2, 259-265.

Cisternas, M., Atwater, B.F., Torrejon, F., Sawai, Y., Machuca, G., Lagos, M., Eipert, A., Youlton, C., Salgado, I., Kamataki, T., Shishikura, M., Rajendran, C.P., Malik, J.K., Rizal, Y., Husni, M., 2005, Predecessors of the giant 1960 Chile earthquake, *Nature*, 437, 404-407

Ide, S., Baltay, A. and Beroza, G.C., 2011, Shallow dynamic overshoot and energetic deep rupture in the 2011 Mw 9.0 Tohoku-oki earthquake, *Science*, 332, 1426-1429.

Jankaew, K., Atwater, B.F. Sawai, Y., Choowong, M., Charoentitirat, T., Martin, M.E. and Prendergast, A., 2008, Medieval forewarning of the 2004 Indian Ocean tsunami in Thailand, *Nature*, 455, 1228-1231.

Kayanne, H., Malik, J.N., Ikeda, Y., Echigo, T., Shishikura, M. and Satake, K., 2010, Past giant earthquakes reconstructed from fossil microatolls in the Andaman Islands, Abstract SE11-A011 presented at 2010 annual meeting, AOGS, Hyderabad, India, 5-9 July.

Malik,J.N., Shshikura, M., Echigo, T., Ikeda, Y., Satake, K., Kayanne, H., Sawai, Y., Murty, C.V.R., and Dikshit, O., 2011, Geologic evidence for two pre-2004 earthquake during recent centuries near Port Blair, South Andaman Island, India, *Geology*, 39, 559-562.

Minoura, K., Imamura, F., Sugawara, D., Kono, Y., Iwashita, T., 2001, The 869 Jogan tsunami deposit and recurrence interval of large-scale tsunami on the Pacific coast of northeast Japan, *J. Natural Disaster Sci.*, 23, 83-88.

Monecke, K., Finger, W., Klarer, D., Kongko, W., McAdoo, B.G., Moore, A.L. and Sudrajat, S.U., 2008, A 1,000-year sediment record of tsunami recurrence in northern Sumatra, *Nature*, 455, 1232-1234.

Nanayama F, Satake, K., Furukawa, R., Shimokawa, K., Atwater, B.F., Shigeno, K. and Yamaki, S., 2003, Unusually large earthquakes inferred from tsunami deposits along the Kuril trench, *Nature*, 424, 660-663.

Ozawa, S., Nishimura, T., Suito, H. Kobayashi, T. Tobita, M. and Imakiire, T., 2011, Coseismic and postseismic slip of the 2011 magnitude-9 Tohoku-oki earthquake, *Nature*, 475 , 373-377.

Rajendran, C.P., Rajendran, K., Seshachalam, S., and Andrade, V., 2010, The tsunami geology of the Bay of Bengal shores and the predecessors of the 2004 Indian Ocean event, Abstract T11D-2125 presented at 2010 Fall meeting, AGU, San Francisco, Calif., 13-17 Dec.

Satake, K. and Atwater, B. F., 2007, Long-term perspectives on giant earthquakes and tsunamis at subduction zones, *Annu. Rev. Earth Planet Sci.*, 35, 349-274.

Sawai, Y., Satake, K., Kamataki, T., Nasu, H., Shishikura, M., Atwater, B.F., Horton, B.P., Kelsey, H., Nagumo, T., and Yamaguchi, M., 2004, Transient uplift after a 17th-century earthquake along the Kuril subduction zone, *Science*, 306, 1918-1920.

Sawai, Y., Shishikura,M., and Komatsubara, J., 2008, A study on paleotsunami using hand corer in Sendai plain (Sendai City, Natori City, Iwanuma City, Watari Town, Yamamoto Town), Miyagi, Japan (in Japanese with English abstract), *Ann. Rep. Active Fault Paleoearthq. Res.*, Geological Survey of Japan, 8, 17-70.

Sieh, K., Natawidjaja, D.H., Meltzner, A.J., Shen C.-C., Cheng, H., Li, K.-S., Suwargadi B.W., Galetzka, J., Philibosian, B., and Edwards, R.L. ,2008, Earthquake supercycles inferred from sea-level changes recorded in the corals of west Sumatra, *Science*, 322, 1674-1678.

Paleotsunami study along the Pacific coast of Tohoku, Japan

Yukinobu Okamura[a], Yuichi Namegaya[a], Yuki Sawai[a] , Masanobu Shishikura[a], Kenji Satake[b]

[a]*Active Fault and Earthquake Research Center, Geological Survey of Japan, AIST, Higashi, Tsukuba, Ibaraki, Japan*

[b] *Earthquake Research Institute, University of Tokyo, Yayoi, Bunkyo-ku, Tokyo, Japan*

The pacific coasts of Tohoku Japan have not been preparing against giant tsunamis, though there are a historical document and geological evidence which indicate that these areas have been inundated by giant tsunamis repeatedly during the last thousands years. We have been studying tsunami deposits to evaluate the magnitude of ancient giant tsunamis, however, the tsunami has occurred before our research is used to preventive measures against the tsunami.

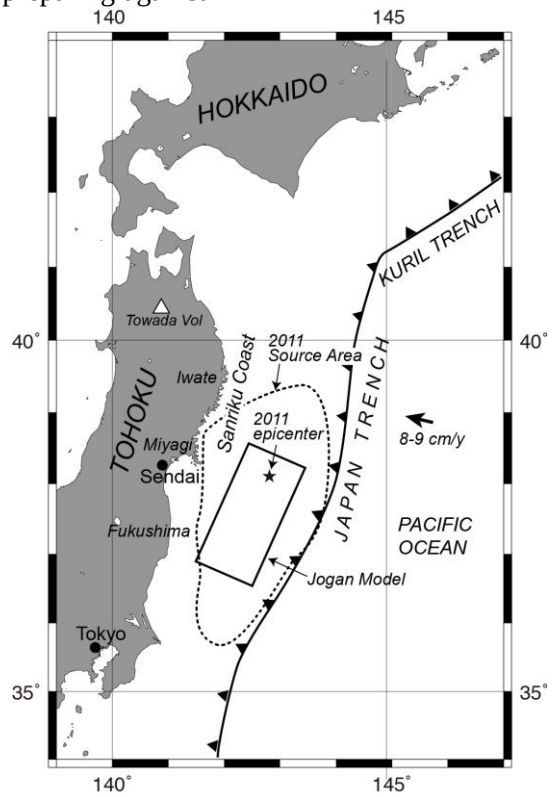

There are many historical documents describing earthquake and tsunami disasters in Japan, which date back to 7th century. Many of the earthquake and tsunami records older than 17th century, however, are insufficient to reconstruct the source model of tsunamis especially in the northeastern Japan. Well-known large tsunamis along the northern Tohoku Pacific coast (Sanriku coast) are the 1611 Keicho-Sanriku tsunami, the 1896 Meiji-Sanriku tsunami, the 1933 Showa-Sanriku tsunami. These tsunamis have been estimated to be higher than 15 m along the Sanriku coast, while they were not so high along the coasts around Sendai and further south.

Before the 16th century, the only reliable historical tsunami in the Pacific coast of Tohoku area is the AD 869 Jogan earthquake which was described in Nihon-Sandai Jitsuroku, one of the national records during the Heian period. The record tells that people cannot stand and many houses fallen during the earthquake. In addition, a giant tsunami inundated around the foot of the castle and swept out everything. The record is presumably based on reports from Tagajo, the location of the government office in Mutsu district (Tohoku area) during the Heian period. The tsunami occurred about 1,140 years ago appears to be comparable to those we experienced on March 11 2011, but the historical record provided no information on the extension of the tsunami inundated area.

Giant tsunamis transport sand from beaches and dunes along coasts to inland swamp and marsh, and left sand sheets as natural records of giant tsunamis. The sand sheet will be covered by mud and peat which are usual sediments in coastal plains and preserved as tsunami deposits. We can obtain information on inundation areas and recurrence intervals of giant tsunamis by surveys of tsunami deposits. There are several coastal plains that satisfy the conditions for preservation of tsunami deposits around Sendai. In fact, tsunami deposits generated by the Jogan earthquake were reported by Minoura et al. (1991). We conducted more detailed survey to construct a reliable source fault model of the Jogan earthquake.

We studied tsunami deposits in Sendai and Ishinomaki Plains of Miyagi Prefecture and small

plains of northern Fukushima Prefecture (Sawai et al., 2007 2008; Shishikura et al., 2007). The study was based on about 400 core samples, taken using hand corers (gauge corer and Russian sampler) and geo-slicer in rice paddy fields. The deposits consist mainly of massive (sometimes laminated), poorly-sorted and graded sand, swamp/marsh peat and mud, and the peat and mud contain sand layers and a volcanic ash. The ash is the To-a tephra layer that fell and deposited during AD 915 eruption of Towada volcano. One of the sandy layers, just below the ash, was regarded as Jogan tsunami in AD869. The Jogan tsunami deposits have been found under the plains approximately 1.5-4.0 km from the shoreline at that time. Several tsunami deposits were found under the Jogan tsunami deposits, and radiocarbon dating suggested that the recurrence interval of the tsunami deposits is 450 to 800 years. Sediments above the ash layer have been cultivated, thus tsunami deposits younger than the Jogan event is scarcely preserved. Exceptionally, we found tsunami deposits above the ash at several sites, suggesting that two tsunami events inundated into the Sendai and Ishinokaki Plains after the Jogan tsunami.

We computed tsunami inundation in both plains from several types of tsunami source models such as outer-rise normal fault (similar to the 1933 Sanriku tsunami), tsunami earthquake (similar the 1896 Sanriku tsunami), interplate earthquakes with variable fault depth, width, length and slip amounts, and an active fault in Sendai bay (Satake et al., 2008; Namegaya et al., 2010). Comparison of the computed inundation areas with the distribution of tsunami deposits indicates that only an interplate earthquake source with 100 km width (top depth of 15 km beneath ocean bottom) and more than 7 m slip (Mw=8.4) can reproduce the observed distribution of tsunami deposits in the two plains.

The model indicates minimum magnitude of the 869 Jogan earthquake, but the 2011 earthquake (Mw=9.0) was much larger than that model. One of the reasons we underestimated the earthquake magnitude is that we assumed that the distribution of tsunami deposit indicate the tsunami inundation area. The survey after the 2011 tsunami showed that tsunami inundation was 1 to 2 km wider than the distribution of tsunami deposits (Goto, et al., 2011). The 2011 tsunami has provided an important opportunity to learn how to evaluate reliable magnitude of ancient earthquakes from geologic records.

References

Goto, K. et al., 2011, New insights of tsunami hazard from the 2011 Tohoku-oki event. Marine Geology, doi:10.1016/j.margeo.2011.10.004.

Minoura, K. and Nakaya, S., 1991, Traces of tsunami preserved in inter-tidal lacusrine and marsh deposits: some examples of from northeast Japan. Journal of Geology, 99, 265-287.

Namegaya, Y. et al., 2010, Numerical simulation of the AD 869 Jogan tsunami in Ishinomaki and Sendai plains and Ukedo river-mouth lowland. Annual Report on Active Fault and Paleoearthquake Researches, no. 10, p. 1-21.

Satake, K. et al., 2008, Numerical simulation of the AD 869 Jogan tsunami in Ishinomaki and Sendai plains. Annual Report on Active Fault and Paleoearthquake Researches, no. 8, p. 71-89.

Sawai, Y. et al., 2007, A study on paleotsunami using handy geoslicer in Sendai Plain (Sendai, Natori, Iwanuma, Watari, and Yamamoto), Miyagi, Japan. Annual Report on Active Fault and Paleoearthquake Researches, no. 7, p. 47-80.

Sawai, Y. et al., 2008, A study on paleotsunami using hand corer in Sendai plain (Sendai City, Natori City, Iwanuma City, Watari Town, Yamamoto Town), Miyagi, Japan. Annual Report on Active Fault and Paleoearthquake Researches, no. 8, p. 17-70.

Shishikura, M. et al., 2007, Age and distribution of tsunami deposit in the Ishinomaki Plain, Northeastern Japan, Annual Report on Active Fault and Paleoearthquake Researches, no. 7, p. 31-46.

Strong Motion Observation System and Project Plan in China

Xiao Jun Li

Institute of Geophysics, China Earthquake Administration, No.5 Minzudaxue Nanlu, Beijing, P.R. China

The development process of the strong motion observation in China is briefly introduced, and the digital strong motion observation network system and the ground motion recordings, especially from the *M8.0* Wenchuan earthquake and aftershocks, are described in detail in this paper. The project of the earthquake early warning systems under construction is also presented.

The strong motion observation in China began in 1962. The first observation work was the deploy of the observation array at the Xinfengjiang reservoir site after the Xinfengjiang reservoir-induced earthquake *M6.1* in March 19, 1962, which consisted of the structural observation stations at the dam and a free field observation station at rock site near the dam. The first strong motion record in China was obtained by the observation station at the Xinfengjiang reservoir site in 1962. After Xingtai earthquake M6.8 on March 8, 1966, 14 permanent free-field stations were deployed, and the mobile observation was carried out for the first time in the word. The development of strong motion observation in China was quite slow. There were only 283 stations and arrays which included 366 sets of accelerometers until 2000, and only about 3000 useful records were obtained. But a lot of mobile observations were made, including about 71 observation actions and 355 stations.

China Digital Strong Motion Observation Network

The mainland of China, in number and density of strong-motion observation stations, was seriously behind the United States, Japan, Iran and Mexico before 2000 (Gao et al, 2001, Zhou, 2006, Nozu, 2004). In order to change the situation and build the National Strong Motion Observation Network System (NSMONS) in China, huge funds were provided by central government to implement the "China Digital Strong Motion Observation Network" project during the National 10th Five-year Plan (2000-2005). The project built the number and distribution of the observation stations and arrays shown in Figure 1. The network focused on regional distribution of permanent stations, seismic intensity stations in major cities for intensity rapid reporting, and special arrays for special research purpose. Furthermore the network was augmented with mobile observations. The network centers were built for record recovery, processing and dissemination, network technical support, network management and maintenance. The network was completed in March 2008 after nearly five years of construction and trial operation. It consisted of 1154 permanent free-field stations, 12 special observation arrays, 200 mobile instruments and a strong-motion observation station management system. The management system included a national center, three regional centers, five intensity rapid reporting centers and local centers of all provinces, municipalities and autonomous regions in mainland of China. The observation stations and arrays resulted in a broad distribution of observation stations and intensive distribution in some local areas.

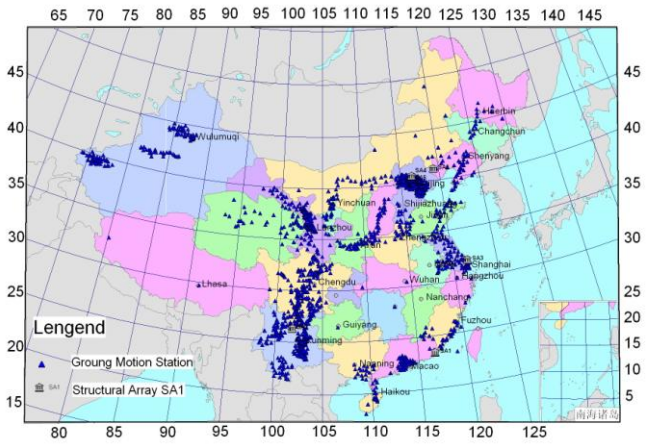

Figure 1. Distribution of stations in the China Digital Strong Motion Observation Network

Reordings from *M8.0* Wenchun Earthquake and Aftershocks

The *M8.0* Wenchuan earthquake occurred in Sichuan Province, China on May 12, 2008, and caused unprecedented loss of human life and widespread severe damage to engineering structures. The fault rupture initiated in the southern Longmenshan and propagated unilaterally toward the northeast for about 300 km, and generated a 240-km-long surface rupture zone along the Beichuan fault and an additional 72-km-long surface rupture zone along the Pengguan fault (Xu, et al., 2009). The earthquake affected areas of six provinces, Municipal and Autonomous Regions including Sichuan, Gansu, Shaanxi, Chongqing, Yunnan, and Ningxia. As of 15 August 2008, a total of 260 aftershocks with magnitude larger than 4.0 had occurred, in which the largest one with a magnitude of 6.4 occurred in Qingchuan on 25 May 2008.

A large number of strong motion records were obtained by the NSMONS from the *M8.0* Wenchuan earthquake and aftershocks. Figure 2 shows the location of strong-motion stations that recorded the main shock. There were 1 350 components of strong motion records, including records from 437 free-field stations and 1 array (8 stations) for topographical effect observation and 2 arrays (10 monitoring points) for structural response observation (Li, Zhou, Yu, et al., 2008, Li, Zhou, Huang, et al., 2008, Lu and Li, 2008). After the main shock, 59 mobile instruments were quickly deployed in the earthquake disaster area as shown in Figure 3 to record ground motions and structural responses from

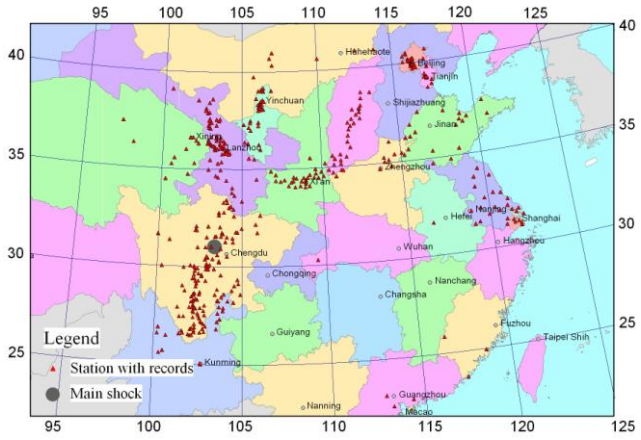

Figure 2. Location of the stations recorded the main shock of Wenchuan earthquake

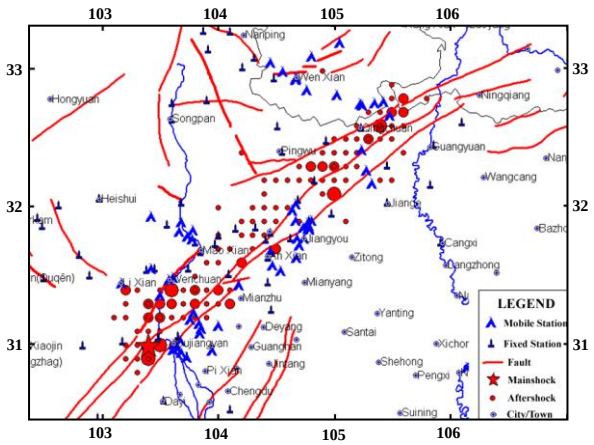

Figure 3. Location of mobile stations recorded aftershocks of Wenchuan earthquake

strong aftershocks. 15 903 components of records were obtained from 949 aftershocks (Li, 2009a, b), in which 9 750 components were recorded by the mobile stations (Li, 2009a). Among the records of the main shock, the largest peak acceleration was recorded at the Wolong station shown in Figure 4 in the hanging wall area with a rupture distance of 23 km, whose peak accelerations were recorded in the east–west, north–south, and up–down directions as 957.7 gal, 652.9 gal, and 948.1 gal, respectively. The characteristics of the acceleration records at Wolong station, with several strong motion parts, showed the fault rupture effects from several segments of the fault. This phenomenon was also found

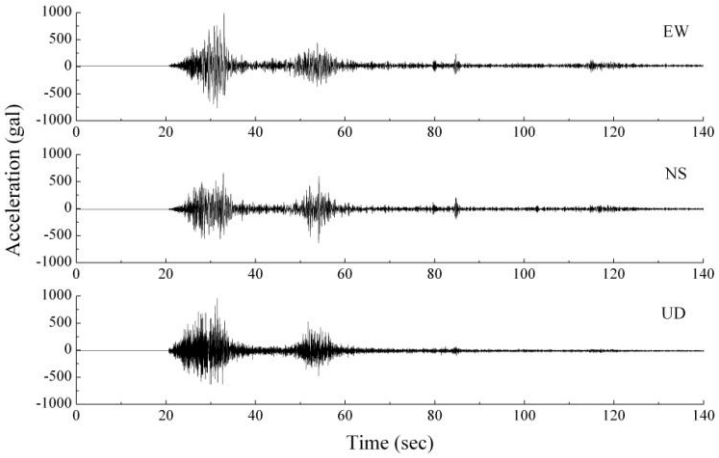

Figure 4. Acceleration records at Wolong station from Wenchuan earthquake

in the records from the *M9.0* Tohoku Earthquake on the 11 March 2011. In the records from aftershocks of Wenchuan earthquake, the largest PGA of 966 gal shown in Figure 5 was recorded by the mobile station in the Qingchuan aftershock *M*4.2 on 10 August 2008.

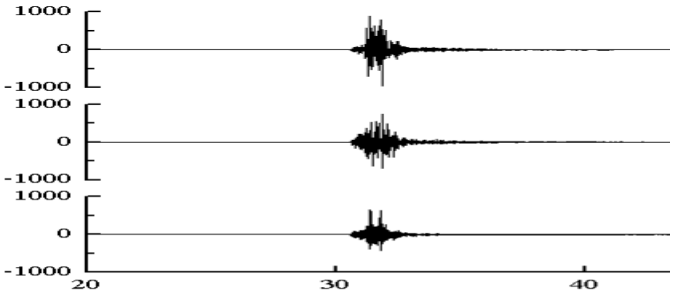

Figure 5. Records from the Qingchuan aftershock *M*4.2 on 10 August 2008 (acceleration (gal) versus time

In addition, there were about 4000 components of strong motion records obtained by the NSMONS from 510 earthquakes except the *M8.0* Wenchuan earthquake and aftershocks in 2007~2009 (Li, 2011) and 2010.

The Demonstrative Earthquake Early Warning Systems under Construction

After the "China Digital Strong Motion Observation Network" project was completed, a new project plan was made immediately, which was to supplement the new stations in the National Strong Motion Observation Network and build demonstrative earthquake early warning systems. The new stations and demonstrative earthquake early warning systems are under construction and would be completed in 2013. Figure 6 shows the distribution of the strong motion stations and earthquake early warning stations. There are 80 strong motion stations, 2 demonstrative earthquake early warning systems each with 80 observation stations and a system center, and a national system center. One of demonstrative earthquake early warning networks is in the Beijing and Tianjin area shown in Figure 7, and another is in the Lanzhou area shown in Figure 8, and the national system center is in Beijing.

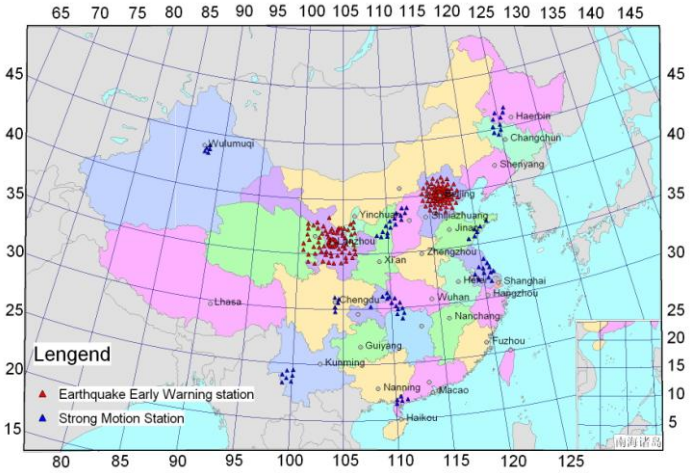

Figure 6. Distribution of the strong motion stations and earthquake early warning systems under construction

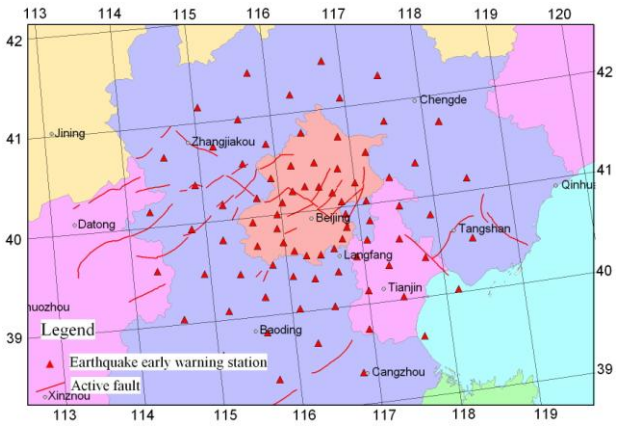

Figure 7. Demonstrative earthquake early warning network in the Beijing and Tianjin area

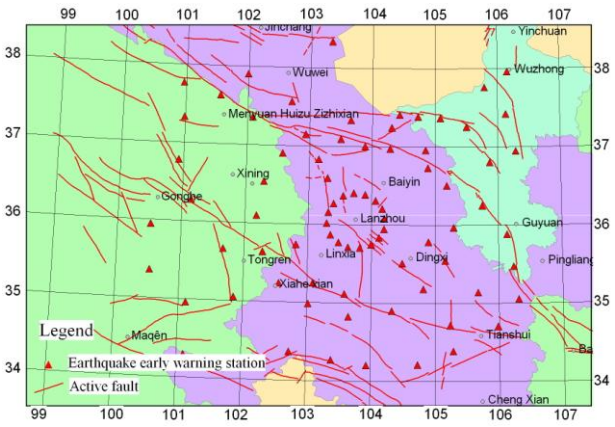

Figure 8. Demonstrative earthquake early warning network in the Lanzhou area

The Wenchuan earthquake records showed that delay of peak ground acceleration arrival was about 54 s between the records at Hanzeng station and Wolong station, and the delay of P-wave arrival

was about 46 s. The Wolong station shown in Figure 9 was near the Yingxiu town which was the most heavy damage area, and the Hanzeng station shown in Figure 9 was near the Beichuan county seat which was the another most heavy damage area in Wenchuan earthquake. If there was an early warning system in the area along the Longmenshan fault area, there was more than 40 s of warning time for the Beichuan county seat. The warning time would be the most valuable seconds for escape.

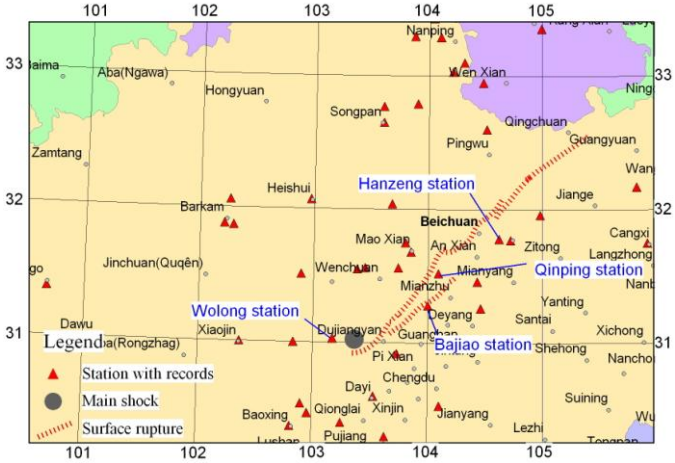

Figure 9. Distribution of the stations recorded the main shock in the fault surrounding area

Acknowledgments

The records used in this study are provided by the National Strong-Motion Networks Center of China. We give our thanks to the National Strong-Motion Networks Center of China and all of the relevant managers and experts. This research work is also supported by the Special Research Fund for Seismic Industry (201108003) and National Key Technology R&D Program (2009BAK55B05).

References

Gao Guangyi, H. Yu, and S. Li, 2001. Strong-Motion Observations in Mainland China. World Information on Earthquake Engineering, 17, 4, 13-18 (in Chinese with English abstract).

Li, Xiaojun, Z. Zhou, H. Yu, R. Wen, D. Lu, M. Huang, Y. Zhou, and J. Cui, 2008. Strong motion observations and recordings from the great Wenchuan earthquake. Earthquake Engineering and Engineering Vibration 7, 3, 235–246.

Li, Xiaojun, Z. Zhou, M. Huang, R. Wen, H. Yu, D. Lu, Y. Zhou, and J. Cui, 2008. Preliminary analysis of strong-motion recordings from the magnitude 8.0 Wenchuan, China earthquake of May 12, 2008. Seismological Research Letters 79, 6, 844–854.

Li, Xiaojun, A. Yu, P. Gan, M. Li, L. Liu, 2008. Survey and Analysis of the Disaster and Engineering Damage of Beichuan County Seat in Ms8.0 Wenchuan Earthquake. Technology for Earthquake Disaster Prevention 3, 4, 352-362 (in Chinese with English abstract).

Li Xiaojun ed-in-chief, 2009a. Uncorrected Acceleration Records of Wenchuan Aftershocks from Mobile Observation Stations. Seismological Press, Beijing, 1–612 (in Chinese).

Li, Xiaojun ed-in-chief, 2009b. Uncorrected Acceleration Records of Wenchuan Aftershocks from Permanent Observation Stations. Seismological Press, Beijing, 1–513 (in Chinese).

Li, Shanyou ed-in-chief, 2011. Uncorrected Acceleration Records of the earthquakes in 2007~2009 from Permanent Observation Stations. Seismological Press, Beijing, 1–269 (in Chinese).

Lu Shoude, Li Xiaojun ed-in-chief, 2008. Uncorrected acceleration records of Wenchuan 8.0 earthquake. Seismological Press, Beijing, 1-302 (in Chinese).

Xu, Xiwei, X.Wen, G. Yu, G. Chen, Y. Klinger, J. Hubbard, and J. Shaw, 2009. Coseismic reverse- and oblique-slip surface faulting generated by the 2008 Mw 7.9 Wenchuan earthquake, China. Geology 37, 6, 515–518.

Yuan Y. F., B. T. Sun ed-in-chief (2008). General introduction of engineering damage of Wenchuan Ms8.0 earthquake. Earthquake Engineering and Engineering Vibration 28, Suppl., 1–16.

Zhou, Yongnian, 2006. Strong-Motion Observation in Mainland China, Recent Developments in World Seismology, 2006, 11, 1-6 (in Chinese with English abstract).

Nozu, Atsushi, 2004. Current Status of Strong-motion Earthquake Observation in Japanese Ports, Journal of Japan Association for Earthquake Engineering, 4, 3(Special Issue), 79-83.

Disaster Process after the 3.11 East Japan Earthquake and Tsunami Disaster

Norio Maki

Research Center for Disaster Reduction Systems, Disaster Prevention Research Institute, Kyoto University, Gokanosyo, Uji, Japan

Impacts from the event

March 11, 2011, North-east Japan suffers from devastating damage by M9 earthquake and induced tsunami. Disaster named the East Japan Earthquake Disaster results in almost 28, 000 human deaths and JPY 17T direct economic impact. M9 earthquake results in five kinds of impact reflecting characteristics of each area.

One is impact of tsunami in local fishing town, especially at Iwate Prefecture. This area hit by tsunami every 30-50 years. Previous one was tsunami in 1960 which caused by gigantic earthquake in Chili. This area was well prepared area against tsunami both in built environment and awareness of people. However, the scale of tsunami was huge and results in devastating damage to built environment and large human casualties.

Sendai is the center of northern part of Japan and has over one million populations also got impact from earthquake shaking and tsunami. Sendai is the city frequently hit by earthquake, and previous one was in 1978. That earthquake disaster caused long time life line system disruption, and the earthquake disaster is called “the first urban area disaster in Japan”. This time, Sendai suffered from life line system disruption. In addition to that, the area near from the sea got devastating tsunami damage. Tsunami inundation reached until 6km inland. Because of concentration about business activities and population, the large economic loss and human casualties comes from Sendai area.

Nuclear power plant failure results in one of the worst nuclear power plant accident in the world. Evacuation order is issued to the people living within 20 km radius. The number of people in designated evacuated area amounts to 75,000. The recovery from the radiation contaminated area is big issues but the impacted area is still in response phase.

Tokyo also suffered from this event. The very first day, fire at oil plant occurred, and stop of commuting train system made about 400 thousand people temporally homeless. Tokyo also experienced a planned blackout for shortage of electricity because of damage from both nuclear power and thermal power stations.

The impact expanded all over the world. Stock price in Tokyo market steeply falls down and the damage of factories in the impacted area stopped factories in the world.

Disaster Response

Our national government and local governments responded those impacts immediately. Setting up of emergency response structure was very fast because disaster occurred at business hour. Teams of emergency responders such as fire fighters, police officers, medical peoples, and self defense force were dispatched to the impacted area soon after the event.

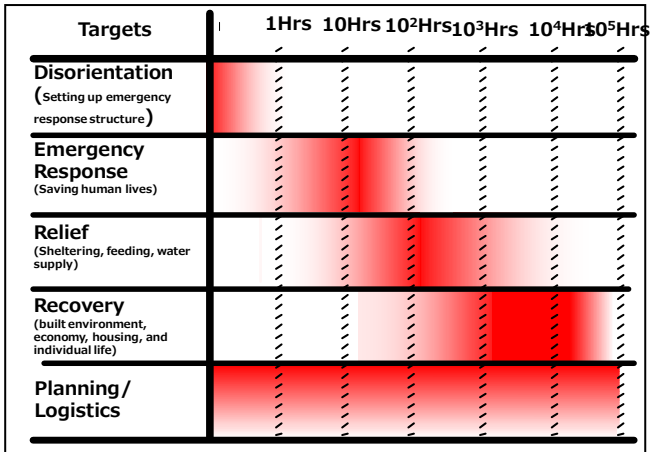

Figure1 Targets of Disaster Response and Recovery

Targets of disaster response are changing according to the time from the event (Fig.1). The first target of response is to save human lives. Number of surviving people flashed away by tsunami are very limited, and operation for saving human lives are concentrated on moving patients in hospital of the impacted area to outside. Relief activities got trouble because of shortage of fuel. However, within a week, food and water supply became stable, and shelters in impacted area were closed within 9month with the completion of a temporary housing.

Accommodating to those targets, local government should conduct various activities. Fig.2 shows the situation of local government response on April 6, 2011. As shown in this figure, within three weeks, relief activities and temporary recovery of lifeline systems becomes stable. However, search and rescue operation still continues, activates toward recovery are very limited. This figure is used to share "a big picture" of disaster response and recovery at Iwate Prefecture.

	Human life				Relief			Lifeline								Social activities							Victims Support						Industry			Recovery					
	S&R	Safety inq	Dead Body	Condolence Money	Food	Fuel	Daily Good	Electricity	Water supply	Gas	Telephone	IT	Mobile Phone	Access	Drainage	Government	Police	Fire Fighting	Emergency Medical	Clinic and Hospital	School	Commercial	Lot for temp Housing	Temp Housing	Survey for Damage	Damage certificate	Life recovery money	Donation	Primary Industry	Small business	Job	Recovery Plan	Debris (public)	Debris (Private)	Debris treatment	Land Use	Public Housing
A City	Y	Y	Y	R	YG	Y	YG	ectric	Y	B	Y	R	Y	G	B	Y	G	R	G	R	Y	B	Y	Y	Y	Y	R	R				B	(Pri	R	B	R	R
B City	Y	R	Y	R	YG	Y	YG	Y	Y	B	Y	R	Y	G	B	Y	G	R	G	R	Y	B	Y	Y	Y	Y	R	R				B	YG	R	B	R	R
C town	Y	B	Y	R		YG		Y	Y	B	Y	Y	Y	G	B	YG	G	Y	G	R	Y	B	Y	Y	Y	Y	R	R				B	YG	R	B	R	R
D village	Y	R	Y	R		YG		Y	Y	Y	Y	R	Y	G	B	YG	G	R	G	G	Y	B	Y	Y	Y	Y	R	R				B	YG	R	B	R	R
E town	Y	R	G	R		YG		Y	Y	Y	Y	R	Y	G	B	YG	G	G	G	G	Y	B	Y	Y	Y	Y	R	R				Y	YG	Y	B	R	R
…	Y	R	G	R		YG		Y	R	G	G	G	Y	G	B	G	G	R	G	G	G	B	Y	Y	Y	Y	R	R				B	YG	R	B	R	R
…	Y	G	G	R		YG		Y	Y	G	G	R	Y	G	B	G	G	G	G	G	G	B	Y	Y	Y	Y	R	R				B	YG	R	B	R	R
…	Y	Y	G	R		YG		Y	Y	G	Y	Y	Y	G	B	G	G	Y	G	G	Y	B	Y	Y	Y	Y	R	R				B	YG	R	B	R	R
…	Y	G	G	R		YG		Y	Y	G	G	G	Y	G	B	G	G	G	G	G	Y	B	Y	Y	Y	Y	R	R				B	YG	R	B	R	R
…	Y	Y	G	R		YG		Y	G	G	G	G	Y	G	B	G	G	YG	G	G	G	B	Y	R	YG	Y	R	R				B	YG	R	B	R	R

Figure 2 Disaster Response Matrixes, on April 6, 2011

Organizational Structure for Response

Local governments are changing their organizational structure according to the phase of disaster response. In Iwate Prefecture, all the emergency responding agencies worked together at the emergency operation center, EOC at the emergency phase. Fig.3 is layout of EOC of Iwate Prefecture. One unique thing about the layout of Iwate is having a helicopter units consisted representatives from all the agencies who own helicopters such as fire department, coastguard, and self defense force including army, navy, and air force. A helicopter is precious limited resources for emergency response, and coordinated use is very important. Emergency response coordination worked well in Iwate Prefecture because all the responding agencies worked together in one room sharing their information.

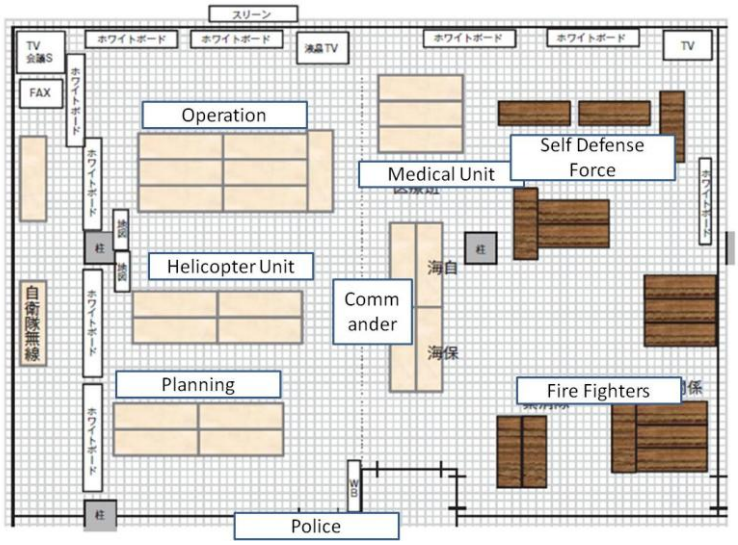

Figure 3 EOC Layouts for Emergency Response

In the relief phase, many departments within a prefecture government are involved in the response in addition to department of emergency response. Coordination among government departments becomes important to conduct effective victims support. In Iwate Prefecture, teams corresponding to specific goal for disaster relief such as a fuel supply, dead body management, victims support, debris management, debris removal, and temporary housing supply. Though liaison offices of each team were selected and conducting meeting every day, information sharing among corresponding people did not go well. It is because they did not work in the same room, and they cannot make simultaneous information sharing and coordination.

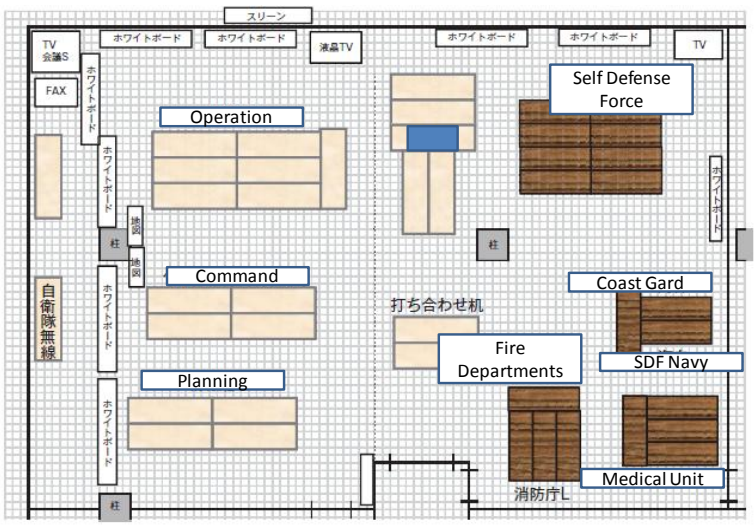

Figure 4 EOC Layouts for Relief Response

Recovery

Local governments worked for recovery from the early phase. Both Miyagi and Iwate

Prefecture published their vision for recovery one month later. Prefecture governments have completed their recovery planning by 6 month except for Fukushima Prefecture. Social impacts in Fukushima Prefecture are different from those in Miyagi and Iwate because of continuous impacts from nuclear power plant accident. And municipality governments have completed their recovery plan until early December. However, planning for detailed land use to be safer city are still continues. National government published their visions for recovery on June 25, 2011, three months after the event. Also parliament have admitted third supplementary budget which is about recovery project in December.

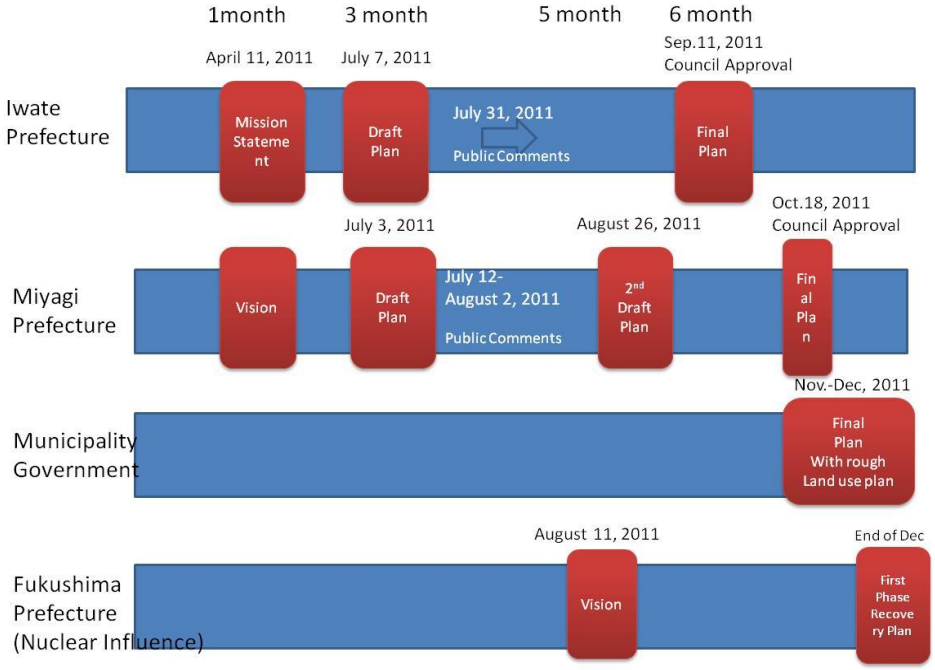

Figure 5 Recovery Planning

Comments and Discussion

Japan has revised their disaster response system based on lessons from the 1995 Kobe earthquake. Those revisions worked well for making emergency response phase effective. However, there still remain issues in relief and recovery phase. Coordination within an organization such as within prefecture governments, national governments did not work well. The system that all the responders work in the same space to share their information, and have enough human resources for information management should be developed. About recovery, slow decision making about land use planning delays business resumption in the impacted area.

The earthquakes, volcanic and tsunami risk management on Kamchatka

Evgeny Gordeev

Institute of Volcanology and Seismology, Far East Branch, Russian Academy of Sciences, Petropavlovsk-Kamchatsky,683006, Russia

Long-lasting observations for earthquakes in Kamchatka showed that on average one earthquake of M=8.5, ten of M=7.2 and one hundred of M=5.9 occur every 33 years. Over the last 50 years from 1961 through 2011, fifteen earthquakes of M >7 occurred in Kamchatka. The strongest earthquake (Mw=7.9) occurred on December 5, 1997 in the north of the Kronotsky Gulf. Within the historical period of observations beginning in 1741, nine earthquakes of M>8, including three earthquakes of M>9 occurred in 1737, 1841 and 1952. The 1952 earthquake generated catastrophic tsunami waves 20 m high. Occurrence of tsunami on the Eastern coast of Kamchatka (the Pacific coast) with the height of waves more than 10 m amounted to 4 per every thousand over the last 6 thousand years. Tsunami warning system was constituted in 2010. The system is composed of three tsunami warning centers located in Petropavlovsk-Kamchatsky, Yuzhno-Sakhalinsk and Vladivostok, 15 broad-band seismic station and 26 strong-motion stations that receive and process data in a real-time mode.

Tsunami warning for the 2011 Great Tohoku Earthquake was issued in 10 minutes.

Tsunami warning systems in Kamchatka and the Kurile Islands are in close cooperation with all Pacific tsunami centers.

There are 30 active volcanoes in Kamchatka and 4-5 of them are continuously active. The explosions of andesitic volcanoes (Bezymianny and Sheveluch) produce strong and fast-moving ash plumes, which can rich high altitude (up to 15 km) in a short time. Bezymianny and Sheveluch are the most active volcanoes in Kamchatka. Two gigantic explosions in the 20-th century took place in Kamchatka (Bezymianny volcano in 1956 and Sheveluch volcano in 1964). The growth of the lava dome in the explosive crater at Bezymianny has been going on from 1956 to present. For the last 5 years 9 strong explosive eruptions at Bezymianny have been associated with the dome-building activity: January 11, 2005 and November 30**;** 2006, May 09 and December 24; 2007, May 11 and October 14-15 2008; August 19, 2009; December 16-17 and May 31, 2010**.**

Since 1980, a lava dome at Sheveluch has been growing at the bottom of the explosive crater, which formed as a result of the 1964catastrophic eruption. Strong explosive eruptions at Sheveluch were associated with the dome-building activity: April 22, 1993; May 19-21, 2001; May 09, 2004;

February 27 and September 22, 2005; December 25-26, 2006; March 29 and December 19, 2007; April 26-28 and September 10-11, 2009.

Strong explosive eruptions from andesitic volcanoes are the most dangerous for aircraft because in a few hours or days they can produce about several cubic kilometers of volcanic ash and aerosols in the atmosphere and stratosphere. Depending on the power of the eruption, its strength and wind speed, ash plumes and clouds can travel thousands kilometers from the volcano for several days, remaining hazardous to aircraft. The International KVERT Project uniting scientists from IVS FEB RAS, KB GS RAS and AVO USGS was established to reduce the risk of encounters of aircrafts with ash clouds from Kamchatka volcanoes.

Scientists analyze seismic, video, visual and satellite monitoring data from Kamchatka volcanoes and provide early warning to the interested air agencies on the state of volcanic hazard.

Earthquake, Tsunami and Volcano Information issued by Japan Meteorological Agency and its endeavor for further applicable tsunami information

Takeshi Koizumi

Seismological and Volcanological Department, Japan Meteorological Agency, 1-3-4 Otemachi, Chiyoda-ku, Tokyo 100-8122, Japan

The Japan Meteorological Agency (JMA) started its nationwide seismological and volcanological observation in 1883, tsunami warning service for local tsunamis in 1949, and that for distant tsunami in 1962, two years after the 1960 Chilean Earthquake. The announcement of volcano information became part of JMA's regular services in 1965.

In the event of large earthquakes, JMA issues information called Earthquake Early Warning (EEW), an earthquake alert which tells the expected seismic intensities (degrees of tremors) around the focus before the strong tremors arrive, followed by information about the observed seismic intensities as well as the location and magnitude of the earthquake. In case of large earthquakes under the sea floor, JMA issues Tsunami Warnings/Advisories in 2 to 3 minutes after the occurrence of the earthquakes based on the estimation of tsunami-genic potential. When volcanic activities become higher, JMA issues Volcanic Warnings/Forecasts. On March 11, 2011 at 05:46 UTC, a M9.0 earthquake officially named as "The 2011 off the Pacific Coast of Tohoku Earthquake" occurred and JMA issued its first tsunami warning/advisory to the Japanese coast in 3 minutes after the earthquake then successively upgraded them based on sea level data recorded at offshore GPS buoys and coastal tide gauge stations. It was pointed out, however, that lower estimation of tsunami height in the first information mistakenly convinced some people not to evacuate. Based on lessons learned, JMA has been making every endeavor to issue further applicable information.

In Japan, a large-scale earthquake with magnitude around 8 is widely expected to hit the Tokai region in the near future (referred to as the Tokai Earthquake). Once anomalous data are detected, JMA issues investigation reports, and if the data are considered to be precursors of the Tokai Earthquake, JMA will convene a committee called Earthquake Assessment Committee for Areas under Intensified Measures against Earthquake Disaster. If the Committee concludes that the Tokai Earthquake is imminent, the Director-General of JMA will report to the Prime Minister, who will then hold a Cabinet meeting and issue a warning statement to the public.

In addition to these domestic services, JMA operates international services on tsunami and volcanic ash clouds. The Northwest Pacific Tsunami Advisory Center (NWPTAC) in JMA provides tsunami advisories for large earthquakes in the northwest and a portion of the southwest Pacific, including South China Sea, to the countries concerned. JMA also provides Tsunami Watch Information (TWI) to the Indian Ocean countries parallel with 3 Regional Tsunami Service Providers (RTSPs) in the region and Pacific Tsunami Warning Center (PTWC) in Hawaii. The Tokyo Volcanic Ash Advisory Center (Tokyo VAAC), operated by JMA, is one of the 9 VAACs in the world, and issues Volcanic Ash Advisories (VAAs) for East Asia and the northwestern Pacific area.

References

Japan Meteorological Agency, 2009. Earthquake and Tsunamis - Disaster prevention -

Japan Meteorological Agency, 2009. Volcanoes - Volcanoes Monitoring and Disaster Reduction -

Roles of Geodetic Methods on Volcanic Eruption Prediction

Makoto Murakami

Institute of Seismology and Volcanology, Hokkaido University

Since the deployment of many receivers around Japanese active volcanoes in mid 1990's, continuous GPS measurement has been demonstrating the usefulness in the volcanic activity monitoring as demonstrated during the 2011 January eruption of Shinmoe Crater of Kirishima volcanic complex in southern Japan, where a deep source inflation was detected prior to the eruption by geodetic analysis. Data around Asama volcano in central Japan also register a good correlation between geodetic signal and volcanic activity. The volcano is repeating eruptions since the prehistoric period. The most recent activity started in 2004 after 20 year long dormancy followed by further two eruptions in 2008 and 2009. Distance change of a baseline spanning over the volcano edifice measured by the continuous GPS shows a series of repeating episodes of inflation and deflation. During the inflation period volcanic activities on the surface (seismicity, fumarole and SO2 emission, etc.) become culminating (Murakami, 2006). All the eruptions after 2004 occurred during inflation period. It is inferred that episodic of magma intrusions from the depth to a shallow reservoir results in the rise and fall of the volcanic activity near the surface. To the present time no apparent periodicity is confirmed in the temporal evolution of the ground deformation. In this presentation, we discuss the possibility of prediction of the beginning of a new episode, based on a certain regularity of the deformation's temporal evolution. It is noteworthy that the temporal change of the baseline length is a chain of successive similar episodes. Each episode shares the similarity in shape but not in magnitude. It is quite interesting that the starting point of each episode drops on a single line suggesting a time-predictability following the same discussion of earthquake predictability. We see similar tendency also around Meakan Volcano, eastern Hokkaido. In this presentation we also discuss the roles of geodetic method in volcanic eruption prediction including the search of possible candidate sites of super eruption.

1952 Near Pyongyang, North Korean Earthquake and it's tectonic implication around the region

Myung-Soon Jun[a], Tae-Seob Kang[b]

[a]*Korea Institute of Geoscience and Mineral Resources, 124 Gwahang-no, Yuseong-gu, Daejeon 305-350, Korea*

[b] *Department of Earth Environmental Sciences, Pukyong National University, 45 Yongso-ro, Nam-gu, Busan, 608-737, Korea*

There was a rather large felt earthquake on March 19, 1952 from Nampo City, west of Pyungyang, the capital of North Korea. The North Korea Seismological Institute estimated the magnitude of the event around 6.5 (Seismological Institute of North Korea, 1987). They might estimate the magnitude from traditional methord, i.e. felt area survey since there was no seismic station that time in the Korean Peninsula. Further more that was during the Korean War. Considering the mild or low seismicity around the Korean Peninsula, this 1952 North Korean event could be the largest event since the 20 century.

For this event, we collected 8 seismogram copies from Japan, China and Russia. However many seismograms show very weak traces. We could digitized rather good quality data only from 3 stations, Abuyama and Matsushiro in Japan and Sverdlovsk in Russia. To determine the earthquake source parameters, we applied moment tensor grid searching method and compare the observed and synthetic seismograms for the above 3 station data. To generate the synthetic seismograms, we applied Mineos program using mode summation method(Master et al., 2007). We found the best fitting with strike 120^{o} , dip 90^{o} , rake 340^{o} and seismic moment $2.45X10^{25}$ dyne-cm, which is relavent with Mw = 6.17(Fig. 1).

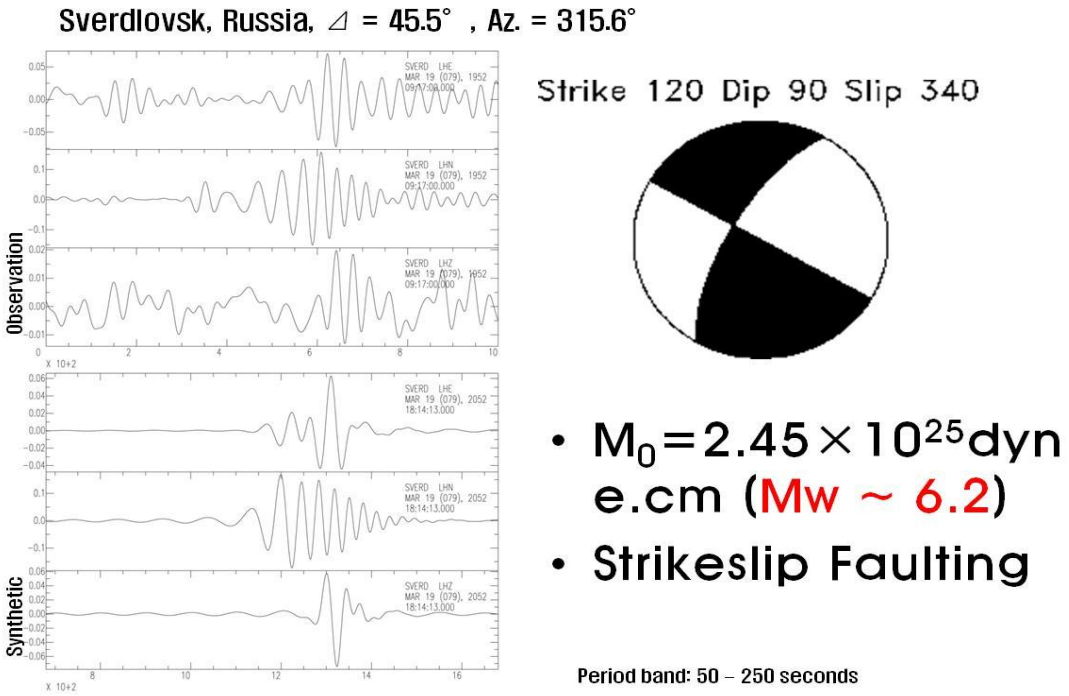

Fig. 1. Comparison of observed and synthetic trace together with simplified mechanism.

Considering the low seismicity around the Korean Peninsula, this event would be the largist event in and around the Korean Peninsula since beginning of 20 century. Their strike-slip mechanism also consistent with the major earthquakes from the region. Jun and Jeon(2010) analyzed 18 intraplate earthquakes with magnitude lager than 4.5 from the last century in and around the Korean Peninsula and found the dominent earthquake source mechanism in the region is predominant strike-slip faulting with small amount of thrust component. Figure 2 shows the earthquake mechanism in and around the Korean Peninsula.

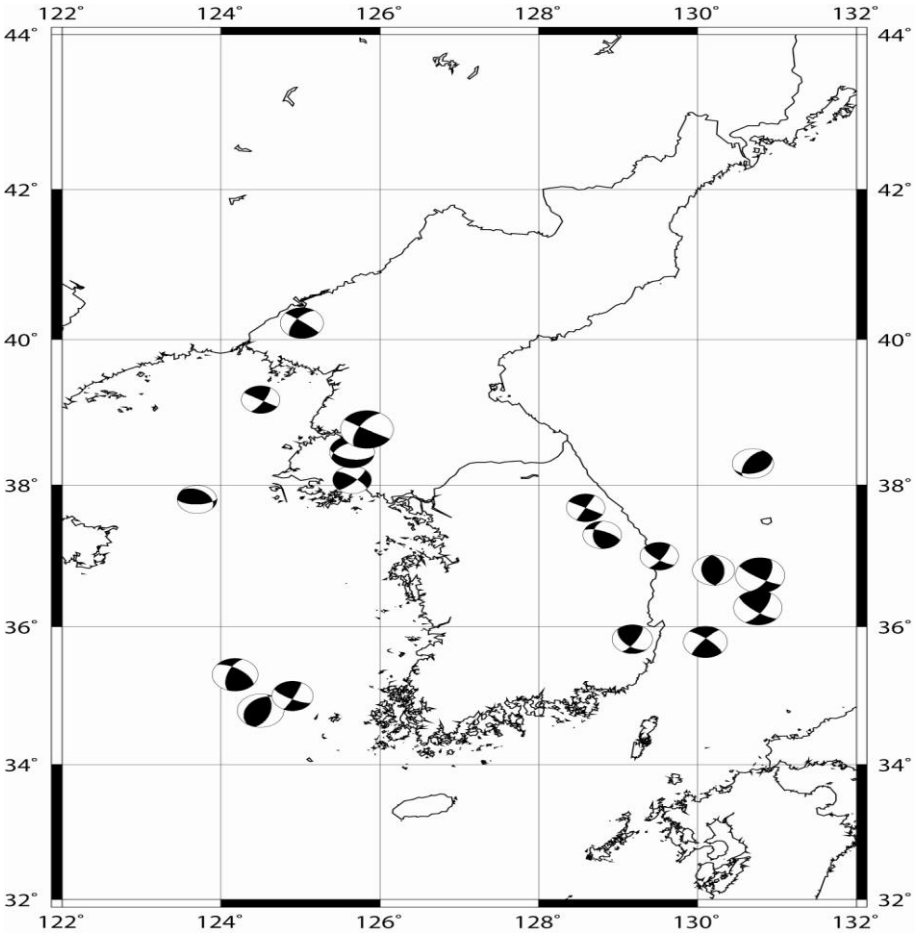

Fig. 2. Simplified earthquake mechanisms in and around the Korean Peninsula.

References

Seismological Institute, 1987. Seismic Catalogue of Korea, p.150.

Masters, G., Barmine, M. and Kientz, S. (2007) Mineos: User Manual version 1.0

Jun M.S. and Jeon J.S. (2010) Focal Mechanism in and around the Korean Peninsula, Jigu-Mulli-wa-Mulli-Tamsa, 13, 198-202.

Seismic hazard assessment in Taiwan: Insights from historical seismicity and radar interferometry analyses

Sin Mei Ng

Department of Geology, Chinese Culture University, 55 Hwa-Kang Road, Yang-Ming-Shan, Taipei, Taiwan 11114

We attempt at providing new insights about the earthquake behaviour in western Taiwan, based on a comparison between historical information and present-day instrumental records. We provide a consistent picture of the earthquake history during the last four centuries and draw some inferences in terms of seismic cycle. Before instrumental seismic observation in Taiwan that started at the end of the 19th century, ancient written earthquake records are available from the ancient Chinese governments and the public concerning the 17th, 18th and 19th centuries. Distribution of casualties and property damage, indicating seismic intensity, can be estimated from archives. Using the Central Weather Bureau (CWB) intensity scale we calibrate the intensity-magnitude relationships from the instrumental seismicity recorded from 1995 to 2005, showing that within the range of historical uncertainties and earthquake depths in western Taiwan, 0-40 km, the depth is not critical in these relationships. With estimated intensities, the magnitudes of historical earthquakes can be evaluated based on a single average empirical relationship between M_L, the local magnitude, and I_0, the epicentral intensity: $M_L = 0.08I_0^2 - 0.04I_0 + 3.41$. Three types of diagrams are then proposed to describe the historical seismicity. The first type involves simple representation of earthquake events according to time and magnitude. The second type involves cumulative plot of the released elastic energy with time, as calculated from reconstructed magnitudes. The third type of diagram shows the evolution of cumulative seismic strain release with time, based on a Benioff's law indicating that the release of elastic strain related to an earthquake is proportional to the square root of the dissipated energy. These curves highlight inferences of historical seismicity analysis in terms of earthquake frequency and seismic cycle duration in the different segments of the front belt and foreland zones of Western Taiwan, with large contrasts suggesting different levels in earthquake hazard.

Following Taoyuan-Hsinchu-Miaoli area was chosen, among five seismogenic zones in western Taiwan, as an investigation area for recent tectonic activity using InSAR persistent scatters. It is because the next possible large earthquake may happen in this region within a decade provided that the time-predictable model is correct and applicable to Taiwan. It is also worth mentioning that Miaoli area cannot be studied because of the lack of satellite images in this region.

Establishment of Taiwan Volcano Observatory at Tatun

Cheng-Horng Lin

Institute of Earth Sciences, Academia Sinica

P O Box 1-55, Nankang, Taipei, Taiwan

In the Tatun volcanic area, just north to the Taipei basin, the geothermal and seismic activities are still very strong in the shallow crust even although there was no volcanic eruption in the human history. Recent study shows that the last eruption might occur around 6000 year ago (Belousov et al., 2010). Combining this result with some previous observations from seismic, crustal deformation, geochemical analyses, and other geological studies in the past decade, volcanic activity in the Tatun volcanic area might not be totally excluded in the future. As a result, careful monitoring of potential eruption in the Tatun volcanic group becomes not only a scientifically interesting topic but also an important issue related to the safety in the whole Taipei area.

To improve the understanding of volcanic characteristics in each volcano group, scientists can employ several different methods such as seismic observation, geochemical analyses, crustal deformation and geothermal monitoring. In the past decade, researchers in several institutions of Taiwan have completed some preliminary volcanic studies in the Tatun volcano and obtained some interesting results. For example, clustering micro-earthquakes and some volcanic tremors have been found in the Tatun volcanic area, some high Helium isotope ratios have been observed from hydrothermal vents and a temporally crustal deformation has been detected through high-precision leveling survey at some particular area. In order to further improve the capability of volcanic monitoring in the Tatun volcano, we plan to integrate all of resource and previous results into one center. Thus, we plan to establish Taiwan Volcano Observatory at Tatun (TVO). To monitor any potentially volcanic activities in the future, this observatory include some real-time monitoring systems as well as site analyses nearby volcanoes. In addition to sharing with scientists, all of the observed results have been demonstrated in real-time at TVO for the education purpose.

Interviewing insights regarding the high fatality rate inflicted by the 2011 Tohoku earthquake

[a]Masataka Ando, [b]Mizuho Ishida, [c]Yoshinari Hayashi and [d]Chiharu Mizuki

a. Institute of Earth Sciences, Academia Sinica, 128 Academia Rd. 2sec., Nankan, Taipei, Taiwan,

b. Japan Agency Marine-Earth Science Technology, 3173-25 Showa, Kanazawa, Yokohama, Japan

c. Faculty of Safety Sciences, Kansai University, 7-1 Shiraume, Takatsuki, Osaka, Japan,

d. Graduate School of Sciences, Hokkaido University, North 10 West 8, Kita, Sapporo, Japan,

The *Mw* 9.0 earthquake, at 14:46 local time caused 20,000 deaths, including missing persons, in Tohoku, northeastern Japan. The shaking intensity in the devastated area was at least VI on the Japan Meteorological Agency intensity scale, a degree that is IX or higher on the MM scale. The strong shaking lasted at least 3 minutes and was described by local residents as the strongest and longest they had ever experienced. The resulting tsunami affected more than 57 cities.

The death toll, including missing persons, and the total population in inundation areas in each were used to calculate inundation death ratios. These high death ratios are particularly unfortunate because most of our interview areas (except for the southeastern coastal plains) are within a 10- to 20- minute walking distance of safe highlands. To understand the causes of the high number of deaths, survivors were interviewed at public evacuation shelters in six cities in mid- April and early June 2011 (Figure 1a). The interviewees, 117 of whom had been in headland and bay areas and 2 of whom had been in the coastal plain at the time of the earthquake, were asked about their own evacuation behavior and that of people whom they had observed. Among 119 interviewees, 37% evacuated to areas that proved to be safe promptly upon feeling very strong and long shaking or receiving tsunami warnings, 29% evacuated to areas with only slight problems, 23% evacuated only after seeing the incoming tsunami that was approaching behind them, and 4% were swept away by the tsunami but were eventually saved. The other 7% of interviewees did not need to evacuate because they had been outside of the affected area when the tsunami hit.

The interviews made it clear that many deaths resulted because current technology and earthquake science underestimated tsunami heights, warning systems failed, and breakwaters were not high enough. However, even if these problems occur in future earthquakes, better knowledge regarding earthquakes and tsunami hazards, coupled with the inherent human instinct to survive, could save more lives. Such basic information can lead local residents to evacuate sooner, so more people could survive a tsunami. To avoid similar high tsunami death ratios in the future, residents, including young children, should be taught the basic mechanism of tsunami generation.

References

Ando, M, M. Ishida, Y. Hayashi and M. Mizuki, 2011, Interviews with survivors of Tohoku earthquake provide insight into fatality rate, EOS, Transactions, AGU, Vol. 92, No. 46: 411-42, 15 Nov.

Lee, S.-J., B.-S. Huang, M. Ando, H.-C. Chiu, and J.-H. Wang (2011), Evidence of large scale repeating slip during the 2011 Tohoku- Oki earthquake, *Geophys. Res. Lett., 38,* L19306, doi:10.1029/ 2011GL049580.

Usami, T. (2003), *Materials for Comprehensive List of Destructive Earthquakes in Japan, [416]–2001*, translated from Japanese, 605 pp., Univ. of Tokyo Press, Tokyo.

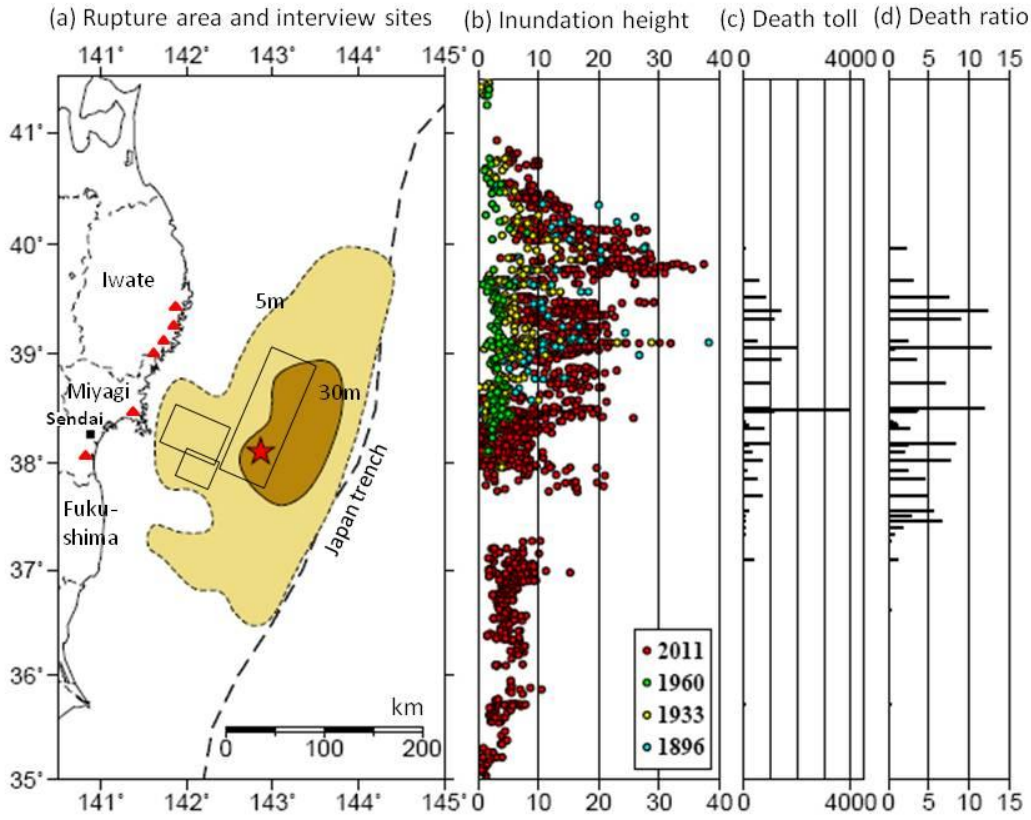

Fig. 1. (a) The rupture area of the 11 March 2011 Tohoku earthquake with 5- meter and 30- meter fault slip contours (Lee et al., 2011). Also shown are the hypocenter of the main shock (star) and the interview sites in this study (triangles). Rectangles are fault planes for the anticipated M 8.0 compound Miyagiken- Oki earthquake. (b) Inundation heights (in meters) along the Japanese coast for the 16 June 1896 (Mw 8.5), 3 March 1933 (Mw 8.4), and 23 May 1960 Chile (Mw 9.5) tsunamis (Usami, 2003) and those of 11 March 2011 (Mw 9.0) tsunami (2011 Tohoku Earthquake Tsunami Joint Survey Group; http:// www.coastal.jp/tsunami2011/). (c) The number of dead and missing persons in each municipality following the Tohoku earthquake. (d) The estimated death ratio (in percent) in the inundation area of each municipality. The figure from Ando et al. (2011).

Current Earthquake and Volcanic Risk Management Activities in the Philippines

Solidum R.U.

Philippine Institute of Volcanology and Seismology, C.P. Garcia Ave., Univ. Philippines Campus, Quezon City 1101 Philippines, rusolidum@phivolcs.dost.gov.ph

The Philippine archipelago is prone to earthquakes, tsunamis and volcanic eruptions due to its geotectonic setting. It has been affected by eruptions from 21 active volcanoes, 90 damaging earthquakes and 40 tsunamis in the past 400 years. These events have caused significant loss of lives and impact to properties and the economy. With the increasing population and rapid urbanization in the country, it is important that earthquake and volcanic risk management efforts must take a whole of society approach, from the national level to the communities. In 2010, the Philippines has legislated a new disaster risk reduction and management act, which takes a participatory, vulnerability reduction and development approach to disasters, emphasizing the importance of preparedness, prevention and mitigation actions than response, recovery and rehabilitation.

As a contribution to disaster risk management efforts in the country, the Philippine Institute of Volcanology and Seismology (PHIVOLCS) is currently undertaking earthquake and volcanic risk management activities that cover volcano, earthquake and tsunami monitoring and warning, hazards and risk assessment, evaluation of volcanic eruption, earthquake and tsunami potential, development of tools for monitoring or hazard and risk assessment, public awareness and preparedness. Several of these activities are collaborative efforts with national and local governments, non-government organizations, and international partners.

In recognition of the increased awareness of the public and need for appropriate preparedness of coastal communities to tsunamis, PHIVOLCS has conducted a national tsunami hazards assessment, developed awareness and preparedness materials for tsunami, piloted community-based preparedness for tsunami and initiated establishment of tsunami early warning systems for selected areas in the country.

PHIVOLCS and several research institutions from Japan led by the National Institute for Earth Science and Disaster Prevention are implementing a project “Enhancement of Earthquake and Volcano Monitoring and Effective Utilization of Disaster Mitigation Information in the Philippines” under the Science and Technology Research Partnership for Sustainable Development (SATREPS) Program of the Japan International Cooperation Agency (JICA) and Japan Science and Technology Agency (JST), The 5 year project from 2009-2014 has 3 components: 1) to improve on the real-time earthquake monitoring through advanced source analyses, intensity observation and rapid information of earthquake parameters and intensity distribution, 2) to evaluate earthquake generation and tsunami potential through GPS, active faults and tsunami studies, 3) integrated real-time volcano monitoring for Mayon and Taal, and 4) to provide disaster mitigation information and promote its utilization among national organizations, local government units, businesses, communities and the public.

PHIVOLCS has also partnered with other institutions to better understand volcanic activities and processes at Mayon with the Earth Observatory of Singapore (EOS), at Taal with the Electromagnetic Signals for Earthquakes and Volcanoes Working Group (EMSEV) of the IUGG and at Kanlaon with European institutions through the project "Mitigate and Assess Risk from Volcanic Impact on Terrains and Human Activities" (MIA VITA).

PHIVOLCS and other national government agencies have also been implementing since 2005 multi-hazard community-based risk reduction activities in several provinces in the Philippines, as supported by other international partners such as Australian Agency for International Development (AusAID) and United Nations Development Programme (UNDP). Activities typically include 1) multi-hazards and risk assessment, 2) establishment of community-based early warning systems for rapid onset events such as tsunami, 3) and the provision of tools, such as the Rapid Earthquake Damage Assessment System hazard and risk assessment software, and results to national and local governments, and training on how to integrate risk reduction into local development planning process.

Eathquake and Tsunami Hazard Assessment in Coastal Areas of Vietnam and Measures for a Seismic Risk Mitigation

Bui Cong Que, Nguyen Hong Phuong

Institute of Geophysics, Vietnam Academy of Science and Technology, 18 Hoang Quoc Viet street, Cau Giay District, Hanoi, Vietnam

Abstract

In coastal areas of Viet Nam concentrated more 20 milion population, a big cities and industrial zones, many constractios of trasport, petroleum industry and tourism. It is the most important and developed zone of national economy and defence. In order to evaluate the earthquake and tsunami hazard and risk in these areas have been carried out a study of seismicity, seismotectonics, recent geodynamics and detail investigation of structural settings of the active fault systems as a seismogenic zones in the territory of Viet Nam and sorounding sea areas. For a study and analysis of a large number of seismic, geological and geophysical data as well as for deterministic seismic and tsunami hazard and risk assessment the probablistic methods of evaluation and a fault- source model and numerical simulation and modeling are developed and used.

On the results of seismic and tsunami hazard assessment the maps of earthquake hazard (PGA) and tsunami hazard in coastal areas of Viet Nam in scales of 1 : 500.000 and 1 : 200.000 are constructed. These maps indicate the strong differences of seismic and tsunami hazard and risk along coastal areas of Viet Nam such as the north and northeast coastal areas has high and relatively high seismic hazard, the central and south central coastal areas characterized by relatively high tsunami hazard with h = 6- 8 m for a return period of 900 years.

In the base of earthquake and tsunami hazard assessment in the coastal areas, the measures for a seismic risk warning and mitigation have been recommended such as detail seismic and tsunami risk evaluation for the areas of a high hazard, establishment and promotion of the National system for earthquake information and tsunami warning, improvement and modernization of the network of broad band seismic stations in Viet Nam and developing and operating the Centre for earthquake information and tsunami warning located in the institute of Geophysics in Hanoi and connected with the network of a seismic and sea level stations and the tsunami warnig centres in the Asia and Asia-Pacific regions.

References

Bui Cong Que, Nguyen Hong Phuong, Nguyen Dinh Xuyen, 2009. Investigation of tsunami sources capable of affecting Vietnam coasts. Procceding of the South China Sea Tsunami Workshop III (SCSTW-3). Nov. 2009. Penang, Malaysia.

Bui Cong Que, Nguyen Hong Phuong, Nguyen Dinh Xuyen, Tran Thi My Thanh, 2010. Study for earthquake and tsunami hazard assessment in coastal areas of Viet Nam and measures for a seismic hazard and risk mitigation. Report of National scientific research project 2007/G45. Ministry of Science and Technology. Hanoi (in vietnamese).

Application of a GIS for Earthquake Hazard Assessment and Risk Mitigation in Vietnam

Nguyen Hong Phuong

Earthquake Information and Tsunami Warning Centre, Institute of Geophysics, Vietnam Academy of Science and Technology, 18 Hoang Quoc Viet street, Cau Giay District, Hanoi, Vietnam

Abstract

The increase of damages and losses due to earthquake and tsunami is not a contingent phenomenon, but a indispensable consequence of population explosion, high speed industrial and infrastructure development, and other social-economical activities. High seismic risk exposure is particularly focused on megacities, industrial centers located in the areas, vulnerable to earthquake impacts, or coastal zones within radius of tsunamis affection. Therefore, planning and investment for strategies on reduce and mitigation of losses and damages due to earthquake and tsunami now become an urgent issue for many countries in the World. Moreover, these strategies have to be made and implemented before the occurrence of earthquake or tsunami in order to avoid much more expenses for the response and recovery activities.

A fault-source model for deterministic seismic hazard assessment in Vietnam was developed based on a database of seismically active faults, Well and Coppersmith relation between earthquake magnitude and fault's parameters (1994) and 10 attenuation equations for regions with different seismotectonic settings. GIS-based tool was developed to help users in assessing hazard caused by a scenario earthquake assumed to be originated by a tectonic fault. The software allows automatic implementation of various stages in a seismic hazard assessment procedure, such as selection of study region and active fault, definition of a scenario earthquake, and hazard calculation. Use of a GIS makes possible the convenient manipulation of loss estimation data concerning building stock and casualties. Results are portrayed on various reports and maps.

The model has been used to assess seismic hazard and loss estimation in Vietnam at various scales, from regional to urban. Results obtained show the advantages of the methodology and technique used. The estimates of damage and human impacts due to earthquakes can help the decision-makers at local, regional and national levels in:

1. Mitigating the possible consequences of earthquakes;
2. Anticipating the possible nature and scope of the emergency response needed to cope with an earthquake/tsunami-related disaster, and
3. Developing plans for recovery and reconstruction following such a disaster.

Application of deterministic seismic risk analysis based on earthquake scenarios can have important contribution in seismic zoning, urban planning and risk management for high priority areas and mega cities of Vietnam.

References

Nguyen Hong Phuong (2005). Development of a Decision Support System for Earthquake Risk Assessment and Loss Mitigation: the Hanoi's Case Study. International Journal of Geoinformatics, Vol.1, No.1, March 2005, pp.191-196.

Nguyen Hong Phuong, Bui Cong Que (2008). GIS application for deterministic seismic hazard assessment in Vietnam. Journal of Geology, Series B, 31, 32, 171-181, 2008.

Earthquake Risk Management in Thailand; Current Status and Future Implication

Niran CHAIMANEE[a]

[a]*Coordinating Committee for Geosciences Programmes in East and Southeast Asia, CCOP Technical Secretariat. 75/10 Rama 6 Road, Ratchathewi 10400, Bangkok, Thailand*

Thailand is situated in the Southeast Asia region where the cross point of two main earthquake belt is located, the Circum-Pacific and Alpine/Himalaya or Mediterranean/Himalaya seismic zones. (Fig. 1). The Indo-Australian and Eurasian boundary zone comprise the convergent margins, including the Burma oblique subduction zone, Andaman thrust and Sunda arc, to the north west, west and south, respectively. The present tectonic stress regime in Thailand is one of transtension, with opening along north-south oriented basins and right-lateral and left-lateral slip on northwest- and northeast-striking faults, respectively.

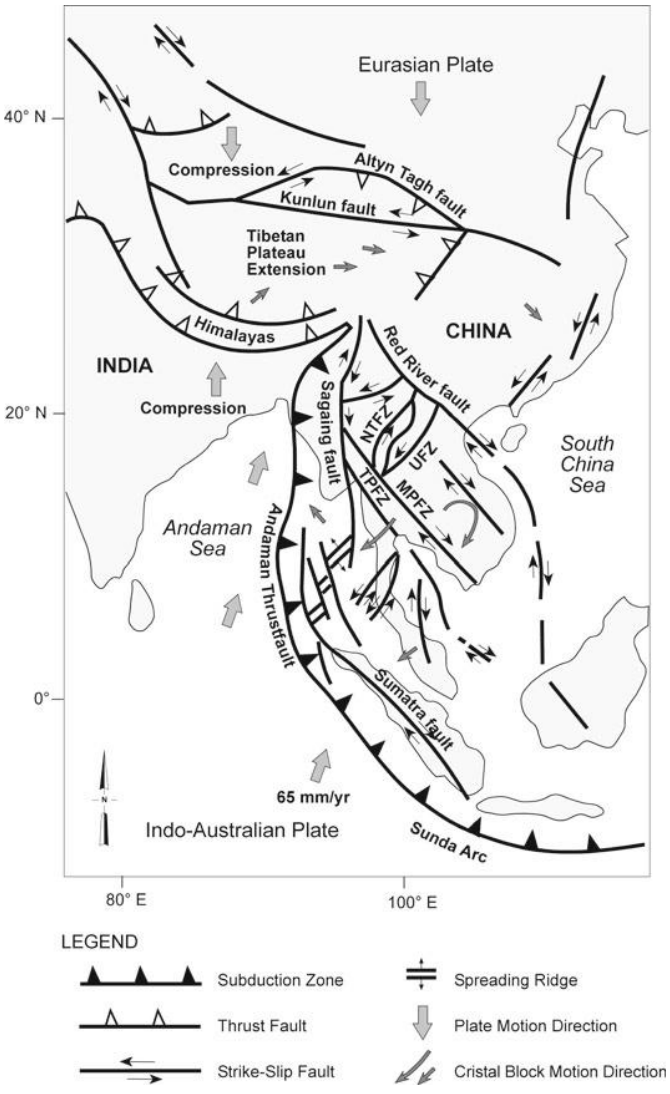

Fig. 1 Major tectonic elements in Southeast Asia and Southern China. *Arrows* show relative directions of motion of crustal blocks during the Late Cenozoic. MPFZ—Mae Ping Fault Zone; NTFZ—Northern Thailand Fault Zone; TPFZ—Three Pagodas Fault Zone; UFZ—Uttaradit Fault Zone. (After Ornthammarath et al. 2010)

Earthquake becomes a common natural disaster that has an extreme and vigorous destruction. One of the causes generating earthquakes is the earth movement along an active fault. In some parts of Thailand, particularly those of the northern and the western regions, earthquake activities were recorded not only by historical/archaeological means but also by instrumental approaches. The coastal areas of Thailand occur along the Gulf of Thailand with a distance of 1,840 km and occur along the west coast of the Thai Peninsular along the Andaman Sea for 864 km. The Andaman Sea coast is a submerging coastline evidenced by the alternation of cliffs and short narrow beaches and drowned valley mouths. The recent 2004 Sumatra Earthquake evidently shows continue horizontal displacement and vertical motion after the earthquake throughout the country (Satirapod et. al., 2008). The assessment, of earthquake impact, ground motion prediction and seismic hazard map were under studying by various agencies and institutions in Thailand. The government regulation and proper measure for earthquake hazards in national level of Thailand will be also discussed.

References

Satirapod C., Simons W.J. and Promthong C., 2008. Monitoring Deformation of Thai Geodetic Network due to the 2004 Sumatra-Andaman and 2005 Nias Earthquakes by GPS. Journal of Surveying Engineering, ASCE/August 2008, 83-88.

Ornthammarath T., Warnitchai P.,·Worakanchana K. and·Zaman S.,2011. Probabilistic seismic hazard assessment for Thailand. · Bull Earthquake Eng., DOI 10.1007/s10518-010-9197-3, 28 pp.

Strategy on Volcanic and Earthquake Hazards Mitigation in Indonesia

Surono

Center for Volcanology and Geological Hazard Mitigation Geological Agency, Jl. Diponegoro 57 Bandung 40122, Indonesia.

Indonesia lies within the collision of three plate tectonics, Indo-Australia, Eurasia and Pasific. As the result, despite the country is enriched with abundant of mineral resources, prosperous land and also decorated with beautiful natural landscape, it also put Indonesia actually prone to geological hazard such as volcanic eruptions and earthquakes. Millions of Indonesian living nearby active volcanoes and in earthquake hazard zones. It is obvious that the strategy on both volcanic and earthquake hazard mitigation is needed.

Center for Volcanology and Geological Hazard Mitigation (CVGHM) of Geological Agency monitors all active volcanoes in Indonesia. The volcanoes are equipped with at least 1 seismometer installed at their flank. The seismic data are transmitted to observatory and head office in Bandung. Some methods such as geochemistry, geophysics and geology surveys are also carried out to support monitoring system. In order to reduce risk due to volcano eruption CVGHM issues early warning system based on instrumental and visual data. The early warning system is defined into 4 alert levels. Level I, it means the activity of the volcano in normal no indication of increasing activity. Level II, the activity tends to increase, though at some volcanoes eruptions may have occurred but threaten only the area around the crater. Level III, if the trend of increasing unrest still continues and eruption may have occurred. At some volcanoes eruptions have occurred but no threatened to inhabitant area. Level IV, when the initial eruption begins to occur as ash/vapor and potentially lead to main eruption, and threaten people living nearby. Aside from alert level, CVGHM also provides volcanic hazard map as a guidance and socialization to people living nearby the volcano.

As for earthquake hazard mitigation CVGHM provides earthquake hazard maps across the country in province scale. The hazard map is created using PSHA methods and developed on EQRM program. The hazard zone is divided into 4, very low earthquake hazard zone, low, moderate and high, respectively.

Creating of Earthquake Hazard Map: An Effort to Mitigate Earthquake Disaster
(Case study: Sulawesi Island Earthquake Hazard Map)

Sri Hidayati, Athanasius Cipta and Rahayu Robiana

Center for Volcanology and Geological Hazard Mitigation Geological Agency, Jl. Diponegoro 57 Bandung 40122, Indonesia

Indonesia occupies an active tectonic zone as the world's three major tectonic plates collides each other. This tectonic condition makes Indonesia an area of pronounced tectonic activity that is prone to earthquakes. Several destructive earthquakes occured in the region during the last decade has caused thousands of casualties, destruction and damage to thousands of infrastructures and buildings. The Aceh earthquake in 26th of December, 2004, which followed by tsunami, accelerates the development in hazard mitigation efforts, as initiated by Indonesia government issued Law No.24/2007 concerning Disaster Management.

The availability of earthquake hazard map throughout the country is a must, since the earthquake mitigation effort is more emphasized on pre-disaster phase. The hazard map is created using PSHA (*Probability Seismic Hazard Assessment*) method and developed on EQRM (*Earthquake Risk Model*) computer program. This method requires inputs of earthquake sources (active fault, subduction zone, diffuse earthquake), site classes and return period. Furthermore GMPE (*Ground Motion Prediction Equation*) for each earthquake zone should be preconcerted.

Earthquake Source Zones are divided into 3 classifications, namely active fault, subduction zone and background. Background is set to accommodate diffuse earthquakes. Fault is a 3D earthquake source model where in distance probability measurement is considered as distance from hypocenter to site. Parameters using for probabilistic analysis are fault trace, slip-rate, dip and dimension of fault. For Sulawesi Island purpose, 10 active faults both onland and sea fault are used (Figure 1). While subduction zone is a model obtained from well determined seismotectonic data. Parameters needed for this source model are subduction area, dip, slip rate, a- and b-value that calculated from historical earthquake and the depth of subduction slab.

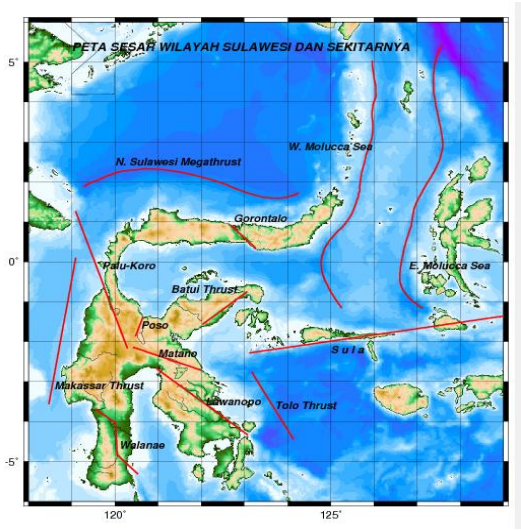

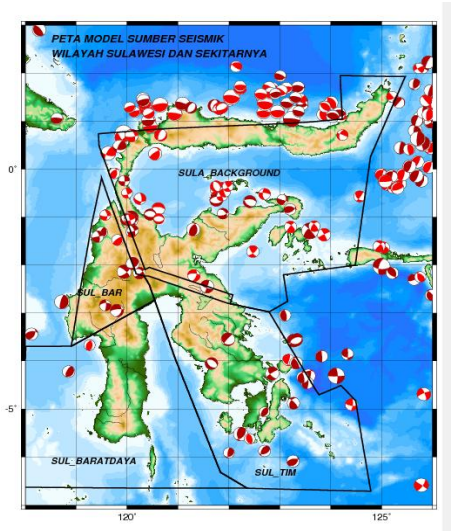

Figure 1. Fault and Subduction traces used in simulation (left) and background source model (right)

Background source model is used to accommodate earthquake which may occur randomly out of the fault zone, and also to predict larger scale earthquake which occurred near the location of small and medium historical earthquakes. Background source model is fit for unidentified source parameter of earthquake which occurred in history.

Site classes are determined by considering geological and morphological aspects. Those aspects are used to construct geomorphic class, and then estimated-vs30 for each grid point is calculated. Based on availability of geological and topographic maps, the geomorphic classifications are introduced as in Table 1 below. Geomorphic map of Sulawesi Island with 1.1 km of resolution were developed and shows that Sulawesi were divided into 14 geomorphic classes (Figure 2). Furthermore estimated-vs30 is calculated from geomorphic class, and then site class is arranged as NEHRP (*National Earthquake Hazard Reduction Program*) classification.

Tabel 1. Geomorphic Classification

SLOPE	**ELEV**	**LITHOLOGY**	**GEOMORPHOLOGICAL UNIT** (Wakamatsu et al, 2006)	**NOTES**
>15	>700	T products	Mountain (1a, 1b)	independent to lithology
	<700	T products	Hill (3)	independent to lithology
		Volcanic (Q)	Volcanic Hill (6)	
5-15			Mountain footslope (2)	independent to lithology
		Volcanic (Q)	Volcanic footslope (5)	
≤5		Alluvium, colluviums, fluvial etc	• Valley bottom lowland (10) • Alluvial fan (11) • Back marsh (13) • Abandoned river channel (14) • Delta and coastal lowland (15) • Marine sand and gravel bars (16)	Colluviums fluvial
Active volcano			Volcano (4)	Eruption centers
Terrace			• Rocky strath terrace (7) • Gravelly terrace (8)	• Brecciated, geo. structure • Alluvium, Geo. Structure
		Volcanic ash	Terrace covered by volcanic ash soil (9)	
5-15		Sand (Q)	Sand dune (17)	
Others			• Reclaimed land (18) • Filled land (19) • Natural levee (12)	• Engineered • engineered • Barrier, parallel to river/coast, sand bar

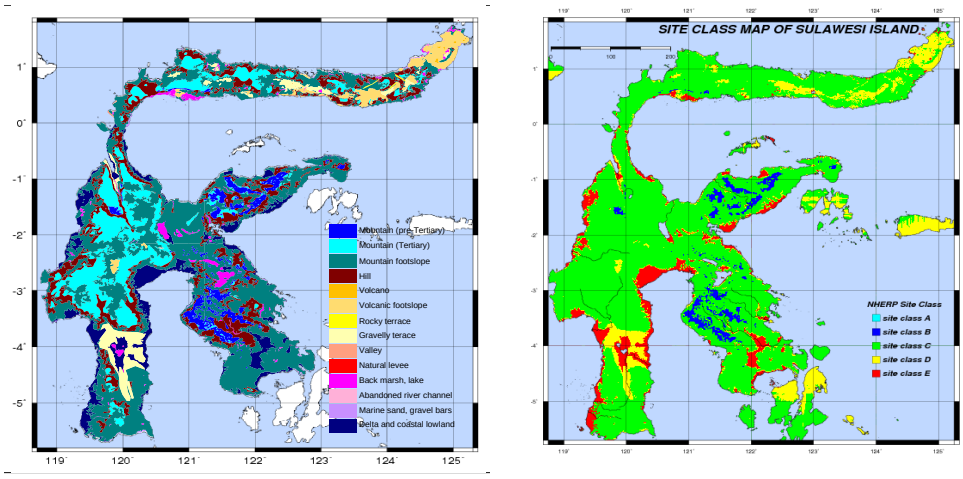

Figure 2. Geomorphic map of Sulawesi (left) and site class map of Sulawesi (right).

Since specific **attenuation functions** for Indonesia are not available yet, the use of attenuation functions from regions which has similar geologic and tectonic condition are inevitable, the attenuation functions are as follow (in Masyhur *et al*., 2010):

a. Shallow crustal for fault source model and shallow background: Boore-Atkinson(2008); Campbell-Bozorgnia (2006); Chiou-Youngs (2008)
b. Subduction interface, for subduction source model: Zhao with variable vs30 (2006); Atkinson-Boore (2003); Youngs, et al (1997).
c. Deep intraslab for deep background source model: Atkinson-Boore (2003); Youngs, at al (1997)

Results

The results are PSHA maps of Peak Ground Acceleration (0.0 second) on bedrock and soil, 0.2 second and 1.0 second spectral accelerations. These maps represent the 10% probability of exceedance in 50 years (475 years return period). The Sulawesi earthquake hazard map were created based on the estimated intensity, which obtained by converting the acceleration level on 1.0 second RSA (*Response Spectral Acceleration*) (Figure 3, left). The hazard levels are divided into four classifications, they are very low (MMI < V), low (VII > MMI ≥ V), moderate (VIII > MMI ≥ VII), and high (MMI ≥ VIII) respectively (Figure 3, right).

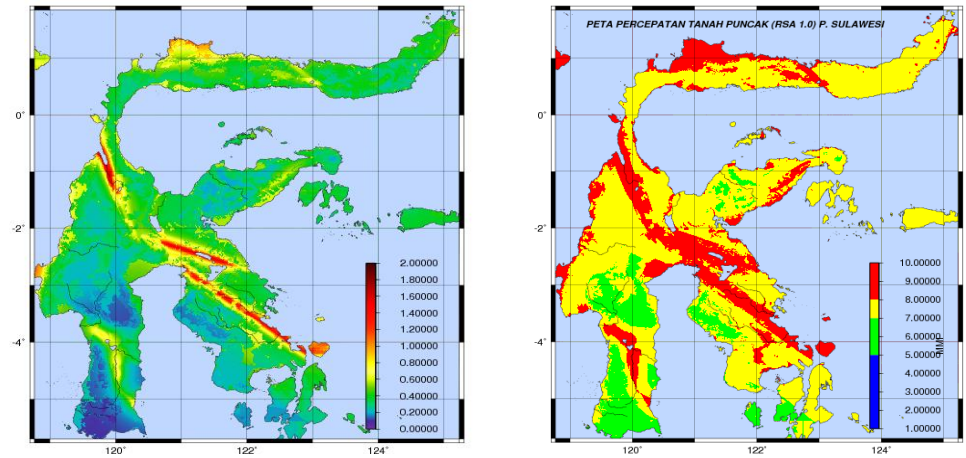

Figure 3. Acceleration map on RSA 0.0 s (left) and Earthquake Hazard Map (right)

References

Irsyam, M., Sengara W., Aldiamar, F., Widiyantoro, S., Triyoso, W., Natawidjaja, D.H., Kertapati, E., Meilano, I., Suharjono, Ridwan, M., 2010, *Summary of Study Development of Seismic Hazard Map of Indonesia for Revision of Hazard Map in SNI 03-1726-2002*, Bandung, Indonesia

Wakamatsu, K. Matsuoka M, K. Hasegawa, 2006, GIS-based Nationwide Hazard Zoning Using the Japan Engineering Geomorphologic Classification Map, Proceedings *of the 8th U.S. National Conference on Earthquake Engineering*, Paper No. 849, California, USA

Vulnerability, Capacity and Community Empowerment in Hazard Zone Areas, A Challenge in Hazard Mitigation in Indonesia

Supriyati Andreastuti

Center for Volcanology and Geological Hazard Mitigation,
Geological Agency, Ministry of Energy and Mineral Resources, Indonesia

ABSTRACT

Indonesia is prone to hazard due to its tectonic setting and geological condition, therefore, it is susceptible to geological disaster, such volcano eruptions, landslides, earthquakes and tsunamis. Areas potential to these hazards are mostly highly populated. The risk becomes higher as those areas also a tourist destination or source of income for people living surrounding. In some cases, less people are living in hazard zone areas with difficult access due to geographic condition, mainly around active volcanoes. These facts are also contributed by infrequent and occasionally long repose activity.

In Indonesia, the increase of frequency and magnitude of disaster events recently, lead to disaster management program become one of national priorities. Improvement of disaster mitigation strategies includes mitigation services and technologies were implemented to develop capacity building of local governments and communities.

In order to carried out effective disaster mitigation, National Disaster Management Agency was established in 2008. In its development, regional (33) and district disaster management agency offices (497) were also established.

Survey on 120 respondents from hazard mitigation officials, those have variation in educations and experiences showed that there were 4 most influence aspects, from the most dominant, are coordination, communication, early warning and types of hazard to dealing with. These indicate that disaster management is important beside how early warning was communicated according to types of hazard. Coordination, cooperation and communication are essential in hazard mitigation to reach optimum result in risk reduction. These are supported by good and effective early warning system and communication amongst stake holders and public to facilitate the process of warning information.

Most problems arise in hazard mitigation activities are understanding early warning and source of information and experience to disaster. These vulnerability factors would affect awareness of communities Therefore, continuous information, training and intensive communication of authorities with public is important to improve capacity and capability of institutions and communities. On the other hand, mitigation activities process becomes more effective where practical involvement of communities, legal and policies were implemented.

In turn successful mitigation need to be supported by urban planning of potential hazard zone areas, empowerment of communities and policies.

Geoscience as a component of an all-of-government approach to recovery from the Canterbury earthquake sequence of 2010-2011

Kelvin Berryman

Director, Natural Hazards Research Platform Manager, GNS Science, Lower Hutt, k.berryman@gns.cri.nz

Abstract

The Canterbury earthquake sequence is the most significant event in New Zealand since World War II. The impacts have consumed >8% of New Zealand's GDP, which, on a per capita basis, are perhaps eight times the impact of Hurricane Katrina on the US economy and four times the economic impact of the recent Tohoku earthquake and tsunami in Japan.

In Canterbury, geoscience information and has contributed significantly to civil defence crisis management and more recently to an all-of-government recovery effort coordinated through the Canterbury Earthquake Recovery Authority (CERA), and regional and local authorities in Canterbury. The earthquake sequence has comprised three main shocks (as of early October), spaced at intervals of several months, each with particular spatial and temporal impacts. The extended duration of the sequence has resulted in major social, community, education, and economic disruption, creating much uncertainty in relation to the feasibility of land remediation in liquefaction damaged areas, and in judging the appropriate time to begin infrastructure, residential and commercial rebuild.

The earthquakes have also resulted, in some parts of the region, ground shaking that has been much more severe than planned for in building codes. The appropriateness of codes, what residual capacity there should be in buildings and infrastructure to protect from rare but potentially catastrophic events, and whether a "city factor" is required to protect the socio-economic function of large cities, also needs input from the geoscience community. Crucial decisions for reconstruction and rehabilitation of communities is requiring substantial and on-going coordinated input from seismologists, geologists, geotechnical engineers, landuse planners, structural engineers, landslide specialists, hazard and risk modellers, and social scientists. CERA is the coordinating agency, and geoscience input to their activities is a feature of this crisis, more so than in any previous natural hazard event in New Zealand.

VHub – a virtual community and cyberinfrastructure for collaboration in volcano research and risk mitigation

Greg A. Valentine, Center for Geohazards Studies, University at Buffalo

VHub (short for VolcanoHub, and accessible at vhub.org) is an online platform for collaboration in research and training related to volcanoes, the hazards they pose, and risk mitigation. The underlying concept is to provide a mechanism that enables workers to share information with colleagues around the globe, thereby building a volcanology "virtual community." Collaboration occurs around several different points: (1) modeling and simulation; (2) data sharing; (3) education and training; (4) volcano observatories; and (5) project-specific groups. VHub is evolving as new capabilities and participating organizations are being added.

Modeling and simulation are playing increasingly important roles in volcano-related work, both for improving our understanding of volcanic processes and for forecasting hazards and risk. Volcanology can be thought of in terms of a hierarchy (Figure 1). At the base (foundation), theoretical and numerical modeling is a tool for basic research, along with experimentation and field studies. Computational fluid dynamics (CFD), for example, is providing important new insights into the dynamics of pyroclastic flows, the hazardous conditions they produce, and the deposits that are left in the geologic record. Such tools are highly complex, require years of expertise to develop and use properly, and are computationally intensive and time consuming. An example of such a CFD model is mfix (see mfix.org), which solves mass, momentum, and energy equations for multiphase flows. Most CFD models are not useful in a practical sense for risk assessment because of these complexities and the difficulty of incorporating many sources of uncertainty that are associated with real situations at volcanoes. Instead, risk assessment commonly must account for a wide range of potential scenarios, processes, and uncertainties, and must be communicated in a straightforward way that can be used by decision makers who might not have a strong background in science and engineering. Thus, the tools at the top of the hierarchy (Figure 1) are highly simplified representations of complex natural processes. At an intermediate level, models that are less complex than first-principles CFD models but that are still focused on specific processes (such as pyroclastic flows, or tephra fallout), are used to explore uncertainties in those individual processes. Two examples of such models are the energy cone model for pyroclastic flows, and Tephra2 for atmospheric dispersion and fallout. Volcanology and risk assessment advance more rapidly when there is strong interaction between the different levels of the hierarchy, for example, when simple risk models are used to identify parameters that produce the most uncertainty in risk, and those parameters are explored in more detail with CFD and intermediate-level models.

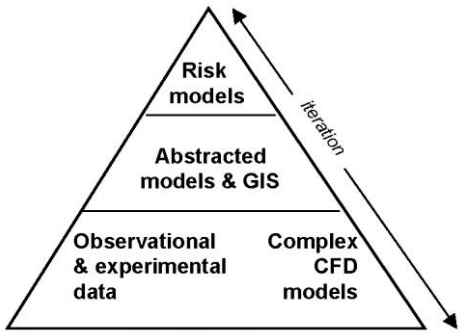

Figure 1. Modeling hierarchy.

VHub promotes modeling and simulation in two ways: (1) middle- and upper-tier models can be implemented on VHub for online execution. This eliminates the need to download and compile a code on a local computer. VHub can provide a central "warehouse" for such models that should result in broader dissemination, including to developing countries where researchers and observatory staff might not have advanced computing equipment or expertise. VHub also provides a platform that supports the more complex CFD models by enabling the sharing of code development and problem-solving knowledge, benchmarking datasets, and the development of validation exercises.

VHub also provides a platform for sharing of data and datasets. The VHub development team is currently working with major global database efforts such as the Smithsonian Global Volcanism Program and Bristol University's VOGRIPA project. The main goal of these collaborations is to use

VHub's online capabilities to promote access, sharing, and analysis of data within those databases. VHub is implementing the iRODS data sharing middleware (see irods.org). iRODS allows a researcher to access data that are located at participating data sources around the world (a "cloud" of data) as if the data were housed in a single virtual database. This approach is being used in several other disciplines; in particular, astronomy provides an analog for where iRODS might lead. In astronomy, observatories (analogous to volcano observatories) around the world are constantly collecting, and locally archiving, data measured by telescopes and other detectors. An astronomer who wants to find all data that exist for a particular location in the sky can access that cloud of data via iRODS. The common link is in the metadata; for this to work in volcanology the community will need to agree on metadata standards and formats, while the raw data themselves can be stored in different formats that suit the local environment.

Education and training is another important use of the VHub platform. Audio-video recordings of seminars, PowerPoint slide sets, and educational simulations are all items that can be placed onto VHub for use by the community or by selected collaborators. An important point is that the "manager" of a given educational resource (or any other resource, such as a dataset or a model) can control the privacy of that resource, ranging from private (only accessible by, and known to, specific collaborators) to completely public. For example, currently there are at least three workshops that have been uploaded onto VHub. One of them is completely private; another is accessible for people who request permission from the manager, and the third is available to anyone. Materials for use in the classroom are being loaded onto VHub. The development team is working on a suite of interactive simulations aimed at illustrating the controls on important volcanic processes. Users of these resources can range from university professors to high school teachers to observatories who are teaching stakeholders about volcanic hazards.

VHub has partnered with three observatories (Pasto Volcano Observatory; Montserrat Volcano Observatory; and Osservatorio Vesuviano). The goal of these partnerships is to ensure that VHub evolves in a way that is useful not just for the research community but also for observatories who have real-world hazard and risk mitigation problems. The observatories have identified the importance of being able to share monitoring data and analysis tools with experts in at other observatories, in a way that provides control of the data. The observatories are also contributing forecasting tools for specific hazards.

Finally, VHub is a very useful platform for project-specific collaborations. For example, a small group of researchers from three institutions are collaborating on a volcanic field in the western USA. They have developed a group site on VHub where they share documents, datasets, maps, and have ongoing discussions using the discussion board function. The group site is set up to be completely private, so that visitors to VHub do not even see the group listed under the "Groups" menu. Conversely, a there is a large effort to develop a user facility for large-scale experiments on volcanic processes. Any visitor to VHub can see this listed as a group, but to participate they must request membership from the group manager. This allows the group to "filter" new members to ensure that they are serious participants.

VHub is a platform that could potentially prove very powerful in collaborating and communicating about circum-Pacific volcanic hazards. It is easy to set up an account at vhub.org and anyone can then organize groups, and upload or use resources. Because VHub is a relatively new effort (began in January 2010, went online in June 2010), the number of available resources is still somewhat small and the format of the site will continue to evolve. However, we hope that VHub eventually becomes a central "hub" for volcano related research and risk mitigation, just as its relative, nanohub.org, has become a central resource for the nanosciences community.

VHub is funded by the U.S. National Science Foundation.

Growth of International Collaboration in Monitoring Volcanic Ash Eruptions in the North Pacific

John C. Eichelberger[a] and Christina Neal[b]

[a]*Volcano Hazards Program, US Geological Survey, MS904, 12201 Sunrise Valley Dr, Reston, VA, USA 20192*
[b]*Alaska Volcano Observatory, US Geological Survey, 4210 University Dr, Anchorage, AK, USA 99508*

Nearly continuous ocean-lithosphere subduction from Japan through the Kuril Islands, Kamchatka Peninsula, Aleutian Islands, and into Alaska creates one of the most geologically active and hazardous regions on Earth. Disasters have resulted from great earthquakes, including three (Kamchatka 1952, Alaska 1964, Honshu 2011) of the five M>9 ever recorded, with destruction spread across the Pacific by tsunamis. More than 200 potentially active volcanoes in this region threaten aircraft, communities, commerce, and infrastructure, with multiple eruptions occurring in a typical year. Among the larger historical eruptions are Usu in 1663 (3 km^3 bulk volume), Bezymianny in 1956 (3 km^3), Tolbachik in 1975 (2 km^3), and Katmai in 1912 (30 km^3), largest of the 20th century. Impacts of such events transcend national boundaries. Risks from shared geohazards can be minimized by increased cooperation and exchange in monitoring, analysis, and expertise. In the last two decades, great strides have been made by Japan, Russia, and the United States in developing a collaborative approach to detecting and warning of ash eruptions in the North Pacific.

Growth of volcano monitoring in Alaska and the Russian Far East

Although many volcanoes have long been monitored in Japan in recognition of the hazard they present to people and infrastructure on the ground, until about two decades ago the volcanoes of the Russian Far East and Alaska were more often viewed as subjects for scientific research. The eruption of Alaska's Mount Redoubt Volcano in 1989 and the resulting near-disastrous encounter of a Boeing 747 aircraft with an ash cloud changed this perception. Fortuitously, the Alaska Volcano Observatory (AVO), a partnership of the USGS, University of Alaska Fairbanks Geophysical Institute, and Alaska Division of Geological and Geophysical Surveys had recently been established, and one of its first tasks was to increase the level of instrumentation of Redoubt. Despite an accurate short-term warning that an explosive eruption was possible, lines of communication and awareness of the hazard to aviation were clearly inadequate. This prompted efforts within the United States to improve detection of unrest and onset of explosive eruptions, provide rapid and coordinated messages from volcano observatories and weather offices to the aviation industry, and raise awareness of the problem by the aviation industry and the Federal Aviation Administration (FAA). It was also recognized that much of the ash over Alaska and US-managed international air space comes from Kamchatka.

In the aftermath of the 1989-90 Redoubt eruption, AVO received an increase in U.S. Government funding to expand basic monitoring infrastructure and add new capabilities in satellite remote sensing. Scientific and operational staff from AVO and the U.S. National Weather Service (NWS) began to work closely to improve detection and warning of ash events in the North Pacific. In 1993, the first written ash eruption response plan was published, outlining each agency's roles and responsibilities during an eruption. In addition to AVO, NWS, and FAA, the current plan includes the U.S. Air Force and Coast Guard, and the State of Alaska environmental and emergency response agencies. Beginning in 1996, with additional funding from FAA for AVO, monitoring networks were established solely because of the threat posed to aircraft, probably for the first time worldwide. At present, 30 of the 52 historically active volcanoes in Alaska are monitored by real-time seismic networks, some with continuous GPS and webcams as well.

The 1990s also saw widespread recognition of the threat from active, explosive Russian volcanoes prompting a Russian-US collaborative effort to establish two eruption monitoring and reporting scientific organizations in the Russian Far East. The Kamchatka Volcanic Eruption

Response Team (KVERT) was founded in 1993 in Petropavlovsk-Kamchatsky, involving staff of the Institute of Volcanic Geology and Geochemistry (IVGG, now the Institute of Volcanology and Seismology or IVS) and the Kamchatka Experimental and Methodical Seismological Department (KEMSD, now the Kamchatkan Branch of Geophysical Survey or KBGS). The Sakhalin Volcanic Eruption Response Team (SVERT), based at the Institute of Marine Geology and Geophysics in Yuzhno-Sakhalinsk, became operational in 2004. Both organizations took advantage of the large body of knowledge and expertise about Russian volcanoes whose development began in the Soviet era and continues now with increasing participation by Japanese and American scientists. SVERT relies primarily on satellite remote sensing to monitor the Kuril volcanoes. KVERT and KBGS colleagues maintain seismic instruments and a number of webcams on the more active Kamchatka and northern Kuril volcanoes, and conduct regular satellite surveillance. Despite hundreds of ash clouds produced in Kamchatka and the Kurils in the past 20 years, no significant, damaging encounter by aircraft has occurred.

To improve communication to meteorological authorities and the aviation industry, AVO and KVERT now use a highly formatted message called a Volcano Observatory Notice for Aviation (VONA) that contains only the critical information needed by pilots, dispatchers, and other aviation managers pertaining to an ash event. The VONA has been accepted by the International Civilian Aviation Organization (ICAO) and encouraged for adoption around the world. AVO, KVERT, and SVERT also use a four-step color code for aviation warnings, ranging from GREEN for repose to RED for explosive eruption or explosive eruption imminent. This system is likewise endorsed by ICAO.

Japan-Kamchatka-Alaska Subduction Processes (JKASP)

As international collaborations and awareness of geohazards grew, volcanologists and seismologists from Hokkaido University, the Institute of Volcanology and Seismology (then IVGG), the University of Alaska Fairbanks, and the USGS began a series of approximately biennial week-long JKASP workshops. The founding meeting was held in Petropavlovsk-Kamchatka in 1998, and the series in 2011 began its third cycle through Petropavlovsk-Kamchatsky, Sapporo, and Fairbanks. The purpose of the workshop series is to create a geoscience community and promote collaborative science where, because of great distances and political obstacles, little had existed before. Another primary goal was to provide opportunities for students to learn how to do science in the harsh environment of the northern Pacific region and to appreciate the importance of international collaboration and understanding other cultures.

An early achievement was the founding by the University of Alaska Fairbanks, Kamchatka State University, and Hokkaido University of the International Volcanological Field School. The school has held sessions in Kamchatka, Hokkaido, and Alaska, currently with annual two-week, for-credit summer sessions at Mutnovsky-Gorely volcanoes in Kamchatka and Katmai National Park in Alaska. Although originally intended for students from Japan, Russia, and the U.S., it is now providing field experience at active volcanoes for hundreds of students from all over the world. Another product of JKASP workshops was a volume of papers on the region jointly edited by Russian, Japanese, and American scientists and published by the American Geophysical Union. The workshops also encouraged and/or provided a forum for many bilateral projects, including Russia-Japan work in the Kurils; Russia-US investigation of Bezymianny Volcano; Russia-US study of paleotsunamis; and an ambitious Germany-Russia land and sea investigation encompassing neotectonics, geology, and geochemistry known as Kuril-Kamchatka and Aleutian Marginal Sea – Island Arc Systems (KALMAR).

JKASP-2011 had as its theme “Mitigating Risk through International Volcano, Earthquake, and Tsunami Science”. Abstracts for the meeting provide a comprehensive summary of recent and ongoing projects and are available at http://www.kscnet.ru/ivs/slsecret/jkasp_2011/index_eng.htm.

Development of Volcanic Ash Advisory Centers (VAACs)

In response to in-flight engine failure incidents, the International Civil Aviation Organization (ICAO) and its International Airways Volcano Watch program (IAVW) created nine Volcanic Ash Advisory Centers (VAACs) in the mid-1990s. The nine VAACs are responsible for issuing rapid formal notices to aviation when volcanic ash in the atmosphere is a threat. The Tokyo, Anchorage, and Washington VAACs must work in close coordination as ash from Russian and Alaskan volcanoes can rapidly transit all three VAAC areas of responsibility. VAACs use volcano-observatory reports, pilot reports, geostationary and polar-orbiting satellite data, and ash-dispersion models as the basis for their advisories. As an ash cloud drifts downwind, responsibility for issuing advisories generally passes from one VAAC to the next (Fig. 1).

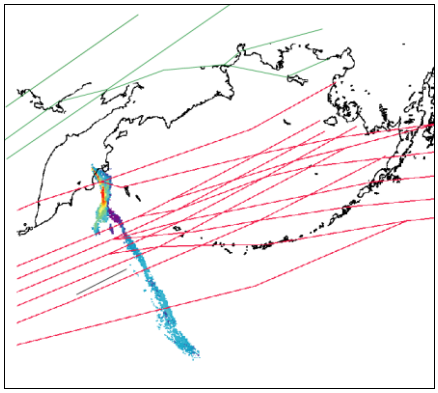

Fig. 1a: Ash plume from 1994 eruption of Kliuchevskoi crossing primary North Pacific air routes (D. Schneider, USGS)

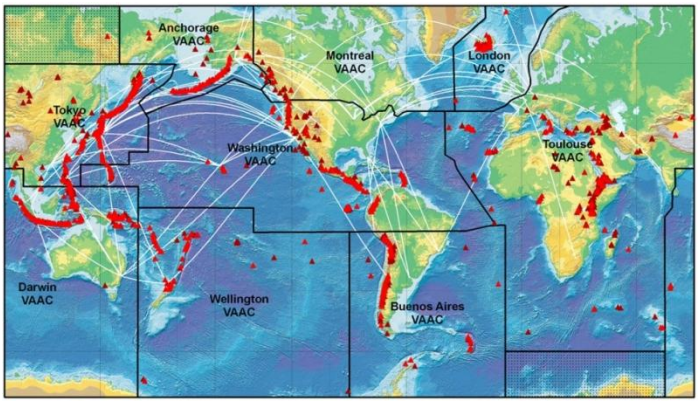

Fig. 1b: Areas of responsibility for Volcanic Ash Advisory Centers (VAACs). Ash clouds from Japan, Kurils, Kamchatka, and Aleutian arc volcanoes first traverse airspace that is the responsibility of the Tokyo, Anchorage, or Washington VAAC. Red triangles are active or potentially active volcanoes.

A recent example of coordinated international response in the North Pacific

The 2009 eruption of Sarychev Volcano in the central Kurils was a successful recent example of international cooperation during a dangerous explosive eruption. The location of this eruption and drift of ash clouds in nearly all directions required multiple VAACs, Air Route Traffic Control Centers, and Meteorological Watch Offices to issue warning messages, posing significant challenges to message coordination. Formal aviation warnings were the immediate responsibility of the Tokyo VAAC and the Aviation Meteorology Centers (AMC) in Petropavlovsk and Yuzhno-Sakhalinsk; the Washington and Anchorage VAACs began issuing alerts when ash neared and entered their areas of responsibility. SVERT assigned an aviation level of concern color code and provided updates on the ongoing activity via e-mail messages to international aviation and meteorological agencies and local authorities. Lacking any ground-based monitoring equipment, SVERT relied on satellite observations to track the eruption. SVERT Information Releases were posted on the web and mirrored on the website of AVO. AVO staff also conducted telephone call-downs to US aviation and meteorological authorities to assist in disseminating key information about the eruption and path of the ash cloud, also assisting in the monitoring of the region through satellite imagery in their twice daily remote sensing reports. Despite multiple ash clouds above 8000 m altitude and many hundreds of flights crossing the region during the period of eruption, no aircraft encountered ash during flight.

Lesson of Eyjafjallajokul

The Icelandic eruption of 2010 demonstrated that volcanic ash clouds from a small eruption of a well-monitored volcano can paralyze the aviation industry and a continent. A combination of unfortunate weather patterns, limitations in the accuracy and validation of ash cloud models, and a

complicated air traffic management environment led to a dramatic shutdown of airspace. Ripple effects were felt worldwide because of the huge volume of traffic that normally moves into and out of Europe. Gaps in planning and challenges validating model forecasts in real time were contributing factors to the largely economic disaster, estimated at 5 billion Euros.

Relative to trans-ocean air routes and neighboring continents, the position of Iceland in the North Atlantic is analogous to that of the Aleutians in the North Pacific. Lesser disruption due to recent historical events in the North Pacific, however, does not mean we are adequately prepared. Indeed, only a third of the potentially active volcanoes of Alaska and Russia are monitored by *in situ* networks. Satellite remote sensing, while of enormous value, is limited by weather and access to data in real-time. Not all Observatories are 24/7 operations and challenges in communication across languages and time zones persist. Inconsistent techniques of analysis and reporting lead to occasional confusion among recipients of warning messages and insufficient and/or interrupted funding make frequent interaction with counterparts problematic. Moreover, against this backdrop of challenge is an ever increasing vulnerability as population, air traffic, and global economic interconnectedness continue to grow.

A way forward

Volcanologists, meteorologists, and air traffic authorities in our region can be proud of the high level of vigilance and responsiveness in the face of nearly constant volcanic activity and increasing vulnerability. To meet these ongoing challenges, however, we support efforts to encourage a more coordinated and formal international approach to mitigating the risk from eruptions in the North Pacific. Specifically, we suggest the following initiatives and emphases that would require contributions from all involved:

1. Make bilateral (US-Russia and Russia-Japan and US-Japan) agreements to share expertise, technology, real-time monitoring data, and lessons learned and exchange personnel in order to: (1) improve our collective ability to assess and warn of eruptions, (2) modernize and expand monitoring networks and adopt best practices, (3) further interoperability and a clear, coordinated response.

2. Develop a consistent format and reliable mechanism for global daily volcano observatory reporting coordinated by the World Organization of Volcano Observatories (WOVO). Unlike the better integrated meteorological field with its World Meteorological Organization (WMO), WOVO is an unfunded, wholly volunteer commission of a scientific society.

3. Collaborate to increase access to satellite remote sensing data from all international sources in as near real-time as possible, with a particular emphasis on Synthetic Aperture Radar (SAR), which can image volcanoes through weather, ash, and steam clouds. One step to improve data access is to apply for designation of the region as a Natural Laboratory of the Global Earth Observing System of Systems.

4. Seek ways to involve young scientists and students to ensure continuity and vitality of volcano hazard science in the region.

Such approaches will help to mitigate earthquake and tsunami risk as well.

EOS activities toward Volcanic Risk Mitigation

C.G. Newhall

Earth Observatory of Singapore, Nanyang Technological Univ., 50 Nanyang Ave, N2-01a-10, Singapore 639798

The Earth Observatory of Singapore (EOS) was established in early 2009, in response to concern in Singapore raised by the December 2004 Andaman-Sumatra earthquake and by rising global concern about climate change. The chief proponent and now-Director is Prof. Kerry Sieh, and there are three broad science subgroups, Tectonics (led by Prof. Paul Tapponnier), Volcanism (led by myself), and Climate (group leader not yet selected).

EOS' mission is scientific research toward a safer and more sustainable world. That's a lofty goal. Each of our groups is defining how it can best – but also realistically -- contribute toward this goal. In the volcano group, my colleagues and I have opted to have four main projects:

- Laboratory Volcanoes
- Magma Plumbing
- WOVOdat, and
- Exploratory Volcano projects. This last project is a composite of several small projects.

Because Singapore has no active volcanoes of its own (!), we have arranged with colleagues from neighboring countries to work with them on several volcanoes that we think have special lessons to tell and where improved knowledge would improve forecasts (by host-country scientists) and public safety. All of these were selected for their position along a spectrum of degassing behavior, from open to plugged, because degassing behavior has a major influence on eruptive style and hazard. We have started work with PHIVOLCS at Mayon (open degassing); and with CVGHM at Gede (semi-plugged); and Salak (plugged). We are proposing to work also at Ulawun (open degassing) with colleagues from RVO and Australia. Each project will develop multiparameter monitoring infrastructure and geologic/petrologic knowledge that will make these laboratories for future studies. Since other foreign groups have similar interests we will in some cases be coordinating and sharing data with other groups, in addition to PHIVOLCS, CVGHM, and RVO.

The Magma Plumbing project, led by Dr. Fidel Costa, will focus on the timescales and rates of magma processes, based on disequilibrium features in the minerals and on correlation of crystal stratigraphy, diffusion, and reaction rims with instrumental monitoring data. This project will work on the Laboratory Volcanoes and on selected other volcanoes.

The WOVOdat project is presently hosted by EOS. It is compiling the collective monitoring experience of the world's (WOVO) volcano observatories into a centralized, web-accessible, easily searchable database. Its two main uses will be for research on pre-eruptive unrest, and for reference during volcanic crises. Those who attempt probabilistic forecasts of eruptions will find a wealth of cases in WOVOdat that can be translated into probabilities for progressive, early nodes on an event tree, e.g., the annual probability of unrest at a given volcano, and the conditional probabilities that unrest is of magmatic origin, that magma will erupt, and that it will do so with a specified Volcanic Explosivity Index (VEI).

The design and pilot testing of WOVOdat is complete, and we are now in the enormously challenging data population stage. We seek only historical data – those which are 2 years old or older. The purpose of this latency or grace period is so that scientists who collect the data have time to analyse and publish them first. We also seek only processed data, e.g., earthquake catalogue data rather than waveforms, though a few representative waveforms from each volcano are welcome. Even after 2 years, raw data are kept by the observatories, and "ownership credit" of the processed data remains with the observatory. WOVOdat is not intended as the primary source of data about any single volcano; its purpose is primarily for comparisons, searches for patterns across many volcanoes, etc.

We have had early WOVOdat assistance from NIED and GSJ (AIST), and have had preliminary discussions with JMA and university colleagues. To date, only a very small amount of data from Japan has been compiled into WOVOdat and we certainly hope to add the extensive volcano monitoring experience of Japanese observatories and scientists.

The Exploratory projects are varied. A few are ongoing explorations, e.g., using JAXA/ GoSAT (Ibuki) data to estimate volcanic CO_2 emission from space. This is not easy, and to date there are only a few cases where the PI (Florian Schwandner) has been able to correlate CO_2 with SO_2 and to make preliminary estimates of CO_2 outgassing. Other exploratory projects are short, one-off, relatively narrow field projects, e.g., describing and dating a specific debris avalanche deposit, or following up with ground truth after InSAR detected inflation, or capturing scientific lessons from an eruption.

We are a start-up group that is gradually defining useful niches in which we can make our best contributions. We want to be collaborative and to be good neighbors.

Recent volcanic crises in the USA and Europe: some case studies

B.F. Houghton[a], R.J. Carey[a,b], T. Thordarson[c]

[a] *National Disaster Preparedness Training Center, University of Hawai`i, Honolulu, HI, USA*
[b] *CODES, University of Tasmania, Hobart, Australia*
[c] *School of Geosciences, University of Edinburgh, Edinburgh, United Kingdom*

Eyjafjallajökull 2010

The 2010 eruption of Eyjafjallajökull volcano, in Iceland, was of low intensity (VEI 3), but long-lived, with two episodes over 52 days. Locally the eruption was well anticipated. Iceland had experienced a diverse range of eruptions in the last 3 decades and the volcano was well monitored. The net result was knowledge that this eruption was likely to occur about 3 years beforehand, and that the eruption was imminent in late 2009. Prior to 2010, volcanic hazard assessments (2003-2005), evacuation planning (2005-2006) and testing (2009-2010) of the systems occurred. Internationally, severe disruption to international air traffic led to an unprecedented breakdown of global airspace with a $5 billion cost.

The international impact was both severe and unanticipated. On 15 April 2010, about 80% of Europe's aircraft were grounded for six consecutive days, causing the highest level of air travel disruption since the Second World War. The 2010 eruption showed how even eruptions of low mass eruption rate (MER) have significant impacts. During the second phase of the eruption much of European airspace was closed due to the drifting volcanic plume and some 180,000 flights were cancelled at a total cost of at least 1.5 billion €.

Figure 1: Eruption of Eyjafjallajökull volcano showing the two characteristic hazards associated with episode 2: Plumes containing fine ash rising to up to 8 km elevation and jökulhlaups (glacial floods). *Photograph: Magnús Tumi Guðmundsson, University of Iceland.*

The response to an ash and aviation crisis is challenging, and changes since 2010 include: i) better understanding of the behaviour of ash, its effects on jet aircraft, as well as its dispersion; ii) definition of responsibilities and roles within and between agencies; and iii) information distribution and dissemination in a coordinated and timely fashion.

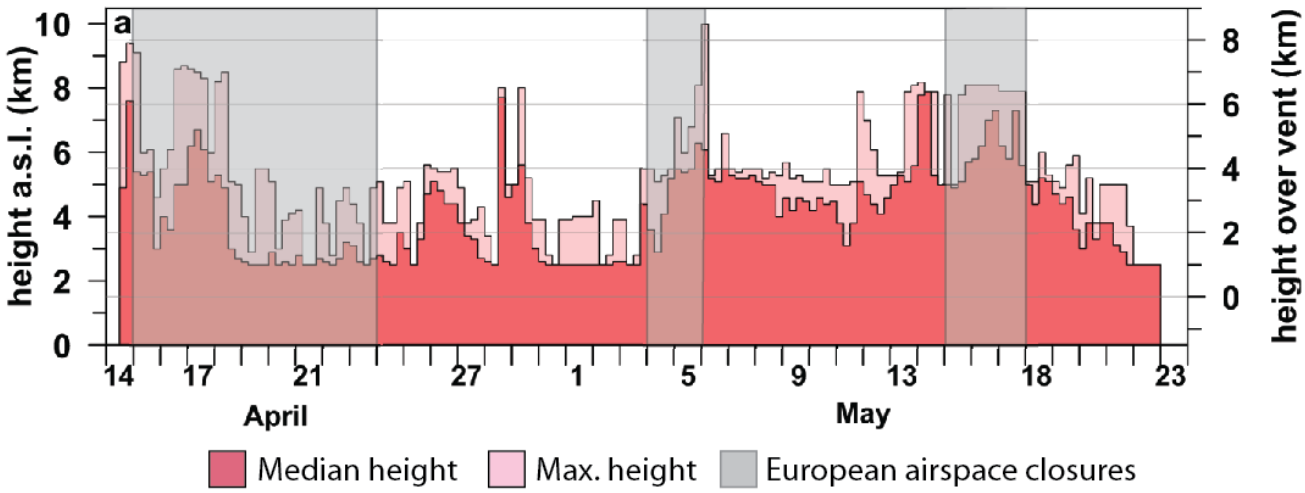

Figure 2: A plot of the maximum and median plume height in kilometers (vertical axis) versus time in days throughout April and May 2010 (horizontal axis). *Thorvaldur Thordarson, unpublished data*.

St Helens 2004-2008

The onset of renewed activity at Mount St. Helens in 2004 was extremely newsworthy as the catastrophic eruption of May 18, 1980 was still fresh in the minds of many people. Public and media interest necessitated an intensive response from emergency managers, public officials & USGS scientists.

Figure 3. The intense media response to the re-awakening of Mount St. Helens. *Photograph Cascades Volcano Observatory, U. S. Geological Survey.*

In the face of uncertainty, this eruption entailed a crisis of crowd and information control, rather than a serious threat to public safety. Uncertainty associated with eruption size and duration was difficult to communicate. The public has very little real experience with volcanoes on which to base their thinking.

The situation brought on a rapidly changing communication situation which required timely flow of information to emergency responders. The situation was in flux and there was always at least a short lag time between the event, its interpretation, and restatement to the media and public. There was a wide range of public response that ranged from curiosity to fears of a 1980-like eruption. These concerns were common among officials as well as the public and required careful attention. Crowd control (visitors and media) was a major challenge for response agencies. Additionally, the media desired frequent access to scientists—from before sunrise through sunset—to satisfy TV programming needs. Since there was no declaration of emergency, no supplementary funding for response was provided to agencies.

Figure 4: Changes of media interest associated with different information statements and physical changes of activity at St. Helens. Volcano seismicity is shown as the red line. The number of contacts with the CVO website is shown as the grey colored histogram. *Data source: Cascades Volcano Observatory, US Geological Survey.*

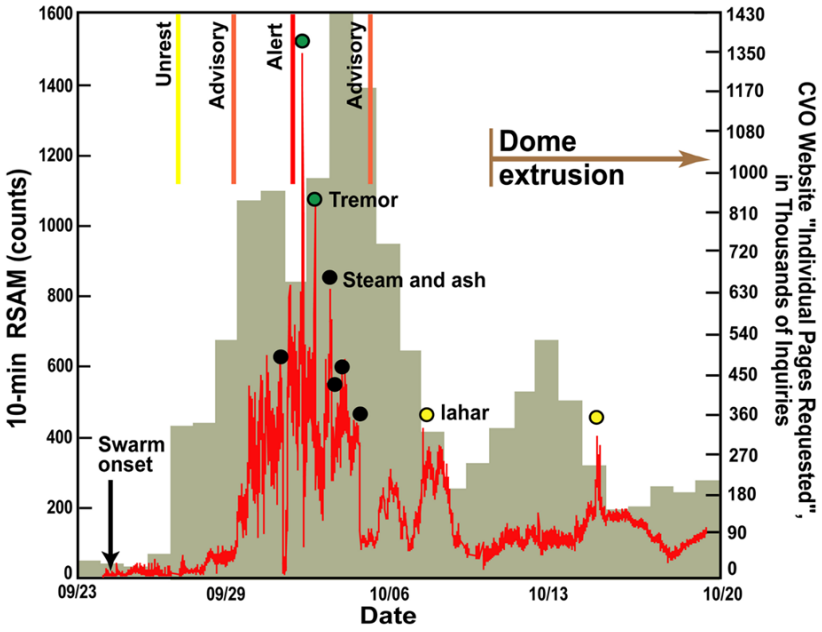

Redoubt 1989-1990

The Redoubt case study has been chosen to illustrate that if monitoring, research and outreach occur and are communicated well pre-eruption crisis, volcanic crises can be mitigated successfully. Due to the high occurrence rate of eruptions in Alaska (~ 1 per year) collaboration, communication and interaction between different agencies in Alaska has been established and well practiced. Interagency partnerships are effective with a record of successfully mitigating hazards associated with airborne ash.

Heightened activity began in July 2008 in a typical fashion with increases of both gas emissions and seismic activity. 8-9 months of precursory activity facilitated alert levels changes to proceed gradually. The eruption began with a minor explosion of steam and ash on March 15. A major explosive event occurred on March 22, and subsequently AVO recorded more than 19 explosions.

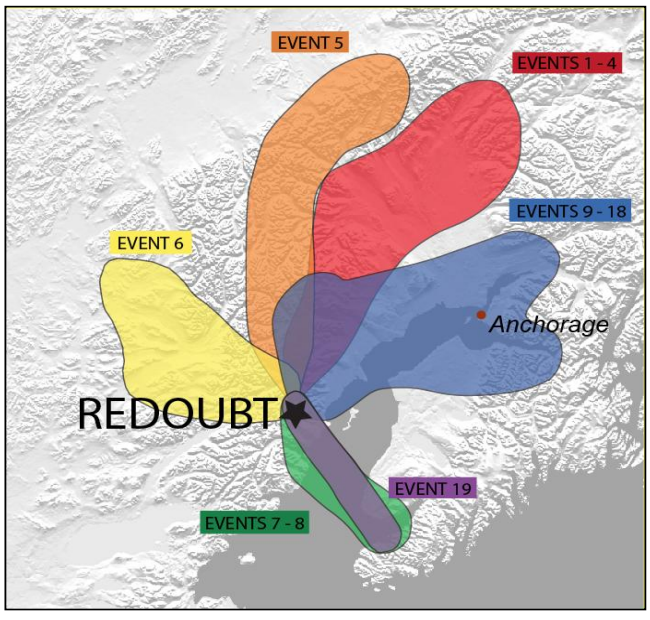

Figure 5. The map shows the ash fallout lobes mapped by Alaska Volcano Observatory staff for different phases of the 1989-1990 Redoubt eruption. Ash fall impacts to Anchorage were mostly on 25-28 March and 4 April 2009, however relatively light ash falls impacted several rural communities, and infrastructure. Ash fall in Anchorage had minor health and economic impacts. *Kristi Wallace, U.S. Geological Survey.*

Plume heights exceeded 15 km (50,000 feet) on many occasions. The largest explosion occurred on April 4, lasting > 30 minutes, and was comparable in size to the largest event of the 1989/1990 eruption. Three major lahars occurred on March 23, March 26, and April 4, which inundated the Drift River valley and reached the Cook Inlet and affected the Drift River Oil Terminal. After the April 4 explosive event the growth of the lava dome continued for approximately 3 months.

The economic impacts to the region were significant due to the length of the eruption and the ash fall on Anchorage during 25-28 March and 4 April. Kenai ash fall resulted in business closures; however some businesses reported increased sales as residents prepared themselves by purchasing emergency and ash cleanup supplies. The timing, spring and early summer, resulted in a loss of tourism revenue. Interruption to aviation between 22 March and 5 April was intermittent, and led to flight route changes and cancellations. More significantly, the complete closure of Anchorage airport on 28 May resulted in economic impacts of over $2M. .

Acknowledgements: The case studies were assembled with Carolyn Driedger, John Ewart, Cynthia Gardner, Christina Neal, Willie Scott, and Kristi Wallace and Chris Waythomas, from U. S. Geological Survey, and Magnús Tumi Guðmundsson, of University of Iceland, for a FEMA-supported Volcano Crisis Awareness course.

References

Devenish, B. 2010. NAME predictions of ash dispersion from Eyjafjallajökull. 2010 Fall Meeting, American Geophysical Union, San Francisco, USA.

Höskuldsson, Á. 1999. Áhrif eldgosa á Íslandi á flugsamgöngur yfir Norður Atlandshafi – Skýrsla fyrir samgönguráðuneytið. (Effects of Icelandic eruptions on air traffic across the North Atlantic – A report prepared for the Iceland Ministry of Transportation). South Iceland Institute of Natural History, 37 pp.

Mastin, L.G.; Schwaiger, H.; Denlinger, R.P. 2010. Why do models predict such large ash clouds? An investigation using data from the Eyjafjallajökull eruption, Iceland. 2010 Fall Meeting, American Geophysical Union, San Francisco, USA.

Miller, T. P. and Chouet, B. A., (eds.) 1994. "The 1989-1990 eruptions of Redoubt Volcano, Alaska," Journal of Volcanology and Geothermal Research 62: 1-316.

Palsson, T., Conference Summary and Conclusions. Atlantic Conference on Eyjafjalljökull and Aviation. September 2010. http://en.keilir.net/keilir/conferences/eyjafjallajokull

Sherrod, D.R., Scott, W.E., and Stauffer, P.H., eds., 2008, A volcano rekindled; the renewed eruption of Mount St. Helens, 2004-2006: U.S. Geological Survey Professional Paper 1750, 856 p. and DVD-ROM [http://pubs.usgs.gov/pp/1750/].

Till, A. B., Yount, M. E., and Riehle, J. R.. 1993. "Redoubt volcano, southern Alaska: a hazard assessment based on eruptive activity through 1968". U.S. Geological Survey Bulletin B 1995: 1-19.

Waythomas, C.F., Dorava, C., Miller, T.P., Neal, C.A., McGimsey, R.G. 1998. "Preliminary Volcano-Hazard Assessment for Redoubt Volcano, Alaska." US Geological Survey Open-File Report 97-857.

VOGRIPA and the 'Global Volcano Model'

Steve Sparks[a], Sian Crosweller[a], Sue Loughlin[b], Lee Siebert[c], Paul Kimberly[c], Natalie Ortiz[a], Laura Hobbs[a], Koji Kiyosugi[d], Shinji Takarada[e]

[a]*Department of Earth Sciences, University of Bristol, Wills Memorial Building, Queens Road, Bristol, BS8 1RJ, UK*
[b]*British Geological Survey, Murchison House, West Mains Road, Edinburgh, EH9 3LA, UK*
[c]*Smithsonian Institution, Global Volcanism Program, NMNH NHB-119, Washington, DC 20013-7012, United States*
[d]*Department of Geology, University of South Florida, 4202 East Fowler Avenue, Tampa, Florida 33620, United States*
[e]*Geological Survey of Japan, AIST, Site 7, 1-1-1, Higashi, Tsukuba, Ibaraki 305-8567, Japan*

Over 600 million people live close enough to active volcanoes to be affected when they erupt [1-3]. Volcanic eruptions cause loss of life, significant economic losses and severe disruption to people's lives, as highlighted by the recent eruption of Mount Merapi in Indonesia. The eruption of Eyjafjallajökull, Iceland in April and May 2010 illustrated the potential of even small eruptions to have major impact on the modern world through disruption of complex critical infrastructure and business. The effects in the developing world on economic growth and development can be severe. There is evidence that large eruptions can cause a change in the earth's climate for several years afterwards [4,5]. Aside from meteor impact and possibly an extreme solar event, very large magnitude explosive volcanic eruptions may be the only natural hazard that could cause a global catastrophe. The last really significant caldera-forming eruption of this size occurred at the volcano of Tambora in Indonesia in 1815 when over 70,000 people lost their lives. The eruption caused crop failure and food shortages in New England and elsewhere due to summer frosts. A similar eruption or larger explosive eruption today could also have severe regional or global consequences.

VOGRIPA (Volcano Global Risk Identification and Analysis Project) originated as part of the Global Risk Identification Programme (GRIP) under the auspices of the United Nations and World Bank. GRIP is a 5-year programme aiming at improving global knowledge about risk from natural hazards. VOGRIPA is an international partnership led by Bristol University and including the Smithsonian Institution, Geological Survey of Japan, British Geological Survey, University of Buffalo (SUNY), University of South Florida and Munich Re. VOGRIPA is also a formal IAVCEI project. The objectives are to create a spatially-enabled global relational database of volcanic hazards and vulnerability information that can be analysed to show locations at high risk from volcanism, identify gaps in knowledge about hazards and risk, and allow scientists and disaster managers to analyse risk within a global context of systematic information. A database of large magnitude explosive eruptions reaching back to the Quaternary has been created, with extreme-value statistics being used to evaluate the magnitude-frequency relationship, and it includes an assessment of how the quality and completeness of records affect the results. This relational database is anticipated to go on-line and be

interactive from April 2012.

There is now a growing international network developing the Global Volcano Model (GVM) that would make systematic evidence, data and analysis of volcanic hazards and risk widely accessible. In addition to collating and developing more databases, the GVM project will develop analysis and modelling tools to assess volcanic hazard and risk. The GVM project would also complement and interface with other major international initiatives, notably including the Global Volcanism Program of the Smithsonian Institution (USA), VHub (a US-led effort to develop an online collaborative environment for volcanology research and risk mitigation, including the development of more effective volcanic hazards models), WOVOdat (a database on precursors to volcanic eruptions), the Volcano Observatory Best Practice programme and the International Volcanic Health Hazards Network. The GVM project has parallels with the Global Earthquake Model (GEM) in intention and scope of providing an authoritative source for assessing volcanic risk.

References

[1] Tilling, R.I., Peterson, L.W. 1993. Lessons in reducing volcanic risk. Nature, 364, 277-279;
[2] Small, C., Naumann, T. 2001. The global distribution of human population and recent volcanism. Environmental Hazards 3, 93–109;
[3] update to 2009 World Bank population data;
[4} Rampino and Self. 1994. Climate-volcanic feedback and the Toba eruption of ~74,000 years ago.Quaternary Research, 40, 69-80;
[5] Thordarson & others. 2009. Effects of megascale eruptions on Earth and Mars, Special Paper 453, The Geological Society of America.

The role of multidisciplinary research and collaboration for improving the resilience of communities to volcanic risk

David Johnston[a], Graham Leonard[a], Emma Doyle[a], Julia Becker[a], Douglas Paton[b], Kevin Ronan[c], Bruce Houghton[d], Chris Gregg[e], Shane Cronin[f], Tom Wilson[g], Carol Stewart[a], Vicki Johnson[a], Jan Lindsay[h], Gill Jolly[i], Sally Grant[a], Victoria Sword-Daniels[j]

[a]*Joint Centre for Disaster Research, GNS Science/Massey University, Wellington, New Zealand*
[b]*School of Psychology, University of Tasmania, Launceston, Australia*
[c]*School of Psychology, Central Queensland University, Rockhampton, Australia*
[d]*Department of Geology & Geophysics, University of Hawaii, United States*
[e]*Department of Geoscience, East Tennessee State University, United States*
[f]*Massey University, Palmerston North, New Zealand*
[g]*Department of Geological Sciences, University of Canterbury, Christchurch, New Zealand*
[h]*School of Environment, The University of Auckland, New Zealand*
[i]*GNS Science, Taupo, New Zealand*
[j]*Civil Environmental and Geomatic Engineering, University College London, United Kingdom*

Introduction

Significant portions of the world's population are at risk from the impacts of volcanic activity (Witham 2005). While the timing of eruptions may be unknown or uncertain, their impacts and long term effects can be assessed. Recent eruptions, such as Chaiten Volcano, Chile, and Mt. Merapi, Indonesia, have demonstrated the devastating impacts of volcanic activity on nearby landscapes and communities. The 2010 Eyjafjallajökull eruptions, although small by world standards, highlighted the vulnerability of the modern day global society to minor eruptions. Volcanic crises must be planned for using a comprehensive risk management approach that links reduction, readiness, response and recovery activities. In this paper we discuss the importance of multi-disciplinary research to enhance community education programs and emergency response, and highlight three example programs that are utilizing this approach to address these issues at national and international levels.

Over the last few decades it has been recognized that integrated multi-disciplinary research is needed to provide an understanding of the social, economic and cultural factors that influence the development of strong communities that are resilient to the impacts of volcano hazards and able to respond effectively when events occur (Ronan et al., 2000, Gregg et al., 2004, Gaillard & Dibben, 2008). The benefits of a multi-disciplinary approach include: (1) improvements in governance structures and processes, such as policy and legislative frameworks, planning (including land use), governance institutions and leadership; (2) identification of the characteristics that make people, communities, organizations and other social structures resilient, and the impediments that prevent it; (3) improvement in emergency management and disaster relief procedures and processes; (4) more efficient and effective recovery after an event; and (5) improved uptake and value of hazard related research investment. Other less direct benefits include: (6) the capture of emerging trends (e.g., how an aging population effects community resilience and what this means for research and policy); (7) a better understanding of the relationship between economics, resilience and recovery; (8) an assessment of the impact of hazards on society (including social, economic, environmental, cultural impacts); (9) a better understanding of vulnerability and how society perceives its own vulnerability; (10) strengthening of the evidence-base at the research/policy interface; and (11) a better understanding of the linkages between the stakeholders, frameworks and institutions.

Understanding the elements of effective education programs

Public education programs are a key element of an effective risk management strategy (Finnis et al., 2006). For most volcanologists and risk managers, estimates of risk are based on objective analyses of the likelihood of a hazard event and its consequences within a specific area. However, research frequently shows us that there are considerable differences between expert assessments of risk and the way in which risk is interpreted and acted on by individuals and other groups in our community (often including local and central government) (Paton & Johnston, 2006). Social scientists are aware that people's understanding of and response to risk are determined not only by scientific information or direct physical consequences, but also by the interaction of psychological, social, cultural, institutional and political processes. Perceived risk can be amplified or attenuated through the operation of personal, social psychological and community factors. Effective risk management must involve the consideration of the wide spectrum of social factors that determine levels of acceptable risk and influence human behavior. It is important that risk management be seen as a multi-disciplinary activity and that it works, accordingly, to develop models that reflect the dynamic and contingent nature of risk phenomena.

Most public education initiatives focus only on increasing awareness and knowledge about hazards, without addressing the other factors that influence adaptive capacity and resilience. An increased understanding of a hazard is only one aspect that can influence preparation and appropriate response during an event (e.g., evacuation and warning compliance and resilience overall). A significant issue for public education with respect to preparedness is people's *motivation* and *intention* to prepare for volcanic disasters (Paton & Johnston, 2006). Individuals first need to become motivated to confront the hazardous aspects of their environment, and then form intentions to actually make preparations. It is important to understand the beliefs and attitudes that underpin people's responses to risk so that intervention strategies can be targeted to enhance these motivations and intentions, while also addressing any biases that may be present. This may involve strategies that emphasize the salience of hazard issues for community members.

Contemporary research has highlighted that improved preparedness is likely to accrue from enhancing community members' beliefs in the feasibility of mitigating hazard effects through personal actions (i.e., to counter beliefs that hazards have totally catastrophic effects, also known as 'action coping') and enhancing beliefs in personal competency to implement these activities (i.e., self-efficacy) (see Paton & Johnston, 2006). Furthermore, ownership of responsibility for action is an important variable. Changing these factors requires a mix of public education, social policy, training and empowerment strategies. Trust is another important facet in converting preparedness intentions to actions (Paton, 2008). If people have trust in an information source, they are more likely to adopt protective measures.

Linking research activities in emergency management and response

The UN's International Strategy for Disaster Risk Reduction calls for the development of research in the area of warning system effectiveness and improved disaster response and recovery. Recent multiple catastrophes and the difficulty of coordinating responses underscore the urgency of developing appropriate human and technological systems to deal effectively with such disasters. In response to these imperatives, disaster management is maturing from an ad-hoc, practice-based approach into a scientific discipline in its own right. A number of national, regional and international initiatives have been developed to strengthen the links between countries and between disciplines.

During a volcanic crisis situation, response personnel and government or public body officials have to make critical decisions regarding their response in 'naturalistic conditions' that are

characterized by ill-structured problems, uncertain and dynamic environments, and ill-defined and competing goals, all within a short time and high stress environment (Johnston et al., 1999, Crichton & Flin, 2002, Galley et al., 2004). Effective emergency management decision-making is thus critically dependent upon the correct evaluation of event characteristics and an accurate situation assessment. This requires expertise through experience, pre-planning activities and training to recognize both the situation and the appropriate course of action. These characteristics are developed and enhanced through multi-organizational and multi-disciplinary planning activities, collaborative exercises and simulations (Paton & Jackson, 2002), as well as a thorough analysis of past events and response capability.

Finally we discuss three multi-disciplinary programs, which have been developed to address the international and national issues associated with volcanic crises.

IRDR

The Integrated Research for Disaster Reduction (IRDR) (http://www.irdrinternational.org/) is a decade-long integrated research program co-sponsored by the International Council for Science (ICSU), the International Social Science Council (ISSC), and the United Nations International Strategy for Disaster Reduction (UN-ISDR). It is a global, multi-disciplinary approach to dealing with the challenges brought about by natural disasters, mitigating their impacts, and improving related policy-making mechanisms. The IRDR Program endeavors to bring together the natural, socio-economic, health and engineering sciences in a coordinated effort to reduce the risks associated with natural hazards.

Cities on Volcanoes Commission

The International Association of Volcanology and Chemistry of the Earth's Interior (IAVCEI) has a number of commissions working towards reducing volcanic risk. The Cities and Volcanoes Commission (http://cav.volcano.info/) aims to provide a linkage between the volcanology community and emergency managers, to serve as a conduit for exchange of ideas and experience between "volcano cities", and promote multi-disciplinary applied research, involving the collaboration of physical and social scientists and city officials. The Commission is open to all IAVCEI members with no charge for membership. We aim to develop a close link with the International Volcanic Health Hazard Network (IVHHN) and the World Organization of Volcano Observatories (WOVO).

Local Case Study: Auckland, New Zealand

Auckland, New Zealand's largest city and a vital link in the country's economy, is built on the potentially active basaltic Auckland Volcanic Field (AVF). Although the volcanoes in Auckland are small and their eruptions have been infrequent, the risk associated with future activity is very high given the physical and economic vulnerability of Auckland (population 1.3 million; 2006 census). In recognition of this, in 2008 the New Zealand government ran Exercise Ruaumoko, a test of New Zealand's nationwide arrangements for responding to a major disaster resulting from a volcanic eruption in Auckland. The exercise took approximately 18 months to plan, and included the participation of over 120 organizations at local, regional and national levels. Exercise Ruaumoko provided an excellent and rare opportunity to test a large number of mitigation, scientific and technical procedures in this uncertain geological environment. One significant development in volcanic hazard and risk research and volcanic crisis management in New Zealand that evolved out of Exercise Ruaumoko is the 7-year multidisciplinary, multi-agency DEtermining VOlcanic Risk in Auckland

(DEVORA) research program (http://www.iese.co.nz/Volcanology/DEVORA). The program is co-funded by the Earthquake Commission (EQC), Auckland Council, GNS Science and various universities, and aims to provide a much-improved strategy and rationale for appropriate risk mitigation. The program began with a detailed assessment of what is already known about the volcanic hazard and risk in Auckland (see Lindsay 2010), and is now systematically addressing information gaps. An integrated geological model of the AVF is being developed, and a rigorous probabilistic hazard analysis of the AVF is shedding light on the most likely scenarios and patterns in evolution of the field in space and time. The likelihood of Auckland being impacted by ash from other North Island volcanoes is also being evaluated. Over the next few years the new data will be used to develop a risk framework for Auckland, providing local authorities, utility companies, infrastructure providers and the public with a more accurate assessment of their susceptibility to volcanic activity.

References

Crichton, M., & Flin, R. (2002). Command Decision-making. In R. Flin & K Arbuthnot (Eds.), Incident Command: Tales from the hot seat (pp. 201-238). Aldershot, England: Ashgate Publishing Limited.

Finnis, K., Johnston, D., Becker, J., Ronan, J. & Paton, D. 2007. School and community-based hazards education and links to disaster resilient communities. *Regional Development Dialogue* 28: 99-1008.

Gaillard J.-C., Dibben C. eds. (2008) Volcanic risk perception and beyond. *Journal of Volcanology and Geothermal Research*, 172(3-4).

Galley, I., Balm, R., Paton, D. Johnston, D. 2004. The Ruapehu Lahar Emergency Development Plan process: an analysis. *Australasian Journal of Disaster and Trauma Studies*. Online Journal (http://www.massey.ac.nz/~trauma/).

Gregg, C.E., Houghton, B.F., Paton, D., Swanson, D.A., Johnston, D.M. 2004. Community preparedness for lava flows from Mauna Loa and Hualālai volcanoes, Kona, Hawai‘i. *Bulletin of Volcanology* 66: 531-540.

IESE (Institute of Earth Science and Engineering Aotearoa), 2008. DEVORA: About the DEtermining VOlcanic Risk in Auckland project, http://www.iese.co.nz/Volcanology/DEVORA.aspx.

Johnston, D.M., Paton, D., Houghton, B. 1999. Volcanic Hazard Management: Promoting integration and communication. In: Ingleton, J. (ed.), Natural Disaster Management, Tudor Rose, Leicester, England, p. 243-245.

Lindsay, J.M.: Volcanoes in the big smoke: a review of hazard and risk in the Auckland Volcanic Field. in: Williams A.L., Pinches G.M., Chin C.Y. McMorran T.J. and Massey C.I. (eds). Geologically Active. Delegate Papers of the 11th Congress of the International Association for Engineering Geology and the Environment (IAEG). 2010 Taylor & Francis Group, London.

Paton, D. 2008. Risk communication and natural hazard mitigation: How trust influences its effectiveness. *International Journal of Global Environmental Issues*, 8, 2-16.

Paton, D. & Johnston, D. 2006. Disaster Resilience: An integrated approach. Springfield, Ill., Charles C. Thomas.

Paton, D. & Jackson, D.M. 2002. Developing disaster management capability: an assessment centre approach. *Disaster Prevention and Management*, 11(2), 115-122.

Ronan, K.R., Paton, D., Johnston, D.M., Houghton, B.F. 2000. Managing societal uncertainty in volcanic hazards: A multidisciplinary approach. *Disaster Prevention and Management* 9: 339-349.

Witham, C. 2005. Volcanic disasters and incidents: a new database, *Journal of Volcanology and Geothermal Research*, 148, 191-233.

Public Release of Estimated Impact-based Alerts for Global Earthquakes using the U.S. Geological Survey's PAGER System

David J. Wald[a], Kishor S. Jaiswal[a], K. D. Marano[a], and D. Bausch[b]

[a]*National Earthquake Information Center, U. S. Geological Survey, 1711 Illinois Street, Golden, CO, 80401, USA*
[b]*Federal Emergency Management Agency (FEMA), Denver Federal Center, Denver, CO, 80225, USA*

In September 2010, the U.S. Geological Survey (USGS) began publicly releasing earthquake alerts for significant earthquakes around the globe based on estimates of potential casualties and economic losses (Figure 1). These estimates significantly enhance the utility of the USGS Prompt Assessment of Global Earthquakes for Response (PAGER) system, which has been providing estimated ShakeMaps and computing population exposures to specific shaking intensities since 2007. Quantifying earthquake impacts and communicating estimated loss estimates (and their uncertainties) to the public, the media, humanitarian, and response communities are the culmination of several important new, evolving components of the PAGER system.

First, the operational PAGER system now relies on empirically-based loss models that account for estimated shaking hazard and population exposure, and employ country-specific fatality and economic loss functions derived using analyses of losses due to recent and past earthquakes (Jaiswal et al., 2009, 2010). In some countries, our empirical loss models are informed in part by PAGER's semi-empirical (Jaiswal and Wald, 2010) and analytical loss models (Wald et al., 2008), and building exposure and vulnerability data sets, all of which are being developed in parallel to the empirical approach (Jaiswal et al., 2010). Second, human and economic loss information is now portrayed as a supplement to existing intensity/exposure content on both PAGER summary alert messages (available via cell phone/email) and Web pages. Loss calculations also include estimates of the economic impact with respect to the country's Gross Domestic Product (GDP).

Third, in order to facilitate rapid and appropriate earthquake responses based on our probable loss estimates, in early 2010 we proposed a four-level Earthquake Impact Scale (EIS; Wald et al., 2010). Instead of simply issuing median estimates for losses—which can be easily misunderstood and misused—this scale provides ranges of losses from which potential responders can gauge expected overall impact from strong shaking. EIS is based on two complementary criteria: the estimated cost of damage, which is most suitable for U.S. domestic events; and estimated ranges of fatalities, which are generally more appropriate for global events, particularly in earthquake-vulnerable countries. Alert levels are characterized by alerts of green (little or no impact), yellow (regional impact and response), orange (national-scale impact and response), and red (international response). Corresponding fatality thresholds for yellow, orange, and red alert levels are 1, 100, and 1000, respectively. For damage impact, yellow, orange, and red thresholds are triggered when estimated US dollar losses reach 1 million, 100 million, and 1 billion+ levels, respectively.

Finally, alerting protocols now explicitly support EIS-based alerts. Critical users receive PAGER alerts i) based on the EIS-based alert level, in addition to or as an alternative to magnitude and population/intensity exposure-based alerts, and ii) optionally, based on user-selected regions of the world. The essence of PAGER's impact-based alerting is that actionable loss information is now available in the immediate aftermath of significant earthquakes worldwide based on quantifiable, albeit uncertain, loss estimates provided by the U.S. Geological Survey's National Earthquake Information Center (NEIC).

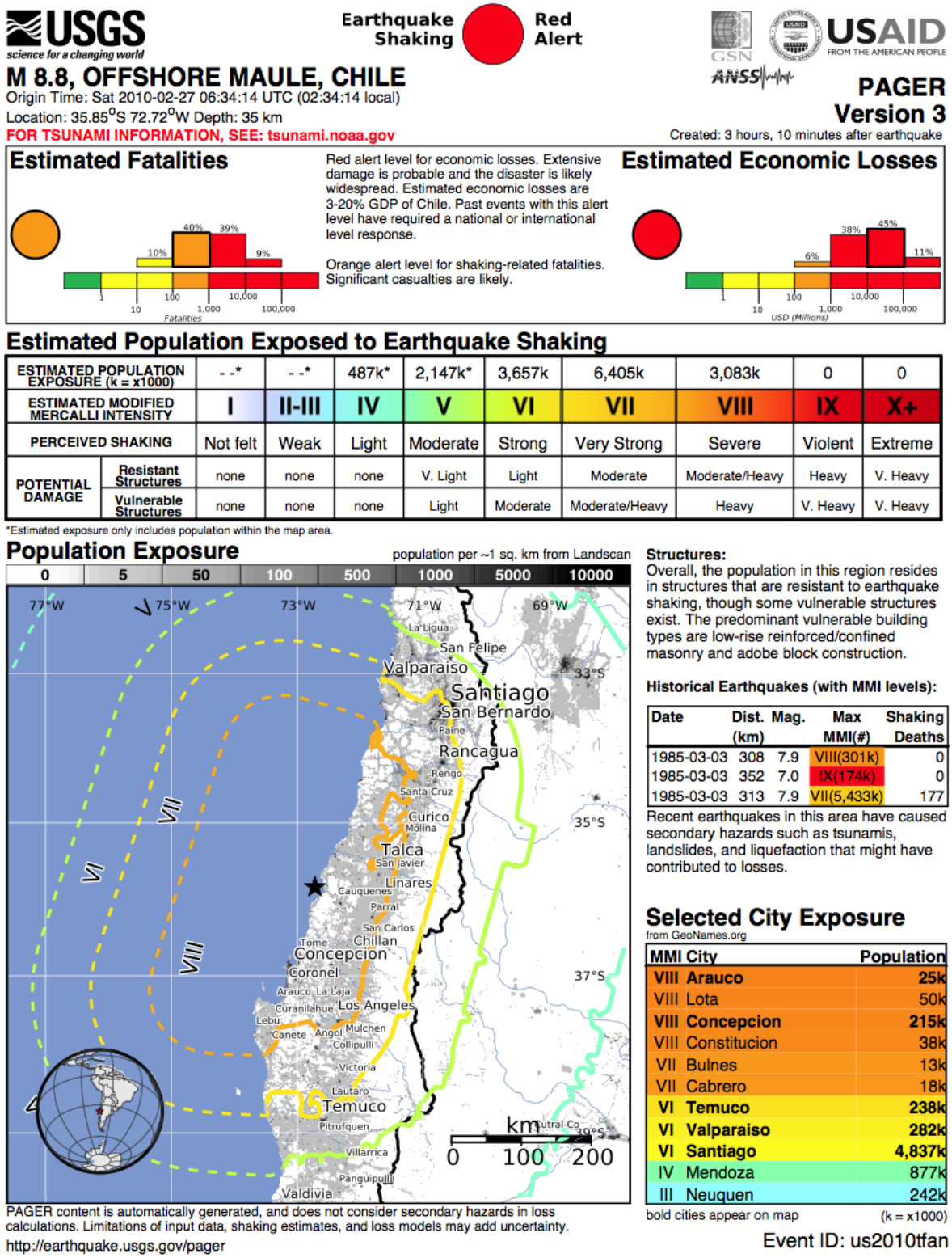

Figure 1. Example PAGER summary figure for the M8.8 Chile earthquake of 2010 showing population density, contoured intensity level (lower left), population exposed per color-coded intensity level (middle), selected cities with population and intensity level (lower right), vulnerable structures, relevant historical earthquakes (middle right), and color-coded impact scale indicating the alert level.

In Figure 1 we provide an example of PAGER's "onePAGER" summary and EIS for the M8.8 Chile earthquake of 27 February 2010. This summary figure indicates both the fatality-based (left) and economic-based (right) color-coded alerts and their likelihoods. The wording (top-center) is alert-level dependent and is meant to provide a rough gauge of the losses, the likely geographic extent of the impact, and the typical level of response, all based on PAGER's historical event database (Allen et al., 2009a). The selected alert level contains the median loss estimate and therefore has the highest likelihood; the uncertainty in the alert level can be gauged by the histogram, depicting the probability that actual losses could be in adjacent alert levels (or loss/fatality ranges). News reports for this earthquake confirm over 500 fatalities and financial losses of approximately $30 billion **(**Associated Press, 13 June, 2010**).** PAGER estimates based on the global ShakeMap (Wald et al, 2008) were constrained by reported intensities and fault dimensions, and resulted in a red earthquake-shaking summary alert, based on an orange-alert level for fatalities and a red-alert level for economic losses.

PAGER loss estimates and associated alerts are generated automatically by the USGS within 30 minutes of any magnitude 5.5 or larger event globally, and for any ShakeMap generated in the US (M>3.5). The estimated impacts are controlled primarily by: i) the distribution and severity of shaking, ii) the population exposed at each shaking intensity level, and iii) how vulnerable that population is to building damage at each intensity level, which is dominated by the degree of seismic resistance of the local building stock. The PAGER system takes a ShakeMap as the primary hazard input; then, based on a comprehensive worldwide population database (LandScan; Bhaduri et al., 2002), computes the population exposed to each level of shaking intensity. With this approach, PAGER automatically identifies earthquakes that will be of societal importance based on the total population exposed to higher intensities. Since these calculations are available well in advance of ground-truth observations or news accounts, they can play a primary alerting role for domestic (U.S.) as well as international earthquake disasters.

It is helpful for users to be aware of the likely frequency of potential alerts when signing up for notifications; too infrequent alerts result in the lack of familiarity with the information content; conversely, too frequent alerts tend to be more easily ignored. Figure 2 shows a global map of the spatial distribution of events and the fatality-based alerts that they would have produced over the past 35 years (1973 to 2008) based on the ShakeMap Atlas (Allen et al, 2009b), PAGER-CAT (Allen et al., 2009a), and the Earthquake Impact Scale approach to gauging impact (Wald et al., 2010). The spatial distribution reflects contributions from relative hazard, population exposure, and building vulnerability. There would have been approximately 17,792 green, 568 yellow, 52 orange, and 49 red fatality-based alerts during those years. Red alerts were comprised of 36 events with greater than 1,000 and 13 events with greater than 10,000 fatalities. Over that time period there were approximately 15 yellow, 1-2 orange, and 1-2 red fatality-based alerts per year.

In the U.S., the fatality-based alerting levels are, as expected, much less frequent. Hence, domestic alerting based on economic impact is more suitable for response. For economically-based alerts, since 1980 within the United States, the reported losses would have been associated with about 116 green, 30 yellow, 7 orange, and 3 red alerts or, approximately, 1 yellow per year; 1 orange per 4 years, and 1 red alert per 10 years.

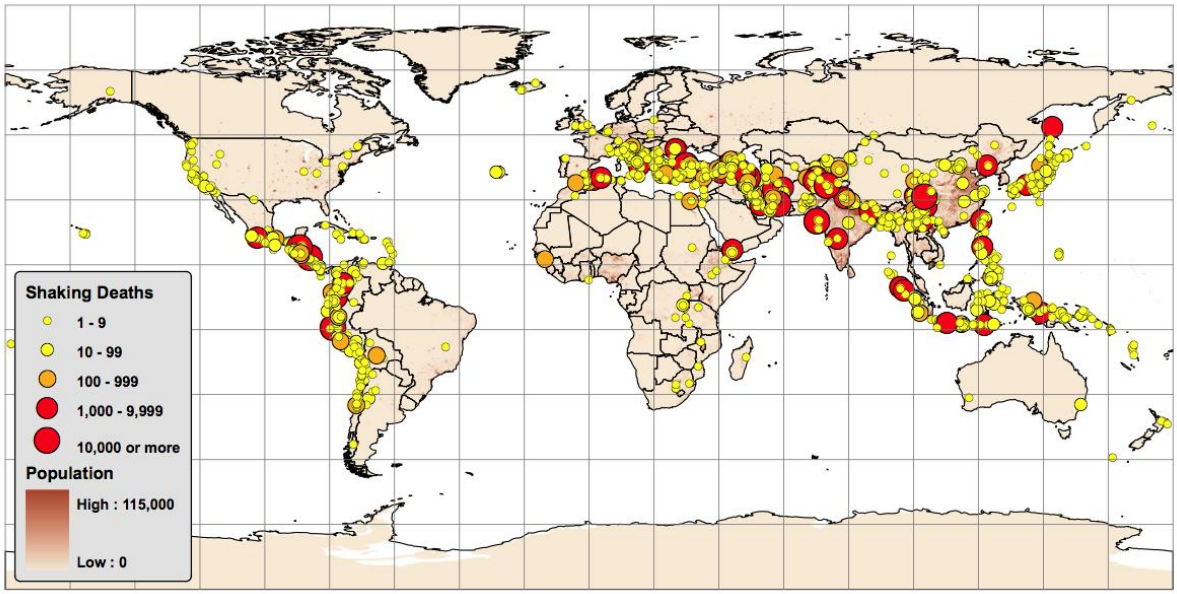

Figure 2. Map of fatality-based alert levels that would be triggered given the observed fatalities for events in the PAGER-CAT v2008_06.1 (Allen et al., 2009a), during 1970 thru mid-2008. The legend provides the fatality threshold for color-coded alert level. Over the past thirty-eight years there would have been approx. 17,792 green (not shown in figure), 568 yellow, 52 orange, and 49 red alerts (approximately 15 yellow, 1-2 orange, and 1-2 red alerts per year).

References

Allen, T.I., Marano, K.D., Earle, P.S., Wald, D.J. (2009a) PAGER-CAT: a composite earthquake catalog for calibrating global fatality models. *Seismol. Res. Lett*. 80(1):57–62.

Allen, T.I., Wald, D. J., Earle, P. S., Marano, K. D., A. J. Hotovec, Lin, K, and Hearne, M. G. (2009b). An Atlas of ShakeMaps and population exposure catalog for earthquake loss modeling, *Bull. Earthq. Eng., v. 7, DOI: 10.1007/s10518-009-9120-y*.

Bhaduri, B., Bright, E., Coleman, P., Dobson, J. (2002). LandScan—locating People is What Matters, *Geoinformatics* 5(2):34–37.

Jaiswal, K., and Wald, D. J. (2010). Development of a Semi-Empirical Loss Model Within the USGS Prompt Assessment of Global Earthquakes for Response (PAGER) System, *Ninth U.S. National and Tenth Canadian Conf on Eq. Engineering*, Paper 1095, 10 pp.

Jaiswal, K. S., D. J. Wald and H. Crowley (2010). An Empirical Model for Estimating Economic Losses Due to Large Worldwide Earthquakes, *Proc. 14th European Conf. Earthquake Eng. (14ECEE*), Ohrid, Macedonia, 9 pp.

Jaiswal, K. Wald, D. J., and Hearne, M. (2009). Estimating Casualties for Large Worldwide Earthquakes Using an Empirical Approach, *U.S.G.S. Open-File Report* 2009-1136, 78 p.

Wald, D. J., K. Jaiswal, K. D. Marano, and D. Bausch (2010). An Earthquake Impact Scale, Natural Hazards Review, published ahead of print, Jan 3, 2011, 42 pp.

Wald, D. J., P.S. Earle, K. Porter, K. Jaiswal, and T.I. Allen (2008). Development of the USGS's Prompt Assessment of Global Earthquakes for Response (PAGER) System, *Proc. 14th World Conf. Earth. Eng.*, Beijing, 8 pp.

Extreme Seismic Hazards and Societal Implication

Alik Ismail-Zadeh [a b c]

[a] *International Institute of Earthquake Prediction Theory and Mathematical Geophysics, Russian Academy of Sciences, Profsoyuznaya str. 84/32, Moscow 117997, Russian Federation*
[b] *Karlsruhe Institute of Technology, Geophysical Institute, Hertzstr. 16, Geb. 6.42, Karlsruhe 76187, Germany*
[c] *Institut de Physique du Globe de Paris, 1, rue Jussieu, Paris 75238, France*

The vulnerability of human civilizations to natural disasters is growing due to the proliferation of high-risk objects, clustering of populations, and destabilization of large cities. Today a single earthquake may take up to several hundred thousand lives, and cause material damage up to several billions EURs with a possible chain reaction expanding to a world-wide financial crisis and economic depression (comparable and even more severe than the current financial crisis and economic recession). "A large earthquake in (or close to) Tokyo might result in a world financial crisis, because many Japanese companies, which invested considerable funds in foreign enterprises, will withdraw these funds to rebuild or to restore the city infrastructure after the disaster" (Ismail-Zadeh, 2010). A large earthquake can trigger an ecological disaster if it occurs in close vicinity to a nuclear power plant built in an earthquake-prone area (e.g., in Iran, Japan, or elsewhere).

Extreme (large magnitude) seismic events are manifestations of complex behavior of the lithosphere structured as a hierarchical system of blocks of different sizes separated by faults. Driven by mantle convection these lithospheric blocks are involved into relative movement, resulting in stress localization and earthquakes. Although the lithosphere behaves as a large non-linear system, some integral empirical regularities emerge indicating possibilities for earthquake modeling, forecasting and prediction. I will discuss how extreme seismic events can be simulated numerically in models of block-and-fault dynamics and present a few case studies (e.g., the Sunda Arc, the Tibetan Plateau; Soloviev and Ismail-Zadeh, 2003; Ismail-Zadeh et al., 2007, 2011). The models feature the occurrence of large seismic events, earthquake clustering, and interaction.

A comprehensive quantitative assessment of seismic hazard should be based on multidisciplinary research in (i) geodynamics and geodesy (to reveal zones of tectonic strain and stress localization), (ii) present and historical seismicity (to localize areas prone to strong events), (iii) nonlinear dynamics of the lithosphere (to analyze statistical properties of the earthquake sequences, their clustering and critical transitions), (iv) soil property (to analyze liquefaction and seismic shaking), and (v) classical hazards assessment (to determine peak ground acceleration, response spectra amplitude, and seismic intensity). This approach to seismic hazard should be accompanied by a holistic approach to earthquake prediction and seismic risk assessment (e.g., Beer and Ismail-Zadeh 2003; Cardona 2004), when a convolution of hazard, vulnerability and exposure (as functions of space

and time) should be viewed also from social-psychological (e.g., resilience of community to extreme seismic events) and legal (e.g., role of law in risk reduction; see Paterson 2003) points of view.

Large earthquakes are surprising, and society, as a matter of fact, is poorly prepared to deal with them. Protecting human life and property against earthquake disasters requires an uninterrupted chain of research and civil protection tasks: (i) physical understanding of extreme earthquakes; (ii) geophysical, geodetic and geological analysis of extremes and their monitoring; (iii) modeling of extreme seismicity; (iv) earthquake forecasting and prediction; (v) comprehensive seismic hazard assessment; (vi) assessment of physical and social vulnerability, exposure and risk; (vii) prompt delivery of the scientific forecasts and related information to local authorities in order to undertake preventive measures and to mitigate a large earthquake/tsunami disaster; (viii) enhancement of public awareness; and (ix) public education on disaster risk.

References

Beer, T. and Ismail-Zadeh, A. T. (eds.), 2003. *Risk Science and Sustainability*, Kluwer Academic Publishers, Dordrecht, 256 p.

Cardona, O., 2004. The need for rethinking the concepts of vulnerability and risk from a holistic perspective: a necessary review and criticism for effective risk management. In: *Mapping Vulnerability: Disasters, Development and People*, Bankoff, G., Frerks, G., Hilhorst, D. (eds.), pp. 37-51, Earthscan Publishers, London.

Ismail-Zadeh, A., 2010. Computational geodynamics as a component of comprehensive seismic hazards analysis. In: *Geophysical Hazards: Minimizing Risk and Maximizing Awareness*, T. Beer (Ed.), Springer, Amsterdam, pp. 161-178.

Ismail-Zadeh, A., Le Mouël, J.-L., Soloviev, A., Tapponnier, P., and Vorovieva, I., 2007. Numerical modeling of crustal block-and-fault dynamics, earthquakes and slip rates in the Tibet-Himalayan region, Earth Planet. Sci. Lett., 258, 465-485.

Ismail-Zadeh, A., Le Mouël, J.-L., and Soloviev, A., 2011. Modeling of extreme seismic events, In: *Complexity and Extreme Events in Geosciences*, Sharma, S. et al. (eds.), AGU Geodynamics Series, accepted.

Paterson, J., 2003. Science for risk reduction and sustainable development: the role of law. In: *Risk Science and Sustainability*, Beer T, Ismail-Zadeh A (eds), pp.63-76, Kluwer Academic Publishers, Dordrecht.

Soloviev, A. A., and Ismail-Zadeh, A. T., 2003. Models of dynamics of block-and-fault systems. In: *Nonlinear Dynamics of the Lithosphere and Earthquake Prediction*, Keilis-Borok, V. I., and Soloviev, A. A. (eds.), pp. 69-138, Springer, Heidelberg.

The Global Earthquake Model: Building an Open Source Seismic Risk Model for the World

Ross S. Stein

Chair, GEM Scientific Board
Geophysicist, U.S. Geological Survey, Menlo Park, California

GEM was launched by the Organisation for Economic Cooperation and Development (OECD) in 2009; it is now an international non-profit foundation headquartered in Pavia, Italy (http://www.globalquakemodel.org). GEM is supported by a growing group of twelve public and eight private sponsors in a worldwide collaboration on the leading science and tools to contend with the earthquake threat. All of GEM's sponsors are committed to non-proprietary, open source information being produced for the public good and made useful and understandable to all. In addition, the World Bank, OECD, UN ISDR, and the international societies for earthquake engineering (IAEE), structural engineering (IstructE), and seismology (IAESPEI) have non-voting seats on GEM's Governing Board.

GEM's main objective is to develop a truly open-source platform, OpenGEM, that will allow stakeholders to analyze seismic risk, including the consequences of earthquakes on society and economy, measured over space and time. The global earthquake model is being designed and built by experts and practitioners around the world, and will reflect the needs and knowledge of a variety of prospective users and beneficiaries through GEM's extended partner-network, whereby contributing to increased risk awareness and risk mitigation. A first fully-featured version is scheduled for the end for 2013. GEM's key distinguishing features are these:

- GEM seeks to be comprehensive and innovative: the global earthquake model will not only cover earthquake hazard and risk, but also socio-economic impact, such as forecasting the consequences of earthquakes in terms of deaths, injuries, damage, and national economic losses. There will also be tools to calculate the expected reduction in losses if mitigation measures such as retrofitting have taken place.

- GEM is dynamic: It is an updatable model, featuring various types of output and allowing users to customize input data. In Taiwan, for example, there are competing active fault models, global plate motion models, and shaking attenuation relationships that can be tested by Taiwanese scientists to study their impact on the projections.

- GEM is global: the model will feature global and regional coverage and include where possible currently less monitored areas. This will furnish very detailed coverage for Taiwan, where the necessary data is already of high quality, but will also enable useful coverage for Taiwan's allies in less developed countries.

- GEM is, by design, open access: OpenGEM will be a tool to use for everyone, to cater for the adoption of risk-mitigation actions. It is powered by the software engine, OpenQuake (http://openquake.org). Homeowners will be able to understand what they need, whereas power users, such as Taiwan's scientists and engineers, will be able to access and modify the underlying data layers and modify model assumptions.

- GEM is a cooperative public-private partnership: combining the strengths and objectives of both the public and the private sector, including the insurance, construction, and engineering companies. Both the public and private stakeholders are well-represented by Taiwan's leading public, university, and corporate institutions.

Asia and the circum-Pacific basin are central to GEM's success, both because this is where the greatest population is at risk for earthquakes, and because so much scientific, engineering, and economic expertise is concentrated there. GEM had had its semestral and annual meetings in Singapore, a sponsoring nation, Beijing, and will next meet in Taipei. The ten international consortia building GEM's Global Components Datasets, which runs from Active Faults to Building Fragilities, draw heavily from Asian institutions and scientists.

The IISEE earthquake catalog, "Catalog of Damaging Earthquakes in the World", "IISEE-NET", and BRI strong motion observation

Tatsuhiko Hara

International Institute of Seismology and Earthquake Engineering, Building Research Institute, 1 Tatehara, Tsukuba, Ibaraki, 305-0802, Japan

We introduce two earthquake catalogs available at the website of the International Institute of Seismology and Earthquake Engineering (IISEE), Building Research Institute (BRI). The one is "IISEE's CMTs, Aftershock Distributions, Fault planes, and Rupture processes for recent large earthquakes in the world", which consists of various earthquake information, tsunami simulation results, etc. The other is "Catalog of Damaging Earthquakes in the World", which was compiled by Dr. Tokuji Utsu, and has been inherited by the IISEE. We also introduce strong motion data and information in the fields of earthquake engineering available at the IISEE/BRI web sites.

1. IISEE's CMTs, Aftershock Distributions, Fault planes, and Rupture processes for recent large earthquakes in the world

1.1. Earthquake information

The IISEE has developed an earthquake catalog, "IISEE's CMTs, Aftershock Distributions, Fault planes, and Rupture processes for recent large earthquakes in the world" and since 2008 have been providing it at the following URLs:

http://iisee.kenken.go.jp/eqcat/Top_page_en.htm,
http://iisee.kenken.go.jp/cgi-bin/eqcatalog.newv4/eqcatalog2_eng.cgi.

This catalog contains the following earthquake information for large (Mw≧7.2) earthquakes in the world that occurred since 1994 determined by the analytical techniques developed by the IISEE staff and visiting researchers. The explanations on the technical details are available at the above URLs.

・Centroid moment tensor
- Period: 1994 – October 2010
- Data long period body wave data recorded at GSN stations.

・Aftershock distribution and corresponding fault plane
- Period: January 1994 – 2007
- Data: P-wave arrivals from International Seismological Centre (ISC) CD-ROMs.

・Rupture process
- Period: January 1994 – November 2007
- Data: Tele-seismic broadband waveform data recorded at GSN stations.

Figure 1 shows an example of the solutions in the catalog.

1.2. Tsunami simulation

Results of tsunami simulations and tsunami waveform inversions for recent large earthquakes are available at the IISEE web site. After searching the database, the link button "Tsunami Simulation" is created in case the corresponding tsunami simulation results are available on the IISEE web site. Figure 2 shows the result of tsunami simulation for the February 27, 2010 Chile earthquake.

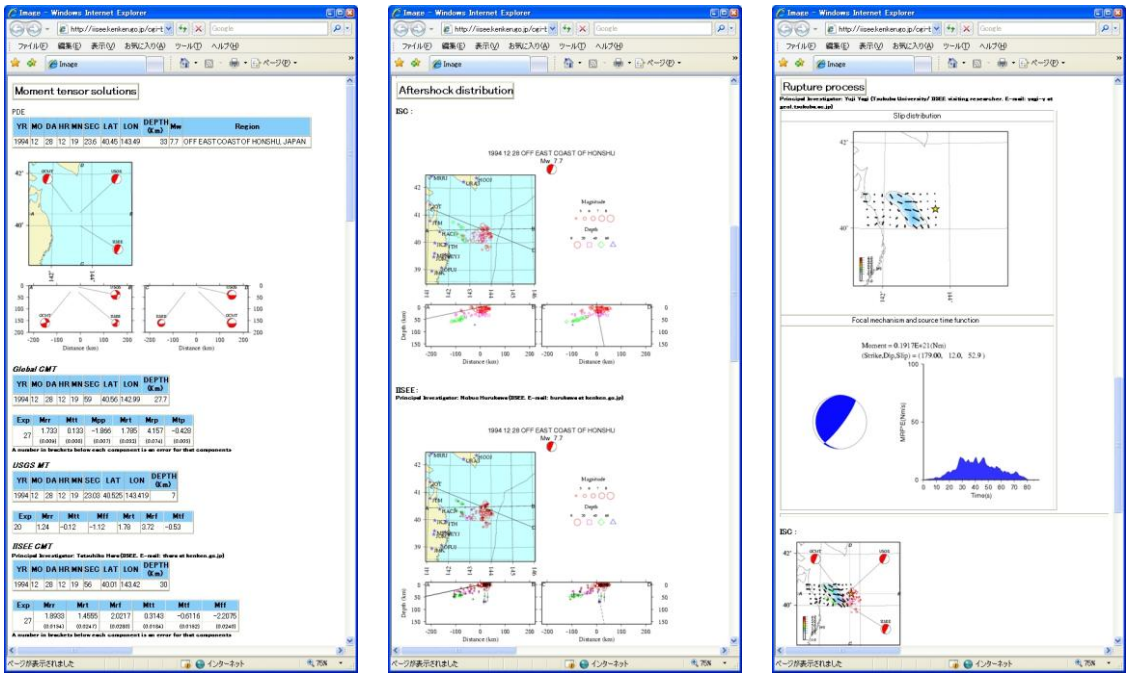

Fig. 1. An example of the solutions in the catalog. The focal mechanisms, aftershock distributions and corresponding fault planes, and rupture process model for the 1994 far east off Sanriku earthquake are show in the left, middle and right panels, respectively.

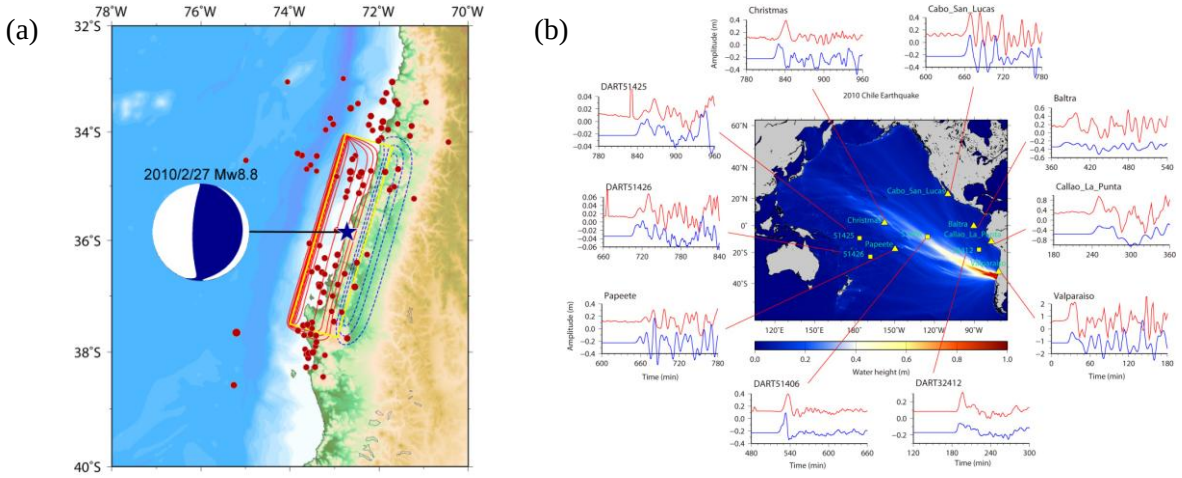

Fig. 2. Tsunami simulation results for the February 27, 2010 Chile earthquake. (a) Seafloor deformation due to a fault model. The red and blue contours indicate uplift and subsidence, respectively (the contour interval is 0.5 m). Aftershocks (determined by USGS) during one day after the mainshock are also shown by red circles. (b) Maximum height of the simulated tsunami and the observed and synthetic tsunami waveforms are shown by red and blue curves, respectively.

1.3. Strong ground motion simulation

Software to perform strong ground motion simulation for seismic bedrock using stochastic Green's function method (Onishi and Horike, 2000) was developed in the BRI research project and results for some large earthquakes are available at http://iisee.kenken.go.jp/eqcat/Top_page_en_s.htm.

In addition, a function to export earthquake source parameters in the IISEE earthquake catalog to calculations of intensities, PGV, and PGA using attenuation relations is available at the search page. Figure 3 shows its interface and an example of calculation.

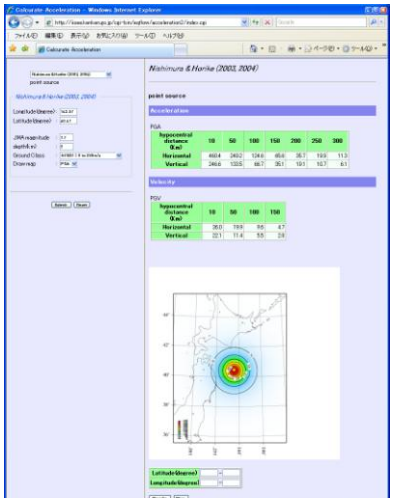

Fig. 3. The interface of the calculator using the attenuation relations.

1.4. Web interface

The IISEE has made a database by including USGS MT solutions, Global CMT solutions, and ISC aftershock distributions, etc. to the above mentioned IISEE earthquake catalog. Also, a KML (Keyhole Markup Language) file is available at the web site, by which the earthquakes registered in the catalog are shown on Google Earth, and the corresponding earthquake information is displayed.

2. Catalog of Damaging Earthquakes in the World

Dr. Tokuji Utsu, Professor Emeritus of Tokyo University, compiled a catalog, "Catalog of Damaging Earthquakes in the World," (Utsu, 1990; Utsu, 2002; Utsu, 2004. The later updates are added by the International Institute of Seismology and Earthquake Engineering), which contains more than 10,000 destructive earthquakes in the world from 3000 B.C. The IISEE has inherited this catalog and its search page on the web site of Earthquake Research Institute (ERI), Tokyo University, developed and maintained by Dr. Toshikatsu Yoshii, Nihon University.

The catalog that Dr. Utsu provided to the IISEE has destructive earthquakes up to June, 26, 2002. The IISEE is continuously updating the catalog, and the current latest event in the database is the earthquake that occurred on December 19 in 2009 in Malawi.

The URLs of the top and search page of this catalog are the followings:

http://iisee.kenken.go.jp/utsu/index_eng.html

http://iisee.kenken.go.jp/utsu/utsuweq_bak_eng.html

3. Information Network on Earthquake Disaster Prevention Technologies (IISEE-NET)

The IISEE conducted a research project entitled “Information Network on Earthquake Disaster Prevention Technologies” between JFY2000 and JFY2002. This project aimed at accumulating and disseminating various technical information effective for disaster prevention efforts in earthquake-vulnerable countries, which includes seismic design codes, seismic networks and activities, seismic damages, and microzonation. The output of this project is available at:

http://iisee.kenken.go.jp/net/index.htm

and is referred to “IISEE-NET”

The IISEE has been improving this site by upgrading and expanding information such as putting a set of free GIS and database software with its instruction.

4. BRI strong motion observation

The Building Research Institute (BRI) has been conducting strong motion observation for building structures since 1957. At present, the BRI is operating more than seventy strong motion stations deploying in major cities throughout Japan. The search page for the BRI strong motion database is at:

http://smo.kenken.go.jp/smdb.

At http://smo.kenken.go.jp/smreport, reports of recent strong earthquakes are also available.

References

Onishi, Y. and Horike, M., 2000. Application of the method for generating 3-component strong ground motions using the stochastic Green's function to the 1955 Hyogo-ken Nanbu earthquake, Journal of Structural Engineering, 46B, 389-398 (in Japanese with English Abstract).

Utsu, T., 1990, Catalog of Damaging Earthquakes in the World (Through 1989), Utsu, Tokuji, Tokyo, 243 pp. (in Japanese).

Utsu, T., 2002, A list of deadly earthquakes in the World: 1500-2000, in International Handbook of Earthquake and Engineering Seismology Part A, edited by Lee, W.K., Kanamori, H., Jennings, P.C., and Kisslinger, C., pp. 691-717, Academic Press, San Diego.

Utsu, T., 2004, Catalog of Damaging Earthquakes in the World (Through 2002), the Dbase file distributed at the memorial party of Prof. Tokuji Utsu held in Tokyo. The revised and extended version is available at http://iisee.kenken.go.jp/utsu/index_eng.html.

GEO Grid Disaster Response Applications and its Activity for the 2011 Tohoku, Japan Earthquake and Tsunami

Masashi Matsuoka[a], Naotaka Yamamoto[b], Hirokazu Yamamoto[b], Ryosuke Nakamura[b], Kazuki Nakamura[b], Shinsuke Kodama[b], Yuko Takeyama[b], Koki Iwao[b], Akihide Kamei[b], Sarawut Ninsawat[b],Satoshi Tsuchida[b], Minoru Urai[c], Isao Kojima[b], Yoshio Tanaka[b], and Satoshi Sekiguchi[b]

[a]*Geoinformation Center, Geological Survey of Japan, AIST, 1-1-1 Higashi, Tsukuba, Ibaraki 305-8567, Japan*
[b]*Information Technology Research Institute, AIST, 1-1-1 Unezono, Tsukuba, Ibaraki 305-8568, Japan*
[c]*The Institute of Geology and Geoinformation, AIST, 1-1-1 Higashi, Tsukuba, Ibaraki 305-8567, Japan*

The GEO Grid is aiming at providing an E-Infrastructure to understand our earth more insightful and more precisely, but faster and easier to worldwide Earth Sciences community (Sekiguchi et al., 2008). The GEO Grid provides large archives of earth observation satellite data, such as Terra/ASTER, ALOS/PALSAR (in present), and JERS-1/OPS and SAR (in near future), securely and rapidly, integrated service with wide variety of geoscientific information such as geologic maps and GIS data, and assembles them easy-to-use formats for potential stakeholders in the several areas, such as resource exploration, environmental conservation, natural hazard evaluation and risk assessment. To provide these services, AIST has constructed systems using Grid and Web service technologies in accordance with general international standards. Several geological maps have been deployed in the GEO Grid system and are open to the public as Web Map Service (WMS) on OGC (Open Geospatial Consortium) international standard.

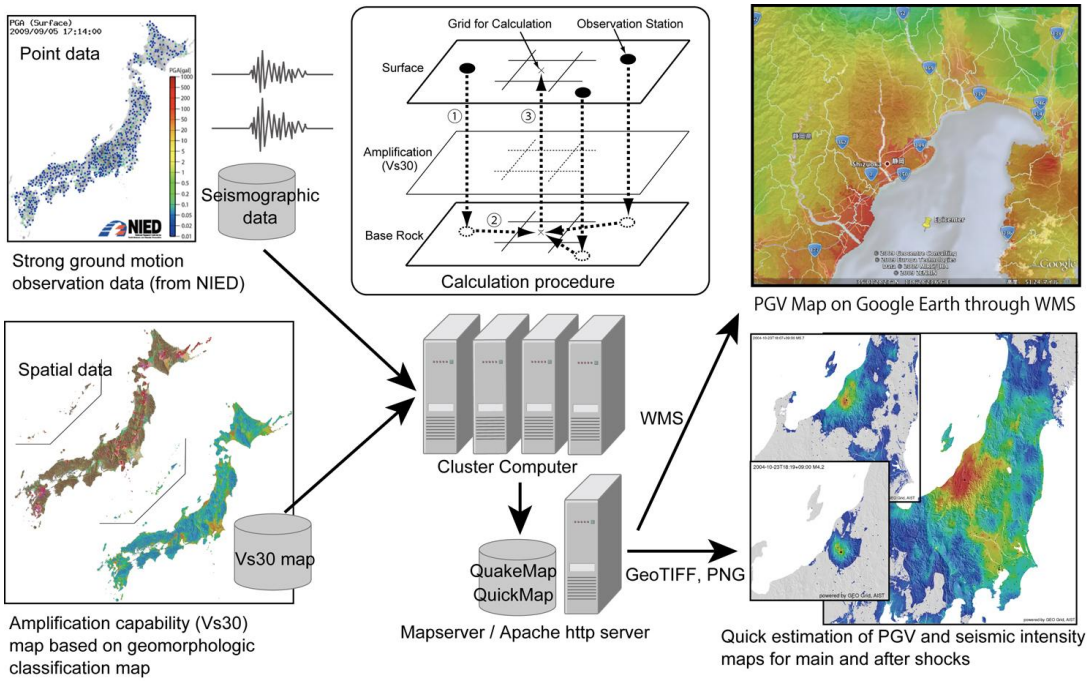

Fig. 1. System Overview and Calculation Procedure of QuiQuake on GEO Grid.

In terms of the applications of hazard evaluation, we have developed some systems for volcanic and earthquake hazards mitigation. A volcanic gravity flow simulation program provides potential dangerous areas of pyroclastic flows caused by volcanic eruptions and can contribute to create volcanic hazard maps. For earthquake hazard estimation, QuiQuake (Quick estimation system for earthQuake maps triggered by observation records) on the GEO Grid is a system which provides wide

ranging and detailed strong ground motion maps, based on information such as peak ground acceleration (PGA), peak ground velocity (PGV), and instrumental seismic intensity (INT), soon after an earthquake occurs. QuiQuake also uses combinations of geomorphologic condition data and observed seismic records. A shake map can help to support decision making for disaster response and business continuity planning (BCP). The amplification capability is estimated from geomorphologic conditions (Matsuoka et al., 2006), based on the Japan Engineering Geomorphologic Classification Map whose spatial resolutions are 7.5 arc-seconds in latitude and 11.25 arc-seconds in longitude (approximately 250m square). The automatic calculation of spatial interpolation, including consideration of attenuation characteristics from the seismic source, is activated by harvesting the seismic data recorded at strong ground motion observation stations operated by the National Research Institute for Earth Science and Disaster Prevention, Japan (NIED). The strong motion maps are published through an OGC-standard web service interface. The schematic flow of the system is shown in Fig. 1.

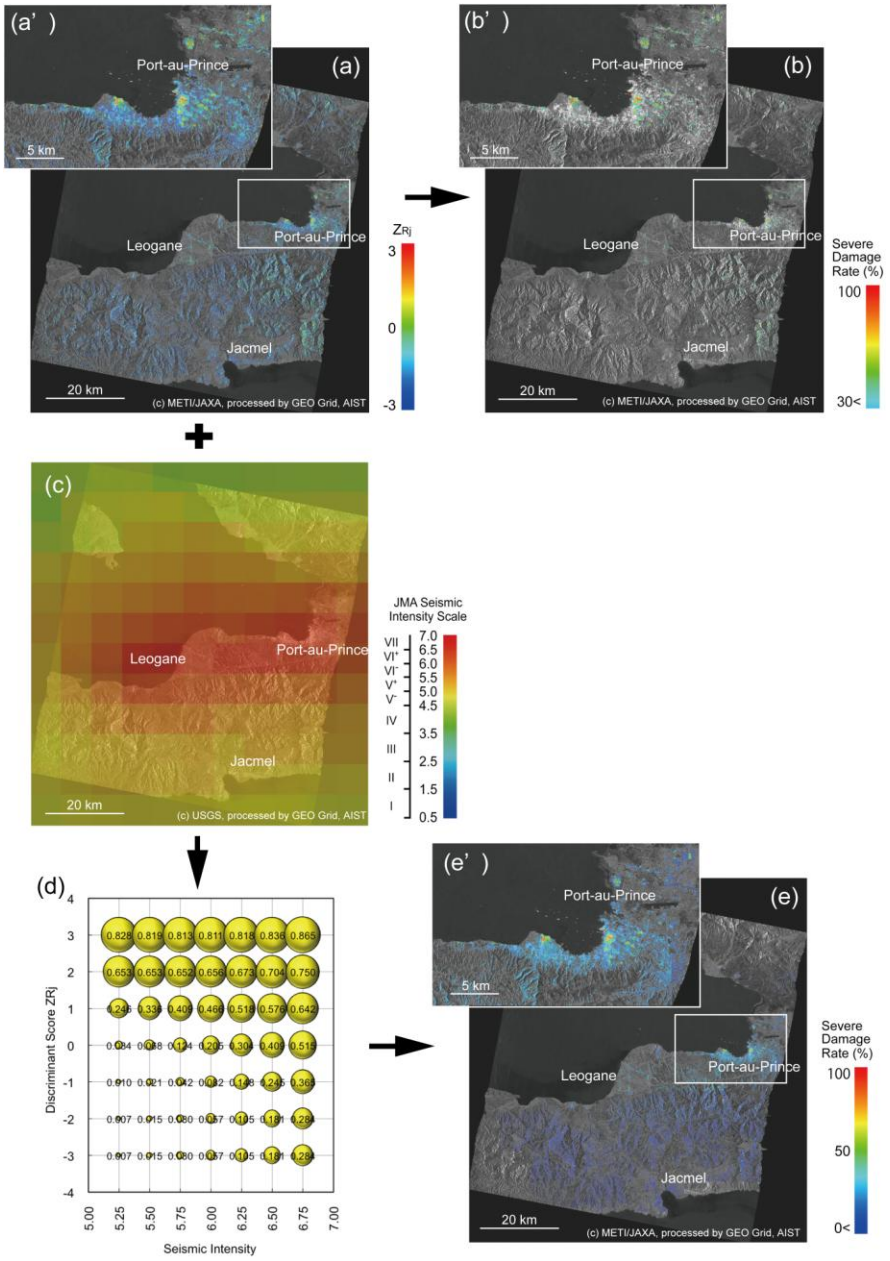

Fig. 2. (a) Distribution of discriminant score, Z_{Rj}, which is the combined variable derived from the correlation coefficient and the difference of the backscattering coefficients calculated by pre- and post-event PALSAR

images. (a') Close up of Port-au-Prince area. (b) Severe damage ratio map of buildings estimated by the conversion from Z_{Rj} using a likelihood function model. (b') Close up of Port-au-Prince area. (c) Seismic intensity map calculated by PGV map from USGS ShakeMap. (d) Estimated severe damage ratio (average value) after integration and probability updates for all 49 possible combinations of a likelihood function by Z_{Rj} and a fragility function by seismic intensity. (e) Integrated severe damage ratio (average values) distribution. (e') Close up of Port-au-Prince area.

For risk identification after natural disasters, the large-scale of archived remote sensing data such as Advanced Spaceborne Thermal Emission and Reflection Radiometer (ASTER) and Phased Array type L-band Synthetic Aperture Radar (PALSAR) are available to use from the GEO Grid system. Matsuoka and Nojima (2010) proposed a modeled likelihood function for severe building damage ratio from discriminant scores obtained via regression discriminant analysis, using the difference values and correlation coefficients from pre-event and post-event satellite SAR intensity images of the areas affected by the 1995 Kobe earthquake, as well as damage severity rankings obtained from building damage data of the quake, as explaining variables. Furthermore, the severe building damage ratio distribution can be estimated from SAR images through integration with the fragility function for damage in terms of seismic intensity of earthquakes. Figure 2 shows the estimated results of the 2010 Haiti earthquake.

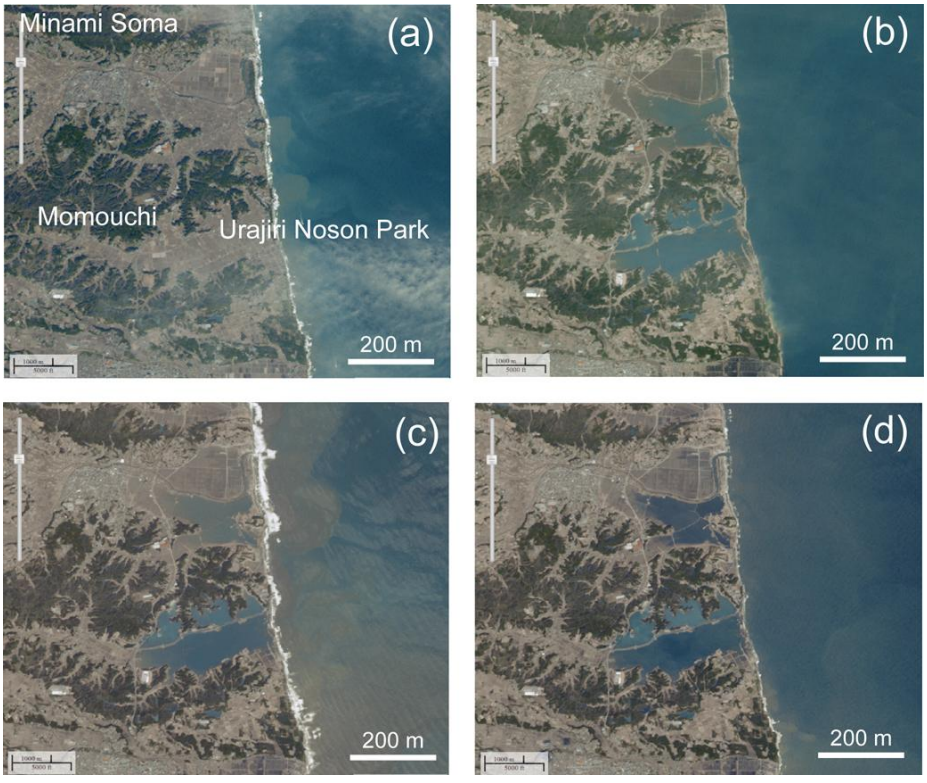

Fig. 3. Time-series ASTER images taken before and after the earthquake and tsunami. (a) Dec. 25, 2008, (b) Mar. 14, 2011, (c) Mar. 19, 2011, (d) Mar. 28, 2011.

In 2011, AIST suffered a sustained power outage because of the major earthquake and resulting tsunami on 11 March that devastated parts of Japan. Though the entire GEO Grid services stopped, we established "GEO Grid Disaster Task Force Team" in order to offer several services: satellite imagery including observation of stricken areas; geological maps; and hazard information, including a strong ground motion map and liquefaction probability. These services are aimed at helping those who are working on emergency responses, research into tsunamis and structural damage, and restoration and rehabilitation of civilian life and economic activities to the wide and long-term disaster. The services

have been designed and developed based on three requirements. The first is “redundancy.” Several services such as the data processing procedures and distribution computational functions of the GEO Grid were migrated to external servers and Cloud system seeking stabilized and redundant operations. The second requirement is “rapidity.” High-speed automatic data processing requires using high-performance computers. The third requirement is “standardization.” Most of the geographic information is open to the public as Web Map Service (WMS) and KML (KMZ), which are international standards for geographic data. Starting again in May, updating the contents had been continued by the GEO Grid services in AIST. Figure 3 shows ASTER time-lapse images of Minami-Soma city. Some areas remain inundated more than two weeks after the tsunami and have suffered subsidence due to the earthquake. Remote sensing plays a key role in monitoring areas such as the evacuation zone due to the Fukushima nuclear plant accident. The contents and footsteps are shown in its web site at http://disaster-e.geogrid.org/.

References

Matsuoka, M., Nojima, N., 2010. Building damage estimation by integration of seismic intensity information and satellite L-band SAR imagery, Remote Sensing, 2(9), 2111-2126.

Matsuoka, M., Wakamatsu, K., Fujimoto, K., Midorikawa, S., 2006. Average shear-wave velocity mapping using Japan Engineering Geomorphologic Classification Map, Journal of Structural Engineering and Earthquake Engineering, 23(1), 57s-68s.

Sekiguchi, S., Tanaka, Y., Kojima, I., Yamamoto, N., Yokoyama, S., Tanimura, Y., Nakamura, R., Iwao, K., Tsuchida, S., 2008. Design principles and IT overviews of the GEO Grid, IEEE Systems Journal, 2(3), 374-389.

National seismic hazard maps for Japan and seismic hazard assessment after the 2011 Tohoku-oki earthquake

Hiroyuki Fujiwara

National Research Institute for Earth Science and Disaster Prevention,3-1Tennodai, Tsukuba, Ibaraki 305-0006, Japan

The Headquarters for Earthquake Research Promotion of Japan published the national seismic hazard maps for Japan in July 2009, which was initialized by the earthquake research committee of Japan (ERCJ) on a basis of long-term evaluation of seismic activity, and on a basis of strong-motion evaluation. The National Research Institute for Earth Science and Disaster Prevention, in the meantime, also promoted a special research project 'National Seismic Hazard Mapping Project of Japan' to support the preparation of the seismic hazard maps (Fujiwara et al. 2009). Under guidance of ERCJ, we have carried out the study of the hazard maps.

The hazard maps consist of two kinds of maps. One is a probabilistic seismic hazard map (PSHM) that shows the relation between seismic intensity value and its probability of exceedance within a certain time period. The other one is a scenario earthquake shaking map (SESM).

The examples of PSHMs are maps of probabilities that seismic intensity exceeds the JMA scale 5-, 5+, 6- and 6+ in 30 or 50 years, and maps of the JMA seismic intensity corresponding to the exceedance probability of 3% and 6% in 30 years and of 2%, 5%, 10% and 39% in 50 years. We classify earthquakes in and around Japan into three categories such as the characteristic subduction zone earthquakes, subduction zone earthquakes, and crustal earthquakes. PSHMs for three earthquake category are also evaluated. For the PSHM, we use empirical attenuation formula for strong-motion, which is followed the seismic activity modeling in the basis of long-term evaluation of seismic activity by ERCJ. Both of peak velocities on the engineering bedrock and on ground surface are evaluated for sites with approximately 0.25km spacing in the basis of the 7.5-Arc-Second Engineering Geomorphologic Classification Database. The JMA seismic intensities on ground surface are evaluated by using an empirical formula.

The SESMs are evaluated for 485 scenario earthquakes of all major faults in Japan. Selection of a specified scenario is essential to make a scenario earthquake shake map. The basic policy of the selection is that we choose the most probable case. We assume several cases of the characteristic source model and compare the results of them to show deviation of strong-motion evaluation due to uncertainties. For the SESMs, based on the source modeling for strong-motion evaluation we adopt a hybrid method to simulate waveforms on the engineering bedrock and peak ground velocity. The hybrid method aims to evaluate strong-motions in a broadband frequency range and is a combination of a deterministic approach using numerical simulation methods, such as the finite difference method, for low frequency range and a stochastic approach using the empirical or stochastic Green's function method for high frequency range. A lot of parameters on source characterization and modeling of underground structure are required for the hybrid method. The standardization of the setting parameters for the hybrid method is studied. We summarize the technical details on the hybrid method based on the 'Recipe for strong-motion evaluation', which are published by the ERCJ.

The national seismic hazard maps for Japan are a comprehensive integration from all of the research aspects conducted by ERCJ. It contains information of all necessary data for producing the maps. To cross-check and promote the use of the national seismic hazard maps, an engineering application committee was established by NIED. Under the committee guidance, we have developed an open web system to provide seismic hazard information interactively, and name this system as Japan Seismic Hazard Information Station, J-SHIS (http://www.j-shis.bosai.go.jp/). We aim to distribute a process of uncertainty evaluation and to meet multi-purpose needs in engineering fields. The information provided from J-SHIS includes not only results of the hazard maps but also various information required in the processes of making the hazard maps, such as data on seismic activity, source models and underground structure.

The Tohoku-Oki earthquake (Mw 9.0) of March 11, 2011, was the largest event in the history of Japan. This magnitude 9.0 mega-thrust earthquake initiated approximately 100 km off-shore of Miyagi prefecture and the rupture extended 400 - 500 km along the Pacific plate. Due to the strong ground motions and tsunami associated by this event, approximately twenty thousand people were killed or missing and more than 220 thousands houses and buildings were totally or partially destroyed. This mega-thrust earthquake was not considered in the national seismic hazard maps for Japan. By comparing the results of the seismic hazard assessment and observed strong ground motions, we understand that the results of assessment were underestimated in Fukushima prefecture and northern part of Ibaraki prefecture. Its cause primarily lies in that it failed to evaluate the M9.0 mega-thrust earthquake in the long-term evaluation for seismic activities. On the other hand, another cause is that we could not make the functional framework which is prepared for treatment of uncertainty for probabilistic seismic hazard assessment work fully. Based on lessons learned from this earthquake disaster and the experience that we have engaged in the seismic hazard mapping project of Japan, we consider problems and issues to be resolved for probabilistic seismic hazard assessment and make new proposals to improve probabilistic seismic hazard assessment for Japan.

We propose the following four issues to be solved for improvement of seismic hazard assessment for Japan.

1) Modeling of seismic activity with no oversight to low-probability earthquakes.
2) Preparation of strong ground motion maps considering low-probability earthquakes.
3) Development of methodology for selecting appropriate scenario earthquakes from probabilistic seismicity model.
4) Development of methodology for prediction of strong ground motions for mega-thrust earthquakes.

References

Fujiwara, H., et al. 2009. Technical reports on national seismic hazard maps for Japan, Technical note of the National Research Institute for Earth Science and Disaster Prevention, No. 336.

Poster Session

Foyer (First Floor)
10:00, 22 February to 12:00, 24 February
Core Time: 15:00 – 16:00, 23 February

Web Computing Service (WCS) for detecting land cover change caused by volcanic eruptions using Web Map Service (WMS), frequency based change detection algorithm and PALSAR

Joel Bandibas[a], Daisaku Kawabata[a], Minoru Urai[a], Asep Saepuloh[a] and Koji Wakita[b]

[a]*Geoinformatics Research Group, Geological Survey of Japan, AIST, 1-1-1 Higashi, Tsukuba, Ibaraki 305-8567, Japan*
[b]*Geoinformation Center, Geological Survey of Japan, AIST, 1-1-1 Higashi, Tsukuba, Ibaraki 305-8567, Japan*

Introduction

Volcanic eruption is one of the most destructive natural phenomena frequently occurring in most countries located along the Pacific Rim. Timely identification of areas affected by volcanic eruptions is very important for a successful rescue and effective emergency relief efforts. This research focuses on the development of a cost effective and efficient system of identifying areas affected by volcanic eruptions, and the efficient distribution of the information. The developed system is composed of 3 modules which are the Web Computing Service (WCS), Web Map Service (WMS) and the user interface provided by J-iView (fig. 1). WCS is an online system that provides computation, storage and data access services. In this study, the WCS module provides online access of the software implementing the developed algorithm for land cover change detection. It also sends requests to WMS servers to get the remotely sensed data used in the computation. WMS is a standard protocol that provides a simple HTTP interface for requesting geo-registered map images from one or more distributed geospatial databases. In this research, the WMS component provides remote access of the satellite images which are used as inputs for land cover change detection. The user interface in this system is provided by J-iView, which is an online mapping system developed at the Geological Survey of Japan (GSJ) (fig. 2).

Change detection using multi-temporal remotely sensed data could be divided into two broad types: pre-classification and post-classification (Mettemicht, 1999). Post-classification method involves the separate classification of remotely sensed data sets from individual dates. Changes could be determined by the change in land cover types between dates. This method would indicate the areas that undergo change and how they change (e.g. from corn field to residential). Pre-classification methods on the other hand detect changes due to the variations in the brightness or spectral signatures in the images compared. In this method, areas could just be labeled to have "changed" or "not changed", not the type of change. There are several pre-classification methods for detecting land cover change using multi-temporal remote sensing data sets. Image differencing is the most

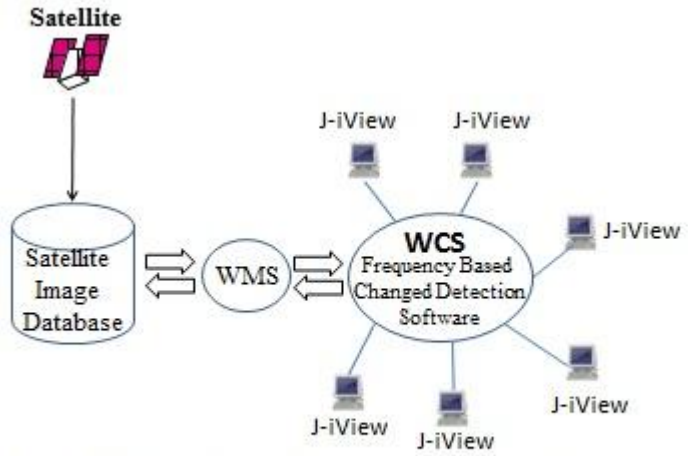

Fig. 1. Web Computing Service (WCS) for detecting land cover change using satellite images provided by a WMS server, a frequency based change detection algorithm and J-iView.

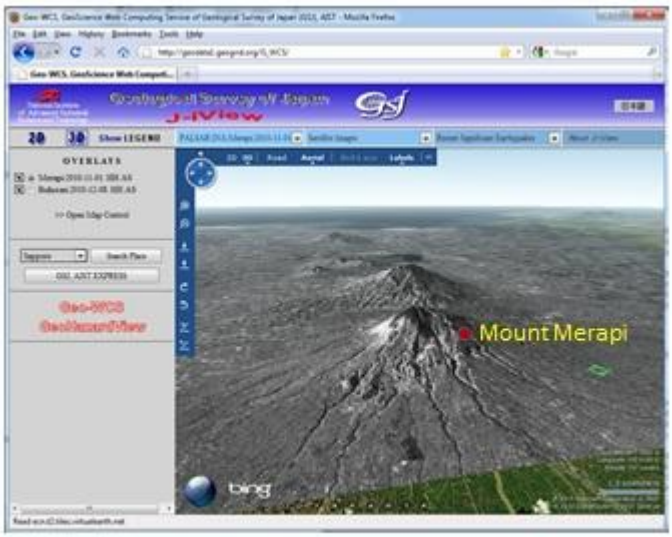

Fig. 2. PALSAR image (HH As) of Merapi volcano taken on November 1, 2010. The image is displayed using J-iView.

common and straightforward method. It is simply the subtraction of the pixel digital values of an image recorded at one date from the corresponding pixel values of the image at the second date (Hayes and Sader, 2001). The output of image differencing indicates that values close to the mean represent areas of 'no change' and magnitude close to +-255 depicts areas of change (Mettemicht, 1999). Image differencing involves the processing of one band of the digital images at a time. Other methods use multiple bands of data for change detection. These include image differencing using bands ratios like vegetation indices and principal component analysis (PCA). In the temporal change detection using PCA, both the surface proportion and the magnitude of the changed area in an image determine which principal component images will contain change information. It is the relative amount of variance between the change area and the unchanged part in an image that determine which particular PCs contain change information (Sing, 1986).

The pre-classification method of detecting land cover change is the more appropriate procedure for mapping areas affected by natural disasters, for identifying damaged areas would not require information about the type of land cover change. Identifying damaged areas involves the determination of the spectral and spatial changes in satellite images taken before and after the occurrence of the disaster. Areas that sustained significant damage should show significant change in the spectral and spatial characteristics. The conventional pre-classification change detection algorithms described above are pixel by pixel based methods of identifying changes of land cover using multi-temporal remotely sensed data sets. However, changes in pixel values between two images are sometimes not good indicator of land cover change. Indeed in many instances, a particular pixel's brightness covering a damaged area would not significantly change. The indications that it covers a damaged area are the changes in the brightness of the surrounding pixels. In many cases, changes in texture are more important in identifying damaged areas than the absolute changes in brightness in images. Delineating damaged areas often involves identifying regions in the image whose texture significantly change in the multi-temporal data sets.

Land Cover Change Detection Algorithm

Several algorithms were developed to determine the spatial signature of pixels in satellite images. One of the earliest spatial signature based algorithms is the contextual identification of pixels or spatial correlation (Khazenie and Crawford, 1989; Alonso and Soria, 1989). A similar method developed by Peddle and Franklin (1989) termed this spatial correlation procedure as gray level-spatial dependency co-occurrence. Gong and Howarth (1992) formulated the frequency based contextual classifier wherein the identity of a pixel is defined by the frequency of occurrence of the different spectral classes of its surrounding pixels. The land cover change detection algorithm used

in this study is based on the contextual method to represent pixel's spatial signature, to detect change in multi-temporal data sets covering areas affected by volcanic eruptions. The unsupervised frequency based changed detection algorithm developed in this study involves 3 stages: 1) the classification of the two images into 15 spectral classes, 2) spatial signature generation using the spectral class occurrence frequency method, and 3) change detection.

The first stage is the segmentation of the two satellite images into 15 spectral classes using the moving averages clustering algorithm described by Richards (1987). The first image was first segmented into 15 spectral classes. The 15 means of the cluster centers of the first image were then used to classify the second image into similar 15 spectral classes. If the two images are exactly the same, the aforementioned clustering sequence should generate two identical clustered images. In the second stage, the spectral class occurrence frequency is defined. The occurrence frequency ***f(i,j,c)*** is the number of times a spectral class ***c*** occurs in the window centered at ***(i,j)***. The window has a square shape with side length ***l***. Spectral classes were labeled from **1** to ***v***, where ***v*** is the total number of spectral classes.

Detecting the difference between the spectral class frequency $f_1(i,j,c)$ of the first image and the frequency $f_2(i,j,c)$ of the second image centering on the same location ***(i,j),*** was carried out by determining the Euclidean distance between the two window frequencies. The pixel window was moved pixel by pixel over the clustered images and the frequency occurrence for each spectral class within the window was computed to generate two frequency tables. The distance between the two frequency tables was computed using the formula

$$d_{(i,j)} = \sqrt{\sum_{c=1}^{v} (f_1(i,j,c) - f_2(i,j,c))^2} \qquad (1)$$

where ***d(i,j)*** is the distance between the two frequencies at pixel location (***i,j***). If the two frequency tables are the same, the distance should be 0. The greater is the distance the greater is the difference between the spatial signatures of the pixels from the two images. In this study, the distance threshold was set at 0.70 after several test runs. Distance values greater than the threshold signify change while values below the threshold means no change. The size of the pixel window used is an important factor in a frequency classifier. If the pixel window is too small, insufficient spatial information is included to characterize a specific land-cover class. If the pixel window is too large, it will result to the inclusion of too much spatial information from the other land-cover classes (Gong and Howarth, 1992). After some preliminary experiments, a 5 x 5 pixel window showed optimum change detection accuracy. This window size was used in the experiment. PALSAR images covering Merapi volcano taken before and after its November 2010 eruptions were used in this study (fig. 2). The developed algorithm aims to detect areas affected by ash falls and pyroclastic flows caused by the eruptions.

Results

This study successfully developed a cheap and efficient system of identifying areas affected by volcanic eruptions. The WCS and WMS technologies make it possible to map areas affected by the disaster by just using a WEB browser. It also shows that satellite images obtained through WMS

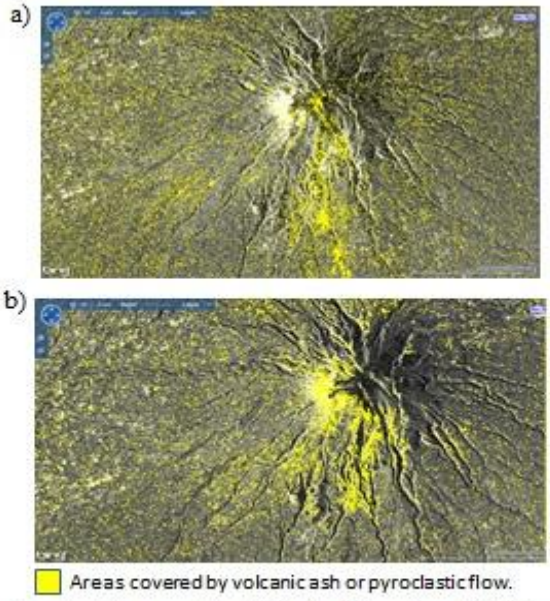

Fig. 3. Maps showing the areas affected by the November 2010 Merapi Eruptions. a) Map generated using low level feature extraction. b) Map generated using the frequency based land cover change detection algorithm.

servers are sufficient inputs for the developed algorithm to identify damaged areas. The frequency based change detection algorithm developed in this study successfully delineated areas affected by ash falls and pyroclastic flows. The accuracy of the algorithm was validated by comparing the results obtained using the established low level feature extraction method as shown in fig. 3. The damaged areas identified by the developed algorithm (fig. 3b) are 86% correlated to the results obtained using the low level feature extraction method (fig. 3a). Higher correlation could be observed in areas covered by volcanic ash shown in thin yellow shades in the maps. However, some discrepancies could be clearly observed in areas covered by pyroclastic flows which are shown in thicker yellow shades. More robust method of determining the accuracies in the identification of the areas damaged by volcanic eruptions would be done later when sufficient field data are already available.

References

Alonso, F.G., Soria, S.L., 1989. Classification of satellite images using contextual classifiers. Proceedings, 12th Canadian Symposium on Remote Sensing, Vancouver, Canada, July 10-14, 1989. 2, 645-646.

Gong, P., Howarth, P.J., 1992. Frequency-based contextual classification and gray-level vector reduction for land-use identification. Photogrammetric Engineering and Remote Sensing 58(4), 423-437.

Hayes, D.J., Sader, S.A., 2001. Comparison of change-detection techniques for monitoring tropical forest clearing and vegetation regrowth in a time series. Photogrammetric Engineering and Remote Sensing 67(9), 1067-1075.

Khazenie, N., Crawford, M., 1989. Spatial-temporal autocorrelated model for contextual classification of satellite imagery. Proceedings, 12th Canadian Symposium on Remote Sensing, Vancouver, Canada, July 10-14, 1989. 2, 497-502.

Mettemicht, G., 1999. Change detection assessment using fuzzy sets and remotely sensed data: an application of topographic map revision. ISPRS Journal of Photogrammetry and Remote Sensing 54(4), 221-233.

Peddle, D.R., Franklin, S.E., 1989. High resolution satellite image texture for moderate terrain analysis. Proceedings, 12th Canadian Symposium on Remote Sensing, Vancouver, Canada, July 10-14, 1989. 2, 653-654.

Sing, A., 1986. Change detection in the tropical forest environment of northeastern India using Landsat. Remote Sensing and Tropical Land Management. John Wiley and Sons, New York, N.Y. 365 pp.

Active fault database of Japan: Gathering and spreading active fault data for earthquake risk management

Toshikazu Yoshioka and Fujika Miyamoto

Active fault and Earthquake Research Center, Geological Survey of Japan, AIST, 1-1-1 Higashi, Tsukuba, Ibaraki 305-8567, Japan

The Active Fault and Earthquake Research Center, GSJ/AIST constructed an active fault database and opened to the public on the internet from 2005 to make a probabilistic evaluation of the future faulting event and earthquake occurrence on major active faults in Japan. The database consists of three sub-database, 1) sub-database on individual site, which includes long-term slip data and paleoseismicity data with error range and reliability, 2) sub-database on details of paleoseismicity, which includes the excavated geological units and faulting event horizons with age-control, 3) sub-database on characteristics of behavioral segments, which includes the fault-length, long-term slip-rate, recurrence intervals, most-recent-event, slip per event and best-estimate of cascade earthquake. Major seismogenic faults, those are approximately the best-estimate segments of cascade earthquake, each has a length of 20 km or longer and slip-rate of 0.1m/ky or larger and is composed from about two behavioral segments in average, are included in the database.

This database contains information of active faults in Japan, sorted by the concept of "behavioral segments" (McCalpin, 1996). Each fault is subdivided into 550 behavioral segments based on surface trace geometry and rupture history revealed by paleoseismic studies. Behavioral segments can be searched on the Google Maps. You can select one behavioral segment directly or search segments in a rectangle area on the map. The result of search is shown on a fixed map or the Google Maps with information of geologic and paleoseismic parameters including slip rate, slip per event, recurrence interval, and calculated rupture probability in the future. Behavioral segments can be searched also by name or combination of fault parameters. All those data are compiled from journal articles, theses, and other documents. We are currently developing a revised edition which is based on an improved database system.

More than ten thousands locality data such as the longitude and latitude, research method, displacement, age of paleofaulting etc. of each surveying sites are also available on the database. These data can be shown from the result view of the segment search.

The URL of the database is as follows:
http://riodb02.ibase.aist.go.jp/activefault/index_e.html

References

McCalpin, J. P., 1996. Application of paleoseismic data to seismic hazard assessment and neotectonic research. McCalpin ed. "Paleoseismology", Academic Press, 439-493.

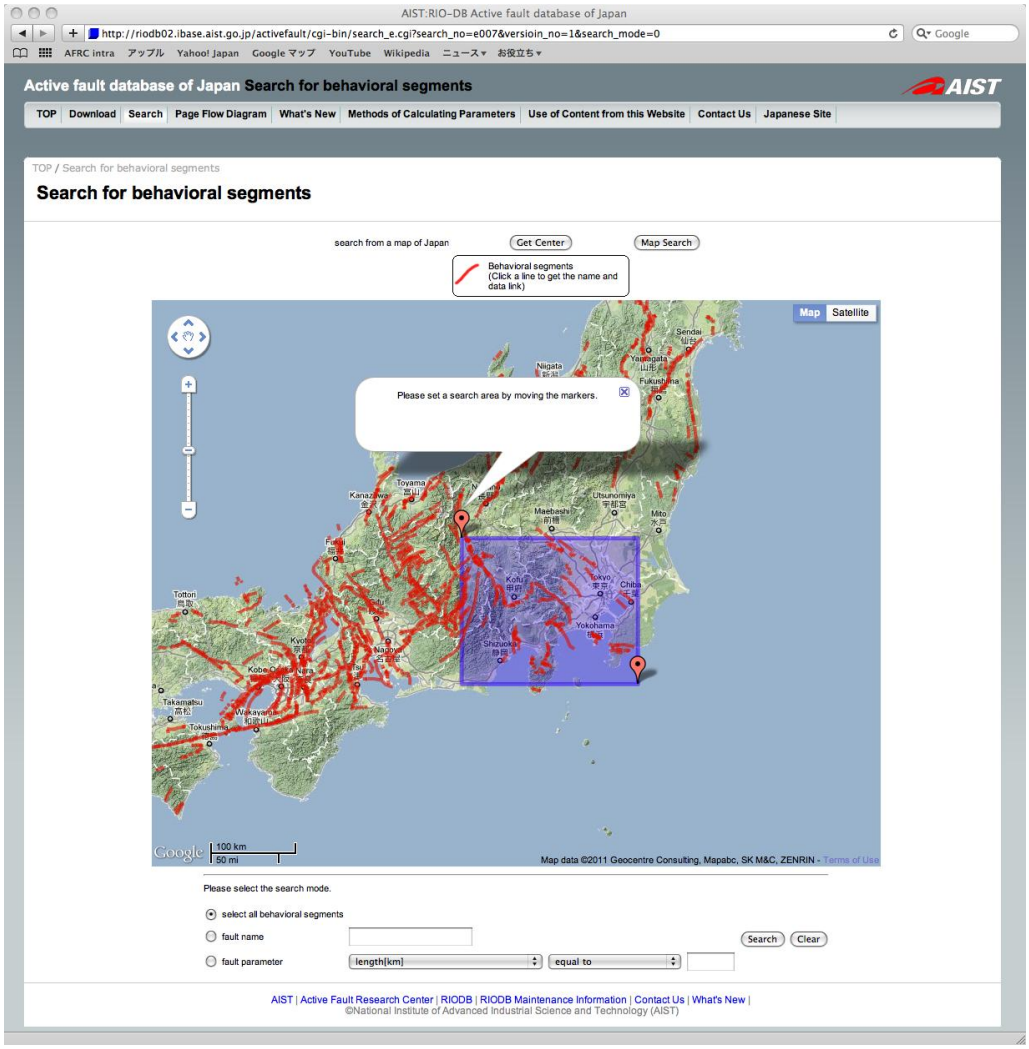

Fig.1 Screen image of search for behavioral segments on the Google Maps

ASTER Image Database for Volcanoes

Minoru Urai

Institute of Geology and Geoinformation, Geological Survey of Japan, AIST, 1-1-1 Higashi, Tsukuba, Ibaraki 305-8567, Japan

1. Introduction

The ASTER, which is an earth observing sensor onboard Terra platform and was launched on 1999, is a high spatial resolution imaging spectro-radiometer developed by Ministry of Economy, Trade and Industry, Japan. The ASTER Science Team proposed the 964 active volcano observation plan with ASTER (Urai et al., 1999) and a large number of volcanic ASTER scenes were acquired since June 2000 when the ASTER normal operation was started. The Database is designed to respond to requests from volcanologists for ASTER data. Acquired ASTER volcano images are stored within the database and can be displayed as time-series data, useful for monitoring activity at a particular volcano, as well as potentially useful in the mitigation and response to volcanic disasters. Using the database, you can browse time series of ASTER VNIR, SWIR, TIR and Stereo images that cover 20 km by 20 km fixed area centered at the volcano geographic location. Usually newly acquired scenes will be available within a week. A mosaic is constructed automatically if the volcano is at a scene boundary. 77% of 964 volcanoes have at least one daytime image that has 10 % or less cloud cover.

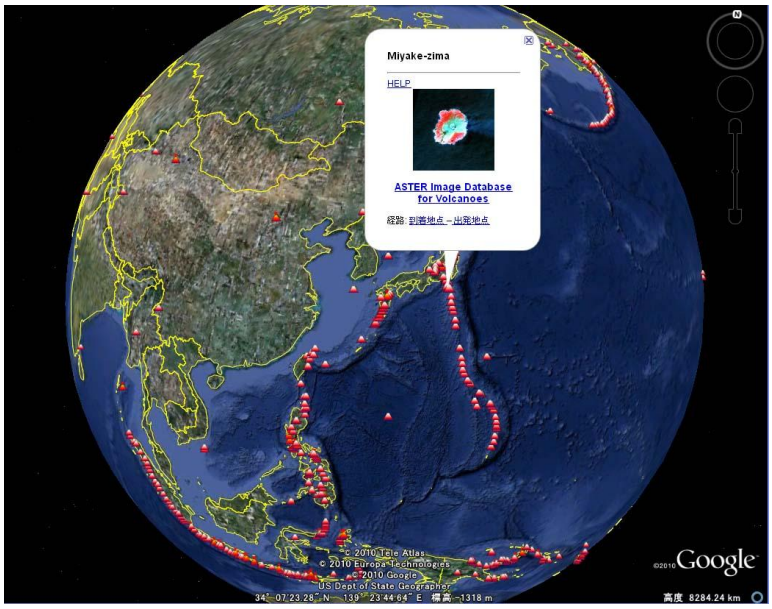

Fig. 1 Google Earth version of the ASTER Image Database for Volcanoes.

You can access the database at **http://igg01.gsj.jp/vsidb/image/index-E.html**. You will see the initial page. Google Earth will be started with volcano location when you click "All volcanoes with Google Earth" (Fig. 1). Clicking the thumbnail image, full resolution image will be displayed.

2. Statistics of the database

ASTER volcano observation is conducted based on ASTER Global Volcano Monitoring plan (Urai et. al., 1999). However, number of observation is depend on volcano. Some submarine volcanoes are rarely observed. Contrary, volcanoes in Iceland and Kamchatka are frequently observed.

Average number of daytime and nighttime observation are 5.0 times/year 5.3 times/year, respectively. The total number of scenes stores in the database is more than 142,000 scenes as of December 2011.

3. Volcanic activity observed with ASTER

Volcanic SO_2 flux can be estimated from the spatial distribution of SO_2 and wind velocity. Since ASTER has both the TIR subsystem and nadir-backward stereoscopic viewing function, we can estimate the volcanic SO_2 flux by the ASTER data alone. However, the nadir-backward These methods are applied to the Miyakejima volcano, Japan. The SO_2 flux derived from ASTER is around 5×10^4 ton/day (Urai, 2004). ASTER VNIR has nadir and backward view to generate DEM. The scale of summit collapse during the April 2007 eruption of Piton de la Fournaise, Reunion Island, western Indian Ocean, was evaluated using before-and-after differential digital elevation models (DEMs) derived from nadir and backward-looking images from the ASTER instrument. The dimensions of horizontal length and width, volume and depth of the depression were estimated as 1,100 by 800 m, $9.6\ 10^7$ m^3 and 320 m, respectively (Urai et. al., 2007). ASTER has TIR to observe surface temperature. Large surface thermal anomalies that were 4 km long, 1.5 km wide and represent an area of 3.85 km^2 were detected in cloud free nighttime on May 4, 2007, at the Piton de la Fournaise (Urai et. al., 2007). Sarychev Peak has been one of the most active volcanoes on Kuril Islands. Most recently it repeated its violent eruptions in June 2009. The volume of volcanic products in Matua Island discharged from Sarychev Peak was estimated, and there was a 0.08 km^3 difference between ASTER and PRISM DEM Data. The plume height was estimated as high as 10 km using ASTER images (Urai and Ishizuka, 2011).

4. Conclusions

ASTER was launched on December 1999 and has observed many volcanic eruptions. Through these observations, ASTER's ability to monitor volcanic activities, such as thermal anomalies, topographic changes, volcanic gases, among others, has been validated. The ASTER Image Database for Volcanoes helps to promote the use of ASTER images to volcanologists. Statistic analysis of ASTER Image Database for Volcanoes reveals the performance of ASTER Global Volcano Monitoring plan. 77% of 964 volcanoes have at least one daytime image that has 10 % or less cloud cover in eight years ASTER operation.

References

Urai, M., et al., 1999. Volcano Observation Potential and Global Volcano Monitoring Plan with ASTER (in Japanese with English abstract), Bulletin of the Volcanological Society of Japan, 44(3), 131-141.

Urai, M., 2004. Sulfur dioxide flux estimation from volcanoes using Advanced Spaceborne Thermal Emission and Reflection Radiometer - A case study of Miyakejima volcano, Japan, Journal of Volcanology and Geothermal Research, 134(1-2), 1-13.

Urai, M., et al., 2007. Size and volume evaluation of the caldera collapse on Piton de la Fournaise volcano during the April 2007 eruption using ASTER stereo imagery, Geophys. Res. Lett, 34, 1-7.

Urail, M. and Ishizuka, Y., 2011. Advantages and Challenges of Space-borne Remote sensing for Volcanic Explosivity Index (VEI): The 2009 eruption of Sarychev Peak on Matua Island, Kuril Islands, Russia. Journal of Volcanology and Geothermal Research, 208, 163-168.

The geological database of Quaternary volcanoes in Japan

Kuniaki Nishiki[a], Shun Nakano[a], Tatsuyuki Ueno[a], Jun'ichi Itoh[a] and Isoji Miyagi[a]

[a]*Institute of Geology and Geoinformation, Geological Survey of Japan, AIST, 1-1-1 Higashi, Tsukuba, Ibaraki 305-8567, Japan*

A systematically collected dataset about volcanoes, such as the location, ages, and rock types, contributes to comprehensive assessment of the volcanic activities in Japan. The existing database published by the Committee for catalog of Quaternary Volcanoes in Japan in 1999 does not fully reflect the latest geological and chronological data. Our goal is to construct a geological database of Quaternary volcanoes in Japan that uses the latest data, that picks up not only the Quaternary volcanic rocks but also volcanic bodies and intrusive bodies that haven't been checked in previous databases. Additionally, we took account of the change in the definition of Pliocene-Pleistocene boundary from 1.806 Ma to 2.588 Ma proposed by IUGS in 2009, and hence we screened the volcanoes of "Gelasian" stage. This database collects a good deal of information for every volcanoes, for example, the volcano-stratigraphy, eruptive styles, span of activities, position of craters (or estimated eruption center) and list of references. In this presentation, we introduce the dataset of Hokkaido and San'in area.

We hope this database supports a research project for the volcanic hazard reduction, national land utilization (e.g. construction of nuclear facilities) and so on. This database will be published by Geological Survey of Japan (GSJ). In the near future, it will be available on the web.

This research project has been conducted under the research contact with the Nuclear and Industrial Safety Agency (NISA).

References

Committee for catalog of Quaternary Volcanoes in Japan, 1999. Catalog of Quaternary Volcanoes in Japan ver.1.0. The Volcanological Society of Japan.

Japan-Russia scientific research activities for earthquake, tsunami and volcanic disaster mitigation in northwestern Pacific region

Hiroaki Takahashi[a], Mitsuhiro Nakagawa[a], Yuichiro Tanioka[a], Evgeny Gordeev[b], Alexander Khanchuk[c], Victor Bykov[d], Boris Levin[e], Mikhail Gerasimenko[f], Nikolay Schestakov[g], Alexey Malovichko[h], Victor Chebrov[f], Yury Levin[g], Larisa Gunbina[h]

[a]*Graduate School of Science, Hokkaido University, N10W8, Kita-Ku, Sapporo, Hokkaido 060-0810, Japan*
[b]*Institute of Volcanology and Seismology, Far Eastern Branch, Russian Academy of Sciences, 9, Piip Av., Petropavrovsk-Kamchatsky, 683006, Russia*
[c]*Far Eastern Geological Institute, Far Eastern Branch, Russian Academy of Science, 50, Svetlanslaya St., Vladivostk, 690990, Russia*
[d]*Institute of Tectonics and Geophysics, Far Eastern Branch, Russian Academy of Sciences, 65, Kim Yu Chen St., Khabarovsk, 680000, Russia*
[e]*Institute of Marine Geology and Geophysics, Far Eastern Branch, Russian Academy of Sciences,5, Nauki Street, Yuzhno-Sakhalinsk, 693022, Russia*
[f]*Institute of Applied Mathematics, Far Eastern Branch, Russian Academy of Science, 7, Radio Street, Vladivostok, 690041, Russia*
[g]*Far Eastern National University, 27, Oktyabrskaya St., Vladivostok, 690091, Russia*
[h]*Geophysical Survey Headquarter, 189, Lenina Pr., Obninsk, 249030,Russia*
[i]*Sakhalin Branch, Geophysical Survey, Russian Academy of Sciences,2-a, Tikhookeanskaya St.,693010, Russia*
[j]*Magadan Branch, Geophysical Survey, Russian Academy of Sciences, 685024, Russia, 6-b, Skuridin St., Magadan, 685024, Russia*

To clear up the mechanism of earthquake, tsunami and volcanic eruption occurring in northwestern Pacific region and to promote its application to regional disaster mitigation, Hokkaido University and Russian Institutions have continued cooperative scientific research since 1994. Recent comprehensive scientific agreement was signed in 2010 between vice president of Russian Academy of Sciences and Hokkaido University and is valid till 2014. Japan and Russian governments have also operated a program on cooperation in earthquake, volcanic eruption, and tsunami disaster mitigation in their neighboring areas since 2006, and an agreement on cooperation in research and development in science and technology about earthquake and volcanic eruption in Far East Russia since 1997.

Our research activities are strongly connecting with above agreements. A number of research and governmental projects and activities have carried out during recent 20 years. Nowadays, two actual research programs, “Geodynamics in Far Eastern Russia”, and “Eruption Mechanism Investigation in Klychevskaya volcano in Kamchatka”, are in operation under foundation of Graid-in-Aid for scientific research of MEXT.

Objective of former project is to reveal Amurian plate motion by GPS, seismicity and mantle structure, and to evaluate earthquake potential in eastern Japan Sea margin and surrounding areas. We have operated regional seismological network composed by 8 broadband and short-period seismographs in Far Eastern Russia, and local seismological network with 11 short-period one in south Sakhalin. These seismological data are used not only for scientific research but also for monitoring operation by geophysical survey of Russia. Continuous and temporal GPS observations have been done in Sakhalin and Primorsky region. These geophysical investigations have given new knowledge and questions, especially for Amurian plate motion. Several outcomes are published in journals (e.g. Bouroba et al., 2010, Shestakov et al., 2010, Ichiyanagi et al., 2009, Vasilenko et al., 2008).

Second project is strongly connecting with volcanic disaster assessment. It is well known that volcanic eruption occasionally causes catastrophic damages to air traffic as indicated by the 2010

Iceland eruption. Volcanic chain from Japan to Kamchatka has many active volcanoes, and disastrous eruptions have frequently occurred. From the view of disaster operation, monitoring of volcanic activity in this region is very important because main airline between East Asia to North America is flying over this hazardous area. Main goal of this project is to clarify physical mechanism of magma plumping system of island-arc basaltic volcano by geophysical and petrological approaches and to apply new insights for numerical volcano monitoring operation. Klychevskaya volcano is good subject for above aim because of its frequent eruption activities.

Realtime international data exchange on seismological, satellite, and visual instruments are required to realize effective monitoring on earthquake, tsunami and volcanic eruption. We are now challenging to build physical data connection network to distribute monitoring data in northwestern Pacific region. But it is fact that we have so many technical and political problems not yet solved. Paleotsunami surveys also have carried out in Kuril-Kamchatka trench. These prehistorical data is very valuable to evaluate earthquake occurrence interval and its application for tsunami assessment and prediction. We hope that authorities concerned pay more attention to neighboring Russian Far East as a good partner because its scientific activities and monitoring cooperation on geohazards are strongly connecting to national benefit on disaster mitigation field.

References

Bourova, E., K. Yoshizawa, K. Yomogida, 2010. Upper mantle structure of marginal seas and subduction zones in northeastern Eurasia from Rayleigh wave tomography, Phys. Earth Planet. Int., 183, 20-32.

Ichiyanagi, M., H. Takahashi, T. Maeda, M. Kasahara, H. Miyamachi, S. Hirano, R. S. Sen, M. Valentin, C. U. Kim, 2010. Aftershock activities of the Nevelsk earthquake on August 2, 2007, (M6.4), off southwest Sakhalin Island, Russia, by Japan-Russia joint observation, J. Seism. Soc. Jpn., 2, 62, 139-152.

Shestakov, N. V., M. D. Gerasimenko, H. Takahashi, M. Kasahara, V. A. Bormotov,V. G. Bykov, A. G. Kolomiets, G. N. Gerasimov, N. F. Vasilenko, A. S. Prytkov, V. Yu. Timofeev, D. G. Ardyukov and T. Kato, 2010. Present tectonics of the southeast of Russia as seen from GPS Observations, Geophys. J. Int., doi: 10.1111/j.1365-246X.2010.04871.x.

Vasilenko, N. F., B. W. Levon, A. S. Prytkov. C. U. Kim, and H. Takahashi, 2008. Dislocation model of the August 2, 2007, Mw6.2 Nevelsk earthquake, Doklady Earth Sci., 422, 1145-1149.

GEO Grid volcanic gravity flow simulation system for the next-generation real-time hazard mapping: an application to the recent 2011 eruption at Shinmoedake, Kirishima Volcano, Japan

Shinji Takarada[a], Shinsuke Kodama[b], Takahiro Yamamoto[a], Minoru Urai[a]

[a] *Geological Survey of Japan, AIST, Site 7, 1-1-1 Higashi, Tsukuba, Ibaraki 305-8567, Japan*
[b] *Information Technology Research Institute, AIST, Site 2, 1-1-1 Umezono, Tsukuba, Ibaraki 305-8568, Japan*

GEO Grid is an E-Infrastructure to accelerate GEO sciences related information retrieval, storage and processing based on the concept of virtual integration of all data related to earth observation, with certain access management. The GEO Grid system using a set of Grid and Web service technologies would be easy to handle by the end users. Numerical simulation of volcanic gravity flows on volcanoes is one of the major applications of the GEO Grid project. Volcanic disaster mitigation maps (volcanic hazard maps) are available for most major active volcanoes in Japan. A web-based GIS system combining various types of information with real-time numerical simulations are necessary for the next generation of volcanic hazard mapping system. Volcanic gravity flow simulations using the energy cone model are currently implemented on the GEO Grid system (Fig. 1). An interactive user interface to evaluate the probability of an area to be affected by volcanic gravity flows is available on the GEO Grid website. Presently, the volcanic gravity flow simulations are available for 14 volcanoes, such as Kirishima, Unzen, Usu, Merapi and St. Helens. It is also possible to update the digital elevation model (DEM) during the eruptions by taking new ASTER satellite data. Runtime of the simulation is very fast, taking between 10 seconds to 3 minutes, due to the speed of grid computing system. The OGC's Web Coverage Service (WCS) and Web Mapping Service (WMS) are used in the system. The simulation results could be downloaded as shape and KML files. It is thus possible for users to evaluate potential affected area by volcanic gravity flows using Google Earth or GIS system, overlaying evacuation route and various important facilities such as schools and hospitals.

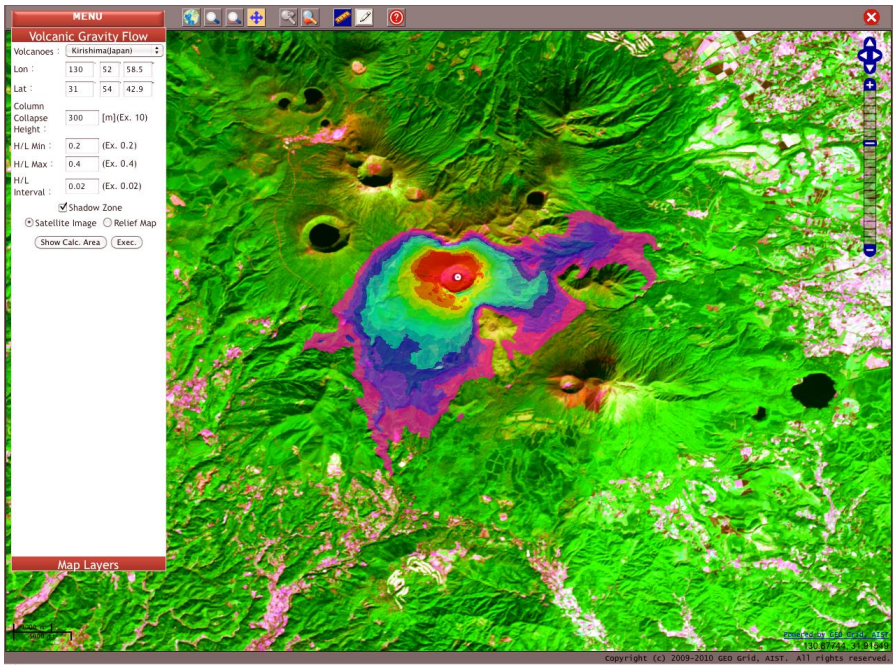

Fig. 1. GEO Grid volcanic gravity flow simulation system. Simulation results on the Shinmoedake, Kirishima Volcano as shown over the ASTER false color composite satellite image.

Phreatomagmatic, vulcanian and sub-plinian eruptions occurred at Shinmoedake, Kirishima Volcano in Kyushu, Japan from Jan. 19, 2011. A total of $3x10^{10}$ kg of volcanic lapilli and ash were ejected and widely distributed to the N120E on Jan 26 and 27. Shinmoedake erupted in ca. 9 ka, ca. 4 ka, 1716-17, 1771-72, and 1959. The major previous eruptions occurred in 1716-17. Phreatomagmatic, vulcanian and sub-plinian eruptions and pyroclastic flows were recorded during the 1716-17 eruptions. The maximum lateral runout distance of the pyroclastic flows was 4.5 km from the vent (Fig. 2). The magnitude of the 2011 eruptions is as large as the 1716-17 eruptions at Shinmoedake volcano (Imura and Kobayashi, 1991). The SiO_2 content of the ejecta from the 2011 eruption is ca. 57%, which is smilar to the ejected materials' SiO_2 content during the 1716-17 products. Hence, similar type of volcanic activity could occur during the 2011 eruption.

The GEO Grid simulation system was used on these eruptions to evaluate the potential pyroclastic flows to the surrounding area from this volcano. The GEO Grid energy cone simulation system is useful to evaluate the potential danger zone in this area. We assumed Soufriere-type pyroclastic flows derived from the column collapse based on the occurrence of the 1716-17 pyroclastic flow deposits. The column collapse height (Hc) was changed from 100 to 1000 m (Figs. 3, 4, 5). The equivalent friction coefficient of pyroclastic flows was estimated from 0.2 to 0.4 based on historical data. The best-fit case was H/L=0.2-0.3 and Hc=300m (Fig. 3) compared to the distribution of the 1716-17 pyroclastic flow deposits (Fig. 2). This result suggests that relatively higher mobility pyroclastic flows (H/L=0.2-0.3) may occur from a column collapse even if the collapse height is only 300 m (=100 m above the crater rim).

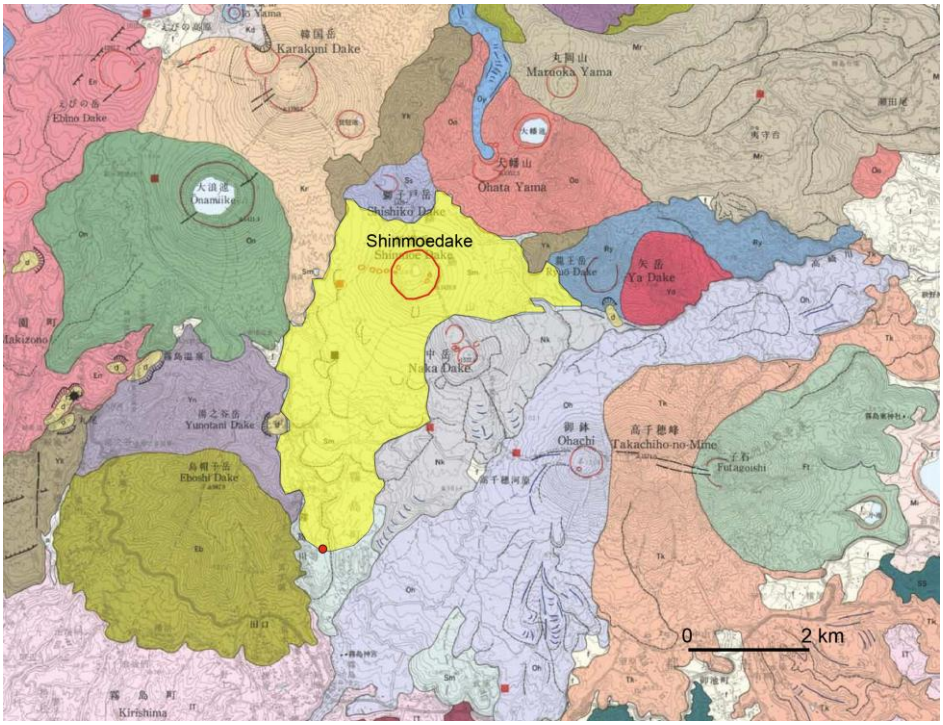

Fig. 2. Geological Map of Kirishima Volcano (Imura and Kobayashi, 2001). Yellow-colored part shown on the geological map indicates the distribution of the 1716-17 pyroclastic flow deposits from Shinmoedake. The red circle at the south margin shows the most distal outcrop of the pyroclastic flow deposit.

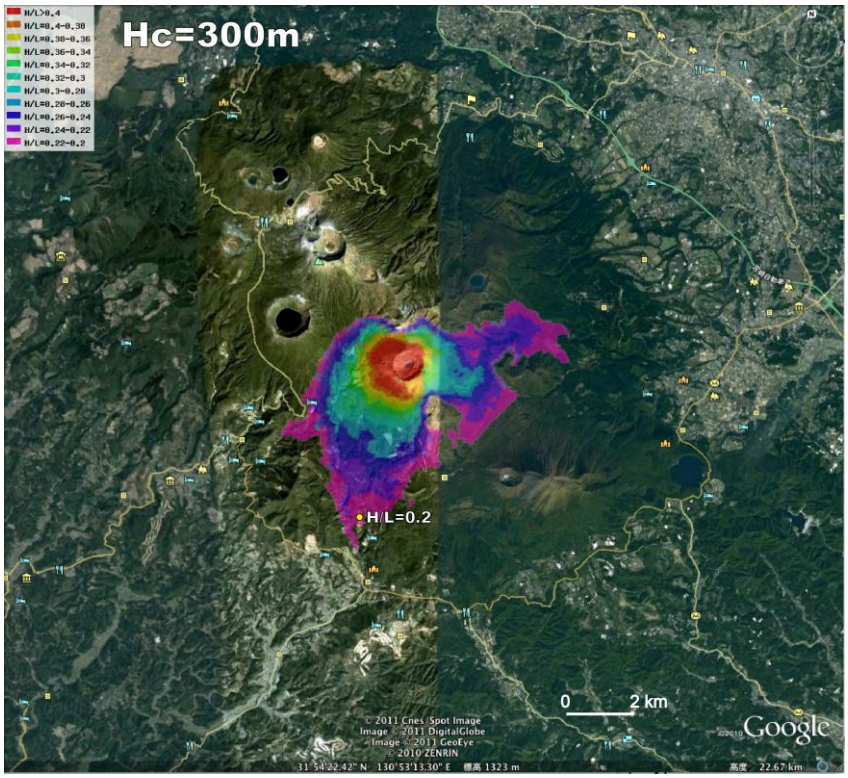

Fig. 3. Result of energy cone simulation (Hc=300m, H/L=0.2-0.4) shown on Google Earth. The point (H/L=0.2) in the figure shows maximum runout distance of pyroclastic flow (4.5km) from the source during the 1716-17 eruptions.

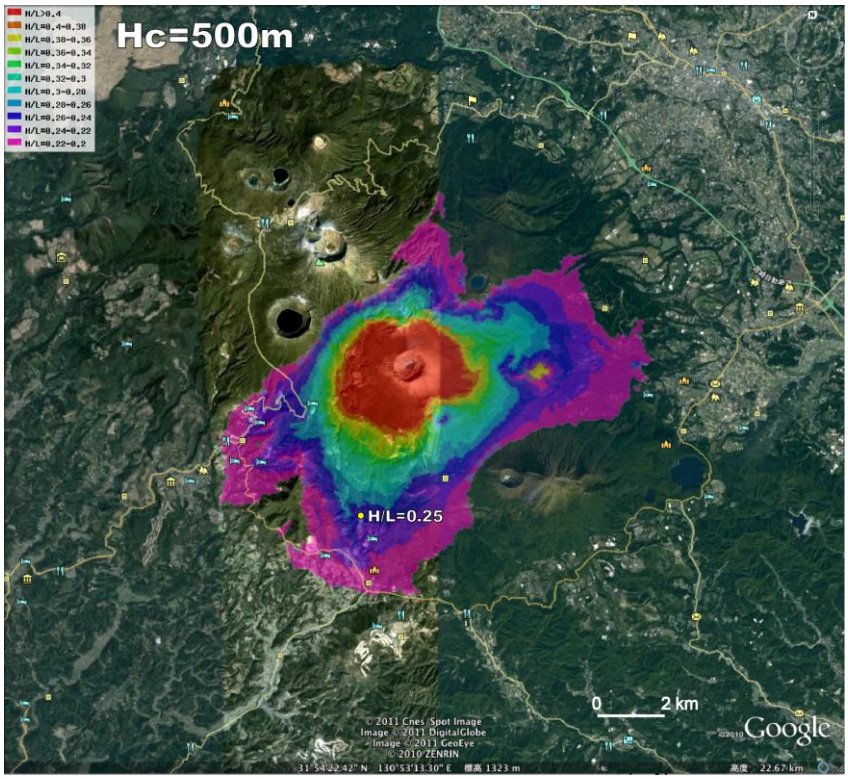

Fig. 4. Result of energy cone simulation (Hc=500m, H/L=0.2-0.4) shown on Google Earth. The point (H/L=0.25) in the figure shows maximum runout distance of pyroclastic flow (4.5km) from the source during the 1716-17 eruptions.

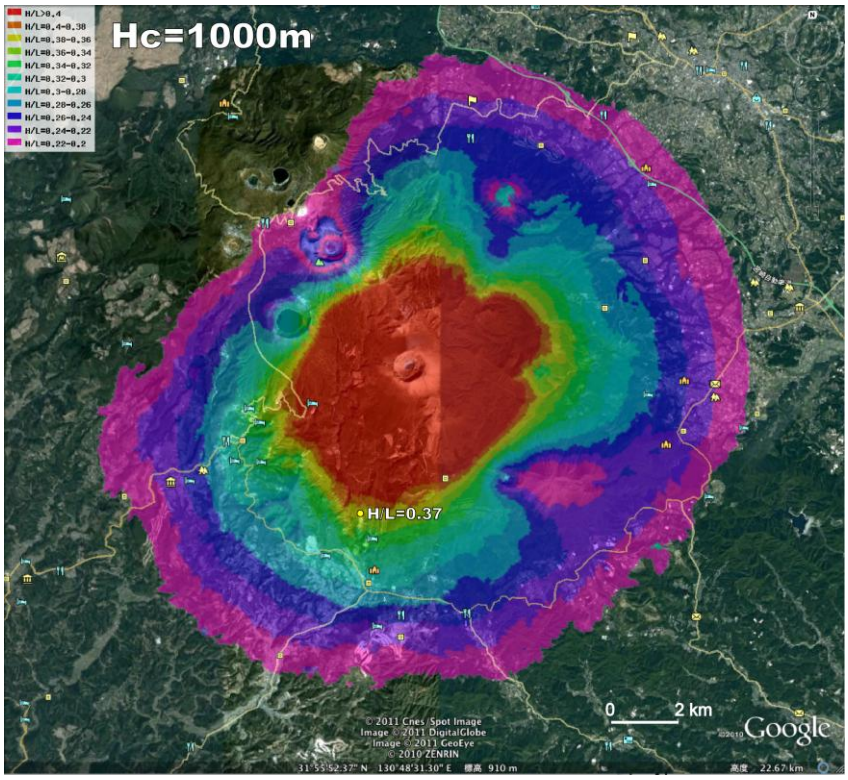

Fig. 5. Result of energy cone simulation (Hc=1000m, H/L=0.2-0.4) shown on Google Earth. The point (H/L=0.37) in the figure shows maximum runout distance of pyroclastic flow (4.5km) from the source during the 1716-17 eruptions.

The ASTER Global DEM (G-DEM, 30m resolution), STRM-3 (90m) and GSI 10m DEM are planned to be installed on the GEO Grid system in the near future. With this information, users could simulate any volcanic gravity flow for any volcano in the world on the GEO Grid simulation system. The energy cone simulation of the GEO Grid system could be applied to other geological hazards such as debris avalanches and landslides. The gravity flow simulation is open to all scientists in the world. More sophisticated simulations such as Titan 2D and LAHARZ, and the usage of ALOS satellite data such as PALSAR and PRISM (2.5m resolution) should be installed on the GEO Grid system in the near future. Collaboration between the GEO Grid and the V-Hub projects is another important target.

The GEO Grid simulation system: http://volcano.geogrid.org/applications/EnergyCone/
User Manual: http://docs.geogrid.org/HowToUse/EnergyCone_en
GEO Grid project: http://www.aist.go.jp/aist_e/aist_today/2009_33/pdf/2009_33_p05_p18.pdf

References

Imura, R., Kobayashi, T. 1991. Eruption of Shinmoedake Volcano, Kirishima Volcano Group, in the last 300 years. Journal of Volcanological Soc. of Japan 36, 135-148.

Imura, R., Kobayashi, T. 2001. Geological Map of Kirishima Volcano. Geological Survey of Japan, 11.

GPS- and InSAR-derived crustal deformation and estimated fault models of the 2011 Tohoku earthquake and the induced inland earthquakes

Tomokazu Kobayashi[a], Mikio Tobita[a], Takuya Nishimura[a], Shinzaburo Ozawa[a], Hisashi Suito[a], and Tetsuro Imakiire[a]

[a]*Geospatial Information Authority of Japan, 1 Kitasato, Tshukuba, Ibaraki 305-0811, Japan*

Preface

The 2011 off the Pacific coast of Tohoku Earthquake (hereafter called "the 2011 Tohoku earthquake") occurred on 14:46, March 11, 2011 (JST), rupturing the plate boundary to the east of northeastern Japn. It is the largest earthquake, of which moment magnitude is 9.0 (by JMA), among all earthquakes ever recorded in the history of seismic observation in Japan. The epicenter locates at off shore of Miyagi Prefecture, where large plate boundary earthquakes, of which magnitude is 7 to 8 but not larger than 8.5, have occurred repeatedly. The 2011 Tohoku earthquake generated a disastrous tsunami hitting the wide area of the Pacific coast from Hokkaido to Honshu causing great damages. In this presentation, we show the crustal deformation associated with the 2011 Tohoku earthquake, observed by geodetic techniques (GPS, GPS/acoustic, and InSAR), and the estimated slip distribution models for the co- and post-seismic deformation. Additionally, we show the InSAR-derived crustal deformation associated with the inland earthquakes probably induced by the 2011 Tohoku earthquake.

Co-seismic deformation

Significant crustal deformation caused by the 2011 Tohoku earthquake was detected by GEONET, the continuous GPS observation network operated by Geospatial Information Authority of Japan (GSI) (Fig. 1). It is notable that a very wide area around the Tohoku and Kanto Districts is affected by the crustal deformation by the 2011 Tohoku earthquake. The maximum movement is recorded at the tip of Oshika peninsula, the nearest place to the epicentric area, where the horizontal displacement reaches 5.3 m. It is the largest co-seismic displacement measured by GEONET since 1994. It is remarkable that all places along the Pacific coast line in the Tohoku and Kanto regions subsided co-seismically. The tip of the Oshika peninsula subsided about 1.2 m. Several tens centimeter subsidence was recorded at many sites from Miyagi to Ibaraki Prefectures coast line.

Slip distribution model

We constructed a distributed slip model for the co-seismic deformation, using GEONET data and seafloor crustal deformation data observed by Japan Coast Guard. We assumed that the co-seismic slip occurred along the plate interface between the Pacific Plate, which is subducting from east, and

the North American plate, where the Tohoku region locates. The slip is estimated by a geodetic inversion based on the method of Yabuki and Matsu'ura (1992). It is notable that the center of the slip area is estimated nearer to the Japan trench, or more eastward, compared with the model inferred using the GEONET data only (Fig. 2). The estimated maximum slip is more than 56 m. The moment magnitude (M_w) is estimated to be 9.0, assuming the rigidity as 40 GPa. This extremely large slip means that the plate boundary in and around this area has been locked very firmly before the earthquake even in the proximity of the trench, and has been accumulating strain energy for a long time.

Post-seismic deformation

GEONET reveals that remarkable crustal deformation is ongoing around the Tohoku and Kanto regions after the 2011 Tohoku earthquake. Horizontal movement toward southeast by east after the mainshock exceeds 50 cm. The pattern of the horizontal movement vectors toward east to southeast means that crustal block on the North American plate, where Tohoku region locates, is moving eastward, overriding onto the Pacific plate, even after the 2011 Tohoku earthquake. However, looking into the detail of the crustal movement pattern, we can note a slight difference between the co-seismic one and post-seismic one. Although all GEONET sites subsided co-seismically, several sites in Miyagi Prefecture and certain sites around Choshi have been uplifting after the earthquake. Some sites locating on the coast of Iwate Prefecture, however, have been still subsiding. Most significant feature of the slip model for the post-seismic deformation is that the center of slipping area is locating a little westward from the center of co-seismic slip area. This means that post-seismic slip along the plate boundary occurs mainly deeper zone compared with co-seismic rapture zone.

Inland earthquakes

Following the 2011 Tohoku earthquake, many inland crustal earthquakes occurred in addition to aftershocks on the plate boundary. Fukushima-Hamadori area and the surroundings is one of the regions where the seismicity drastically changed from a quiescent stage to an active stage. The inland earthquake with M_j7.0 that occurred on April 11, 2011 is the largest inland earthquake since the 2011 Tohoku earthquake, as of this writing. Applying interferometric SAR (InSAR) analysis using ALOS/PALSAR data to the earthquake, we succeeded in obtaining clear co-seismic deformation distributing over ~40-50 km range (Fig. 3). The most concentrated crustal deformation is located ~20 km west of the city of Iwaki. A maximum displacement away from the satellite is observed with ~2.2 m. The striking is that we can identify clear major and minor displacement discontinuities in the InSAR map. The maximum discrepancy in displacement across the discontinuity is approximately 1.6 m. Three main displacement boundaries can be recognized in the source region. The discontinuity

lines run just on the Shionohira, Idosawa and Yunotake fault traces, which are known as active faults (Research Group for Active Faults of Japan, 1991). Field surveys demonstrate that earthquake surface faults, which is of normal fault, appeared with 1.9 m at maximum, and the discontinuity in the interferogram does correspond to the surface rupture locations. Our inferred slip distribution model shows nearly pure normal fault motions on west-dipping planes with moderate-dip-angle (50-65°) for all the three faults (Shionohira, Yunotake, and Idosawa). The west-dipping normal fault motion on the Yunotake fault is correlated with the present-day topographic features, while those on both the Shionohira and Idosawa faults are reversely correlated with the topography.

Acknowledgment: GPS/acoustic data are provided from Japan Coast Guard for the construction of slip distribution model. PALSAR data are provided from Earthquake Working Group under a cooperative research contract with JAXA (Japan Aerospace Exploration Agency). The ownership of PALSAR data belongs to JAXA and METI (Ministry of Economy, Trade and Industry).

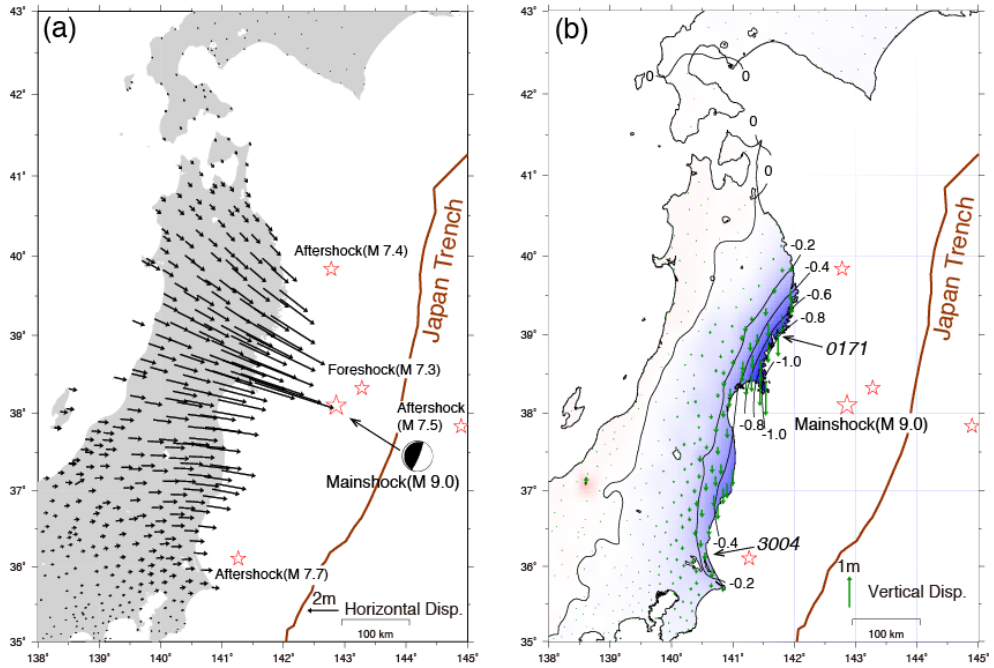

Fig.1 Crustal deformation associated with the 2011 off the Pacific coast of Tohoku Earthquake on March 11, 2011. (a) Horizontal component, (b)Vertical component

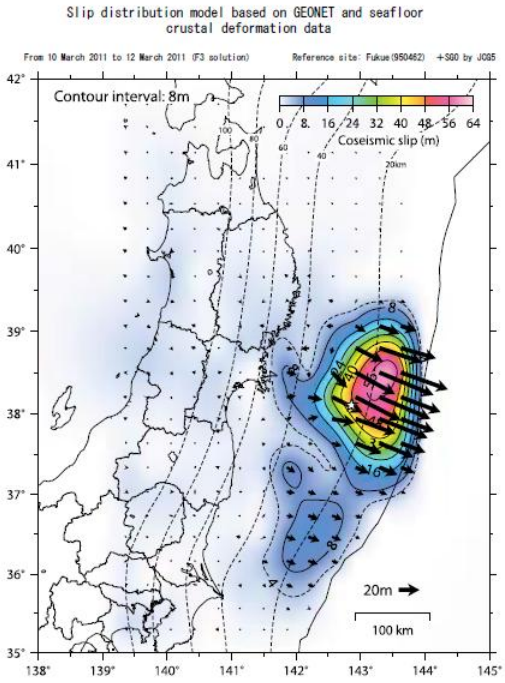

Fig. 2 Slip distribution model of the 2011 off the Pacific coast of Tohoku Earthquake, based on GEONET observation on land and seafloor crustal deformation by GPS/acoustic observations by Japan Coast Guard. (slip distribution model on the plate interface)

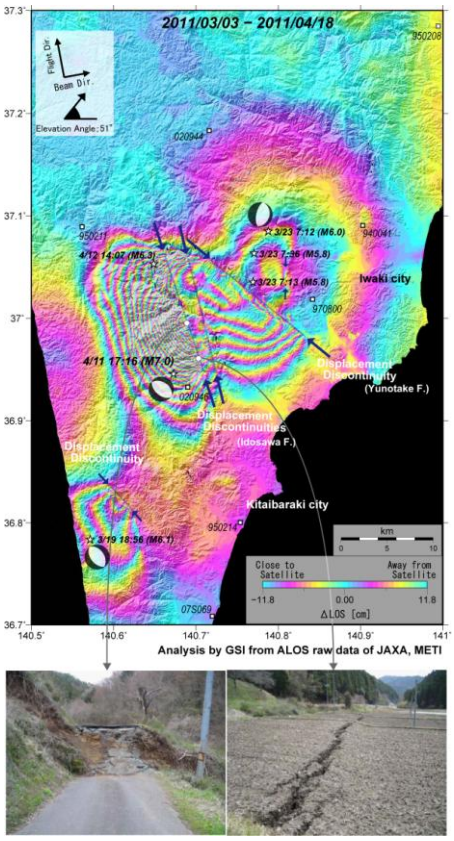

Fig. 3 An interferogram showing crustal deformation associated with the 3/19 (Mj6.1) event, the 3/23 (Mj6.0) event, and the 4/11 (Mj7.0) event. The blue arrows indicate the location of the displacement discontinuities.

Seismic gap and a series of large earthquakes along the Sunda trench and the Sumatran fault

Tomokazu Kobayashi[a] and Mikio Tobita[a]

[a]*Geospatial Information Authority of Japan, 1 Kitasato, Tshukuba, Ibaraki 305-0811, Japan*

Preface: The Sumatra subduction zone is one of the most seismically active regions. Many large megathrust earthquakes have historically repeatedly occurred along the Sunda trench, and the most recent sequence of large ruptures started with the 2004 Mw9.3 Sumatra earthquake. Some parts of the subduction zone is still locked and is likely to break in the next decade or so. To assess the seismic potential along the trench, it is vital to get a better grasp on the spatial extent of each rupture of the seismic sequence after the 2004 event. Also, other seismic hazard potential exists along the Sumatran fault. This fault is the length of ~2000 km with dextral slip motion parallel to the western coast of Sumatra. An oblique convergence between the Eurasian and the Indian/Australian plates along the trench results in a strain partitioning; the Sumatran fault accommodates a component of plate convergence parallel to the trench. There have been more than 20 M6-7 class earthquakes since 1882. In this presentation, we focus on two seismic events: the 2007 Bengkulu earthquake and the 2009 Jambi earthquake. The former is one of the most recent seismic events in a series of major subduction zone earthquakes that began with the 2004 event followed by an Mw=8.7 event on 28 March 2005, while the latter is an inland earthquake that is the first major event at the Sumatran fault since the 2004 event. Satellite synthetic aperture radar (SAR) data can provide detailed and spatially comprehensive ground information. Interferometric SAR (InSAR) analysis has an advantage of detecting ground deformation in a vast region with high precision. We conduct an InSAR analysis for these two events and reveal the spatial extent of each rupture. These results will demonstrate the relationship between the seismic gaps and a series of earthquakes in the Sunda trench and the Sumatran fault, and allow us to discuss the seismic potentials.

The 2007 Bengkulu Earthquake: In this section, we mainly introduce the results of Tobita et al. (2009). A great earthquake with M8.4 (USGS) occurred along the Sunda trench on 12 September, 2009. To map the ground displacement on the Pagai Islands and on the west part of Sumatra Island near the source area, we conduct an InSAR analysis. We use the satellite data of the ALOS/PALSAR which has an L-band sensor with a wavelength of 23.6 cm. The advantage of the L-band sensor is that coherence in interferograms is high even in heavily vegetated areas. For the analysis, we used the orbital paths 445 (29 January, 2007 - 16 September, 2007) and 448 (21 June, 2007 - 21 September, 2007) which cover the west coastal zone of Sumatra Island and the Pagai Islands, respectively. They are strip-map imagery with off-nadir angle of 34.3 degrees. We process the SAR data from a level-1.0 product using a software package GSISAR. We use SRTM (NASAs Shuttle Radar Topography Mission) data with a 3 arc-sec resolution to remove the topographic phase. The ground displacement associated with the earthquake on the Pagai Islands is successfully mapped even in the forest areas. In the interferogram covering the Pagai Islands, approximately fourteen fringes can be recognized between the south end of South Pagai Island (Pulau Pagai Selatan) and the north end of North Pagai Island (Pulau Pagai Utara), indicating that the former has moved 1.7 m toward the satellite relative to the latter. A significant ground deformation in the coastal zone of Sumatra Island is also identified, showing roundish-shaped fringes. The maximum displacement toward the satellite relative to the southeastern edge can be recognized with approximate 60 cm at the region. We inverted the obtained InSAR data to estimate slip distribution on the fault. The slip is estimated as ~2 m at maximum,

located ~50 km south from the southernmost area of South Pagai Island. The rupture length parallel to the trench is ~250 km, and the main slip terminates at the north of South Pagai Island. The estimated slip distribution overlaps with the rupture area of the 1833, but does not reach that of 1797 event which is around Siberut Island off Padang. The remaining unruptured area, namely, the seismic gap suggests that a high seismic potential equivalent to >M8 class does still exists off Padang.

The 2009 Jambi Earthquake: An inland earthquake occurred in the south of Sumatra Island on 1 October, 2009 with M6.6. To map the coseismic displacement, we conducted an InSAR analysis in the same manner as the 2007 Bengkulu event. We used the orbital paths 445 (21 September 2009 - 6 November 2009) for ascending data and 114 (19 January 2009 - 22 October 2009) for descending data. For both paths, clear fringes showing coseismic displacement are identified. The main crustal deformation area concentrates nearly along the Sumatran fault. A result of a 2.5D displacement analysis shows that an eastward motion is inferred with a slight upheaval of ~10 cm in the eastern side of the fault, while in the western side a westward motion is inferred with a slight subsidence of ~10 cm, which is consistent with a right-lateral slip motion. Sieh and Natawidjaja (2000) presented a detailed description of tectonics regarding the Sumatran fault, and they identified 19 fault segments. The rupture area of the 2009 event corresponds to "Dikit segment" they proposed. The Dikit segment is a seismic gap sandwiched between the Siulak segment and the Ketaun segment where Mw=6.7 (USGS) and M=6.2 events occurred in 1995 and 1952, respectively. We may interpret that in a concept of seismic gap hypothesis the 2009 Jambi earthquake was an anticipated event to come.

Acknowledgment: PALSAR data are provided from Earthquake Working Group under a cooperative research contract with JAXA (Japan Aerospace Exploration Agency). The ownership of PALSAR data belongs to JAXA and METI (Ministry of Economy, Trade and Industry).

References

Sieh, K., Natawidjaja, D., 2000. Neotectonics of the Sumatran fault, Indonesia, J. Geophys. Res. 105, 28,295-28,326.

Tobita, M., Ozawa, S., Yarai, H., Nishimura, T., Suito, H., Une, H., Imakiire, T., Amagai, T., Hayashi, F., 2009. Crustal deformation and fault model of the 2007 southern Sumatra earthquake, Chikyu Monthly, 3, 181-188 (in Japanese).

Characterizing Pyroclastic Flow Deposits of a Large Eruption of Mt. Merapi in 2010 using ALOS/PALSAR and ASTER data

Asep Saepuloh[a,b], Minoru Urai[a]

[a]*Institute of Geology and Geoinformation, Geological Survey of Japan, AIST, 1-1-1 Higashi, Tsukuba, Ibaraki 305-8567, Japan*

[b]*Department of Geology, Bandung Institute of Technology (ITB), Jl. Ganesha 10, Bandung 40132, Indonesia.*

Introduction

Detecting pyroclastic flow deposits soon after eruption and their topographic changes after eruption by only optical remote sensing in Torrid Zone are difficult because the clouds, gases, and ashes usually cover thickly the volcano. This study demonstrates the usefulness of a data combination of the Phased Array type L-band Synthetic Aperture Radar (PALSAR) regardless of weather conditions and Advanced Spaceborne Thermal Emission and Reflection Radiometer (ASTER) data. We chose Mt. Merapi in central Java, Indonesia, as a study site (see Fig. 1). The summit of Mt. Merapi is about 2965 m above the sea level and close to the dense populated Yogyakarta City (about 25 km). Merapi activity is characterized by a very frequent eruption ranging from one to five years of time duration (Voight et al., 2000). Serious disasters have been occurred when the dome of lava grows up and collapse to the valley: they are accompanied by hot clouds that usually rise from pyroclastic flows or nuée ardentes. The latest eruption was occurred in November 2010 which caused fatalities to more than hundred people died and serious infrastructure damages. The focus of this paper is to characterize the pyroclastic flow deposits in Novermber 2010 including distribution area (*A*), flow distance (*D*), included angle (α), and collapse direction (γ). The last fifteen years of pyroclastic flow deposits at Mt. Merapi were also used to show the general pattern of the distribution over time.

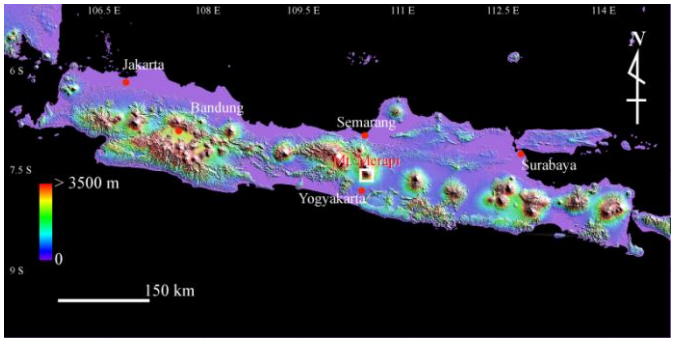

Fig. 1. Location of Mt. Merapi in Central Java, Indonesia.

The Temporal Change of Pyroclastic Flow Deposits

To extract the distribution of pyroclastic flow deposits, we generated the intensity images of SAR data around the summit from single-look complex (SLC) data. The noises from speckle are always incorporated to the image because the backscatter intensity contains reflections of physical quantities from various objects (Hanssen, 2002). Moreover, the high slope gradient also caused the intensity images brighter than flat area. Overcoming the problem, a low level feature extraction was used for ratio of the two intensity

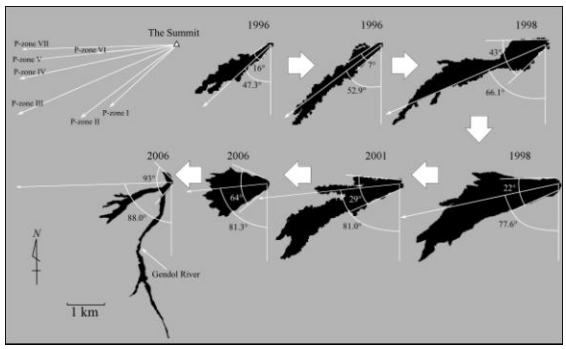

Fig. 2. The change of pyroclastic flow deposits from 1996 to 2006 (Saepuloh et al., 2010).

images. This method is proved effective to extract the pyroclastic flow deposits from the background including speckle noise and slope gradient problem (Saepuloh et al., 2010). After the pyroclastic flow deposits were extracted, the ratio image was geo-coded using DEM SRTM 90 m. About 100 tie points were selected automatically to rectify the image from radar line of sight (LOS) to ground range using polynomial regression. Fig. 2 shows the extracted-pyroclastic flow deposits since 1996 to 2006 using JERS1 and RADARSAT-1 data. The *A* of pyroclastic flow deposits varies over time. The maximum of *A* was achieved in 1998. Generally, the γ of the pyroclastic flow deposits in the past is toward S-SW. The detail explanation about the change pattern each eruption period is discussed in the last section.

To extract the new pyroclastic flow deposits at the latest eruption in November 2010, a pair of ALOS/PALSAR data was used. The acquisitions of the two data are before and after eruption. Their data information is listed in Table 1. Fig. 3A shows the boundary of pyroclastic flow deposits overlaid on a color composite image of ALOS/PALSAR. The flow pattern is similar with the pyroclastic flow deposits in Jun 2006. However, the coverage area is larger than previous eruption. The main paths are toward South and Southwest from the summit. The highest intensities change was occurred at the Southern flank as shown by a massive magenta portion in Fig. 3A. It indicated that the highest damages to the surface layer have been occurred at this area. The hot pyroclastics have flowed and devastated everything on their path. Therefore, surface moisture and texture of the surface layer decrease the intensity value of the image. The pyroclastic flow deposits were also distributed to the Southwestern flank from the summit. Although the intensity of ALOS/PALSAR does not change strongly at the Southwestern flank, the coverage area is larger than distribution at the Southern flank.

Table 1. ALOS/PALSAR used in this study

No	Acquisition date	Path	Row
1	September 12, 2007	93	378
2	November 05, 2010	93	378
3	November 01, 2010	431	704
4	December 17, 2010	431	704

To confirm the distribution of pyroclastic flow deposits, an ASTER thermal infrared (TIR) image was used (see Fig. 3B). The TIR instrument can observe radiance of active lava flows and pyroclastic flows (Ramachandran et al., 2011). The acquisition time of the image is November 1, 2010. To reduce the disturbance of thermal radiance from the environment at day time, the ASTER data at night time was used. Therefore, the high thermal radiance is supposed to be originated from the hot spot of eruption. The massive hot spot was located at the Southern flank from the summit. The position of the hot spot is same with detected pyroclastic flows by ALOS/PALSAR. Another hot spot was located at the Southwestern flank from the summit coincidence also with detection of ALOS/PALSAR.

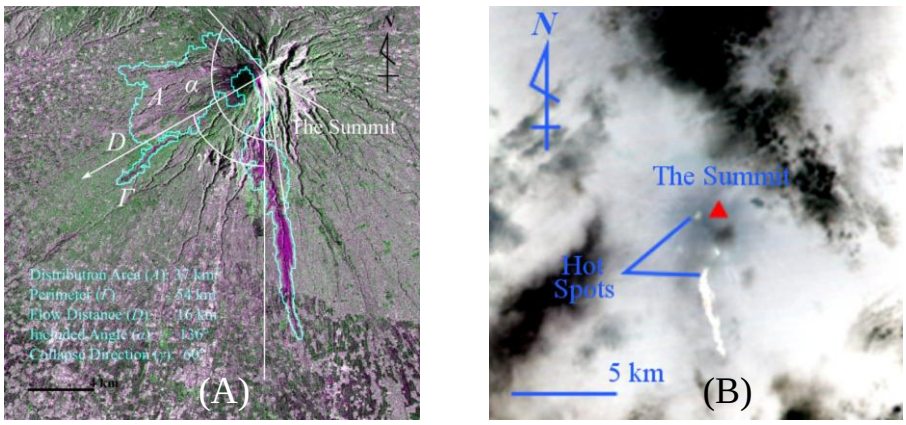

Fig. 3. Boundary of pyroclastic flow deposits overlaid on a color composite of ALOS/PALSAR for R=B=Sept. 12, 2007 and G=Nov. 5, 2010 (A). The hot spots of ASTER image in color composite for R=band 11, G=band 13, and B=band 14 (B).

The Differential Interfermetric SAR (D-InSAR) of Volcano-deformation

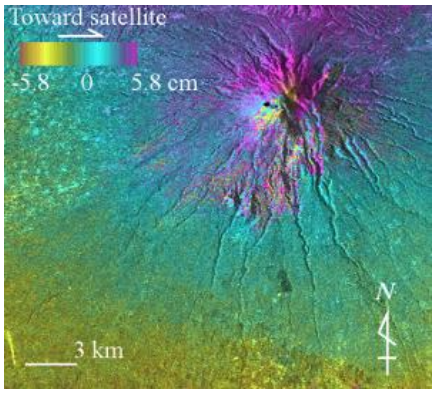

Fig. 4. The interferogram of ALOS/PALSAR shows the strong deformation around the summit

To obtain the deformation in relation to the eruption, we generated the Differential Interfermetric SAR (D-InSAR) of ALOS/PALSAR using GAMMA software. The data pair used to generate the interferogram is shown by no. 3-4 in Table 1. The short perpendicular baseline about 96 m was used to reduce the influence of topographic effect in the interferogram. Fig. 4 shows the interferogram after flattening, orbital and topographical phase correction, and unwrapping. The fringes are supposed to be originated from the deformation phase only. The color order from magenta-yellow-cyan-magenta indicates the uplifting toward satellite. On the contrary, the opposite color order indicates the subsidence. The acquisition dates of the data are before and after eruption. The uplifting phenomena are noticeable clearly around the summit. The highest uplifting was occurred at the remaining edge of the crater in Northeast. The other sides of the crater were already collapse in this period. The collapse of the crater produced pyroclastic flows toward lower topography as shown by fringes discontinuity in the South-Southwest. The fringes discontinuity was caused by low coherency of the two SLC data due to the surface changed.

Discussion

The eruption of Mt. Merapi in November 2010 has a different characteristic in comparison with the last fifteen years of eruption. The peak eruption which is characterized by explosion of large amount pyroclastic flows was occurred in a short period. Fig. 5 shows the characteristics of pyroclastic flow deposits. The abscissa and ordinate axes present the year eruption and characteristics for each eruption period, respectively. The polynomial regression was calculated and overlaid on the true data value to show the trend of the data. Fig. 5A shows that the *A* of the pyroclastic flow deposits is about 7 times larger than the eruption in 2006. The total area covered by pyroclastic flow deposits is about 37 km^2. The maximum of the *D* is about 16 km toward South from the summit (see Fig. 5B). The *A* and *D* at the field should be larger than this calculation because the eruption still continues when the data is acquired. The α has an increasing trend from 1996 to 2010 as shown by Fig. 5C. The eruption in 2010 has the widest angle than the previous eruption. The interesting phenomenon is the contrast trend of the γ from the previous eruption (see Fig. 5D).

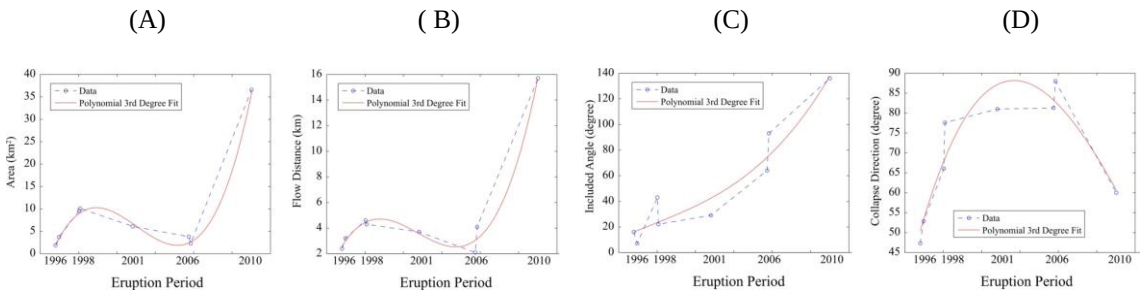

Fig. 5. Characteristics of pyroclastic flow deposits for each eruption period. The polynomial regression was overlaid to show the general trend of the data.

Since the eruption in 1996 to 2006, the trend of γ increased clockwise from the South to the West. However, the γ in 2010 has been changed counter-clockwise from the last fifteen years of eruption. The trend returned to the eruption in 1996. This temporal variation of γ is supposed to be controlled by several factors such as the dome configuration, conduit dislocation, and physical conditions of the magma which ascended through the conduit. In addition, the deformation around the summit can be interpreted that the magma ascended from the deep to the shallow reservoir. The D-InSAR analysis of ALOS/PALSAR which has capability to detect the deformation in millimeter scale (Sandwell et al., 2008), could be used to correlate the internal factor from the magma ascent and the external factor such deformation prior to the dome collapse at the summit. The existence of the hot spots from ASTER TIR images is the evidence that the magma reached to the surface following the dome collapse

Concluding Remark

The pyroclastic flow deposits in the 2010 eruption were detected using the low level feature extraction of the backscatter intensities data. Four characteristics can be calculated: coverage area, flow distance, included angle, and collapse direction. The characteristic of the latest eruption in 2010 has significant differences in which the coverage area, flow distance, and included angle are larger than the last fifteen years of eruption. Moreover, the collapse direction has an opposite trend in comparison with previous eruption. It is similar to the eruption in 1996 toward Southwest from the summit. In addition, the high resolution of the deformation at the summit can be detected using D-InSAR analysis of the ALOS/PALSAR data. The high pressure from magma raised the topography of the summit prior to the dome collapse. The highest uplifting was occurred at the Northeast of the crater. The discontinuity of D-InSAR phase interferogram presented the distribution of pyroclastic flow deposits at the South-Southwest from the summit. The hot spots of ASTER TIR at night time acquisition indicated that the magma from beneath have reached to the surface. Their existence proved that the strong deformation at the summit originated from magma ascent.

References

Hanssen, R.F., 2002. Radar interferometry data interpretation and error analysis. Kluwer Academic Publishers 9-42.

Ramachandran, B., Justice, C.O., Abrams, M J., 2011. Land remote sensing and global environmental change; NASA's Earth observing system and the science of ASTER and MODIS. Springer 245-272.

Saepuloh, A., Koike, K., Omura, M., Iguchi, M., Setiawan, A., 2010. SAR- and gravity change-based characterization of the distribution pattern of pyroclastic flow deposits at Mt. Merapi during the past 10 years, Bulletin of Volcanology 72,221–232.

Sandwell, D.T., Myer, D., Mellors, R., Shimada, M., Brooks, B., Foster, J., 2008. Accuracy and resolution of alos interferometry: vector deformation maps of the Father's Day intrusion at Kilauea 46, 3524 – 3534.

Voight, B., Constantine, E.K., Siswowidjoyo, S., Torley, R., 2000. Historical eruptions of Merapi volcano, Central Java, Indonesia, 1768–1998. Journal of Volcanolology and Geothermal Research 100, 69–138.

Observation network of groundwater and crustal deformation for forecasting the Tokai, Tonankai and Nankai earthquakes

Norio Matsumoto and Naoji Koizumi

Active Fault and Earthquake Research Center, Geological Survey of Japan, AIST, 1-1-1 Higashi, Tsukuba, Ibaraki 305-8567, Japan

Along the Nankai and the Suruga trough, off central to southwest Japan, great earthquakes about magnitude 8 or more have been occurred at intervals of 100 - 200 years. Recent events were the 1944 Tonankai (M 7.9) and the 1946 Nankai (M 8.0) earthquakes along the Nankai trough after 90 - 92 years from the 1854 Ansei Tokai (M 8.4) and Nankai (M 8.4) earthquakes, whereas no earthquake occurs along the Suruga trough after 1854. This anticipated earthquake is referred to as “Tokai earthquake”, and the Japanese Government has been continuing an earthquake prediction program for the anticipated Tokai earthquake since 1978. Japan Meteorological Agency (JMA) is responsible for the prediction of the anticipated Tokai earthquake.

Geological Survey of Japan, AIST has been monitoring groundwater levels at 4 - 15 wells since 1977 to contribute to the prediction of the Tokai earthquake.

We evaluate the detectability of inferred groundwater-level anomalies associated with a preslip at seven groundwater wells observed by GSJ, AIST if the preslip prior to the anticipated Tokai earthquake is assumed to be occurred. In this case the groundwater-level anomalies associated the preslip at HAI, KNG, and OGS exceed the significant anomaly at 38, 3, and 3 hours prior to the Tokai earthquake, This was the first attempt to evaluate detectability of hypothetical preseismic groundwater-level anomalies based on plausible mechanism. Such evaluation is needed if hydrological anomalies are applied to a real-time earthquake prediction.

GSJ, AIST has also established fourteen observation sites in and around focal zones of Nankai and Tonankai earthquakes to monitor groundwater and crustal strain from 2006. The 30, 200 and 600 m-depth wells are constructed in each observation site. Groundwater level and groundwater temperature are observing at each well, and a multi-component borehole strainmeter is deployed at the bottom of either the 600 m-depth or the 200-m depth well. We expect to observe groundwater level and borehole strain changes associated with the short-term slow slip events, preslips and co- and afterseismic crustal deformation.

Long-term variation of pre-caldera volcanic activity in Bali and in Tengger caldera region, East Java

Kiyoshi Toshida[a], Shingo Takeuchi[a], Ryuta Furukawa[b], Akira Takada[b], Supriyati Andreastuti[c], Nugraha Kartadinata[c], Anjar Heriwaseso[c], Oktory Prambada[c], A. Rosgandik[a] Mulyana[c] and Asep Nursurim[c]

[a] *Geosphere Science Sector, Civil Engineering Research Laboratory, CRIEPI, 1646 Abiko, Abiko-shi, Chiba 270-1194, Japan*

[b] *Geological Survey of Japan, AIST, 1-1-1 Higashi, Tsukuba, Ibaraki 305-8567, Japan*

[c] *Center for Volcanology and Geological Hazard Mitigation, Jalan Diponegoro 57, Bandung, Indonesia*

Large-scale, caldera-forming eruptions cause significant effects on both regional and global scale. Large amount of magma need to accumulate over long period of time before large-scale eruption takes place. In order to find the characteristics on the long-term variation of volcanic activity prior to caldera-forming eruptions, we observe stratigraphy and topography, and conduct comprehensive sample collection of volcanic rocks in Bali and Tengger caldera region, East Java. Modal abundance analysis, as well as on-going analysis on whole-rock chemistry and K-Ar dating, are preformed at CRIEPI. Mass fractionation correction method is used for the K-Ar dating. Lava samples having holocrystalline (pilotaxitic or intergranular) groundmass texture are selected for dating analysis in order to obtain accurate and precise ages.

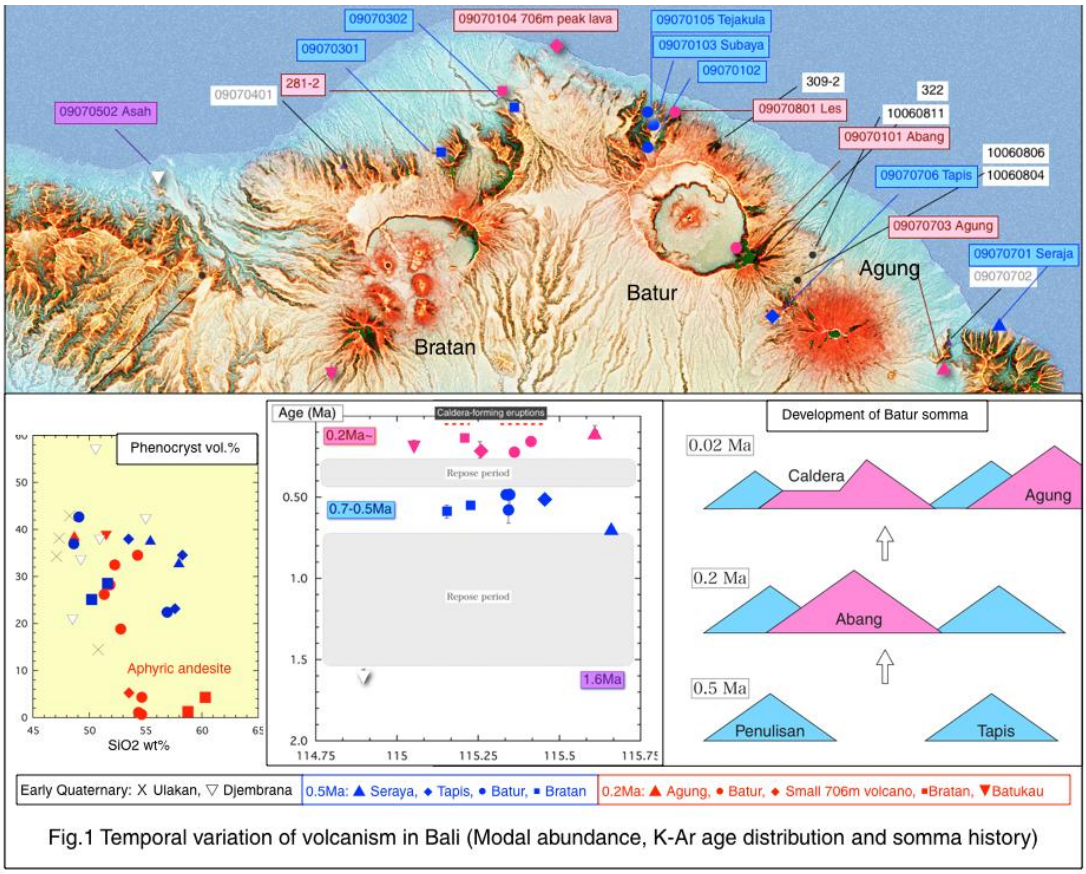

Fig.1 Temporal variation of volcanism in Bali (Modal abundance, K-Ar age distribution and somma history)

1. Batur and Bratan, Bali

We have identified three periods of volcanic activity in Bali. They are 1.6 m.y. BP, 0.7-0.5 m.y. BP, and 0.2 m.y. BP to present. Large somma of both Batur and Bratan caldera volcanoes are constructed by 0.2-0.1 Ma activity, and partly covers 0.6-0.5 Ma volcano to form large shield volcano. Both Batur and Bratan systems have produced caldera-forming eruptions multiple times in the past 30 ky (Furukawa et al., this workshop). The calderas have formed between the peaks of volcanoes from different ages (Fig.1).

Andesites have particular mafic phenocryst assemblage for each period. Hornblende andesite is limited to early Quaternary, and orthopyroxene andesite is limited to 0.5 Ma activity. Clinopyroxene phenocrysts are common to andesites of all ages, except for aphyric andesites of 0.2 Ma activity. They are light-colored in thin sections, indicating their high Mg# and relatively high temperature of magma. The large shield volcanoes of 0.2 Ma consist of aphyric andesite lava layers. The aphyric andesite lavas have relatively higher K2O, TiO2 content and FeO*/MgO ratio. The 0.2 Ma aphyric andesite has also erupted outside of somma at the small volcano located 10 km to the NW of Batur caldera rim. Part of the accumulated aphyric andesite magma of the caldera system may have propagated laterally by dikes.

2. Tengger caldera system, East Java

We have identified at least four active periods in Tengger; they are (1) 1.7 m.y. BP, (2) 0.5 m.y. BP, (3) 0.3 m.y. BP, and (4) 0.1 m.y. BP to present. Much of the somma seem to have formed by pre-caldera period. The start of volcanic activity is similar to Bali, but the two caldera-forming eruptions (Ngadisari and Sand Sea) are much older than Bali. Pyroclastic density current (PDC) deposits of the Ngadisari eruption (Sukapura ingimbrite) is distributed in the northeast apron and foothill. PDC deposits of the Sand Sea eruption are widely distributed at its caldera wall as well as in Ngadisari caldera and in northwest and southwest aprons.

Similarities to Bali include (a) formation of large somma prior to caldera-forming eruption as a result of overlapping volcanoes formed at different periods, (b) clinopyroxene is common phenocryst of basaltic andesite to andesite, and occurence of orthopyroxene andesite is limited to older active period, (c) clinopyroxene phenocrysts are light-colored in thin sections which indicate their high Mg# and high temperature of magma, (d) activity of aphyric andesite that forms shield volcano during intra-caldera period, and (e) the younger aphyric andesites have relatively higher K2O, TiO2 content and FeO*/MgO ratio. Temporal transition of intra-caldera activity from mixed basaltic andesite to uniform and aphyric andesite indicate the accumulation of andesite magma.

(1) Older activity

The northwestern apron of Tengger has dissected topography with wide horseshoe-shaped depression (Kukusan volcano; Takada et al., 2000). Olivine-plagioclase basalt lava at its ridge (G. Tunggangan) is weathered and have onion-like spherulical texture. We have obtained the K-Ar age of 1.7 Ma from this phenocryst-rich lava. Dissected topography is also found at the eastern end of apron. It consists of weathered olivine-orthopyroxene-clinopyroxene andesite lava (Pronggol andesite; Zaennudin et al., 1994).

The outcrop of weathered clinopyroxene-orthopyroxene andesite lava and block-and-ash flow deposit is located at the foot of G. Ider-ider in the south wall of Sand Sea caldera. They are covered by intra-caldera lavas. The andesite contains euhedral orthopyroxene phenocrysts, which is exceptional at Tengger system, along with Pronggol andesite. The block-and-ash flow deposit include basalt block similar to the one at G. Tunggangan.

(2) Pre-caldera activity before first (Ngadisari) caldera eruption

North to northeast apron of the somma is formed in this period with olivine-plagioclase basalt. Ages of olivine-plagioclase basalt lavas at Pananjakan (northwest wall of Sand Sea caldera) agree at 0.5-0.45 Ma for samples from the caldera rim and the foot of the caldera wall. Branggah lava, which forms the northeast apron and is covered by Sukapura ignimbrite, is aphyric basalt with small amount of plagioclase and olivine phenocrysts. Dikes intruded at Pananjakan are also olivine-plagioclase basalts, and are correlated to this period. Olivine-plagioclase basalt lava is also distributed in the western apron.

The K-Ar age of basalt lava from the lowermost unit of Semeru volcano at its southern apron (Jambamgan lava flows 1; Sutawidjaja et al., 1996) is 0.5 Ma. Combined with formation of the north somma of Tengger system, the footprint of Tengger-Semeru volcano cluster (Takada et al., 2000) increased significantly during the pre-caldera period and approached the present extent.

(3) Intra-caldera activity to second (Sand Sea) caldera eruption

Basalt to andesite lavas filled the Ngadisari caldera, and basaltic andesite to andesite lavas formed the south somma in this intra-caldera period. The K-Ar age of basaltic andesite in the southern somma is 0.3 Ma, and is younger than Pananjakan. Based on our K-Ar ages, the somma of Sand Sea caldera therefore consists of volcanoes formed in this and the previous periods. Ngadisari caldera and the intra-caldera units have formed between 0.45-0.3 m.y. BP.

Basalt and basaltic andesite lavas erupted earlier, followed by andesites. Basalts are similar to those of pre-caldera period. Basaltic andesites have heterogenous petrography, which suggest occurence of magma mixing before eruption. Lavas distributed in Ngadisari caldera contain large, unhedral plagioclase and orthopyroxene, clinopyroxene or olivine phenocrysts. The large phenocrysts, especially orthopyroxene and plagioclase, are unhedral and are not in equilibrium to the melt of erupted magma. Groundmass of the lavas have variable crystallinity and chemical composition. Basaltic andesite lavas of the south somma have unhedral clinopyroxene and olivine phenocrysts. Plagioclase phenocrysts are melting from both rim and core. Fot the basaltic andesites, duration of time between the magma mixing and eruption is long enough for phenocrysts to interact with melt, but is short enough to erupt before melting completely. In contrast, andesites are aphyric and have uniform groundmass. The temporal transition from heterogenous basaltic andesite to homogeneous andesite suggests accumulation of andesite magma during the intra-caldera period.

Multiple layers of clinopyroxene-olivine basaltic andesite lavas form the plateau–like topography in the north apron. The age of basaltic andesite lava consiting the plateau at Rambutmoyo waterfall is 0.3 Ma and agrees with the age of south somma. Lavas that fill the depression of Kukusan in the northwest apron are also clinopyroxene-olivine basaltic andesite.

PDC deposit of Sand Sea eruption at the NW caldera wall consist of alternating layers of pyroclastic fall and pyroclastic surge deposits as well as a lava flow layer. The age of the olivine-clinopyroxene-plagioclase basalt lava is 0.3 Ma, which is slightly younger than intra-caldera lavas. Sand Sea caldera was therefore formed at 0.3 m.y. BP, shortly after the intra-caldera activity. The chemistry of air-fall scoria is similar to intra-caldera andesites. The similarity suggests that magmatic process during the intra-caldera period has produced and accumulated magma leading up to Sand Sea eruption.

The shield volcano of basalt and andesite lavas form the east apron. The age of its youngest unit, pyroclastic cones of clinopyroxene-olivine-plagioclase basalt, is 0.25 Ma. The other, older lavas have various weathering texture and phenocryst assemblage, and are likely to have erupted in previous periods.

(4) Present active period

This period started about 0.1 m.y. BP. Units formed in this period are distributed in the northwestern apron, and formed the central cones of Sand Sea caldera, including the active vent (Bromo). The age of aphyric andesite lava in the northwestern apron is 0.08 Ma. Lava and spatter bombs of the central cones (Widodaren, Bromo) are olivine-clinopyroxene basaltic andesite to andesite. Those from Bromo are contain large, unhedral phenocrysts. The large phenocrysts do not represent melt composition of erupted magma, similarly to basaltic andesite lavas which erupted in the earlier part of intra-caldera activity.

Small calderas (Ayekayek, Jambangan) and a group of small pyroclastic cones and maars (Ranu Pane) are distributed between Tengger and Semeru volcano to the south (Sutawidjaja et al., 1996). PDC deposits of Sand Sea eruption do not cover the cones and their scoria deposits in this area. K-Ar ages of the lavas are 0.02-0.04 Ma, which are much younger than the Sand Sea eruption and are consistent with stratigraphy. The lavas are hornblende-clinopyroxene andesite and clinopyroxene-orthopyroxene andesite. They have more variety of phenocryst assemblage and geochemistry compared to central cones of Sand Sea caldera. Therefore, the volcano group seem to have separate crustal magma supply from the contemporary Bromo-Tengger system.

Regarding the future activity of Tengger system, the present activity is characterised as follows based on comparison with older active periods and activities in Bali. (i) Voluminous somma already exists as the cumulative result of previous active periods, which favors the magma accumulation. (ii) The system produces basaltic andesite to andesite magma similar to the intra-caldera period. (iii) The lava and spatter bomb of the current vent, Bromo, have heterogenous phenocryst and groundmass, rather than uniform texture of pre-caldera andesites. In order to estimate the state of andesite magma accumulation, description of petrography and volumetric history of tephra and ejecta from the central cones of Sand Sea caldera is proposed for further study.

Field surveys of this study are conducted as a part of the project "Multi-disciplinary Hazard Reduction from Earthquakes and Volcanoes in Indonesia", supported by SATREPS from JST, JICA, RISTEK and LIPI.

References

Sutawidjaja, I. S., Wahyudin, D., and Kusdinar, E. (1996) Peta Geologi Gunungapi Semeru, Jawa Timur. Direktorat Vulcanologi, Bandung.

Takada, A., Sinulingga, I. K., Surmayadi, M., and Urai, M. (2000) Comparison among volcano complexes with a caldera and without a caldera, East Java (Preliminary report). Research on Volcanic Hazard Assessment in Asia, 93-115.

Zaennudin, A., Andisantono, R. D., Erfan, R. D., and Mulyana, A. R. (1994) Peta Geologi Gunungapi Bromo-Tengger, Jawa Timur. Direktorat Vulcanologi, Bandung.

Explosive eruptions associated with Batur and Bratan calderas, Bali, Indonesia

Furukawa Ryuta[a], Takada Akira[a], Toshida Kiyoshi[b], Supriyati Andreastuti[c], Eka Kadarsetia[c], Nugraha Kartadinata[c], Anjar Heriwaseso[c], Oktory Prambada[c], Yudi Wahyudi[c] and Nizar Firmansyah[c]

[a] *Geological Survey of Japan, AIST, 1-1-1 Higashi, Tsukuba, Ibaraki 305-8567, Japan*

[b] *Civil Engineering Research Laboratory, Central Research Institute of Electric Power Industry, 1646 Abiko, Abiko-shi, Chiba 270-1194, Japan*

[c] *Center for Volcanology and Geological Hazard Mitigation, Jalan Diponegoro 57, Bandung, Indonesia*

In Sunda Arc, caldera forming eruption is frequent as occurring 3times in recent 1000years. The caldera of Krakatau formed in 1883, Tambora in 1815, and Rinjani caldera of Lombok formed in 13th century. So the future caldera forming eruption in Bali should be evaluated from scientific procedure. Our geological study is a corporate work between Indonesia and Japan supported by Japan International Cooperation Agency (JICA) and Japan Science and Technology Agency (JST). We highlights long-term volcanic history of Bali Island, especially focusing on Batur and Bratan calderas including some peripheral volcanoes. We offer a significant contribution towards hazard mitigation at the forthcoming volcanic eruption.

Bratan and Batur calderas are the most famous tourist places in Bali Island and are probable candidate of world geopark. The calderas have prominent depression of 12x8 km and 14x10 km respectively. The calderas are surrounded by flat plateau consist of major pyroclastic flow deposits with subordinating pyroclastic fall deposits and soils. Mt. Agung lying on east of Batur is a undissected stratovolcano with no caldera. As Bratan and Batur calderas are formed by multiple caldera forming eruptions, we need to evaluate long-term forecast of probable caldera-forming eruption.

From 2009 to 2011, we have described more than 200 exposures and have made stratigraphic logs to correlated each deposit which allow us to reconstruct the eruptive history of Bali Island. We newly identified 7 extensive pyroclastic flow deposits which correspond to formation of Batur and Bratan calderas respectively. Radioactive carbon ages of carbonized wood and underlying soil ranges from ca.29 to 6 ka. We also discovered more than 10 plinian pumice and/or scoria fall deposits extensively blanketing west of the Batur caldera. We identified scoria fall deposit from Agung volcano covering Batur area. It suggests sustaining concurrent activities of the Bali volcanoes.

Oldest eruptive products we identified are 29 thousand years before plinian pumice fall deposit and overlying pyroclastic flow deposit. Both deposits respectively thicken toward the present Batur caldera suggesting their source. Southernmost distribution of pyroclastic flow deposit is not sure, because this area is densely populated and lucks outcrops. But southern part of Bali supposed to be isolated island and connected by the sediment supply from the northern volcanic regions. Caldera rim formed by this eruption is not confirmed yet. Carbonized wood root beneath this pyroclastic flow deposit has radioactive carbon date of 23760±70years B.P. (calibrated 2 σ ranges 28812-28086yBP).

Next large eruption is 17 thousand year before consists of pumice fall to the southwest and overlying pyroclastic flow deposit. Outer caldera rim would be formed and proximal welded pyroclastic flow deposit filling inside of the caldera. At the lower non-welded pyroclastic flow deposit we found buried carbonized wood showing ^{14}C age of 14370±70 years B.P. (calibrated 2 σ ranges 17500 to 16980yBP).

The next large eruption is 6ka also made of pumice fall deposit to the southwest and extensive pyroclastic flow deposit. The inner caldera rim must be formed. Sutawidjaja (2009) reported

radiocarbon age for this pyroclastic flow deposit as 5500 years B.P. and we also obtained consistent age dating as 5550±50 years B.P. (calibrated to 6310 cal.yBP).

Youngest large eruption is four thousand years before. Pumice fall deposit blanketing west of Batur and relatively minor pyroclastic flow deposits intervened. Pyroclastic cone (Sayang) was also formed in southwest of caldera.

We obtained the chronology and magnitude of large-scale explosive eruptions from Batur and surrounding volcanoes. Older volcanoes are basalt and andesite stratovolcanoes with no evidence of caldera formation. Age of them are shown by Toshida et al. (2010 and this workshop). For Batur and Bratan calderas, there are three caldera forming eruptions among last 30000 years (once in 10000years). We have less information from 4ka to present, and from 0.2Ma to 30ka.

We appreciate valuable support from Rendang Volcano Observatory, CVGHM, Bali.

References

Sutawidjaja, I. S., 2009. Ignimbrite Analyses of Batur Caldera, Bali, based on 14C Dating. Jurnal Geologi Indonesia, 4, 189-202.

Toshida, K., Takeuchi, S., Furukawa, R., Takada, A., Andreastuti, S., Kartadinata, N. and Heriwaseso, S (2010) K-Ar ages and long-term distribution of volcanic activity around calderas in Bali and East Java. International Workshop on Multi-disciplinary Hazard Reduction from Earthquakes and Volcanoes in Indonesia.

Development of risk assessment simulation tool for optimal control of a low probability - high consequence disaster

Hiroki Yotsumoto[a], Kikuo Yoshida[a], Hiroshi Genchi[a], Kiyotaka Tahara[a], Kiyotaka Tsunemi[a], Hideo Kajihara[a], Yuji Wada[a], Ryoji Makino[a], Kazuya Inoue[a], Yukinobu Okumura[b], Yasuto Kuwahara[b], Haruo Horikawa[b], Masayuki Yoshimi[b], Yuichi Namegaya[b]

[a] *Research Institute of Science for Safety and Sustainability, AIST, Onogawa 16-1, Tsukuba, Ibaraki 305-8569, Japan*
[b] *Active Fault and Earthquake Research Center, AIST, 1-1-1 Higashi, Tsukuba, Ibaraki 305-8567, Japan*

1. Introduction

Japan faces an urgent need of developing a science-based decision-making system to strengthen society and industries against earthquakes and/or other disasters since great earthquakes are anticipated to occur at high probabilities beneath the Tokyo Metropolitan area and along the Tokai, Tonankai and Nankai areas.

Conventional risk assessment methods for chemical substances has been developed to control the risks of relatively high-probability events (such as the chronic impacts of chemicals), however, they are difficult to directly apply to unsteady and sudden disasters such as earthquakes. On the other hand, risk assessment for primary earthquake hazards (strong shaking, tsunami etc.) has been investigated and they have been applied in earthquake insurances and the business continuity plans (BCP) of companies. The Cabinet Office and the Fire and Disaster Management Agency have respectively developed a tool and system for estimating possible damages caused by the anticipated Tokai, Tonankai and Nankai Earthquakes. However, no system are able to handle multifarious and multitiered secondary effects of earthquakes such as great damages by tsunami, radioactive contamination caused by the nuclear power plant accident, and the impacts of the shredded supply chains on the industry.

Therefore, there is an urgent need of constructing comprehensive, interdisciplinary simulation technologies of risk assessment to estimate the multitiered effects of primary hazards and secondary damages and to assess the risks of damages in order to help people take the optimum actions during a low-probability but high consequence disaster, which may cause huge economic and social damages.

The National Institute of Advanced Industrial Science and Technology will start an interdisciplinary study in this year, cooperation of the Active Fault and Earthquake Research Center, which has a potential of assessing earthquake hazards, and the Research Institute of Science for Safety and Sustainability, which have been developing chemical and environmental risk assessment tools.

This abstract outlines the framework of the study.

2. Framework of the study

Comprehensive risk assessment simulation technologies are to be researched, developed and provided aiming to prevent or mitigate the direct primary damages caused by large-scale earthquakes and tsunami and relevant and indirect secondary damages, such as nuclear power and chemical plant accidents and destruction of production and distribution network. (See Fig. 1).

The next-generation risk assessment simulation technologies, which help people to take optimum actions during low-probability but high-consequence disasters, consist of 1) a subsystem for estimating the primary hazards, 2) a subsystem for quantifying the hazards of secondary disasters, and 3) a risk assessment subsystem. (See Fig. 2).

The subsystem for estimating the primary hazards will be a software for estimating the earthquake intensities in major industrial zones, which spreads in Kanto and the Pacific side of western Japan, during large earthquakes, such as the anticipated Tokai, Tonankai and Nankai earthquakes, and the tsunami inundation.

The second subsystem will be a software for quantifying the damages to the transportation network and lifelines, fire damages, and diverse damages to the industries caused by disturbance to the production and distribution network across regional and national boundary as well as the damages of human health caused by spread of radionuclides and toxic chemical substances by nuclear power and chemical plants accident.

The third subsystem will be a software for simulating the risk of loss of lives, destruction of houses and fire damages, which are estimated by municipal governments and from the systems of the Cabinet Office and the Fire and Disaster Management Agency, and the risk of human health and damages of production and distribution systems, which are estimated from the results of the first and second subsystems, by using common indices such as money and disability-adjusted life years (DALY). The assessed risks will be displayed in figures, tables and maps.

3. Contents of the study

To develop the risk assessment technologies, a feasibility study is to be conducted in this year. It involves surveying the primary hazards of the Tohoku Earthquake, such as the earthquake intensities and inundation, and its secondary damages to the major industries, governments and the human health, jointly with the municipal governments and industries hit by the earthquake. Based on the results, model districts will be decided for the anticipated Tokai, Tonankai and Nankai Earthquakes; the relationship will also be organized among disasters, damages and hazards; and the topics of assessing the risks will be clarified.

4. Future

The risk assessment simulation will enable the national and municipal governments and industries to quantitatively assess the multiplex risks of primary hazards and secondary damages and assist them in making decisions, such as in formulating disaster prevention measures and urban planning by municipal governments, designating industrial areas in strong zones against disasters, and establishing optimum production areas and distribution networks.

The results of the study will enable the scale of secondary damages, which has been desultorily and fragmentary estimated, to be quantitatively and comprehensively simulated and will introduce the concept of quantitative risk assessment and management in the disaster prevention measures of the national and municipal governments and the industries.

After the feasibility study, a database of estimated primary hazards and secondary damages will be prepared and incorporated in the risk assessment simulation system. The topics found in the feasibility study will be investigated and the three subsystems of the risk assessment simulation system will be developed.

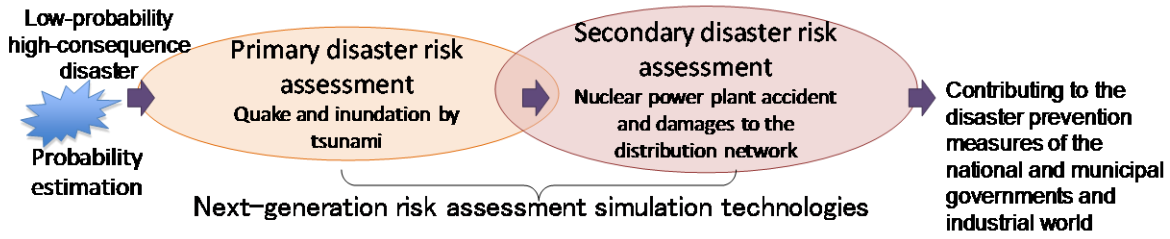

Figure 1. Position of next-generation risk assessment simulation technologies

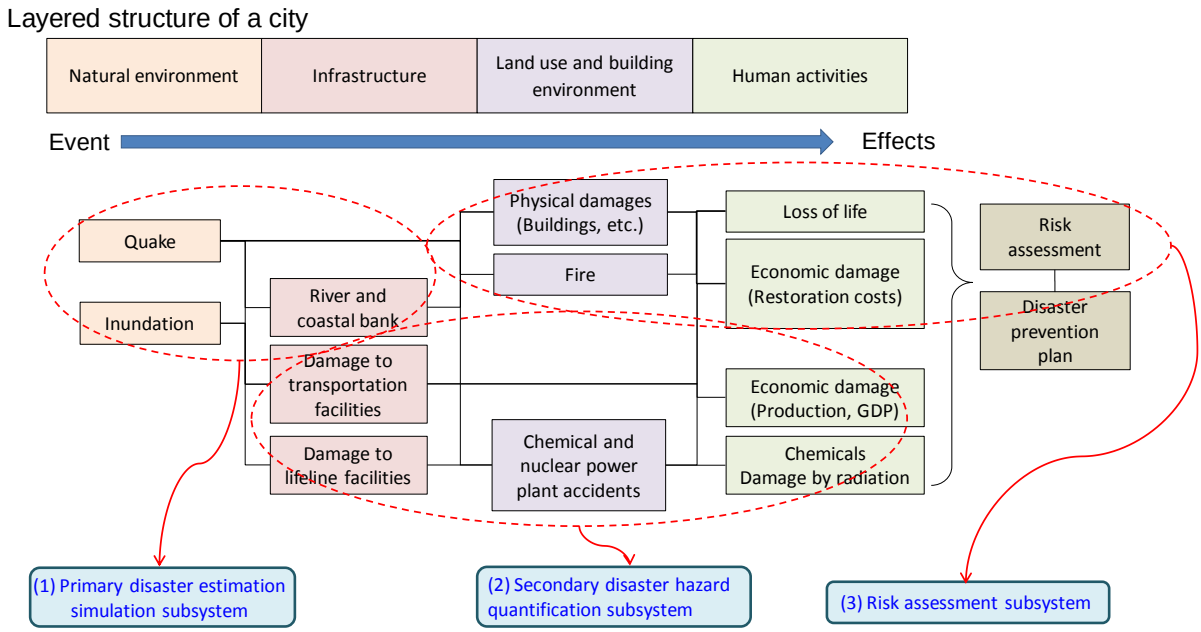

Figure 2. Framework of the risk assessment simulation system

Geological Evaluation of Frequency and Process of Caldera-forming Eruption: A compiled study of Indonesian caldera volcanoes

Akira Takada, Ryuta Furukawa[a], Kiyoshi Toshida[b] , Supriyati Andreastuti, Nugraha Kartadinata[c]

[a]Geological Survey of Japan, AIST, 1-1-1 Higashi, tsukuba, Ibaraki 305-8567, Japan
[b]Geosphere Science Sector, Civil Engineering Research Laboratory, CRIEPI, 1646 Abiko, Abiko-shi, Chiba 270-1194, Japan
[c]Center for Volcanology and Geological Hazard Mitigation, Jalan Diponegoro 57, Bandung, Indonesia

There are various volcanoes in the world. Almost volcanoes erupted frequently. However, some volcanoes seem to be quite for preparing a large-volume eruption with caldera formation. What is a caldera-forming eruption? Compared with usual eruptions, a caldera-forming eruption, erupted volume~ 10-1000 km3, causes huge direct damages, wide-spread pyroclastic flow, air fall, lahar, tsunami, and global impacts such as climate change; The recovering time is more than 10 years for climate, ocean, food, human health, traffic, buildings, and 100-1000 years for land use (Fig. 1). Japanese have forgotten a caldera-forming eruption, because the last one occurred 7,000 years ago. Indonesia was suffered twice for the last 200 years, and three times within 1000 years. The total victims amount to 130,000, which is 55 % of the total ones from eruptions in the world during the last 200 years.

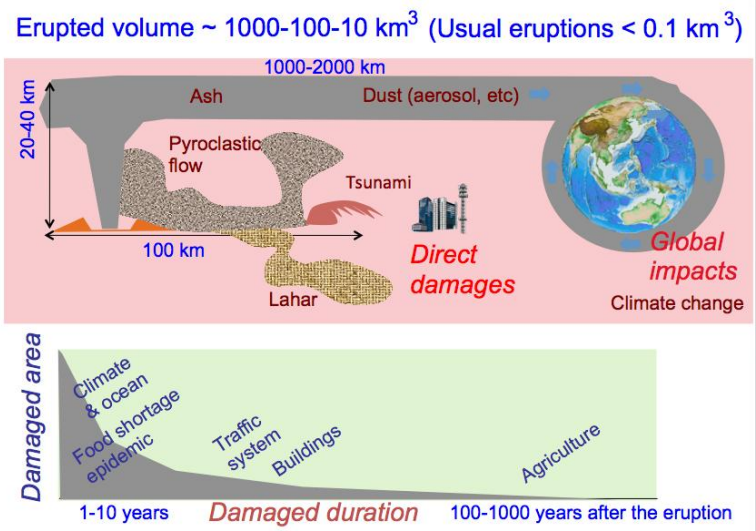

Fig. 1. Caldera-forming eruption

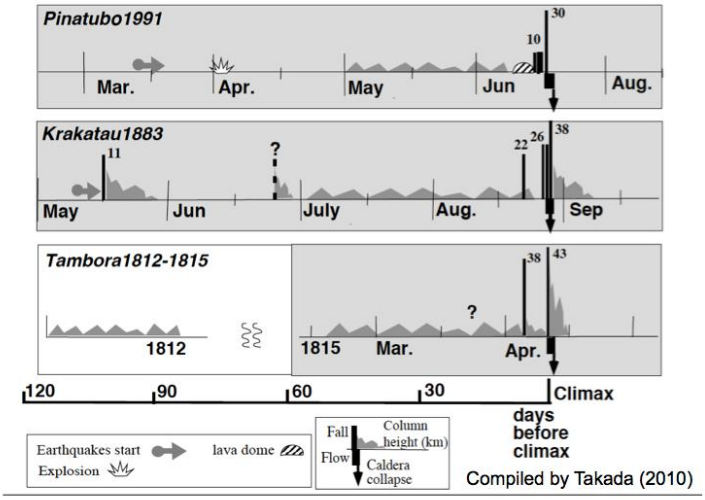

Fig. 2. The short-term process to the caldera-forming eruption

We have questions on the caldera-forming eruption. (Q1) Can we get a precursor sign for the eruption (where, when, what volume)? (Q2) Is not the eruption infrequent (< once / 100 years)? (Q3) Can we evaluate the next candidate for hazard mitigation? We carried out the JST-JICA project as follows. (1) The first is to study the process to the caldera forming eruption, that is, the quantitative eruptive history of target volcano to caldera-forming eruption, especially, multi-caldera volcanoes in Bali (Furukawa et al., G-EVER1 poster). (2) The second is to clear the frequency of the caldera-forming eruption, that is, the temporal and spatial distribution of the eruption in East Java and Bali (Toshida et al., G-EVER1 poster). (3) The third (this paper) is to evaluate volcanoes base on the obtained geological data, in order to answer (Q1) and (Q2). The results will contribute to the answer of (Q3).

The short-term evolution: During the last a few months, we may catch the short-term process as the progressive activity to the climax eruption (Fig. 2). The upper is the example of Pinatubo 1991 eruption, Philippine (Harlow et al., 1996; Hoblitt ea al., 1996; White et al., 1996; Wolfe and Hoblitt, 1996). The second is that of Krakatau 1883 (Rampino and Self, 1982). The third one is that of Tambora 1815 (Junghuhn, 1854; Self et al., 1984, Stothers, 1984; Yamamoto et al., 2000; Takada and Yamamoto, 2008). There occurred a lot of small eruptions and hydrothermal explosions during the last a few months just before the climax. Moreover, there occurred unusual wide-range hydrothermal activity, 2-5 km-wide, before the climax, suggesting the existence of an active large volume magma beneath the summit.

The long-term evolution: There was a large shield or stratovolcano constructed with a large eruption rate before the caldera forming eruption, for example, Tambora, and Tenggar. In contrast with those volcanoes, Kelute has never cause the caldera-forming eruption (Fig. 3). The eruption rate is far smaller than those of volcanoes with caldera. For example, we compiled the eruptive history of caldera

volcano, Tambora (Takada et al., 2000; Matsumoto et al., 2000), and Rinjani (Takada et al., 2003; Nasution et al., 2003; Furukawa et al., 2004; Furukawa et al., 2005). The corporation project between GSJ and VSI got the scenario that, during the last 10,000 years, the eruption rate decreased, eruption style changed to more explosive, and chemical composition changed (Fig. 4).

The cluster of volcano complex is composed of several volcanoes with repose periods. If the magma flux increases, the volcano can evolve into the caldera-forming stage. The schematic diagram of the cumulative eruptive volume with time shows the evolution process of the ideal volcanoes with caldera-forming eruption (Fig. 5). In the future, we may be able to evaluate a volcano evolving to the caldera-forming eruption, based on the basic data on the process and frequency of the caldera-forming eruption.

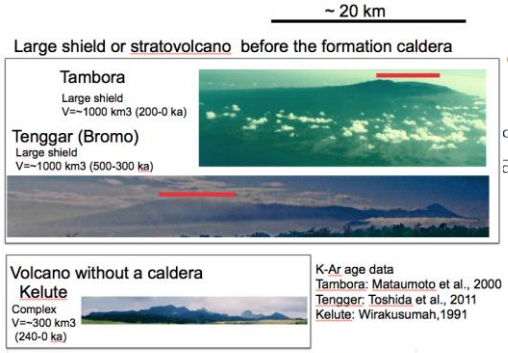

Fig. 3. Volcanoes with calderas and without calderas

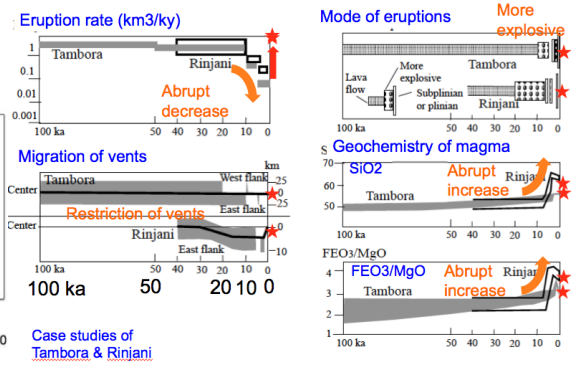

(Takada et al., 2000; Matsumoto et al., 2000, Takada , 2010)

Fig. 4. Long-term evolution to the caldera-forming eruption

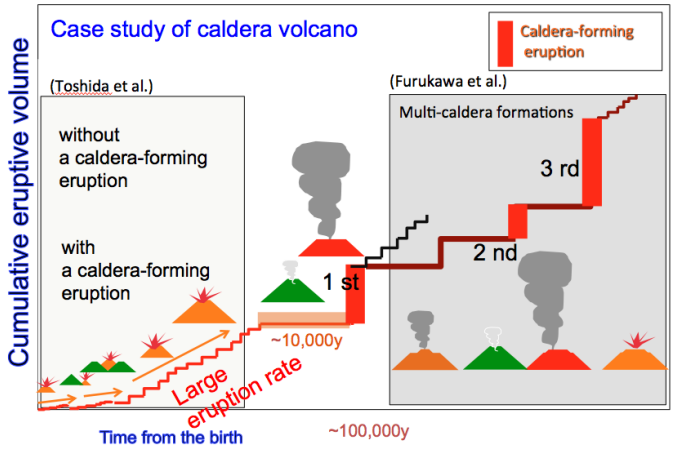

Fig. 5. Long-term evolution of the caldera volcano

On the prediction of scaling relationships governing the runouts of short-lived fluidized granular flows

L.Girolami[1,2], T.H. Druitt[1], O. Roche[1]

[1] *Laboratoire Magmas et Volcans, Université Blaise Pascal, CNRS-IRD, 63038 Clermont-Ferrand, France.*

[2] *Geological Survey of Japan, AIST, 1-1-1 Higashi, Tsukuba, Ibaraki 305-8567, Japan.*

Pyroclastic flows are a major hazard around volcanoes and there is an urgent need to develop quantitative models of their flow and sedimentation behaviour in order to make predictions of their impact on the environment. Although field observations from deposits (Branney and Kokelaar, 2002) and approximate measurements of frontal velocity (Levine and Kieffer, 1991; Loughlin et al., 2002) exist, their hazardous behaviour developed on a broad range of spatial and temporal scales requires more detailed studies. Laboratory-scaled experiments can play an important role both in helping to describe precisely the physical processes developed during propagation as well as in infering the flow dynamics from deposits morphology.

Despite the significant progress made on the physics of dry granular flows since the last decade (GDRMidi, 2004; Lajeunesse et al., 2005; Lube et al., 2005; Forterre and Pouliquen, 2008), research on fluidized granular flows (in which the interstitial fluid plays an important role) remains poorly understood. In this study, we conducted laboratory dam-break experiments of synthetical powders (EZ and FCC commonly used in the oil industry) generated by the release of hot (200°C) gas-fluidized mixtures down a smooth, horizontal channel.

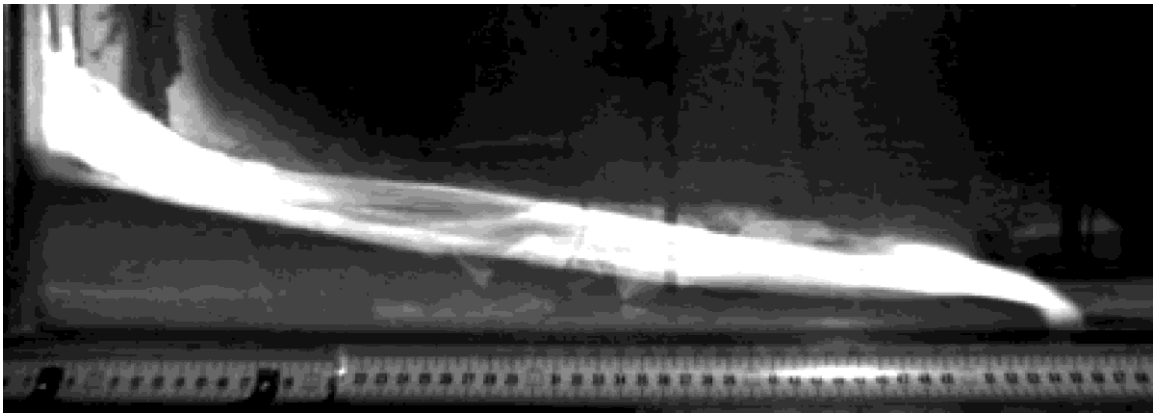

Fig. 1 – Dam-break collapse of a hot, initially fluidized granular mixture.

The sets of experiments presented here, varying the initial mixture geometries (initial aspect ratio '*a*' and initial expansion '*E*' especially) in a wide range, aims to gain insights into the physics of initially fluidized granular flows.

Results obtained in this study are compared with those obtained previously in Girolami et al. (2008) with the ash material, then discussed. The flow dynamics reveals different aspects. First, at

constant initial expansion, the flows are controlled entirely by gravity while the maximum flow velocity (measured during the dominant phase of transport) is given by $2gh_0$. Second, at varying initial expansion, the flows are controlled both by gravity and fluidization effects, these latter extending the runouts relatively to that of initially non-expanded (incipiently fluidized; $U=U_{mf}$) flows. The additive nature of this law provides a smooth transition from non-expanded to expanded flows. Two possible scalings are proposed to explain it. The first one (1) assumes that the excess time (t_{xs}) and distance (x_{xs}) observed from initially expanded flows are governed by an excess of potential energy available before release due to the expansion state of the mixture, then increasing the mean frontal velocity during the principal phase of transport by a factor two. The second one (2) assumes that t_{xs} and x_{xs} are governed by the sedimentation processes from initially expanded mixtures (*i.e.* hindered settling) that decrease the aggradation velocity of the basal deposit formed progressively during the principal phase of transport.

References

Branney, M.J., Kokelaar, P., 2002. Pyroclastic density currents and the sedimentation of ignimbrites, Geological Society Memoir, 27, 152 pp.

Forterre, Y. and Pouliquen, O., 2008. Flows of dense granular media, Annual Review of Fluid Mechanics, 40, 1-24.

GDR MiDi, 2004. On dense granular flows, European Physical Journal, E14, 341-365.

Girolami, L., Druitt, T. H., Roche, O. and Khrabrykh, Z., 2008. Propagation and hindered settling of laboratory ash flows, Journal of Geophysical Research, 113, doi:10.1029/ 2007JB005074.

Lajeunesse, E., Monnier, J. B. and Homsy, M., 2005. Granular slumping on a horizontal surface, Physics of Fluids, 17, 103302.

Levine, A. H. and Kieffer, S. W., 1991. Hydraulics of the August 7, 1980, pyroclastic flow at Mount St. Helens, Washington, Geology, 19, 1121-1124.

Loughlin, S. C., Calder E. S., Clarke A. B., Cole P. D., Luckett, R., Mangan M., Pyle D., Sparks R. S. J., Voight B. and Watts R. B., 2002. Pyroclastic flows and surges generated by the 25 June 1997 dome collapse, Soufriere Hills Volcano, Montserrat, in: The Eruption of Soufriere Hills Volcano, Montserrat From 1995 to 1999, edited by T. H. Druitt and B. P. Kokelaar, Geological Society Memoir, 21, 191-210.

Lube, G., Huppert, H. E., Sparks, R. S. J. and Freundt, A., 2005. Collapses of two-dimensional granular columns, Physical Review, E72, 041301.

The observation with Remote GNSS Monitoring System

Eiichirou Harima

Geospatial Information Authority of Japan, 1 Kitasato, Tsukuba, Ibaraki 305-0811, Japan

Remote GNSS Monitoring System has been developed for the purpose of conducting an autonomous GNSS observation. This has made it possible not only to install the system in the area where there is no ordinary electricity nor telephone services, but also to urgently install and operate it if volcanic activity intensifies. Remote GNSS Monitoring System is automatically conducting the GNSS observation and data communications by using a control device which is equipped with an automatic recovery function. The electric power is supplied for the system by photovoltaic power generation, and the satellite communications are used for the data communications. Furthermore, some of the latest Remote GNSS Monitoring Systems are experimentally monitoring the state of volcanos via the web camera.

To monitor the Baegdusan volcano before the next magmatic eruption

Aurélien Dupont and Sung-Hyo Yun

Pusan National University, Busan 609-735, Republic of Korea

The Baegdusan volcano is an intraplate volcano (Zhao et al., 2009) located in the Changbaishan volcanic region (41.98° N ; 128.08° E), on the Sino-Korean border in the eastern part of Jilin Province and North Korea (Zhao et al., 2010). Baegdusan stratovolcano began to form about 1 million years ago. Major eruptions are occured 170,000 and 4,000 years ago. Minor eruptions are described in 1668, 1702 and 1903.

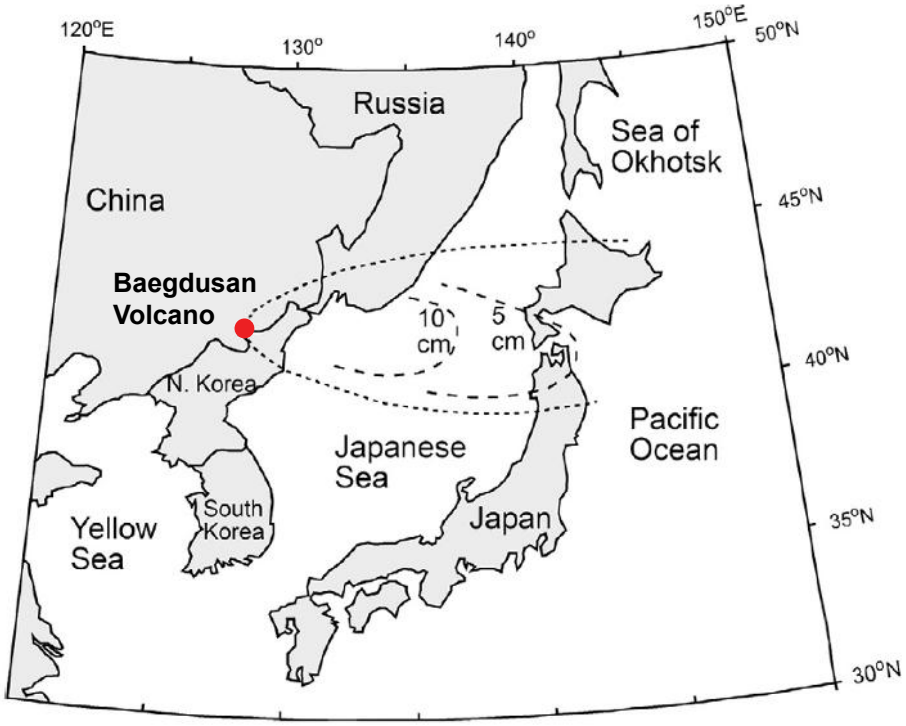

Fig. 1 Locality of the Baegdusan stratovolcano and distribution of the tephras of the Millennium eruption. Modified from Zou et al., (2010).

One of the most eruptive destructive eruptions (VEI 7) from the Baegdusan volcano about 1000 years ago is one of the largest eruptions on the Earth in the last millennium (Horn and Schmincke, 2000). It involved more than 20-30 km^3 of magma (DRE). The Plinian column was estimated to have a maximum height of 25 km. A widespread ash fall deposit has been traced across the Sea of Japan to Hokkaido and is several centimeters thick at more than 1,000 km from the source (Zou et al., 2010). Unwelded pyroclastic flows associated with collapse events of Plinian eruption column extended more than 70 km from the crater rim. Lahar deposits extended over 230 km downstream along the rivers (Mainville, 2010). This event was large enough to have a global impact and is comparable in magnitude to the 1815 eruption of Tambora, Indonesia. The Millennium eruption formed a large caldera with a diameter of about 5 km and area of 20 km^2, that filled with water. Currently the lake has a maximum depth of 374 m and an area of ~ 9.8 km^2 with a water surface elevation of 2189 m. It has a volume of 2 km^3. Baegdusan is the most active volcano in China (Wei et al., 2003) and it is a highrisk volcano because more

than 100,000 people live on or near the slopes with the addition of many tourists in summer (Stone, 2010).

A seismic crisis starts in June 2002 with swarms of tremors. The China Earthquake Administration (CEA) have traced the epicenter around 5 km beneath the surface (Liu et al., 2011). Over the next 3 years Baegdusan shuddered, sometimes experiencing more than 200 spasms in a month. Activity crested on 19 March 2003, when more than 500 tremors where recorded. But after a swarm in May 2005, Baegdusan's seismicty receded to backgrounds levels (fewer than 10 earthquakes per month). Observations showed that Baegdusan rose about 68 mm over that period - five times the rate before the shaking started. Swarms of volcanic tremor and deformation, well above baseline, suggesting increased gas pressures in the magma but these evidences of the pressure buildup simply stops abruptly, is probably the signature of a deep intrusion (Moran et al., 2011).

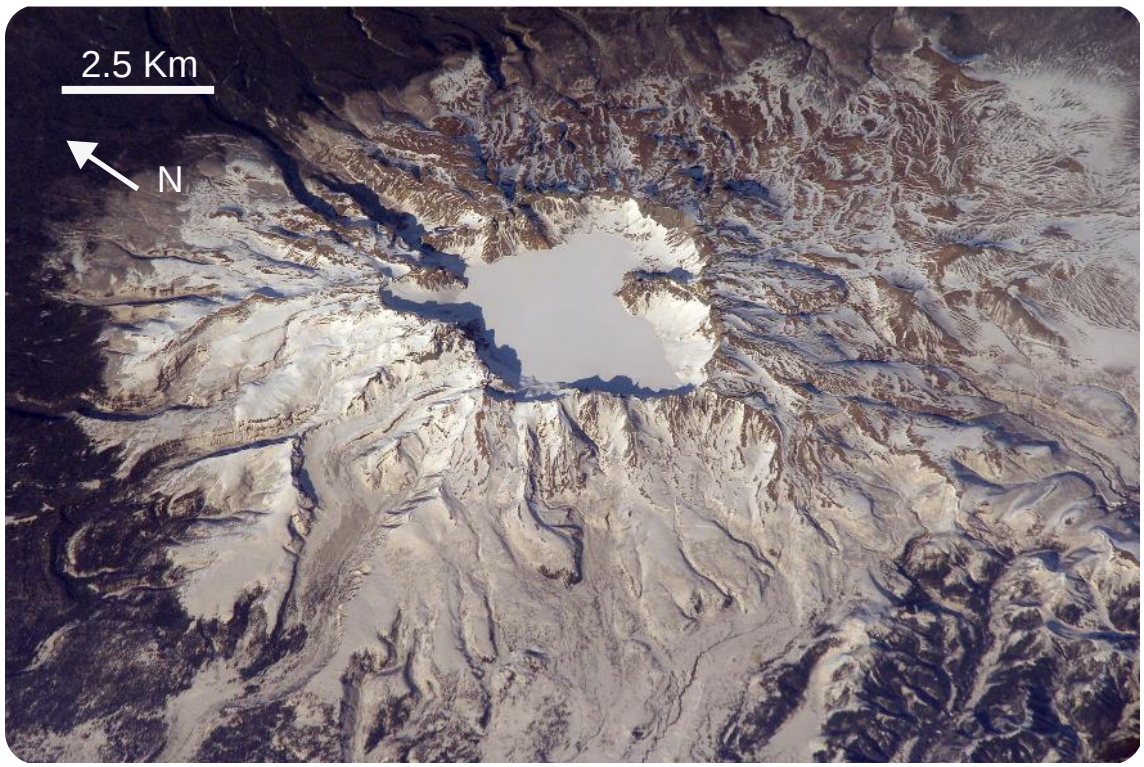

Fig. 2 Baegdusan volcano. The photography was acquired from the International Space Station on April 4, 2003 with a Kodak 760C digital camera with an 800 mm lens. © NASA/JSC.

The current activity is most disturbing because the CEA have determined, over the past 2 years, that the caldera rim has flumped a few centimeters even as the surrounding land continues to rise. In 2008, Korean scientists discovered a new fumarole, or gas vent, near the east flank, 40 km from the caldera. Odd burst of sulfur dioxide was observed and fluctuations were measured in hot springs, on the north flank, in November 2011. Two years ago temperatures suddenly have increased up to ~ 2-3^{o} C on average (Stone, 2011). What is going on? Answer to this question requires data and an international scientific collaboration. We plan to monitor the Baegdusan volcano to characterize its seismic, acoustic and hydrostatic activity. The goal of this project is to isolate a possible precursor of the next magmatic eruption.

References

Horn, S., and H. U. Schmincke, 2000. Volatile emission during the eruption of Baitoushan Volcano (China/North Korea) ca. 969 AD. Bulletin of Volcanology 61, 537–555.

Liu, G., J. Yang, L. Wang, and J. Sun, 2011. Analysis of Tianchi volcano activity in Changbai Mountain, NE China. Global Geology 14(1), 44–53.

Manville, V., 2010. An overview of break-out floods from intracaldera lakes. Global and Planetary Change 70, 14–23.

Moran, S. C., C. Newhall, and D. C. Roman, 2011. Failed magmatic eruptions: late- stage cessation of magma ascent. Bulletin of Volcanology 73, 115–122.

Stone, R., 2010. Is China's riskiest volcano stirring or merely biding its time ? Science 329, 498–499.

Stone, R., 2011. Vigil at North Korea's Mount Doom. Science 334, 584–588.

Wei, H., R.S.J. Sparks, R. Liu, Q. Fan, Y. Wang, H. Hong, H. Zhang, H. Chen, C. Jiang, J. Dong, Y. Zheng, Y. Pan, 2003. Three active volcanoes in China and their hazards. Journal of Asian Earth Sciences 21, 515–526.

Zhao, D., Y. Tian, J. Lei, L. Liu, and S. Zheng, 2009. Seismic Image and origin of the Changbai intraplate volcano in East Asia: Role of big mantle wedge above the stagnant Pacific Slab. Physics of the Earth and Planetary Interiors 173, 197–206.

Zhao, D., and L. Liu, 2010. Deep structure and origin of active volcanoes in China. Geoscience Frontiers 1, 31–41.

Zou, H., Q. Fan, and H. Zhang, 2010. Rapid development of the great Millennium eruption of Changbaishan (Tianchi) Volcano, China/North Korea: Evidence from U-Th Zircon dating. Lithos 119, 289-296.

The impacts on structures by volcanic eruption – A case study of the 1990-1995 eruption on Unzen Volcano, Japan

Daisuke Nagai

Mt.Unzen Disaster Memorial Hall, 1-1 Heisei Town, Shimabara City, Nagasaki, 855-0879, Japan

Japan Islands had met repeatedly earthquakes, tsunami and volcanic disasters. The event on 11 March, 2011 effected a big impact to the world. The problems of nuclear power plants are continuing. In future, the effect of volcanic eruption against the buildings including houses and nuclear power plants is an important theme to the risk management. This study focused on a case study of the 1990-1995 eruption on the Unzen Volcano. The eruption resulted in the deaths of 44 people and destroyed houses. Houses around the volcano are mainly wood frame and reinforced structures. Dynamic overpressure was estimated from damaged houses. These houses were destroyed by pyroclastic surge. Overpressure conditions based on studies from nuclear testing and atomic bomb on Nagasaki, Hiroshima. Data in this study were collected horizontally on disaster area. In the axial zone, dynamic overpressure was above 35 kPa. Almost houses were removed, remained only the basement. Around this area, all people were deathbed. While in peripheral zone, dynamic overpressure was about 3 kPa. Many houses remained standing with a few damages. Several people were alive around this area. The data bases such this study has a clear implication for the risk planning of natural disaster and building the power plants.

Re-evaluation of Mw of the 1707 Hoei earthquake

Yuzo Ishikawa

Active Fault and Earthquake Research Center , AIST, 1-1-1 Higashi, Tsukuba, Ibaraki 305-8567, Japan

It was well known that the 1707 Hoei earthquake was the one of the largest event in Japan. The magnitude of the Hoei earthquake was estimated as M8.6 in the Science Table 2011 version, using the felt area and M8.8 or 8.9 by Usami(2003). It is a standard way for the historical events. But, the length of the source faults of the Hoei earthquake was very long as about 600km from Suruga bay to off Ashizuri peninsular (Aida, 1981a,b). It is longer than the one of 2011 East Japan event Mw9.0. It was thought that the magnitude of the Hoei earthquake was underestimated and it must be re-evaluated.

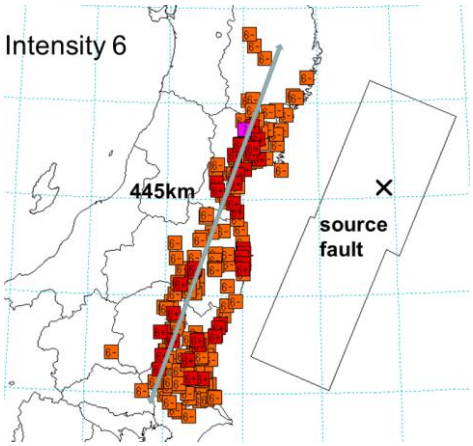

The formula of estimating the magnitude of historical events in and around Japan proposed by Muramatsu(1969) was commonly used. He gathered the intensity distribution of more than 10 events in and around Japan to get the empirical formula between the length of seismic intensity (JMA scale) 5 or 6 area to the magnitude. He got the good formula for magnitude range from 6 to 8.1. The limitation of the lack of data for large events was not regarded to estimate the magnitude of the Hoei earthquake, because there was no data of such large magnitude. Now we got the intensity distributions for large magnitude, ex 2003 Tokachi earthquake Mw8.0 and 3-11 earthquake Mw9.0.

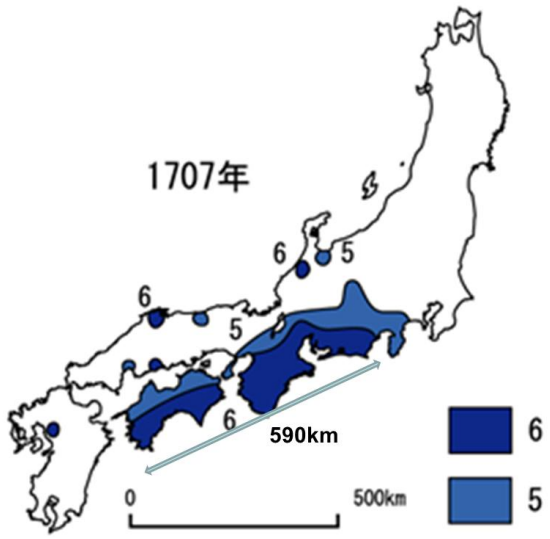

The size of the aftershock distribution was also used to get the magnitude proposed by Utsu et al(1965). PDE data was used to check their formula for mega events and the estimated the aftershock area of the Hoei earthquake..

Finally, we estimated the magnitude of the 1707 Hoei earthquake using the length of the area of intensity 6 and the aftershock distribution of 3-11, The results is obtained that Mw 9.1 to 9.3 is suitable for the Hoei earthquake.

Long-term and short-term Volcanic Risk Assessment based on New Geologic Maps of Tokachidake and Tarumae Volcanoes, northern Japan

Yoshihiro Ishizuka and Ryuta Furukawa

Institute of Geology and Geoinformation, Geological Survey of Japan, AIST, 1-1-1 Higashi, Tsukuba, Ibaraki 305-8567, Japan

GSJ has provided geologic maps of active volcanoes in Japan with distribution and age of ejecta in the past, and its characteristic features since 1980. Newly published geologic maps - Tokachidake and Tarumae volcanoes- allow us to read their long-term and short-term volcanic risk assessment.

Tokachidake Volcano

The Tokachidake volcano group, southwestern end of the Kurile arc, is one of the most active volcanoes in Japan with an eruptive history spanning approximately 1.0 Ma. The volcano group extends 25 km consisting of at least twelve volcanic edifices. Historical eruptions accompanied with basaltic pyroclastic materials had occurred around the center of the volcano group in the interval for 26~36 years in 1926, 1962 and 1988-89. Ishizuka et al (2010) have mapped the 55 geologic units in the area of 270 km^2 centered on the active craters using by traditional mapping methods, airborne laser scanner data, and new 33 K-Ar and 16 radiocarbon ages (Fig.1). This result gave us new views for the eruptive history of the volcano group that: 1) the volcanic activity had spread 300,000 years ago, and converged monotonically afterwards to its central part, and 2) basaltic magmas were erupted in the whole area of the volcano group whereas felsic magmas were extruded only in its central part. It becomes possible that recent historical eruptions are re-interpreted by getting these long-term viewpoints. We can evaluate the current volcano observation network concentrated in the center of the volcano group to be right based on the long-term volcanic risk assessment.

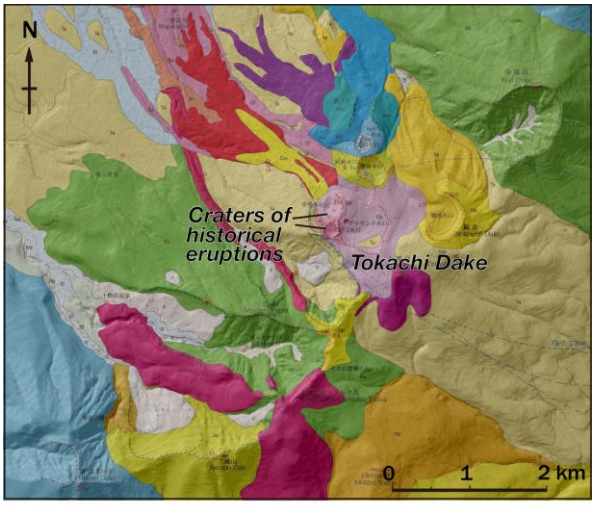

Fig.1 Geologic map of Tokachidake Volcano (central part) combined with topographic relief.

Tarumae Volcano

Tarumae Volcano is located on the important area for the Hokkaido economy that the airport, harbor, railroad and highway are concentrated. The volcano repeated large-scale eruptions in the past 10,000 years, and it is characteristics that the eruptions brought pumices and volcanic ashes to the wide area in Hokkaido. Furukawa and Nakagawa (2010) showed detailed isopach maps of ejecta for the eruptions and their eruption magnitude. The magnitude of the eruptions in the 17th and 18th century (Ta-a and Ta-b) is estimated to be large (Fig.2). However, the magnitude of the eruption is decreasing since the 19th century and it resembles to sequence of previous activity stage of 2,500 -2,000 years before. The next eruption is expected as small magnitude judging from this short-term assessment. On the other hand, as the repose period between each activity stages is decreasing, next eruption is possibly large magnitude if Tarumae Volcano transferred into next activity stage

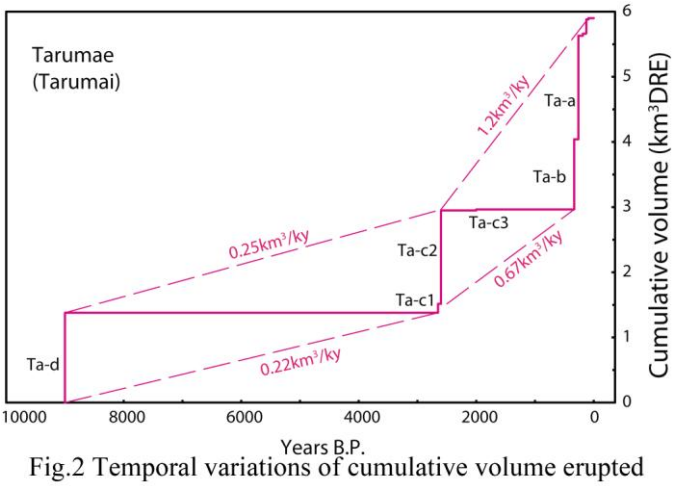

Fig.2 Temporal variations of cumulative volume erupted in the past 10,000 years for Tarumae Volcano.

We believe that geologic maps with new technique are powerful tools for the long-term and short-term volcanic risk assessment of each volcano. They will give fundamental data for the preparation of hazard maps published by the local government.

References

Furukawa, R. and Nakagawa, M. (2010) Geological map of Tarumae Volcano. Geological Survey of Japan, AIST, 8p. (in Japanese with English abstract)

Ishizuka, Y., Nakagawa, M. and Fujiwara, S. (2010) Geological map of Tokachidake Volcano. Geological Survey of Japan, AIST, 8p. (in Japanese with English abstract)

How Many Explosive Eruptions are Missing from the Geologic Record? Analysis of the Quaternary Record of Large Magnitude Explosive Eruptions in Japan.

K. Kiyosugi; C.B. Connor
Department of Geology, University of South Florida, Tampa, FL, United States

R. S. J. Sparks; H. S. Crosweller
Earth Sciences, University of Bristol, Bristol, United Kingdom

L. Siebert
Global Volcanism Program, Smithsonian Institution, Washington, DC, United States

S. Takarada
Geological Survey of Japan, AIST, Tsukuba, Japan

1. Introduction

To support assessments of environmental and societal impacts of volcanism on global, regional and local scales and provide basic information on global explosive volcanism, the Large Magnitude Explosive Volcanic Eruptions database (LaMEVE) is created as a component of the VOGRIPA (Volcanic Global Risk Identification and Analysis Project) database of volcanic hazards, which is being developed as part of the Global Volcano Model (GVM). The LaMEVE database attempts to include all known explosive eruptions, which is dated (~ 1.8 Ma), source volcano is known and magnitude or VEI (Volcanic Explosivity Index) is 4 or greater. The database contains information about the age of eruptions, deposit type, pyroclastic ejecta volume, VEI, magnitude, intensity, geochemistry, source volcano location, data source of volcanic records, errors and uncertainties with indices of data reliability. It is publically available online (http://www.bgs.ac.uk/vogripa) and currently contains information on 2853 Quaternary volcanoes and over 1800 explosive eruption records from the last 1.8 My.

Here we analyzed explosive eruptions of the Japanese islands, which are included in the LaMEVE database, to understand the preservation potential of eruptions with time in Japan.

2. Data

The LaMEVE database of VOGRIPA has been systematically compiled from primary and secondary sources. Major data sources of explosive events in Japan included by the database are as follows:

1) The one million year tephra database
(http://gunma.zamurai.jp/database/index.php?kind=1m&mode=)

2) 2000 year eruption database
(http://gunma.zamurai.jp/database/index.php?kind=2k&mode=)
Data source 1) and 2) are organized by Prof. Hayakawa at the Gunma University, Japan.

3) Active volcano database of Geological survey of Japan
(http://riodb02.ibase.aist.go.jp/db099/index-e.html)

4) Quaternary volcano catalog of the Volcanological Society of Japan (http://www.geo.chs.nihon-u.ac.jp/tchiba/volcano/index.htm)

5) Atlas of tephra in and around Japan. Univ Tokyo Press, Tokyo (Machida and Arai., 1993)

Because many tephra units called with different names in these data sources, eruption history of each volcano was constructed based on these source databases at the beginning of the compilation process to find overlapped units. When unit age was different between these data source, original articles of the source databases were referred and one of the data, which was suitable to keep coherent stratigraphic relationship, was included in our dataset. Finally our data consists of 696 explosive eruptions. Half of them occurred within the last 65 ka. 77% of the total eruptions occurred since 200 ka; the oldest eruption in the database is 2.25 Ma. In addition, percentages by eruption magnitude are: VEI 4 (40%), VEI 5 (42%), VEI 6 (13%) and VEI 7 (5%). Fig. 1a shows cumulative number of different VEI eruptions with time. Because it is reasonable to assume that smaller eruptions occur more frequently, fewer VEI 4 eruptions than VEI 5 eruptions indicates that small eruptions are missing in our dataset. Survivor function, which is the normalized cumulative number of events, shows steeper decreases of smaller VEI eruptions with time and suggests that smaller eruptions are more rarely preserved than larger ones (Fig. 1b). Therefore erosion of units must be the main reason of missing record.

3. Analysis and results

Preservation rate of event is calculated with moving average:

$$r_m = 2n/(d_{m+n}-d_{m-n}) \quad ...eq.1$$

where r_m and d_m are the preservation rate and age of the mth youngest event respectively. 2n is the number of events to calculate the preservation rate of mth event.

The change of identified eruptions in the geologic record with time shows two major trends (Fig. 2a). The likelihood of an eruption preserved in the last 10 to 100 ka follows an exponential trend, suggesting that many young deposits are rapidly eroded and are missing from the geologic record. Older deposits exhibit a gentler trend, indicating that once the deposit is initially preserved it is more likely to be identified in the geologic record than suggested by simple exponential decay. Therefore double exponential decay function is applied to model the preservation rate (Fig. 2b):

$$R_t = R_1 \exp(-l_1 t)+R_2 \exp(-l_2 t) \quad ...eq.2$$

where R_t is the preservation rate of events that occurred t years ago. R_1 is the initial value of preservation rate of units which will quickly disappear with time due to erosion. R_2 is the initial value of preservation rate of units which will be preserved for a long time but finally become unidentifiable in the long period. l_1 and l_2 are decay constants of the exponential decay function. The preservation trends are detrended after modeling by eq.2. The result suggests 97 % of VEI 4 events are missing from the record after 100 ka, whereas 40 % for VEI 5 to 7 are missing after this time period (Fig. 3). These results indicate that eruption probabilities based on long term recurrence rate must account for the potential for even large eruptions to be missing from, or unidentified in, the geologic record.

4. Acknowledgments

The work was partially supported by the Nuclear Waste Organization of Japan (NUMO).

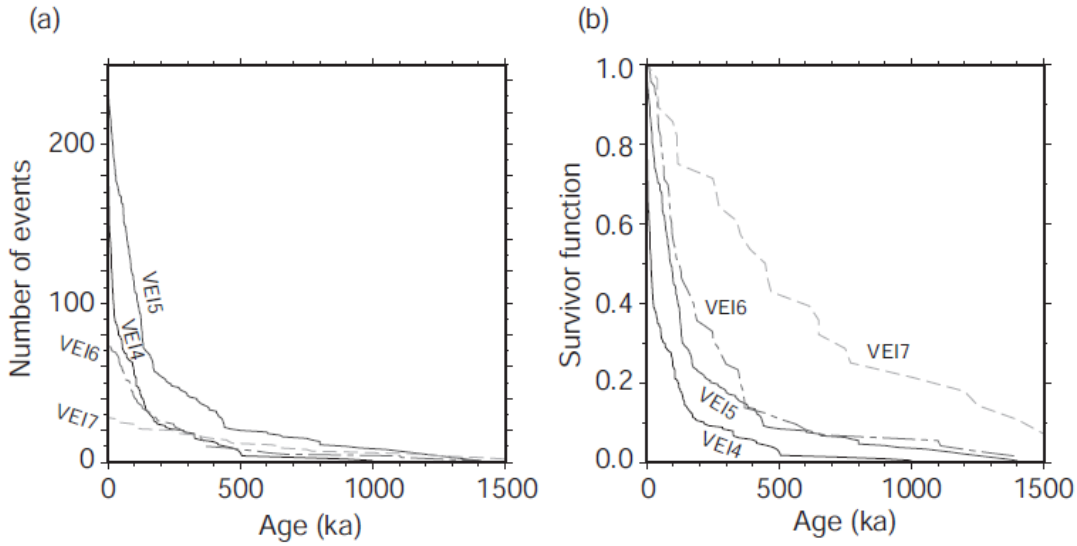

Fig. 1. Decrease of the included dataset with time. (a) Cumulative number of events. (b) Survivor function.

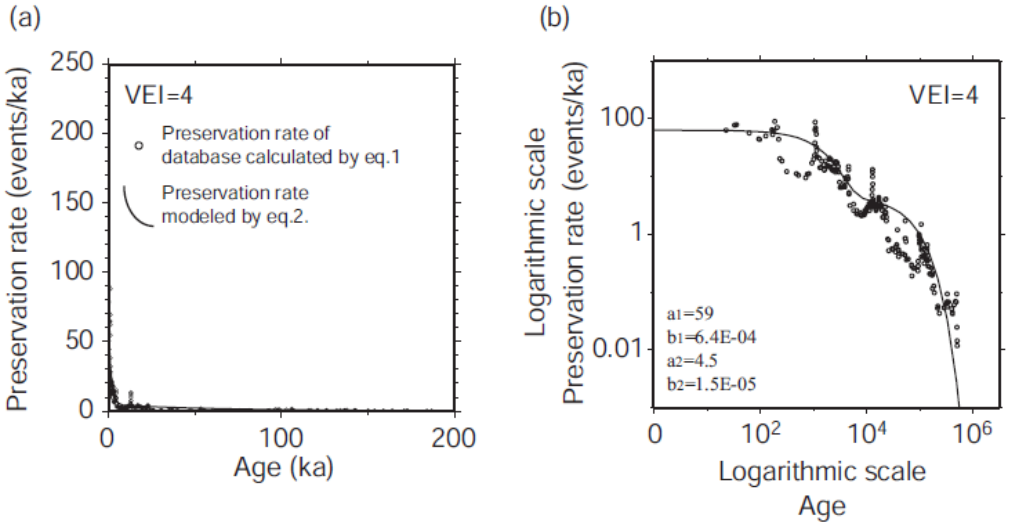

Fig. 2. Example of preservation rate change with time and model fitting (VEI=4, n=3). (a) Linear scale. (b) Logarithmic scale.

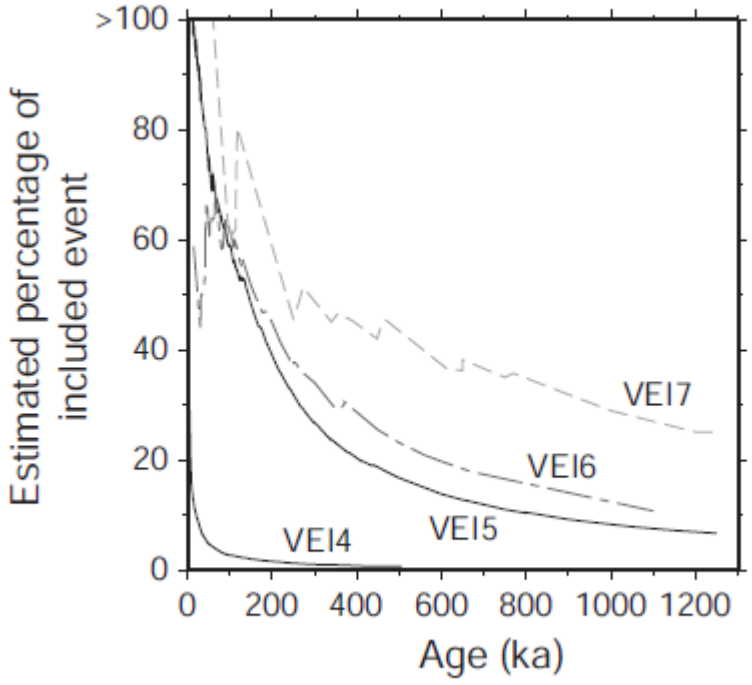

Fig. 3. Percentage of missing events with time.

Electric Power Failures in the 2011 off the Pacific Coast of Tohoku Earthquake

Gaku Shoji[a], Dai Takahashi[b]

[a]*Associate Professor, Faculty of Engineering, Information and Systems, University of Tsukuba, 1-1-1 Tennodai, Tsukuba, Ibaraki 305-8573, Japan*

[b]*Graduate Student, Graduate school of Systems and Information Engineering, University of Tsukuba, 1-1-1 Tennodai, Tsukuba, Ibaraki 305-8573, Japan*

The 2011 off the Pacific Coast of Tohoku earthquake caused severe damage on lifeline systems such as water treatments, energy supply systems, communication networks and transportation facilities. Among them, electric power failures occur at maximumly 4,858,580 houses in the areas offered by Tohoku Electric Power Co (as of March 17, 2011) (Tohoku Electric Power Company, Inc, 2011) and at maximumly 4,050,000 houses in the areas offered by TEPCO (as of March 11, 2011) (TEPCO, 2011). The damage assessment is significant to implement the associated data for risk assessment on power failures and induced consequences at a hazardous region for the future disaster prevention. From the reason, we collect the data by surveying the related web sites on power failures during the 2011 off the Pacific Coast of Tohoku earthquake for cities and towns at Ibaraki, Tochigi, Chiba, Saitama and Kanagawa prefectures and Tokyo Metropolitan areas, and by interviewing to the local government sectors and TEPCO branch office sectors. The total of subject cities and towns is 313 as shown Fig 1.

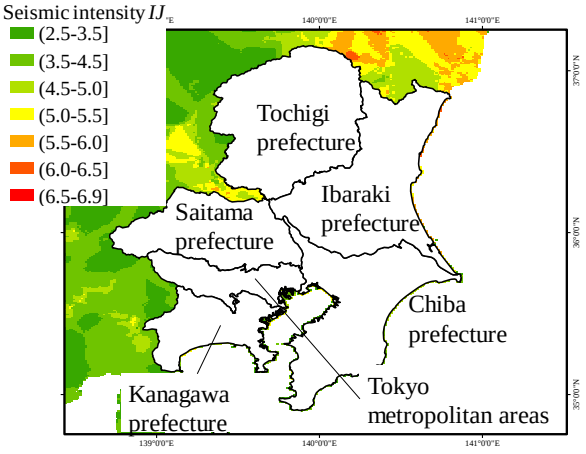

Ibaraki: 32 cities, 10 towns and 2 villages
Tochigi: 14 cities and 12 towns
Chiba: 36 cities, 17 towns,1 village and 6 wards
Tokyo: 25 cities, 2 towns,1village and 23 wards
Kanagawa: 19 cities, 13 towns,1 village and 28 wards
Saitama: 39 cities, 23 towns,1 village and 10 wards

Fig.1 Subject cities and towns, and spatial distribution of seismic intensity *IJ*

Based on collected data, we analyze whether power failures occurred or not, the number of

households and houses affected by power failures at a city i $N^{PF}{}_i$, and the restoration periods D_{RP}. We quantify the relative frequency $f^{R}{}_{PF}$ defined as the ratio of the number of the affected cities and towns by the total number of subject cities and towns at a same class for seismic intensity IJ. In addition, we quantify two damage ratios $R^{h}{}_i$ and $R^{c}{}_i$ at a city i, defined as the ratio of the number of affected households or houses $N^{PF}{}_i$ by the number of $N^{h}{}_i$ and $N^{c}{}_i$,

Fig 2 shows the relation of relative frequency $f^{R}{}_{PF}$ with seismic intensity IJ. $f^{R}{}_{PF}$ shows 0.33 at 3.0-3.1 IJ. $f^{R}{}_{PF}$ increases to 0.50-0.60 as IJ of 3.2 to 5.1 although $f^{R}{}_{PF}$ shows zero at 3.2-3.3 IJ, 0.33 at 3.6-3.7 IJ and 0.44 at 4.0-4.1 IJ. $f^{R}{}_{PF}$ increases to 0.78-1.00 as IJ of 5.2 to 6.1.

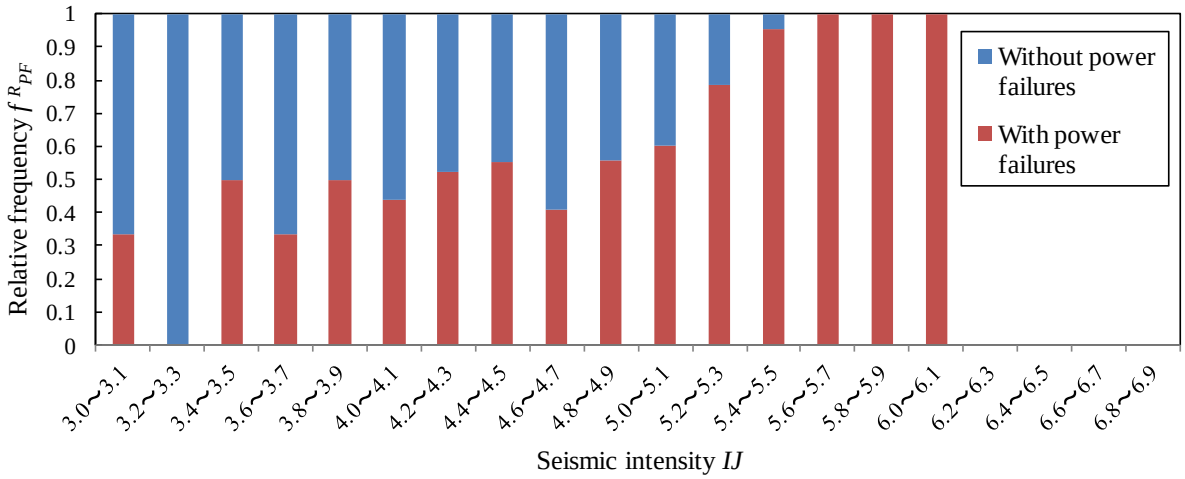

Fig.2 Relation of relative frequency $f^{R}{}_{PF}$ with seismic intensity IJ

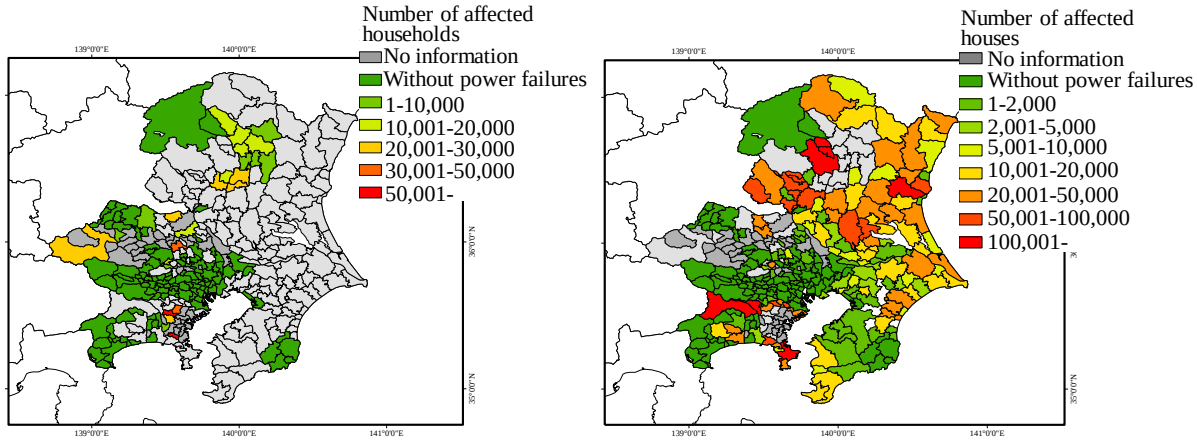

(a) $N^{h}{}_i$ (b) $N^{c}{}_i$

Fig.3 Spatial distribution on power failures by the number of affected households $N^{h}{}_i$ and houses $N^{c}{}_i$

Fig.3 shows spatial distribution on power failures by the number affected households $N^{h}{}_i$ and houses $N^{c}{}_i$. From Fig.3(a), two wards at Midori ward and Sakae ward, Yokohama city show large damage over 50,000 households. From Fig.3(b), 12 cities and towns at Ibaraki and 7 cities and towns

at Tochigi show larger N^i_h over 20,000. 2 cities at Saitama and 3 cities and towns at Chiba also show larger N^i_h over 20,000. N^h_i shows over 100,000 houses at the boundary regions between Tokyo metropolitan areas and Kanagawa.

Fig.4 shows spatial distribution on power failures by the damage ratio R^h_i, R^c_i. From Fig.4(a), eastern areas at Tochigi show higher R^h_i over 0.9 and western areas at Saitama show higher R^h_i over 0.7. Midori ward and Sakae ward at Yokohama city show higher R^h_i over 0.7. From Fig.4(b), 21 cities and towns at Ibaraki and 12 cities and towns at Chiba show higher R^c_i over 0.6.

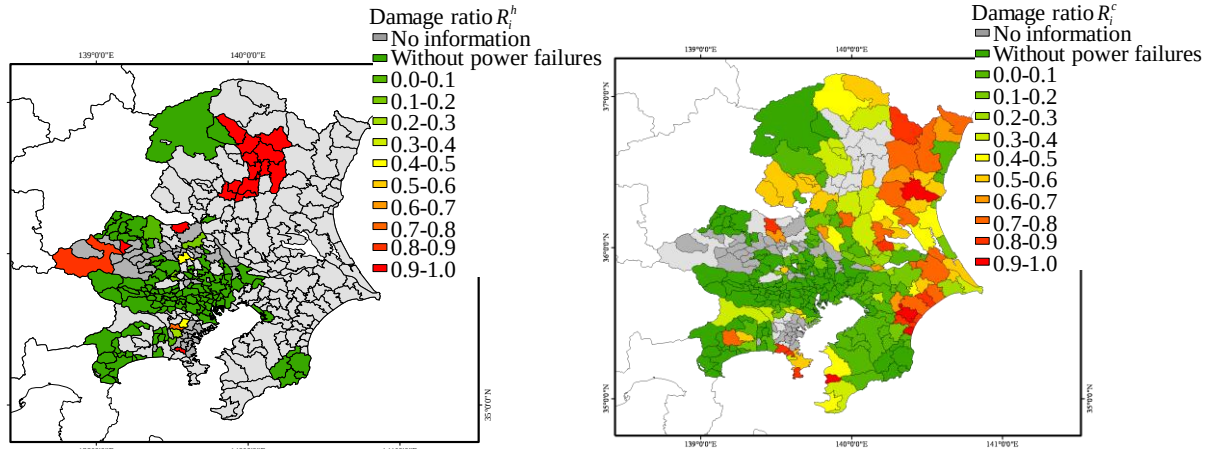

(a) Damage ratio R^h_i (b) Damage ratio R^c_i

Fig.4 Spatial distribution on power failures by the damage ratio R^h_i, R^c_i

Fig 5 shows frequency of damage ratio R^h_i and R^c_i dependent on seismic intensity IJ. From Fig.5(a), frequency on R^h_i of 0.0 to 0.4 becomes high as IJ of 3.0 to 4.5 whereas frequency on R^h_i of 0.7 to 0.8 becomes low at the same range of IJ. Frequency on R^h_i of over 0.8 becomes high as IJ over 4.7. From Fig.5(b), frequency on R^c_i of 0.0 to 0.6 becomes high as IJ of 3.0 to 4.7 whereas frequency

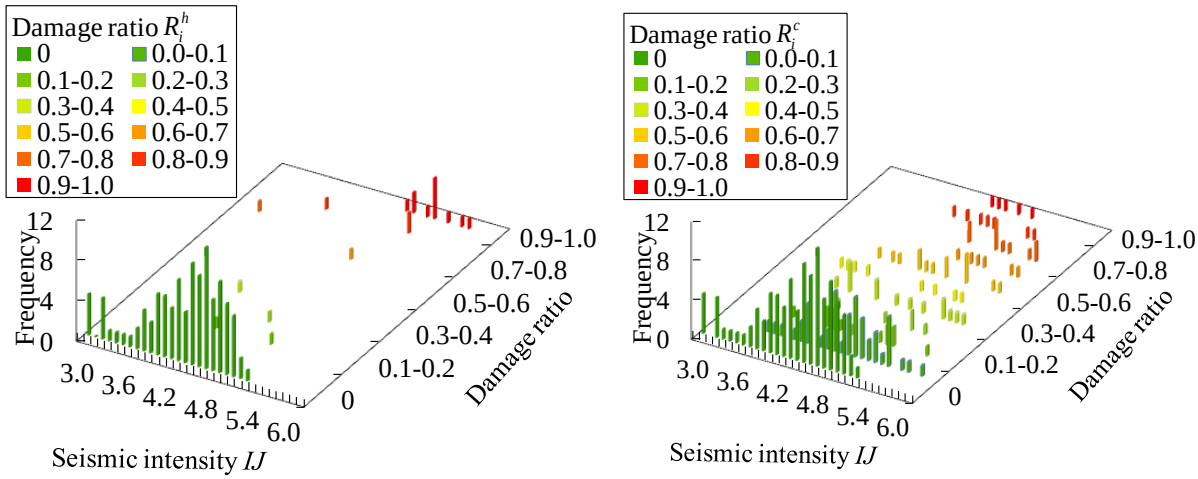

(a) Frequency on R^h_i (b) Frequency on R^c_i

Fig.5 Frequency of damage ratio R^h_i, R^c_i dependent on seismic intensity IJ

on R^c_i of 0.6 to 0.9 becomes low at the same range of *IJ*. Frequency on R^c_i of over 0.6 becomes high as *IJ* over 4.8

Fig.6 shows relation of the restoration period D_{RP} with seismic intensity *IJ*. Fig.7 shows spatial distribution by the restoration periods D_{RP}. From Fig.6, D_{RP} at *IJ* of 3.0 to 4.5 shows 0.3 to 0.7, that is nearly half a day. D_{RP} for two cities at *IJ* over 4.5 reach 1 day, D_{RP} for one town *IJ* of 4.7 becomes 2 days and D_{RP} for one city *IJ* of 5.0 becomes 5 days. Moreover maximum D_{RP} at *IJ* over 5.0 is 7 days at Kashima city, Ibaraki. From Fig.7, longer D_{RP} over 4 days shows in northern areas and coastal areas at Ibaraki than in the other areas. On the other hand, shorter D_{RP} within 1 day shows in the areas at Saitama and Kanagawa.

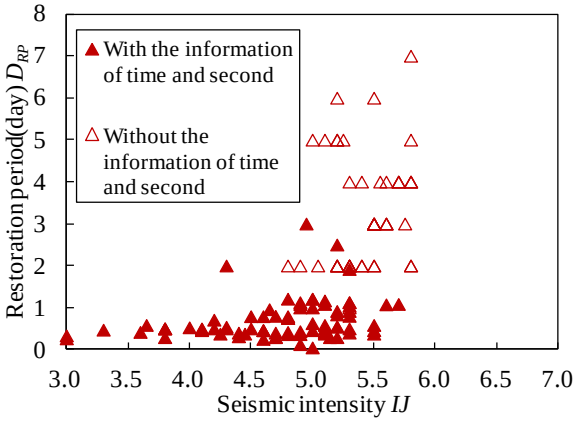

Fig.6 Relation of the restoration periods D_{RP} with seismic intensity *IJ*

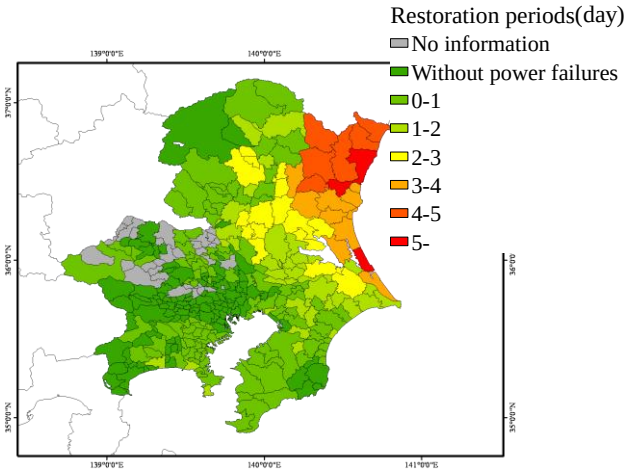

Fig.7 Spatial distribution of the restoration periods D_{RP}

References

Tohoku Electric Power Company, Inc. HP (2011). *Emergency Information* http://www.tohoku-epco.co.jp/emergency/9/index.html

TEPCO HP(2011). *Influence on our facilities during the 2011 off the Pacific Coast of Tohoku earthquake* http://www.tepco.co.jp/index-j.html

Design for Hybrid Database System for Volcanological Research and Outreach Program on Eruptive History

Mitsuru Okuno[a, b], Naoyuki Tsuruta[b, c], Yukihisa Nishizono[b, d], Masayuki Torii[e]
Hirohito Inakura[d], Tetsuo Kobayashi[b, f], Members of the International Research Center for Eruptive History and Informatics[b]

[a]*Faculty of Science, Fukuoka University, Nanakuma, Jonan, Fukuoka, 814-0180 Japan*
[b] *International Research Center for Eruptive History and Informatics, Fukuoka University, Nanakuma, Jonan, Fukuoka, 814-0180 Japan*
[c] *Faculty of Engineering, Fukuoka University, Nanakuma, Jonan, Fukuoka, 814-0180 Japan*
[d] *West Japan Engineering Consultants Inc., Watanabe-dori, Chuo, Fukuoka, 810-0004 Japan*
[e] *Kumamoto Gakuen University, Oe, Kumamoto, 862-8680 Japan*
[f] *Graduate School of Science and Engineering, Kagoshima University, Korimoto, Kagoshima, 890-0065 Japan*

The International Research Center for Eruptive History and Informatics, Fukuoka University, which will be established from April 2012, aims to construct a new database system not only for academic purposes but also for general interests. This system is designed to be fully automatic to enable simultaneous input of research publication. The locations and photo-images of various outcrops are basic information. The data in the system are divided into three categories (Fig. 1: 1 open to the public, 2 open to authorized person and 3 for personal use) to reserve priority of researchers.

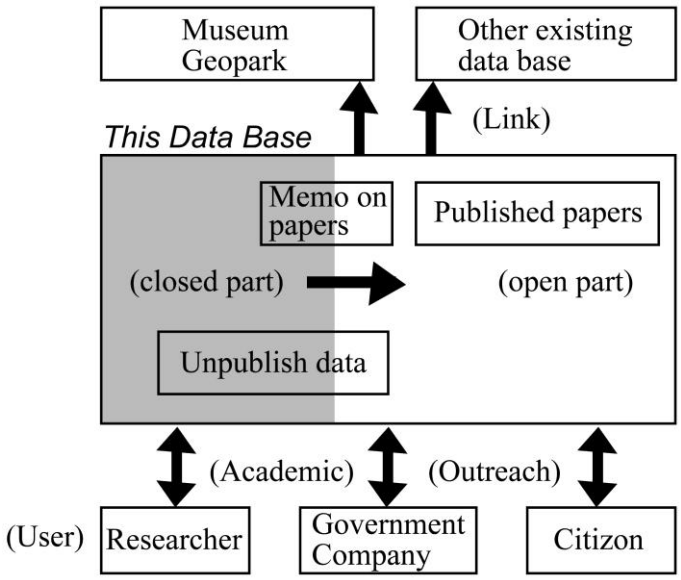

Fig. 1 Schemtic diagram of hybrid data base

This system can provide a platform for various collaborative studies in volcanology. The center will also publish issues of the international journal, "Eruptive History and Informatics" that will include the publication of data such as description of outcrops with accompanying analytical data, as well as reviewed papers on volcanoes around the world. Publications in English will be link with the database mentioned above.

Hosted by：Geological Survey of Japan, National Institute of Advanced Industrial Science and Technology (AIST)

Supported by：Ministry of Economy, Trade and Industry (METI), Ministry of Education, Culture, Sports, Science and Technology (MEXT), Ministry of Foreign Allairs of Japan (MOFA), Japan Meteorological Agency (JMA), National Research Institute for Earth Science and Disaster Prevention (NIED), Building Research Institute (BRI), Earthquake Research Institute, University of Tokyo (ERI), Disaster Prevention Research Institute, Kyoto University (DPRI), United States Geological Survey (USGS), EuroGeoSurveys, GNS Science, Asian Disaster Reduction Center (ADRC), Coordinating Committee for Geoscience Programmes in East and Southeast Asia (CCOP), Circum-Pacific Council (CPC), Global Earthquake Model (GEM), International Union of Geodesy and Geophysics (IUGG), International Assosication of Seismology and Physics of the Earth's Interior (IASPEI), International Association of Volcanology and Chemistry of the Earth's Interior (IAVCEI), Geological Society of Japan, Seismological Society of Japan, Volcanological Society of Japan, Japan Association for Quaternary Research, and Japanese Society for Active Fault Studies

Organizing Committee Chairperson：Eikichi TSUKUDA, Director General of GSJ

Organizing Committee：Geological Survey of Japan, AIST